Imact of clay minerals on the establishment of microbial communities driving nutrient turnover during early phases of soil development

Tanuwidjaja, Irina

University of Zagreb

FACULTY OF AGRICULTURE

Irina Tanuwidjaja

IMPACT OF CLAY MINERALS ON THE ESTABLISHMENT OF MICROBIAL COMMUNITIES DRIVING NUTRIENT TURNOVER DURING EARLY PHASES OF SOIL DEVELOPMENT

DOCTORAL THESIS

Zagreb, 2023

Sveučilište u Zagrebu

AGRONOMSKI FAKULTET

Irina Tanuwidjaja

UTJECAJ MINERALA GLINA NA USPOSTAVU MIKROBNIH ZAJEDNICA KOJE POKREĆU KRUŽENJE NUTRIJENATA U RANIM FAZAMA RAZVOJA TLA

DOKTORSKI RAD

Zagreb, 2023.

University of Zagreb
FACULTY OF AGRICULTURE

Irina Tanuwidjaja

IMPACT OF CLAY MINERALS ON THE ESTABLISHMENT OF MICROBIAL COMMUNITIES DRIVING NUTRIENT TURNOVER DURING EARLY PHASES OF SOIL DEVELOPMENT

DOCTORAL THESIS

Supervisors:
Prof. Mirna Mrkonjić Fuka, PhD
Prof. Michael Schloter, Dr. rer. nat. habil.

Zagreb, 2023

Sveučilište u Zagrebu
AGRONOMSKI FAKULTET

Irina Tanuwidjaja

UTJECAJ MINERALA GLINA NA USPOSTAVU MIKROBNIH ZAJEDNICA KOJE POKREĆU KRUŽENJE NUTRIJENATA U RANIM FAZAMA RAZVOJA TLA

DOKTORSKI RAD

Mentori:
Prof. dr. sc. Mirna Mrkonjić Fuka
Prof. dr. rer. nat. habil. Michael Schloter

Zagreb, 2023.

Bibliography data
Scientific area: Biotechnical sciences
Scientific field: Agriculture
Scientific branch: Ecology and environmental protection
Institution: University of Zagreb Faculty of Agriculture, Department of Microbiology
Supervisors of doctoral thesis: Prof. Mirna Mrkonjić Fuka, PhD
Prof. Michael Schloter, Dr. rer. nat. habil.
Number of pages: 155
Number of figures: 33
Number of tables: 9
Number of appendices: 0
Number of references: 329
Doctoral thesis defense date: 27th of February 2023
The members of the PhD defense committee:
Prof. Sanja Sikora, PhD
Assoc. prof. Kristina Krklec, PhD
Assoc. prof. Ana Bielen, PhD

The doctoral thesis is deposited in:
National and University Library in Zagreb, Ulica Hrvatske bratske zajednice 4 p.p. 550, 10 000 Zagreb
Central Agricultural Library, Faculty of Agriculture, Svetošimunska cesta 25, 10 000 Zagreb.

The topic of the thesis has been accepted at the session of the Faculty Council of the University of Zagreb Faculty of Agriculture, held on the 13th of November 2018, and approved at the session of the Senate of the University of Zagreb on the 13th of February 2019. The title of the topic was amended by the Senate resolution on the 24th of May 2022 and supplemented by the resolution in English on the 17th of January 2023.

UNIVERSITY OF ZAGREB
FACULTY OF AGRICULTURE

Statement of originality

I, **Irina Tanuwidjaja**, hereby declare that I have independently written the doctoral thesis under the title:

IMPACT OF CLAY MINERALS ON THE ESTABLISHMENT OF MICROBIAL COMMUNITIES DRIVING NUTRIENT TURNOVER DURING EARLY PHASES OF SOIL DEVELOPMENT

With my signature I guarantee:

- that I am the only author of this doctoral thesis
- that doctoral thesis is the original result of my work and that while writing it, I did not use any other sources except ones already cited
- that I am familiar with the terms of the Ethic codex of the University of Zagreb (sec.19).

Zagreb, _____

_____
Signature of the PhD student

Doctoral thesis grade

The dissertation was defended at the University of Zagreb Faculty of Agriculture on the _____ in front of the members of the PhD defense committee:

1. Prof. Sanja Sikora, PhD _____
2. Assoc. prof. Kristina Krklec, PhD _____
3. Assoc. prof. Ana Bielen, PhD _____

Supervisor Prof. Mirna Mrkonjić Fuka, PhD

University of Zagreb Faculty of Agriculture

Department of Microbiology

Svetošimunska cesta 25, 10 000 Zagreb, Croatia

Mirna Mrkonjić Fuka was born in Zagreb in 1976. She graduated from the Faculty of Science in Zagreb in 2002 and received her PhD at the Technical University of Munich (TUM) in 2007 with a thesis on the structural and functional diversity of proteolytic bacteria in the soil. Since 2007 she has worked at the Department of Microbiology at the Faculty of Agriculture, University of Zagreb, where she was appointed Professor in 2022. Her main scientific interests include the analysis of functional and structural diversity of bacterial communities in complex ecosystems, molecular-biological identification of lactic acid bacteria, and selection of starter and bioprotective cultures. Mirna Mrkonjić Fuka teaches at the Faculty of Agriculture of the University of Zagreb, where she coordinates seven courses at the undergraduate and graduate levels. She was a supervisor of one doctoral, nine bachelor, and twenty-one master theses and supervisor of three student work rewarded with a Rector's Award. Mirna Mrkonjić Fuka has obtained several awards and acknowledgments (DAAD, FEMS, ERASMUS, CEEPUS, Society of University Teachers, and Other Scientists in Zagreb) for her scientific and academic work. She has participated in several international (Erasmus+, TEFSI (2019-2020), Tempus IV Program (2015-2017), See-Era, Net Plus (2010-2012), European Regional Development Fund (2006-2007), DFG-German Research Foundation (2002-2005)), and national projects (MZO (2007-2013) and The Agency for Payments in Agriculture, Fisheries and Rural Development (2021-2024)) of which she was the leader of one bilateral project with Germany (2012-2013), two with Austria (2014-2015, 2022-2023), one with Slovenia (2016-2017) and one with China (2018-2019) as well as the leader of the project founded by Croatian Science Foundation (2014-2017) and project founded by The Agency for Payments in Agriculture, Fisheries and Rural Development (2021-2023). Since 2007 Mirna Mrkonjić Fuka has spent more than fifteen months at renowned foreign universities and scientific research institutions BOKU, Austria; TUM, Germany; Helmholtz Zentrum Munich, Germany; Vitoria University, Wellington, New Zealand; Huazhong University, Wuhan, NR China). Mirna Mrkonjić Fuka is a member of the Croatian Microbiological Society, a member of the Board for the Use of GMOs at the Croatian Ministry of Health, and was a member of the Steering committee of the Institute for Agriculture and Tourism in Poreč. She has held more than 25 lectures at renowned international scientific research institutes and congresses and has published more than 30 scientific papers cited 495 times according to WOS.

Supervisor Prof. Michael Schloter, Dr. rer. nat. habil.

Technical University of Munich

Chair of Soil Science, TUM School of Life Sciences (Weihenstephan)

Emil-Ramann-Straße 2, 85 354 Freising, Germany

Michael Schloter was born in 1966. He studied biology at the University of Munich and obtained his diploma in 1990. He then received his PhD at the University of Bayreuth in the working group of Prof. Klingmüller. After several postdoc positions, he became the leader of the working group “Functional Microbial Ecology” at the Institute for Soil Ecology at the GSF National Research Center in 2002. Furthermore, Michael Schloter became the director of the Research Unit for Environmental Genomics at the Helmholtz Center Munich in 2011. In 2011 he was awarded the Heinrich Baur Prize for outstanding scientific achievements in the field of agricultural research and related disciplines. The main focus of his work is the examination of the genetic diversity of microbiota in different environmental compartments where his main goal is to understand the interaction between microbes and various hosts such as plants, its meaning for ecosystem functionality and performance, and to manage the microbial genetic resources in soils for sustainable agriculture, mainly for the production of high quality, healthy food. In addition, he is involved in several human microbiome initiatives. Michael Schloter is recognized as one of the world’s most-cited researchers (top 1%) according to the Web of Science. His research group has published more than 150 papers in the last 5 years in scientific journals such as Nature and PNAS. Michael Schloter has been teaching at TUM and closely collaborating with colleagues and faculty members in the Department of Life Sciences since 2001 and was appointed honorary professor of microbiology in 2010. He also serves as an editor of numerous international journals (since 2003), and a reviewer for DFG and EU (since 2007).

Acknowledgements

First of all, I would like to express my sincere gratitude to my PhD supervisors prof. Mirna Mrkonjić Fuka, PhD, and prof. Michael Schloter, dr. rer. nat. habil. for their continuous support, time, effort, motivation, and immense knowledge. Their guidance helped me throughout the research and writing of this thesis.

I am also grateful to my defence committee, prof. Sanja Sikora, PhD, assoc. prof. Kristina Krklec, PhD, and assoc. prof. Ana Bielen, PhD, who generously shared their knowledge and experience with me.

My special thanks go to Karin Pritsch, PhD, for her invaluable advice, feedback, and generous support in all areas.

I would also like to express my gratitude to the entire EGEN/COMI and IBÖE/BIOP group at Helmholtz Zentrum München. Maria, Anne, Martin, Vjera, Antonis, Urška, Matea, Christian B., Christian K., Christoph, Florian, and many others, thank you for your generosity and encouragement, your humour, and the fun times we had at and outside work. Thanks to your friendship, my time in Germany was a true gift.

I would also like to express my sincere gratitude to all my colleagues at the Faculty of Agriculture, Department of Microbiology (Prof. Sikora, Mirna, Ivana, Nataša, Sanjica, Petra, Laura, Sandra, Dragica, Sali, Darija) for the welcome, help, advice, support, laughter and above all for the truly unique working atmosphere.

And finally, none of this would have been possible without my family and friends (you know who you are) and Toni's endless support, patience, and complete lack of self-preservation instinct. Thank you...

The research presented in this doctoral thesis was performed under the supervision of prof. Mrkonjić Fuka, PhD and prof. Michael Schloter, Dr. rer. nat. habil. in the framework of the scientific project “Biotic and abiotic factors that drive the function of microbial communities at biogeochemical interfaces in different soils (BAMISO)” which is part of the Priority programme SPP 1315 “Biogeochemical Interfaces in Soil” funded by German Research Foundation (DFG). The research was conducted at the Research Unit for Comparative Microbiome Analysis (COMI) at the Helmholtz Center Munich and the University of Zagreb Faculty of Agriculture, Department of Microbiology.

Summary

Soil is an integral part of every terrestrial ecosystem where it facilitates various ecosystem processes, including nutrient cycling (carbon (C), nitrogen (N)), and turnover (phosphorus (P)). The interaction between soil microbiota and soil constituents, such as clay minerals and organic matter leads to the formation of hotspots of microbial diversity and activity. Moreover, microbial metabolism actively shapes the habitat in which they live and influences soil formation together with other physical, chemical, and biological factors.
Soil formation is a lengthy process based on the interaction of complex physical, chemical, and biological processes where microorganisms play an essential role as they drive nutrient availability and nutrient storage mainly if no plants are available. Furthermore, microbial diversity and function in the soil are affected by various abiotic and biotic factors, including mineral composition, and clay minerals in particular. Even though it was shown that different minerals can support and select different microorganisms, thus shaping the microbial community and function in soils, it is unknown how clay minerals influence the establishment, diversity, and adaptation of functional microbiota involved in nutrient cycling and turnover in the early stages of soil development. Therefore, this research aimed to improve our understanding of how clay minerals impact the establishment and diversity of microbial communities driving C, N, and P turnover during the early stages of soil development by combined analyses of the bacterial abundance and diversity with qPCR and T-RFLP respectively, and an in-depth analyses of microbial diversity and functional genes involved in C and N cycling, and P turnover based on a metagenomic shotgun sequencing of artificial soil microbiota.
This study using artificial soils of different mineralogy (montmorillonite (MT), illite (IL), montmorillonite+charcoal (MT+CH), and illite+ferrihydrite (IL+FH)) has shown that soil properties, clay mineral composition in particular, strongly influence the establishment of different microbial communities during soil development. However, only two clay minerals (MT and IL) with different specific surface areas and charges that influence the nutrient availability, showed a strong effect on the bacterial community structure and function over the long-term incubation. Similar values of total organic C (13.5 ± 0.9 in MT and 11.6 ± 0.7 in IL), total N (1.5 ± 0.1 in MT and 1.3 ± 0.2 in IL), and total P (396 ± 20 in MT and 384 ± 29 in IL) content were detected in both soils. Consequently, the C:N:P ratios were very similar as well (82:7:1 in MT and 90:11:1 in IL) indicating C, N and P depleted system. However, based on the analysis of genes present in both soils, it is obvious that microorganisms have developed different strategies to overcome nutrient depletion in MT and IL. The degradation of recalcitrant C compounds such as cellulose (*bglX, bglB*) and chitin (*nagZ, hexA-B, hex*), N depolymerisation, and mineralization (*pepA, pepN, pepD, pip, clpP, clpX, aguB, hmgL, hutH, CTH, sdaA/sdaB, dsdA, tdcB*) and assimilation (*gudB/rocG, gdhA/GLUD1, gdhA/GLUD2*), together with effective P uptake and use of the internal poly-P pool (*ppa, ppx, pstSCAB*) were characteristic for MT. In contrast, starch (*amyA*) and chitin (*chiA*, *CHIT1*) were preferable C sources in IL. Furthermore, the higher abundance of denitrification related genes (*narG, nirS, nifH*) in IL indicates that N depletion was potentially overcome by the more efficient consumption of alternative N sources, such as chitin (*chiA*, *CHIT1*) when compared to MT. Lastly, higher abundances of genes encoding alkaline phosphatases (*phoA*, *phoD*), glycerophosphoryl diester phosphodiesterase (*ugpQ*), and glycerol-3-phosphate transporter system (*ugpBAEC*) indicate that IL microbiota utilizes organic P sources to overcome P depletion.
Overall, the results of this study significantly contribute to better understand the effect of clay minerals on the establishment of microbial communities that drive nutrient turnover, revealing different microbial strategies in adapting to and overcoming nutrient depletion during the early phases of soil development.

Keywords: soil formation, clay minerals, microbial diversity, functional microbiota, carbon and nitrogen cycle, phosphorus turnover, qPCR, T-RFLP, next-generation sequencing

Prošireni sažetak

Utjecaj minerala glina na uspostavu mikrobnih zajednica koje pokreću kruženje nutrijenata u ranim fazama razvoja tla

Tlo je heterogena smjesa različitih mineralnih, organskih i bioloških komponenti i kao takvo predstavlja jedno od najsloženijih staništa u kojem mikroorganizmi obitavaju. Interakcije između mikroorganizama i čvrste faze tla, kao što su minerali glina i organska tvar uzrokuju stvaranje reaktivnih ploha koje predstavljaju žarišta mikrobne raznolikosti i aktivnosti. Sama veličina i fizikalno-kemijska svojstva ovakvih mikrostaništa ovise o izvornom matičnom supstratu. Među abiotičkim čimbenicima koji utječu na karakteristike mikrostaništa, ističe se mineralni sastav tla, točnije minerali glina. Dokazano je da minerali glina utječu na biogeokemijsko kruženje i mobilizaciju hranjivih tvari, kao što su ugljik (C), dušik (N) i fosfor (P). Prisutni su u svim tlima i sedimentima gdje tvore glavnu frakciju koja utječe na veličinu specifičnih reaktivnih površina. Smatraju se regulatorima kationske izmjene i mjestom adsorpcije organskih i anorganskih spojeva, čime utječu na dostupnost hranjivih tvari te posljedično na preživljavanje, metabolizam i funkciju mikroorganizama. Stoga, različiti mikroorganizmi naseljavaju tla s različitim mineralnim sastavom. Mikroorganizmi svojim metabolizmom aktivno mijenjaju stanište u kojem obitavaju te utječu na razvoj tla zajedno s ostalim biološkim, fizikalnim i kemijskim čimbenicima. Istovremeno, mikroorganizmi imaju središnju ulogu u biogeokemijskom kruženju svih kemijskih elemenata, među kojima se ugljik, dušik i fosfor smatraju esencijalnima. Njihova uloga u kruženju kemijskih elemenata je od posebnog značaja u ranim fazama razvoja tla. Obzirom da ugljik i dušik ne nalazimo u izvornom matičnom supstratu, potencijalni izvori ugljika i dušika u tlu uključuju taloženje organskih tvari i fiksaciju ugljika odnosno dušika od strane autotrofnih mikroorganizama. Fosfor, s druge strane, je prisutan u ranim fazama razvoja tla, prvenstveno u anorganskom obliku kao sastavni dio matičnog supstrata, te stoga njegova mobilizacija ovisi isključivo o mineralnom trošenju supstrata koje pak ovisi o aktivnosti i sposobnosti otapanja i mineralizacije od strane mikroorganizama. Međutim, još uvijek se ne zna u kojoj mjeri minerali glina utječu na sastav, razvoj i adaptaciju mikrobiote uključene u kruženje makronutrijenata u ranim fazama razvoja tla, zatim koje funkcionalne mikrobne grupe pokreću kruženje tvari u osiromašenim ekosustavima te koje procese i mehanizme koriste da nadvladaju nedostatak C, N i P tijekom produžene inkubacije tala. Na temelju navedenog postavljene su sljedeće hipoteze: u umjetnim tlima različitog mineralnog sastava razvit će se različite mikrobne zajednice (**H1**), produžena inkubacija umjetnih tala dovest će do iscrpljenja bioraspoloživih oblika ugljika, dušika i fosfora i postupne prilagodbe i razvoja mikrobnih zajednica sposobnih iskorištavati teško dostupne oblike C, N i P (**H2**), nedostatak bioraspoloživog ugljika uzrokovat će adaptaciju mikrobnih gena uključenih u kruženje ugljika (**H3**), mikrorganizmi će nadvladati nedostatak bioraspoloživog N i P recikliranjem organskog N i P i efikasnijim unosom N i P u mikrobne stanice (**H4**) i konačno, funkcionalna mikrobiota sastojat će se primarno od tzv. generalista odnosno mikrobnih grupa prilagođenih širokom spektru ekoloških čimbenika sa sposobnošću iskorištavanja različitih izvora hranjiva među kojima će samo nekoliko grupa pokretati sve procese uključene u kruženje C, N i P, dok će zastupljenost specijalista tj. uskospecijaliziranih mikrobnih grupa koje pokreću neki specifičan proces u kruženju C, N i P biti će zanemariva (**H5**). Stoga, ciljevi ovog rada su ispitati utjecaj minerala glina na uspostavu, raznolikost i aktivnost mikrobnih zajednica, identificirati procese i mikrobne grupe koje pokreću kruženje makronutrijenata tijekom ranih faza razvoja tla i identificirati mehanizme koje mikroorganizmi koriste da nadvladaju nedostatak C, N i P tijekom produžene inkubacije tala.

Za ispitivanje postavljenih hipoteza korištena su dva pristupa. Utjecaj minerala glina na dostupnost hranjivih tvari, bakterijsku brojnost te uspostavu, raznolikost i aktivnost mikrobnih zajednica (**H1**) ispitan je u preliminarnom eksperimentu u kojem su pripremljena umjetna tla (n=4) koja se međusobno razlikuju po sastavu minerala gline. Ova tla su, uz

kvarcni pijesak i prah, sadržavala jednu od sljedećih komponenti koje se često pojavljuju u prirodi: monmorilonit (MT), ilit (IL), montmorilonit+drveni ugljen (MT+CH) ili ilit+ferihidrit (IL+FH). Za svako umjetno tlo pripremljeno je 9 nezavisnih ponavljanja, mase do 500 g. Na početku eksperimenta, svako je umjetno tlo inokulirano mikrobnim inokulatom koji potječe od Ap horizonta prirodnog luvisola i sterilnim stajskim gnojem. Sterilni stajski gnoj je ponovno dodan svim umjetnim tlima 562. dan inkubacije. Inkubacija umjetnih tala završena je nakon 842 dana. Pretpostavljano je da će se do ovog trenutka, ovisno o tipu minerala glina, formirati mikro- i makro-agregati usporedivi onima u prirodnim tlima. Ovako pripremljenim umjetnim tlima potom je dodan biljni materijal u triplikatima. Kako bi se provjerilo da li su umjetna tla usporediva s prirodnim tlom, jedan uzorak luvisola (Scheyern) je u triplikatima tretiran biljnim materijalom. Istovremeno, pripremljene su i kontrole koje su se od umjetnih tala i luvisola razlikovale samo po tome što im nije dodan biljni materijal. Sva tla su dodatno inkubirana tijekom 63 dana u mraku, uz održavanje stalne vlage. Uzorci su uzeti 0., 7., 21. i 63. dan nakon dodavanja biljnog materijala. Utjecaj minerala gline na dostupnost ugljikovih spojeva i aktivnost mikroorganizama određena je na temelju WEOC (organski C koji se može ekstrahirati vodom) vrijednosti, brojnost na temelju C_{mic} vrijednosti i kvantifikacijom 16S rRNA gena, a raznolikost bakterijskih zajednica na temelju T-RFLP analize 16S rRNA gena amplificiranog početnicama 6-FAM-27f i 1401r.

Primijećeno je da u svim umjetnim tlima, bez obzira na prisutne minerale gline, WEOC vrijednosti opadaju odmah nakon dodatka biljnog materijala, što se može objasniti povećanom mikrobnom aktivnošću i trenutnim iskorištavanjem lako dostupnog ugljika od strane mikroorganizma. Iako je isti trend zamijećen u svim umjetnim tlima, nešto niže WEOC vrijednosti su detektirane u umjetnim tlima koja sadrže MT u usporedbi s tlima koja sadrže IL, što ukazuje na bržu izmjenu hranjivih tvari u MT, kao i nešto višom stopom mikrobne respiracije. U prirodnom tlu, s druge strane, opadanje WEOC vrijednosti je detektirano tek kasnije tijekom inkubacije, u usporedbi s umjetnim tlima, što se može pripisati bolje razvijenim strukturama u prirodnom tlu i organskoj tvari koje bolje i brže vežu raspoložive ugljikove spojeve te ih na taj način privremeno štite od mikrobnog djelovanja. U svim umjetnim tlima, kao i u prirodnom tlu tretiranim biljnim materijalom, mikrobna biomasa se povećala od 0. do 7. dana inkubacije, što je vidljivo iz porasta C_{mic} vrijednosti, i u skladu je s dinamikom WEOC vrijednosti. Bakterijska brojnost, kao što je vidljivo iz broja 16S rRNA kopija gena g^{-1} suhe tvari tla, povećava se u MT, MT+CH i IL+FH umjetnim tlima tek kasnije tijekom inkubacije. Iako su i C_{mic} i broj kopija gena 16S rRNA odraz mikrobne biomase, nesklad između rezultata može se pripisati metodološkim razlikama. Obzirom da je u svim umjetnim tlima detektiran sličan trend u kretanju WEOC i C_{mic} vrijednosti te broju 16S rRNA gena, nije bilo moguće potvrditi H1 hipotezu isključivo na temelju tih parametara. Konačno, na temelju PCA analize T-RF fragmenata 16S rRNA gena, vidljivo je da se bakterijske zajednice u umjetnim tlima značajno razlikuju od bakterijskih zajednica u luvisolu. Nadalje, iz ovih rezultata je vidljivo da na uspostavu i razvoj bakterijskih zajednica u umjetnim tlima najviše utječu minerali gline MT i IL, što se može objasniti razlikama u fizikalno-kemijskim karakteristikama, prvenstveno razlikama u specifičnoj površini i naboju minerala gline, što pak utječe na dostupnost hranjivih tvari mikroorganizmima. Stoga, ovi rezultati potvrđuju hipotezu (**H1**) da određene grupe mikroorganizama preferiraju određene tipove minerala gline, te da posljedično prisutnost minerala gline u tlu utječe na uspostavu, razvoj i raznolikost bakterijskih zajednica.

Ostale hipoteze (**H2-H5**) ispitane su primjenom dubokog sekvenciranja metagenoma umjetnih tala čiji je mineralni sastav najviše utjecao na raznolikost bakterijskih zajednica (MT i IL) nakon 842 dana inkubacije. Obzirom da je izvor hranjiva u obliku sterilnog stajskog gnoja zadnji put unesen prije više od 300 dana, u MT i IL detektirane su niske koncentracije organskog ugljika, ukupnog dušika i fosfora, te vrlo niski stehiometrijski omjeri C:N, C:P i N:P, što ukazuje na nedostatak ugljika, dušika i fosfora u ispitivanim umjetnim tlima koja je usporediva s drugim oligotrofnim ekosustavima. Ovi rezultati ukazuju da su lako dostupna hranjiva potrošena te da su u MT i IL najvjerojatnije zaostali samo teško razgradivi spojevi kao potencijalan izvor makronutrijenata, što potvrđuje hipotezu (**H2**). Zbog nedostupnosti

lako razgradivih C spojeva, mikroorganizmi u MT i IL iskorištavaju teško razgradive C spojeve i mikrobne ostatke. Točnije, u MT mikroorganizmi, primarno koriste celulozu (*bglX*, *bglB*) i hitin (*nagZ*, *hexA-B*, *hex*), a u IL škrob (*amyA*) i hitin (*CHIT1*) kao izvore C. Iako niska zastupljenost gena koji kodiraju enzime uključene u fiksaciju ugljika nije ukazivala na dodatne izvore ugljika, detektirane mikrobnih grupe, točnije članovi koljena Cyanobacteria ukazuju da dio ugljika dospijeva u MT i IL i fiksacijom. Navedeno potvrđuje hipotezu (**H3**) da mikroorganizmi koriste različite mehanizme kako bi nadvladali depleciju ugljika u MT, odnosno IL. Slično kao kod kruženja C, rezultati su pokazali da su mikroorganizmi u MT i IL nadvladali nedostatak lako dostupnih dušičnih spojeva primarno depolimerizacijom, odnosno mineralizacijom složenih organskih N spojeva i mikrobnih ostataka. U MT detektirana je veća zastupljenost gena koji kodiraju ekstracelularne proteaze koje sudjeluju u depolimerizaciji/mineralizaciji dušika i razgradnji bakterijskih staničnih stijenki i proteina (*pepA*, *pepN*, *pepD*, *pip*, *clpP*, *clpX*, *aguB*, *hmgL*, *hutH*, *CTH*, *sdaA*/*sdaB*, *dsdA*, *tdcB*), asimilaciji (*gudB*/*rocG*, *gdhA*/*GLUD1*, *gdhA*/*GLUD2*) i usvajanju dušika (*nrtP*). S druge strane, u IL je detektirana veća zastupljenost gena uključenih u hitinolizu (*CHIT1*), denitrifikaciju (*narH*) i nitrifikaciju (*amoC*, *hao*), što ukazuje da je nedostatak dušika u tlu s IL, za razliku od tla s MT, potencijalno prevladan učinkovitijom potrošnjom alternativnih izvora dušika, kao što je hitin (*CHIT1*). Nadalje, nedostatak lako dostupnih P spojeva mikroorganizmi u MT su nadvladali pojačanim iskorištavanjem unutarstaničnih poli-P (*ppa*, *ppx*) rezervi i povećanjem učinkovitosti unosa fosfora u mikrobne stanice (*pstSCAB*). S druge strane, drukčiji adaptacijski mehanizmi detektirani su u IL, a uključuju pojačano iskorištavanje organskih P oblika pomoću alkalnih fosfataza (kodirane genima *phoA* i *phoD*) i glicerofosforil diester fosfodiesteraze (kodirana genom *ugpQ*) i efikasan transportni sustav glicerol-3-fosfata (*ugpBAEC*), što potvrđuje hipotezu (**H4**). Konačno, mikrobne grupe koje pokreću kruženje ugljika, dušika i fosfora u MT i IL prvenstveno spadaju u visoko zastupljene taksone koji su pronađeni u oba tla, dok je brojnost specijaliziranih mikrobnih grupa specifičnih za MT ili IL iznimno niska, što potvrđuje hipotezu (**H5**).

Ovo istraživanje značajno je pridonijelo razumijevanju učinka minerala glina na uspostavljanje mikrobnih zajednica, identifikaciji funkcionalne mikrobiote koja pokreće kruženje hranjivih tvari i identifikaciji adaptacijskih mehanizama koje mikroorganizmi koriste za prevladavanju nedostatka C, N i P u ranim fazama razvoja tla. U tu svrhu, umjetna tla s točno definiranim karakteristikama su se pokazala kao nezamjenjiv alat koji omogućava istraživanje učinka isključivo jednog određenog parametra, u ovom slučaju, minerala gline. Konačno, metagenomsko sekvenciranje nove generacije trenutno predstavlja jedan od najboljih i sveobuhvatnih pristupa koji istovremeno omogućava istraživanje mikrobne raznolikosti, mikrobnih procesa, kao i povezivanje mikrobnih procesa s točno određenim mikrobnim taksonomskim grupama.

Ključne riječi: razvoj tla, minerali glina, mikrobna raznolikost, funkcionalna mikrobiota, kruženje ugljika i dušika, mobilizacija fosfora, qPCR, T-RFLP, sekvenciranje nove generacije

Table of contents

1. INTRODUCTION 1
1.1. Objective and hypotheses of Ph.D. research 3
2. LITERATURE REVIEW 5
2.1. Soils as a basis for life on Earth 5
2.1.1. Soil development 5
2.1.2. The interplay between biota and their abiotic environment in soils 6
2.2. Nutrient stoichiometry as a driver for microbial activities 9
2.2.1. Carbon cycle 11
2.2.2. Nitrogen cycle 17
2.2.3. Phosphorus turnover 22
2.3. Artificial soils as a tool to study soil development 25
3. MATERIALS AND METHODS 27
3.1. Materials 27
3.1.1. Chemicals 27
3.1.2. Oligonucleotides 28
3.1.3. Kits and master mixes 29
3.1.4. Instruments 30
3.2. Methods 30
3.3. Preparation of artificial soils and experimental design 31
3.3.1. Preparation and maturation of artificial soils 31
3.3.2. Treatment of MT, IL, MT+CH, and IL+FH soils with plant litter 33
3.4. Nucleic acid extraction 34
3.5. Preliminary screening of bacterial diversity and abundance in artificial soils 36
3.5.1 Determination of microbial biomass (C_{mic}) and water-extractable carbon (WEOC) in MT, IL, MT+CH, and IL+FH artificial soils 36
3.5.2. qPCR analysis of pre-incubated artificial soil treated with plant litter 37
3.5.3. Terminal Restriction Fragment Length Polymorphism (T-RFLP) analysis of pre-incubated artificial soil treated with plant litter 38
3.6. In-depth analyses of microbial diversity, functional genes, and microbiota involved in carbon, nitrogen, and phosphorus turnover 39
3.6.1. Measurements of pH, organic carbon, nitrogen, and phosphorus concentrations 39
3.6.2. Library preparation and high-throughput metagenomic sequencing 40
3.6.3. Bioinformatics and statistical analysis 41
4. RESULTS 46
4.1. Effect of clay minerals on bacterial diversity and abundance as shown by preliminary screening 46

4.1.1. Water-extractable carbon (WEOC) and microbial biomass (C_{mic}) 46
4.1.2. qPCR analysis of pre-incubated artificial soil treated with plant litter 51
4.1.3. Terminal Restriction Fragment Length Polymorphism (T-RFLP) analysis of pre-incubated artificial soil treated with plant litter 53
4.2. The influence of different types of clay minerals on phylogenetic and functional diversity and major processes involved in carbon, nitrogen, and phosphorus turnover as shown by metagenomic shotgun sequencing 56
4.2.1. The properties of MT and IL soils 56
4.2.2. Taxonomic and functional differences in MT and IL microbiomes 57
4.2.3. Phylogenetic annotation of MT and IL metagenomes 63
4.2.4. Functional analysis of artificial soil 70
4.2.5. Gene abundance and microbial groups harbouring genes involved in the carbon turnover 73
4.2.6. Gene abundance and microbial groups harbouring genes involved in the nitrogen cycle 82
4.2.7. Gene abundance and microbial groups harbouring genes involved in phosphorus transformation 91
5. DISCUSSION 99
5.1. Influence of clay minerals on the establishment of the microbiome in the early phases of soil development 99
5.1.1. The influence of clay minerals on the dynamics of water-extractable carbon in natural and artificial soils 99
5.1.2. The release of easily degradable carbon and microbial activity 100
5.1.3. The influence of clay minerals on the microbial biomass and bacterial abundance 101
5.1.4. Linkage between bacterial community structure and clay minerals 102
5.2. Microbial diversity and establishment of microbial communities after a prolonged artificial soil incubation as affected by soil mineralogy 103
5.3. Microbial nutrient turnover in montmorillonite and illite containing artificial soils 105
5.3.1. Nutrient limitation in artificial soils 105
5.3.2. Carbon transformations and functional microbiota involved in overcoming carbon depletion 106
5.3.3. Nitrogen transformation and microbiota driving the nitrogen remobilization 110
5.3.4. Microbial phosphorus turnover and microbiota involved in phosphorus recycling 114
5.4. Artificial soil systems as a model for unraveling soil processes 116
5.5. Potentials and drawbacks of the shotgun metagenomic approach 118
6. CONCLUSIONS AND OUTLOOK 123
7. LITERATURE 125

List of abbreviations

3HP	3-hydroxypropionate
3HP-4HB	3-hydroxypropionate-4-hydroxybutyrate
3-PGA	3-phosphoglycerate
Al	Aluminium
ALP	Alkaline phosphatase
Anammox	Anaerobic Ammonium Oxidation
ANRA	Assimilatory nitrate reduction
AOA	Ammonia-oxidizing archaea
AOB	Ammonia-oxidizing bacteria
ATP	Adenosine triphosphate
BNF	Biological nitrogen fixation
BSA	Bovine serum albumin
C	Carbon
Ca	Calcium
CBHs	Cellobiohydrolases
CEC	Cation exchange capacity
CH	Charcoal
C_{mic}	Microbial carbon
COG	Clusters of Orthologous Groups
CTAB	Hexadecyltrimethylammoniumbromide
DEPC	Diethyl pyrocarbonate
Di-4BH	Dicarboxylate/4-hydroxybutyrate
DM	Dry matter
DMSO	Dimethyl sulfoxide
DNRA	Dissimilatory nitrate reduction
dNTPs	Deoxynucleotides
ECM	Ectomycorrhizal fungi
EGs	Endoglucanases
EPS	Extracellular polysaccharides
Fe	Iron
FH	Ferrihydrite
G3P	Glyceraldehyde-3-phosphate
IL	Illite
KEGG	Kyoto Encyclopedia of Genes and Genomes

LiPs	Lignin peroxidases
MANOVA	Multivariate analysis of variance
Mg	Magnesium
Mn	Manganese
MnPs	Manganese-dependent peroxidases
Mo	Molybdenum
MT	Montmorillonite
N	Nitrogen
NCBI	National Center for Biotechnology Information
NOB	Nitrite-oxidizing bacteria
NSAPs	Nonspecific acid and alkaline phosphatase
OC	Organic carbon
P	Phosphorus
PBS	Phosphate-solubilizing bacteria
PCA	Principal component analysis
PEG 6000	Polyethylene glycol 6000
PERMANOVA	Permutational analysis of variance
P_i	Inorganic phosphorus
P_o	Organic phosphorus
PRK	Phosphoribulokinase
P_{total}	Total phosphorus
qPCR	Quantitative polimerase chain reaction
RHP	Reductive hexulosephosphate
rTCA	Reductive tricarboxylic acid cycle
Ru5P	Ribulose-5-phosphate
RuBisCO	Ribulose-1,5-bisphosphate carboxylase/oxygenase
RuBP	Ribulose-1,5-bisphosphate
SDS	Sodium dodecyl sulfate
SOC	Soil organic carbon
SOM	Soil organic matter
sp.	Epecies
SRA	Sequence read archive
SSA	Specific surface area
TC-DNA	Total community DNA
T-RF	Terminal Restriction Fragment

T-RFLP	Terminal Restriction Fragment Length Polymorphism
V	Vanadium
VP	Versatile peroxidase
WEOC	Water-extractable carbon
WL	Wood-Ljungdahl pathway
x *g*	Relative centrifugal force

List of tables

	Page
Table 1. The list of chemicals used in this study.	27-28
Table 2. The list of primers used in this study.	28
Table 3. The list of kits and master mixes used in this study.	29
Table 4. The list of instruments used in this study.	30
Table 5. Model material (modified from Pronk et al., 2012; Vogel et al., 2014) used for artificial soil preparation. For materials with an unknown particle size distribution, total content (%) is indicated for all unknown components (e.g., -100-).	32
Table 6. The composition of buffers used in DNA/RNA co-extraction.	35
Table 7. The properties of artificial soils (MT and IL) after 842 days of incubation. The manure was added twice. The first addition took place at the beginning of the experiment and the second after 562 days of incubation. The values are shown as mean with a standard deviation of three independent replicates (n = 3). Asterisks indicate significant differences in soil properties between MT and IL as shown by the *t*-test ($P < 0.05$).	57
Table 8. The number of reads and average fragment length per replicate before and after quality trimming and removal of contaminant sequences are shown for both forward and reverse reads.	58
Table 9. Diversity indices based on the phyla and families found in the montmorillonite and illite. All values are shown as mean with a standard deviation of three independent replicates (n = 3).	60

List of figures

Page

Figure 1. The interaction between microorganisms and mineral particles in soil aggregate (modified from Huang et al., 2005). Bacterial cells which are enveloped by extracellular polysaccharides (EPS) interact with clay particles. Silt- and sand-size particles surround the bacteria and clay particles and form pores providing the potential binding site for SOM. The aggregate can be additionally stabilized by the attachment of fungal hyphae to the outer surface of an aggregate. The smaller image depicts the adherence mechanisms of clay minerals to the negatively charged bacterial cells: (i) edge-to-face associations, (ii) electrostatic interactions, and (iii) bridging through cations (M^{n+}). 7

Figure 2. The representation of the short-term carbon cycle (modified from Johnson 2016). The carbon cycle is dependent on autotrophic organisms to fix carbon dioxide (CO_2) into organic carbon (CH_2O) during the photosynthesis and on the respiration of heterotrophic organisms which transform the organic carbon into CO_2, under aerobic conditions. Under anaerobic conditions, organic carbon is converted by heterotrophic organisms into methane during methanogenesis. 12

Figure 3. Representation of nitrogen cycle. Main nitrogen transformation processes are colour-coded. Green arrow – nitrogen fixation; yellow arrows – N mineralization (depolymerisation/ammonification) and assimilation; orange arrows – nitrification; purple arrows – dissimilatory nitrate reduction (DNRA), blue arrows – assimilatory nitrate reduction (ANRA); red arrows – denitrification; black arrows – nitrite/nitrate uptake. 19

Figure 4. Representation of phosphorus turnover in soil (modified from Walbridge 1991). The P transformations (weathering, adsorption/desorption, aggregate formation/destruction, ion exchange) that are mainly mediated by abiotic factors are depicted in black, whereas the P transformations mediated by biotic factors, mainly microorganisms, are colour-coded. Dark green arrow – phosphate uptake by plants; turquoise arrow – plant exudation, green arrows – humus degradation; brown arrows – humus formation; yellow arrow – microbial P turnover; blue arrows – P immobilization; orange arrows - P mineralization. 23

Figure 5. Schematic representation of artificial soil. The first phase represents the period between the first and second manure addition (0-562 days) and the second phase, the period between the second manure addition until the end of the maturation period (562-842 days) (modified from Vogel et al., 2014). 33

Figure 6. Design of the experiment with four artificial soils MT, IL, MT+CH, and IL+FH treated with plant litter (modified from Vogel et al., 2014). 34

Figure 7. The predicted genes involved in the microbial C cycle with corresponding enzymes and KEGG KO numbers. Depicted are the enzymes involved in (A) starch metabolism; (B) pectin metabolism; (C) hemicellulose metabolism; (D) cellulose metabolism; (E) chitin metabolism; and (F) carbon fixation. 42-43

Figure 8. The predicted genes involved in the N cycle with corresponding enzymes and KEGG KO numbers. Different processes involved in the N cycle are colour-coded. Orange arrow – N mineralization and assimilation; light green arrow – N_2 fixation; dark green arrows – nitrification; black arrows – denitrification; purple arrows – dissimilatory and assimilatory nitrate reduction; light blue arrows – uptake of extracellular nitrite and nitrate. 44

Figure 9. The predicted genes involved in microbial P turnover with corresponding enzymes and KEGG KO numbers. Different processes involved in P turnover are colour-coded. Dark blue arrow – organic P mineralization and solubilization; light blue arrow – inorganic P mineralization; green arrow – uptake of organic and inorganic P; red arrow – regulation of P turnover. 44

Figure 10. Share of water extractable organic carbon (WEOC) in natural and artificial soils given as mean values (n = 3) and standard deviation at different time points (day 0, day 7, day 21, and day 63) in (A) natural soil, (B) MT, (C) IL, (D) MT+CH, and (E) IL+FH. Green bars represent soil samples treated with plant litter and blue bars untreated soil samples. Asterisks indicate significant differences in WEOC values where $*P < 0.05$ and $**P < 0.01$. 48

Figure 11. C_{mic} values in natural and artificial soils. Green bars represent C_{mic} in soils treated with litter and blue bars C_{mic} in untreated soils. C_{mic} mean values (n = 3) with standard deviation are shown for different time points (day 0, day 7, day 21, and day 63) in (A) natural soil, (B) MT, (C) IL, (D) MT+CH, and (E) IL+FH. Asterisks indicate significant differences in C_{mic} values where $*P < 0.05$ and $**P < 0.01$. 50

Figure 12. Number of copies of 16S rRNA gene in natural and artificial soils. Green bars represent number of copies of 16S rRNA gene per gram of dry soil in soils treated with litter, while blue bars represent number of copies of 16S rRNA gene in untreated soils. Mean values (n = 3) of number of copies of 16S rRNA gene with standard deviation are shown for different time points (day 0, day 7, day 21, and day 63) in (A) natural soil, (B) MT, (C) IL, (D) MT+CH, and (E) IL+FH. Asterisks indicate significant differences in 16S rRNA copy number where $*P < 0.05$. 52

Figure 13. Results of PCA analysis of T-RF profiles of microbial communities originating from natural soil (Luvisol, from Scheyern, Germany) and artificial soils. T-RFLP was performed on all soils in triplicates (n = 3). (A) natural soil and all artificial soils, and (B) artificial soils. Natural soil and artificial soils with different compositions are depicted with different colours (purple – natural soil, yellow – MT, green – IL, blue – MT+CH, and red – IL+FH), different sampling times with distinct shapes (rhomb – day 0, circle – day 7, triangle – day 21 and square – day 63), and samples treated with litter are depicted with open symbols and untreated with closed symbols. 55

Figure 14. Principal component analysis (PCA) of montmorillonite (MT, n = 3) and illite (IL, n = 3) soil metagenomes (A) and microbiota harbouring genes involved in C (B), N (C), and P turnover (D). (A-D) the first two components based on relative, Hellinger transformed abundance on the family level are shown. Arrows represent families that have the largest influence on metagenome separation. No significant changes between the MT and IL were detected. 62

Figure 15. Relative abundance of prokaryotic families in artificial soils containing MT and IL. Sequences were aligned against the NCBI-nr database and annotated with MEGAN5. Relative abundance was calculated based on the number of all assigned reads. The mean relative abundance with standard deviations (n = 3) of the twenty most abundant taxa is shown. Asterisks indicate significant differences in prokaryotic families between two metagenomes ($P < 0.05$). 64

Figure 16. Relative abundance of prokaryotic families involved in C turnover in artificial soils containing MT and IL. Sequences were aligned against the NCBI-nr database and annotated with MEGAN5. Relative abundance was calculated based on the number of all assigned reads. The mean relative abundance with standard deviations (n = 3) of the twenty most abundant taxa is shown. Asterisks indicate significant differences in prokaryotic families involved in C turnover in artificial soils ($P < 0.05$). 66

Figure 17. Relative abundance of prokaryotic families involved in N turnover in artificial soils containing MT and IL. Sequences were aligned against the NCBI-nr database and annotated with MEGAN5. Relative abundance was calculated based on the number of all assigned reads. The mean relative abundance with standard deviations (n = 3) of the twenty most abundant taxa is shown. 68

Figure 18. Relative abundance of prokaryotic families involved in P turnover in artificial soils containing MT and IL. Sequences were aligned against the NCBI-nr database and annotated with MEGAN5. Relative abundance was calculated based on the number of all assigned reads. The mean relative abundance with standard deviations (n = 3) of the twenty most abundant taxa is shown. Asterisks indicate significant differences in prokaryotic families involved in P turnover in artificial soils ($P < 0.05$). 70

Figure 19. Rarefaction curves based on KO-Ids identified in montmorillonite and illite-containing artificial soils. Depicted is the number of observed KO ID of subsampled KEGG hits where the amount of KEGG hits was randomly chosen from the metagenome for each replicate. 71

Figure 20. Metabolic and functional diversity in artificial soils containing montmorillonite (MT) and illite (IL). Sequences were aligned against the KEGG database and annotated with MEGAN5. Relative abundance was calculated based on the number of all assigned KEGG reads. The mean relative abundance with standard deviations (n = 3) is shown. Asterisks indicate significant differences in metabolic and functional diversity in artificial soils ($P < 0.05$). 72

Figure 21. Relative abundance of enzymes involved in carbon turnover in artificial soils containing MT and IL. Obtained sequences were aligned against the KEGG database and annotated with MEGAN5. Relative abundance was 74

calculated based on the number of reads assigned to the C cycle. The mean relative abundance with standard deviations (n = 3) of predicted genes involved in (A) cellulose, (B) hemicellulose, (C) chitin, (D) starch, and (E) pectin metabolism, and (F) C fixation is shown. Asterisks indicate significantly different ($P < 0.05$) annotated reads in the artificial soils containing MT and IL.

Figure 22. Correlation between the abundance of genes involved in cellulose (*bglX/bglB*, *celB*, *CBH1*), hemicellulose (*abfA*, *gmuG*), chitin (*chiA/CHIT1*, *nagZ/hexA-B/hex*), starch (*amyA*, *SGA1*, *nplT*), and pectin (polygalacturonase) degradation, and carbon fixation (*aclA/aclB*, *coxL/coxM/coxS*, *cooS*, *rbcL/rbcS*), and soil pH, and C:N:P stoichiometry in artificial soils containing (A) MT and (B) IL. Blue colours represent the positive, and red negative correlation. Darker colour and larger circle diameter indicate a stronger correlation. White squares indicate the absence of correlation. Grey squares indicate significant correlation ($P < 0.05$). 76

Figure 23. Relative abundance of prokaryotic families involved in the carbon cycle in the artificial soils containing MT and IL. Obtained sequences were assigned on the functional level by aligning against KEGG, and on the taxonomic level against the NCBI-nr database. Relative abundances were calculated based on the number of reads assigned to the C cycle. The colour intensity in the heatmap represents the relative abundance of families associated with a C cycle in montmorillonite and illite. Twenty most abundant families are depicted. 78

Figure 24. Distribution of shared and unique families involved in the C cycle in the artificial soils containing montmorillonite (MT) and (IL). The reads were functionally assigned with KEGG and taxonomically with the NCBI-nr database. Shown are the mean values of the most abundant families involved in cellulose, hemicellulose, and chitin degradation. Relative abundances were based on the number of all reads assigned to the C cycle. 80

Figure 25. Distribution of shared and unique families involved in the C cycle in the artificial soils containing montmorillonite (MT) and (IL). The reads were functionally assigned with KEGG and taxonomically with the NCBI-nr database. Shown are the mean values of the most abundant families involved in starch, and pectin degradation, and C fixation. Relative abundances were based on the number of all reads assigned to the C cycle. 81

Figure 26. Relative abundance of predicted prokaryotic genes encoding enzymes involved in the nitrogen cycle in artificial soils containing MT and IL. Obtained sequences were aligned against the KEGG database and annotated with MEGAN5. Relative abundance was calculated based on the number of all assigned KEGG reads. Values are shown as the mean with standard deviation (n = 3). Asterisks indicate significant differences ($P < 0.05$) in the number of annotated reads between the MT and IL soils. 83

Figure 27. Correlation between the abundance of genes involved in depolymerisation/ammonification (*ureC/ureB/urea, chiA, pepA, pepN, pip, pepD, clpP, clpX, aguB, hmgL, hutH, CTH, sdaA/sdaB, dsdA, tdcB, echA, cynS,* nitrilase, formamidase), N assimilation (*glnA, gltS/gltD/gltB, gudB, gdhA*), denitrification (*narG/narH/narI*, *narA/narB*, *nirK/nirS*, *norB/norC*, *nosZ*), dissimilatory nitrate reduction (*nirB/nirD*, nrfA/nrfH), assimilatory nitrate reduction (*nirA*, *narB*, *nasA/nasB*), nitrification (*amoB*/*amoC*, *hao*), nitrite and nitrate uptake (*nrt*, *nrtA/nrtB/nrtC/nrtD*), and soil pH, and C:N:P stoichiometry in artificial soils containing (A) MT and (B) IL. Blue colours represent the positive, and red negative correlation. Darker colour and larger circle diameter indicate a stronger correlation. White squares indicate the absence of correlation. Grey squares indicate significant correlation ($P < 0.05$). 85

Figure 28. Relative abundance of prokaryotic families involved in the nitrogen cycle in the artificial soils containing MT and IL. Obtained sequences were assigned on the functional level by aligning against the KEGG database, and on the taxonomic level against the NCBI-nr database. Relative abundances were calculated based on the number of reads assigned to the N cycle. The colour intensity in the heatmap represents the relative abundance of families associated with the N cycle in montmorillonite and illite. Twenty most abundant families are depicted. 87

Figure 29. Distribution of shared and unique families involved in the N cycle in the artificial soils containing montmorillonite (MT) and illite (IL). The reads were functionally assigned using KEGG and taxonomically with the NCBI-nr database. Shown are the mean values of the most abundant families involved in N mineralization, N assimilation, denitrification, DNRA, ANRA, nitrification, and N uptake. Relative abundances were based on the number of all reads assigned to the N cycle. 89-90

Figure 30. Relative abundance of predicted prokaryotic genes encoding enzymes involved in phosphorus turnover in artificial soils containing MT and IL. Obtained sequences were aligned against the KEGG database and annotated with MEGAN5. Relative abundance was calculated based on the number of all assigned KEGG hits and values were shown as mean with standard deviation (n = 3). Asterisks indicate significant differences ($P < 0.05$) in the number of annotated reads between the investigated soils. 92

Figure 31. Correlation between the abundance of genes involved in P regulation (*phoB*, *phoR*), P mineralization (*phoN*, *olpA*, *phoA, phoD, ugpQ, appA,* 3-phytase, *phnW, phnX, phnA, ppa, ppx, phnK, phnL, phnN*), organic P uptake (*phnC, phnD, phone, ugpA, ugpB, ugpC, ugpE*), inorganic P uptake (*pstA*, *pstB*, *pstC*, *pstS*), and P solubilization (*gcd*), and soil pH, and C:N:P stoichiometry in artificial soils containing (A) MT and (B) IL. Blue colours represent the positive, and red negative correlation. Darker colour and larger circle diameter indicate a stronger correlation. White squares indicate the absence of correlation. Grey squares indicate significant correlation ($P < 0.05$). 94

Figure 32. Relative abundance of prokaryotic families involved in phosphorus turnover in the artificial soils containing MT and IL. Obtained sequences were assigned on the functional level by aligning against the KEGG database, and on the taxonomic level against the NCBI-nr database. Relative abundances were calculated based on the number of reads assigned to the microbial P turnover. The colour intensity in the heatmap represents the relative abundance of families associated with a P turnover in artificial soils containing montmorillonite and illite. Twenty most abundant families are depicted. 96

Figure 33. Distribution of shared and unique families involved in the P turnover in the artificial soils containing montmorillonite (MT) and illite (IL). The reads were functionally assigned using KEGG and taxonomically using the NCBI-nr database. Shown are the mean values of the fifty most abundant families involved in P solubilization, mineralization, and uptake. Relative abundances were based on the number of all reads assigned reads. 98

1. INTRODUCTION

Soils are one of the most complex systems and an integral part of terrestrial ecosystems, responsible for maintaining various services including carbon storage, nutrient cycling, and turnover, water dynamics and quality, soil fertility, regulation of aboveground and belowground diversity, biotic regulation, filtering and buffering, and transformation of potentially harmful substances (Haygarth and Ritz, 2009; Paul et al., 2021; Uroz et al., 2015). They consist of different mineral, organic and biological compounds associated in complex hierarchical structures.

Soils develop from the underlying bedrock through a series of complex physical, chemical and biological processes whose rate is determined by various factors, such as climate, bedrock type, time, microorganisms, and plants. Microorganisms may contribute to the weathering of inorganic bedrock by enzymatic reactions, pH reduction, synthesis of agents such as cyanide, oxalate, and gluconic acid, and excretion of siderophores (Cuadros, 2017; Mavris et al., 2010; Napieralski and Roden, 2020; Štyriaková et al., 2012). The progression of mineral weathering is characterized by the release of smaller particles i.e. primary and secondary minerals whose interaction leads to the formation of micro- and macro-aggregates with different physiochemical properties that stabilize the soil organic matter (SOM), thus promoting the development of microhabitats and subsequent spatial allocation of soil microorganisms.

The interaction between microbes and soil constituents, such as clay minerals and organic matter results in the formation of highly reactive interfaces (Kögel-Knabner et al., 2008; Totsche et al., 2018), that represent hotspots of microbial diversity and activity. The size and physicochemical characteristics of the different microhabitats are strongly driven by the initial parent material. The resulting abiotic soil properties and specific surface areas (SSA) strongly determine water and nutrient availability for microbes. Uroz et al. (2015) showed that minerals present in soil play an important role in the biogeochemical cycle. They are ubiquitous in soil and sediments and form a main fraction of SSA, and can therefore be considered as a regulator of cation exchange, and the site of organic matter, nutrient, and pollutant adsorption (Vogel et al., 2014) and as such, greatly influence the survival, activity, and function of microorganisms (Chaerun et al., 2005). However, the size of SSA and the exact adsorption site on the clay mineral depend on the type of clay minerals present in the soil. For instance, in addition to the large external specific area, the swelling clay mineral montmorillonite possesses an additional large internal surface area where water and nutrients can be retained. In contrast, non-swelling illite exhibits only external surfaces and consequently, smaller reactive surfaces (Vogel et al., 2014). Furthermore, Vogel et al.

(2015) have shown that the influence of clay minerals on microbial diversity increases with soil aging, while the influence of metal oxides decreases (Babin et al., 2013; Steinbach et al., 2015).

In addition to mineral composition, other environmental factors, such as nutrient availability, pH, and redox conditions (Lombard et al., 2011) support different microorganisms, hence shaping the microbial community structure and function in soils (Boyd et al., 2007). For example, soils with high nutrient input support the formation of microbial hot spots. The soil-litter interface is an example of a such hot spot where soluble litter compounds are highly available. They are characterized by high microbial activity, growth, and C turnover. In addition, the availability and quality of substrates vary during the decomposition which leads to the succession of microorganisms (Poll et al., 2008). On the other hand, microorganisms play a central role in most biogeochemical transformations and subsequent provision of available carbon (C), nitrogen (N), phosphorus (P), and other nutrients, hence strongly influencing the terrestrial ecosystem services such as the development of plant communities and plant production. Nannipieri et al. (2003) estimated that microorganisms are involved in about 90 % of soil processes. In addition, a large diversity of soil microbiota is still considered a black box (Simon and Daniel, 2011). Hence, the information on the exact number of species in a unit of soil is unknown. Furthermore, most functional traits, such as nutrient cycling and turnover are a result of the close interaction of microbial communities.

The source of important macronutrients in initial soils differs. C and nitrogen (N) are not part of mineral composition and are scarce in initial soils. The potential sources of C include the deposition of allochthonous organic matter, such as plant litter, insects, and cyanobacterial and algae communities (Hodkinson et al., 2003; Stibal et al., 2008). Potential sources of N, on the other hand, include N fixation and deposition (Brankatschk et al., 2011). Thus, the supply of C and N progressively increases with soil maturation (Vitousek et al., 2010). In contrast, phosphorus (P) is part of inorganic bedrock and P mobilization is mostly dependent on mineral weathering. Since it is mainly found in inorganic form adsorbed to the mineral surfaces or in organic form incorporated in biomass or soil organic matter, it frequently acts as a limiting nutrient in terrestrial ecosystems. P availability, in initial soils, is at large the function of microbes in mediating the P distribution between the available pool in soil solution and the total P in the soil through solubilization and mineralization processes (Richardson and Simpson, 2011).

Even though microorganisms are well-established as the driving force behind nutrient cycling and turnover (Bardgett and van der Putten, 2014; Bender et al., 2016; Wagg et al., 2014), the effect of mineral composition on microbial structure, functional diversity, and

subsequent nutrient cycling, especially during soil formation remains unclear. However, the emergence of methods such as high-throughput metagenomic sequencing could not only help identify the main microbial drivers of C, N, and P transformations, but it could also provide a deeper insight into adaptation strategies microorganisms develop to overcome C, N, and P depletion in early stages of soil development.

1.1. Objective and hypotheses of Ph.D. research

Because community structure and function of soil microbiota are constrained by C:N:P ratios of ecosystem and nutrient resources, the ecological stoichiometry can help predict a relationship between soil microorganisms, nutrient availability, and nutrient recycling, as well as possible constraints on biogeochemical processes. Furthermore, stoichiometric ratios in soil regulate how elements, C, N, and P in particular, vary based on different nutrient sources at different levels of the organization including cellular, individual, population, community, at the ecosystem level.

It is known that microbial abundance and function are influenced by the interaction of biotic and abiotic factors. However, the influence of mineral composition on microbial structure, and subsequent macronutrient cycling in the early stages of soil development remains unclear. Furthermore, we aim to identify the main microbial drivers of C, N, and P turnover in oligotrophic terrestrial ecosystems and to gain a deeper insight into the mechanisms related to the early stages of soil formation.

In this respect, the following questions were addressed, and hypotheses were tested in experiments with artificial soil mixtures:

H1: Do different minerals, types of clay minerals in particular, select for specific microorganisms and thus shape distinct microbial communities and activity?

Considering that different clay minerals show different characteristics, variable surface area, and charge, in particular, which influence the nutrient availability, we hypothesize distinct microbial communities will develop according to mineral composition.

H2: How does a prolonged incubation after the last external organic matter addition impact the bioavailable organic matter, nitrogen, and phosphorus content in artificial soil?

Following the consumption of bioavailable nutrients in form of easily degradable carbon compounds, organic nitrogen and external organic phosphorus, and microbial cross-feeding, depletion of bioavailable forms of C, N, and P will develop, with only

recalcitrant forms of C, N, and P remaining in the artificial soil system thus leading to adapted microbial communities.

H3: Which strategies do microorganisms develop to overcome carbon depletion in the early stages of soil development?

Since carbon turnover is the critical step in all ecosystems, soil included, and soil microorganisms play a pivotal role in carbon cycling, a core microbiota, similar to natural ecosystems, and an adaptation of carbon-associated genes will develop.

H4: Which strategies do microorganisms adapt in the early stages of soil development to overcome N and P shortage/limitation?

Considering the bioavailability and expected limited nitrogen and phosphorus concentration after a prolonged maturation, for microorganisms to adapt and survive, they need to develop strategies, such as recycling mineral and organic N and P, as well as an increase in N and P uptake which will be reflected in the soil metagenome.

H5: Will the functional microbiota associated with C, N, and P turnover mostly consist of a generalist or specialists?

Since C, N, and P are crucial macronutrients essential for the survival of microorganisms, the functional microbiota should consist of generalists and highly abundant taxa, with only a few taxa with the potential for driving all processes involved in C, N, or P cycling. Taxa unique for a single artificial soil type with a potential to drive a specific process are expected in a very low abundance.

The objective of this thesis is to investigate the influence of soil mineral composition on bacterial community structure in the early stages of soil development, and subsequently to identify processes and microbial drivers of macronutrient cycling. Since natural ecosystems are extremely complex, it is difficult to detect an exclusive influence of soil mineral composition on microbiota in early soil developmental stages. Hence, simplified artificial soil systems with a well-defined composition where the influence of environmental factors and higher organisms, such as plants are excluded, were selected in this study.

2. LITERATURE REVIEW

2.1. Soils as a basis for life on Earth

Soils are an integral part of terrestrial ecosystems where they play a pivotal role in maintaining ecosystems services such as nutrient cycling and turnover, carbon storage, and turnover, water dynamics, regulation of aboveground diversity, biotic regulation, filtering and buffering, and the transformation of potentially harmful elements and compounds (Haygarth and Ritz, 2009; Paul et al., 2021). A central role in most biogeochemical transformations and the subsequent provision of available carbon (C), nitrogen (N), phosphorus (P), and other nutrients is played by microorganisms. Hence, strongly influencing all terrestrial ecosystem services. On the other hand, soil physical and chemical properties including quantity and quality of soil organic matter (SOM), pH, and redox conditions strongly influence the microbial community structure dynamics and function in soils (Bardgett and Caruso, 2020; Bardgett and van der Putten, 2014; Lombard et al., 2011).

2.1.1. Soil development

Soil is a heterogeneous mixture of different mineral, organic and biological compounds that are associated in complex hierarchical structures. It develops from an underlying inorganic bedrock over a long time through complex physical, chemical, and biological processes between lithology, topography, climate, time, plants, and microorganisms (Egli et al., 2018; Egli et al., 2011). Environmental processes like freezing and thawing, heating and cooling, and abrasion from wind, water, and ice masses, have a strong influence on rock weathering. Although lichens, algae, mosses, fungi, bacteria, and archaea are known to colonize rock and other mineral surfaces, the true extent of their impact on mineral weathering is difficult to quantify. However, several researchers have shown that soil microorganisms can enhance mineral weathering through different mechanisms, including (1) enzymatic oxidation or reduction of mineral components, (2) production of a redox agent, and inorganic and organic acids and consequent local reduction of pH, (3) production of alkali, (4) production of ligand which forms a highly soluble product with a mineral component, (5) production of complexing agents such as cyanide, oxalate and gluconic acid, and (6) excretion of transport vehicles, like siderophores (Cuadros, 2017; Mavris et al., 2010; Napieralski and Roden, 2020; Štyriaková et al., 2012).

Rock weathering processes result in disintegration of rock to smaller particles or chemical transformations. Chemical weathering of rocks can result in precipitation and/or formation of secondary minerals like oxides and clay particles. The rearrangement of those minerals,

flocculation and cementation lead to aggregation (Duiker et al., 2003; Wilpiszeski et al., 2019). Aggregation is strongly driven by SOM, mineral components like metal oxides and hydroxides and clay particles, and microorganisms. SOM represents a nucleus and a binding agent in the formation of aggregates. Metal oxides, metal hydroxides, and clay particles also act as an aggregator, where metal ions form bridges between mineral and organo-mineral particles, and clay. In addition to binding particles together they influence SOM decomposition and turnover (Lavallee et al., 2020; Pronk et al., 2013). SOM, the main factor in the promotion and stabilization of aggregation is susceptible to microbial decomposition. Hence, microbial activity promotes not only the stabilization of soil structures through the production of organic substances capable of binding soil particles, but also destabilizes it by decomposing SOM, making an aggregation a dynamic and perpetual process in soil (Baldock, 2002; Merino-Martín et al., 2021).

Furthermore, weathering of the bedrock contributes to the soil-forming processes by releasing the constituent elements in soluble forms that are available to soil microorganisms and plants (Zaharescu et al., 2020). The bedrock (soil parent material) is initially colonized by organisms capable of photosynthesis and nitrogen fixation which produce organic matter, thus supporting the growth of chemoorganotrophic bacteria and fungi (Meier et al., 2019). Microorganisms, together with various physical processes, further promote the dissolution of bedrock into smaller particles and the formation of cracks in the rocks. With time, the formation of soil particles in the before-mentioned cracks provides the habitat for pioneering plants. Root-bacteria associations between those early plants and soil microorganisms facilitate the nutrient and water supply of plants (Donhauser and Frey, 2018; Schulz et al., 2013). The growth of plant roots furthers the rock fragmentation, and the root excretions increase the microbial abundance and promote the development of microbial activity hotspots in the rhizosphere. As the weathering proceeds the soil depth increases and it becomes able to support more complex and larger organisms. Therefore, soil development is a very complex, dynamic, and long-lasting process, dependent on climatic, various abiotic, and biotic factors, that can take hundreds to thousands of years (Hunt et al., 2021).

2.1.2. The interplay between biota and their abiotic environment in soils

Soil development is characterized by the formation of micro- and macroaggregates with different physicochemical properties which allow the development of microhabitats and subsequent spatial allocation of soil microorganisms. Mineral and organic soil components and microorganisms form a continuous system where all components are constantly in

contact with each other (Figure 1) (Baveye et al., 2018; Cuadros, 2017; Huang et al., 2005; Merino-Martín et al., 2021).

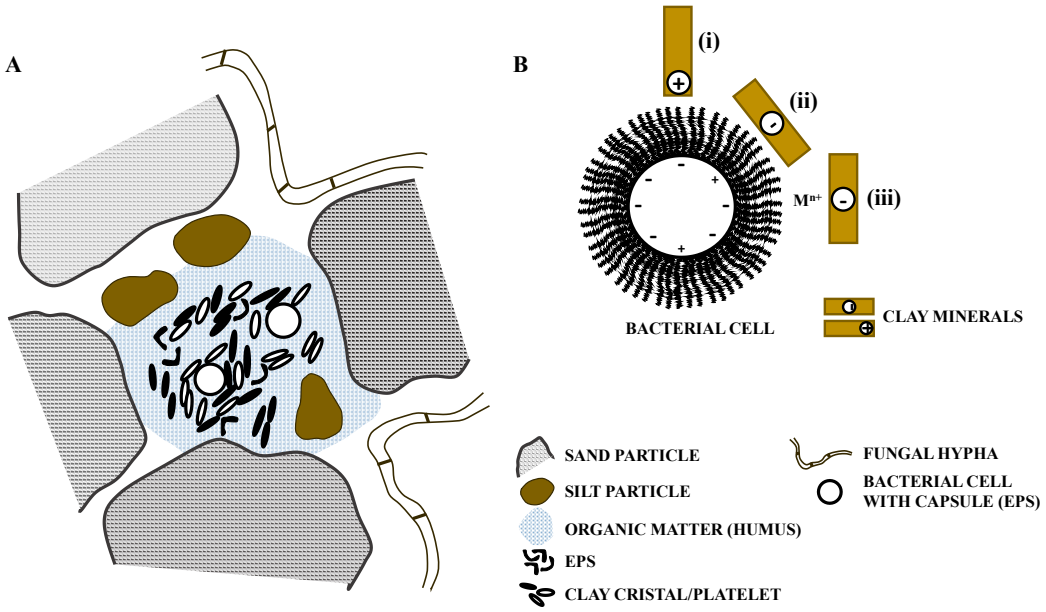

Figure 1. The interaction between microorganisms and mineral particles in soil aggregate (modified from Huang et al., 2005). Bacterial cells which are enveloped by extracellular polysaccharides (EPS) interact with clay particles. Silt- and sand-size particles surround the bacteria and clay particles and form pores providing the potential binding site for SOM. The aggregate can be additionally stabilized by the attachment of fungal hyphae to the outer surface of an aggregate. The smaller image depicts the adherence mechanisms of clay minerals to the negatively charged bacterial cells: (i) edge-to-face associations, (ii) electrostatic interactions, and (iii) bridging through cations (M^{n+}).

The interaction between microbes, minerals, and other soil constituents, such as clay particles and organic matter results in the formation of highly reactive interfaces (Kögel-Knabner et al., 2008; Totsche et al., 2018), that represent hotspots of microbial diversity and activity. Those hotspots are highly structured, heterogeneous, and discontinuous (Stotzky, 1997, Totsche et al., 2018; Vogel et al., 2022).

All minerals show potential for microbial colonization where they act as an attachment site and nutrient source for microorganisms, thus contributing to different soil functions, including nutrient cycling, soil fertility, and water quality (Uroz et al., 2015). The minerals differ according to their nutrient composition, dissolution rate, and subsequent weatherability. Hence, they can be considered as a reactive site for potential cation

exchange. However, it remains unclear if the microbial colonization of mineral surfaces is a random process, if it is controlled by environmental conditions, or by mineral characteristics. Several researchers have shown that mineral colonization is strongly dependent on environmental factors suggesting that the mineral colonization represents an adaptation mechanism where microorganisms colonize different mineral surfaces as a means of protection from unfavorable external factors such as extreme temperatures, pH, irradiation, nutrients availability, and water content (Leinemann et al., 2018; Sun et al., 2020; Wang et al., 2017). For example, both Chan et al. (2012) and Wierzchos et al. (2011) have shown that the establishment of hypolithic communities in the world's major deserts and the microbial colonization of gypsum crust in the Atacama Desert, was dependent on the moisture content, where higher colonization rates were determined in the environment with higher moisture content. Other factors such as the availability of carbon and oxygen (Boeddinghaus et al., 2021; Mauck and Roberts, 2007) influence the microbial colonization of minerals. Ionic strength and pH show a strong effect on surface binding forces with a subsequent increase of bacterial attachment to the mineral surface of microcline and quartz (Scholl et al., 1990; Uroz et al., 2015). Nutrient scarcity has increased the incidence of phosphate-solubilizing bacteria (PBS) in grassland soils with low-P status (Mander et al., 2012) and the incidence of soil bacteria effective in solubilizing minerals (Acidobacteria Gp2 and Alphaproteobacteria) in a less fertile non-pygmy terrace in the Mendocino site (Uroz et al., 2014).

Other researchers have shown that bacterial communities colonize different minerals depending on their characteristics including size, porosity, charge, composition and complexity. Abdulla (2009) investigated granite fragments and showed that actinomycetes preferably colonized minerals with higher porosity. Analyses of different sandstone fractions showed bacterial colonization preferences towards the smallest fractions. Regarding the mineral composition, it was shown that they are poor in carbon and nitrogen, but they may contain essential micronutrients (Certini et al., 2004). Hence, the chemical composition and dissolution rate of minerals can represent an important driver for the selection of distinct microbial communities.

Furthermore, clay minerals in the soil are highly reactive due to their high specific surface area (SSA) and cation exchange capacity (CEC), thus binding not only many organic and inorganic molecules, but binding extracellular microbial enzymes essential for organic matter degradation and nutrient acquisition as well (Turner et al., 2014; Zhang et al., 2019; Zhu et al., 2018a). In addition, different microorganisms play an important role in the dissolution of clay minerals which may result in the increase or decrease of organic carbon (OC) availability, and in the mobilization of essential macronutrients, such as nitrogen (N), and phosphorus (P). All those factors may directly influence the C, N, and P bioavailability

and consequently the C:N:P ratios in soil, thus strongly influencing the biogeochemical processes and elemental turnover and cycling (Wang et al., 2020).

2.2. Nutrient stoichiometry as a driver for microbial activities

The biogeochemical cycling of numerous chemical elements found in soil is essential to maintain multiple ecosystem functions, including soil fertility, plant production, climate regulation, etc. However, it is still unclear how and why multiple-element turnover changes in terrestrial ecosystems depend on soil composition, type and age, environmental factors, vegetation, and climate (Ochoa-Hueso et al., 2021).

It is well established that soil microorganisms and their enzymes have an essential role in regulating the transformation of organic matter, plant litter decomposition and mineralization of associated nutrients, nutrient cycling, primary production, and regulation of greenhouse gas emission (Bardgett and van der Putten, 2014; Bender et al., 2016; Wagg et al., 2014). For example, soil bacteria and fungi break down organic matter by using different hydrolytic and ligninolytic enzymes, thus increasing nutrient bioavailability. Furthermore, soil fauna also contributes to the nutrient cycling by comminution of plant litter and organic soil matter and by grazing on microbial biomass (Maaroufi and De Long, 2020; Medina-Sauza et. al., 2019). However, the physiology of soil microorganisms is highly dependent on environmental factors, such as pH, salinity, C substrate quality, and quantity, which drive the establishment of soil communities. Soil bacterial metabolism and growth are, primarily, limited by water availability, followed by C substrate quality and quantity, and finally by other major nutrient availability and concentrations including N and P.

A growing body of evidence points to the fact that the community structure and function of soil microbiota are constrained by C:N:P ratios of an ecosystem and nutrient resources (Maaroufi et al., 2018; Zechmeister-Boltenstern et al., 2015). Ecological stoichiometry can help predict a relationship between soil microorganisms, nutrient availability, and recycling, as well as possible constraints on biogeochemical processes (Maaroufi and De Long, 2020). Furthermore, stoichiometric ratios in soil regulate how elements, C, N, and P in particular, vary based on different nutrient sources at different levels of the organization including cellular, individual, population, community, at ecosystem levels (Wei et al., 2020). However, microorganisms can maintain their C:N:P ratio independently of the C:N:P ratio of the ecosystem they inhabit and its nutrient sources, meaning, that microbial stoichiometry reflects the degree of their elemental homeostasis (Buchkowski et al., 2019). However, soil microbiota, when faced with nutrient imbalances, often constrain their metabolism, growth, and reproduction which can alter the soil population structure and dynamics, trophic interactions and consequently change key ecosystem processes (Frost et al., 2005).

Therefore, nutrient scarcity might decrease microbial activity and consequently inhibit processes such as soil organic matter decomposition, nitrogen, and phosphorus mineralization (Chen et al., 2014; Liu et al., 2020a; Wang et al. 2022; Zhu et al., 2018b). In contrast, when nutrients sufficiently meet microbial stoichiometric requirements, microbial activities are increased, and all mineralization processes are stimulated (Wei et al., 2020; Wei et al., 2019). When C:N:P ratios are much higher and more variable than C:N:P ratios required by microorganisms, microbial communities often shift in favor of dominant strains associated with a distinct C:N:P stoichiometry in response to nutrient levels, thereby maintaining the microbial biomass C:N:P balance (Cui et al., 2020a; Cui et al., 2020b). In particular, N:P is a dominant driver of cellular growth (Elser et al., 2003; Wei et al., 2020).

The nutrient input affects not only the soil nutrient cycling but also the microbial community structure. For example, several researchers have shown that the addition of N and/or P has changed the microbial diversity and structure in different soils (Ho et al., 2017; Leff et al., 2015; Li et al., 2016a; Luo et al., 2020; Zeng et al., 2016). Yet, the changes in microbial community structure could have been caused by other factors, including nutrient availability, soil pH, temperature, plant diversity, etc. as well (Evans et al., 2014; Zhang et al., 2014; Leff et al., 2015; Li et al., 2016b). Some studies have shown that the alteration in microbial community structure has influenced biogeochemical processes and elemental cycling in soil (Delgado-Baquerizo et al., 2016; Habig and Swanepoel, 2015; Mackelprang et al., 2018), whereas others have shown the existence of functional redundancy in soil microbiota, i.e. other microbial species has taken over the same process which was previously driven by lost species thus negating the impact of altered microbial community structure on ecosystem functioning (Louca et al., 2018). Therefore, understanding how nutrient addition affects the microbial communities and how the potential changes in microbial structure are coupled with the elemental cycling, are essential for predicting C, N, and P cycles.

Furthermore, it is well established, that fresh organic matter input often changes SOM mineralization rates, thus causing positive or negative priming effects (Liu et al., 2017; Zhu et al., 2018b). Since soil microorganisms determine the direction and intensity of soil organic carbon (SOC)/soil organic matter (SOM) mineralization depending on exogenous substrate quantity and quality (Shahbaz et al., 2018; Yuan and Chen, 2015), the change in linked N and P mineralization rate might contribute to the succession from opportunist microorganisms that preferentially utilize labile resources to slow-growing microorganisms that can utilize recalcitrant components. *r*-strategist (copiotrophs) with higher nutrient requirements show lower C:N:P ratios than *K*-strategist (oligotrophs) (Fontaine et al., 2003; Zhou et al., 2018). Hence, the priming effect might be dependent on the interaction between these two microbial functional groups, i.e., copiotrophs decomposing the labile C, and oligotrophs native, recalcitrant SOM (Fang et al., 2018).

Altogether, ecosystem and microbial stoichiometry provide a better understanding of soil organic matter (SOM) decomposition and nutrient cycling such as mineralization and immobilization of soil carbon (C), nitrogen (N), and phosphorus (P) (Kaiser et al., 2014). The interaction between C, N, and P turnover processes is intricate and strongly linked, especially in SOM. SOM dynamics are dependent on the microbial decomposers, responsible for the depolymerization and mineralization of SOM, thus acquiring necessary C, N, and P (Cui et al., 2018). Even though in general, C, N, and P turnover play an important role in soil, and particularly in soil development, the exact interactions, mechanisms, and predominant processes in C, N, and P turnover concerning the C:N:P stoichiometry are still unknown.

2.2.1. Carbon cycle

Carbon, nitrogen, and phosphorus are the macronutrients essential for all living organisms, including microorganisms. C, unlike N and P, is mainly considered as an energy source. In soil, the energy balance and multiple element cycling are governed by ecological stochiometry, where C, N, and P cycles are coupled (Liu et al. 2020a; Wang et al., 2022; Zhu et al., 2018b).

The C cycle consists of the C transfer between the atmosphere, oceans, land, and living organisms. In terrestrial and marine ecosystems C cycle is dominated by photosynthesis, respiration, and organic matter formation (Figure 2).

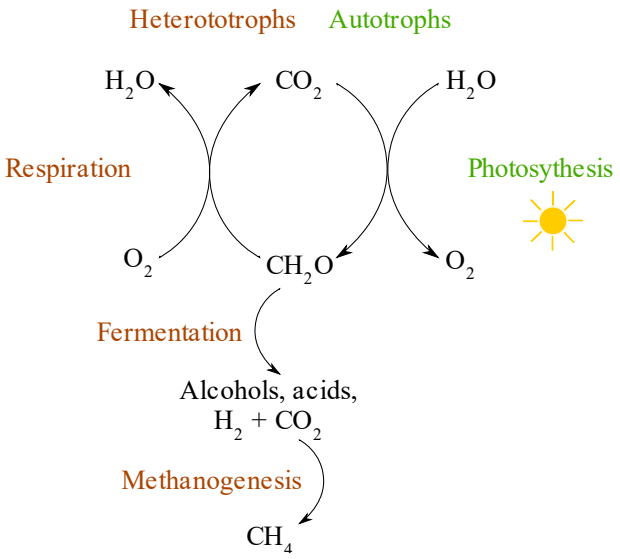

Figure 2. The representation of the short-term carbon cycle (modified from Johnson, 2016). The carbon cycle is dependent on autotrophic organisms to fix carbon dioxide (CO_2) into organic carbon (CH_2O) during the photosynthesis and on the respiration of heterotrophic organisms which transform the organic carbon into CO_2, under aerobic conditions. Under anaerobic conditions, organic carbon is converted by heterotrophic organisms into methane during methanogenesis.

Autotrophic, photosynthesizing plants and chemoautotrophic microorganisms convert inorganic atmospheric carbon dioxide (CO_2) into organic C and deposit it in soil organic matter (SOM) (Lynn et al., 2017; Trumbore 2006). To date, seven carbon fixation pathways, the Calvin-Benson cycle, reductive tricarboxylic acid (rTCA) cycle, Wood-Ljungdahl (WL) pathway, 3-hydroxypropionate (3HP) bicycle, dicarboxylate/4-hydroxybutyrate (Di-4BH) cycle, 3-hydroxypropionate-4-hydroxybutyrate (3HP-4HB) cycle, and reductive hexulosephosphate (RHP) pathway have been discovered in nature (Gong et al., 2018; Kono et al., 2017). The Calvin-Benson, 3HP, and 3HP-4HB cycles occur mainly under aerobic, whereas rTCA, WL, and Di-4HB occur under anaerobic conditions (Gong et al., 2018). The Calvin-Benson cycle is the most widespread carbon fixation pathway, and more than 90% of CO_2 in nature is fixed by plants, algae, and microorganisms using this cycle (Ducat and Silver, 2012). It consists of three parts, carbon fixation, carbon reduction, and ribulose-1,5-bisphosphate (RuBP) regeneration. In the first step, ribulose-1,5-bisphosphate carboxylase/oxygenase (RuBisCO) catalyses the carboxylation of RuBP by CO_2 during which a 6C compound is formed and split into two 3-phosphoglycerate (3-PGA) molecules. The energy needed for this step mainly originates from light, hydrogen, hydrogen sulfide, and sulfur. In the second step, 3-PGA is reduced to glyceraldehyde-3-phosphate (G3P).

And finally, phosphoribulokinase (PRK) catalyses the regeneration of RuBP from ribulose-5-phosphate (Ru5P) (Kono et al., 2017).

Fixed C is released to the atmosphere as CO_2 by heterotrophic microorganisms during the decomposition of organic C of plant, animal, or microbial origin (Liang and Balser, 2011; Lynn et al., 2017) or as methane by archaea during methanogenesis (Lyu et al., 2018). C turnover is closely coupled with the turnover of other elements essential for microbial metabolism, N, and P in particular, and it depends on various environmental factors, such as soil pH, texture, mineral composition, temperature, and water content (Davidson and Janssens, 2006).

Microorganisms and microbial enzymes in soil have a crucial role in breaking down and transforming dead organic material and making it available to other living organisms. One of the main sources of C in the soil is the plant organic matter that originates from above-ground plant litter and its leachates or below-ground root litter and its exudation (rhizodeposition). Rhizodeposition is characterized by a continuous flow of carbon-containing compounds from roots to the soil. Those compounds can be divided into two major groups, easily available and recalcitrant carbon compounds. Simple molecules such as sugars, amino acids, sugar alcohols, organic acids, and more structurally complex secondary metabolites make up the plethora of root exudates and they can be respired and deposited into soil rapidly, within days, or even hours (Witzgall et al., 2021). In contrast, polymers such as lignin, cellulose, and hemicellulose, the typical structural constituents of plant cells (Kögel-Knabner, 2002), represent recalcitrant carbon compounds that need to be depolymerized by extracellular enzymes before they can be taken into the microbial cell and metabolized (Qiao et al., 2019).

Amongst important groups of organisms that participate in carbon cycling are mycorrhizal fungi. They can be divided into two major groups, arbuscular mycorrhizal fungi, obligate symbionts that can only obtain carbon from the host plant, and ectomycorrhizal fungi (ECM), facultative symbionts that can also mineralize organic carbon. It is suggested that up to 30% of total carbon assimilated by plants may be transferred to the fungal partner. The plant carbon that is transferred to the mycelia is then very quickly respired back to the atmosphere (Drigo et al., 2010; Kaiser et al., 2015; Thirkell et al., 2020).

Soil organic matter (SOM) consists of fresh to progressively decomposing plant, microbial, and faunal debris and exudates, and the microbial biomass that is responsible for the primary decomposition of the exudate and detritus (Dungait et al., 2012). It encompasses a series of pools with varying decomposition kinetics, ranging from active pools that can turn over in months to passive pools that can turn over in thousands of years.

The passive pool is composed of recalcitrant constituents whose resistance to decomposition can be attributed to their humified nature. The formation of the humified substances is a result of spontaneous condensation reactions between reactive microbial products and biochemically altered structural biomolecules (Drigo et al., 2010; Wu et al., 2017; Zhang et al., 2018). Some studies suggest that environmental and biological factors may have a far greater influence on the long-term persistence of SOM than the molecular structure of plant litter and the subsequent formation of humus (Tarnocai et al., 2009). It is suggested that SOM persists due to its physical unavailability or inaccessibility to the microbial extracellular enzymes, microorganisms, and the optimal environmental conditions needed for the decomposition due to the entrapment of SOM within soil aggregates and/or sorption to soil mineral phases. Therefore, in addition to the breakdown and release of CO_2 from organic matter, soil microorganisms contribute to the formation of persistent SOM. Also, the soil microorganisms may contribute to the stabilization of soil organic carbon by promoting the formation of microaggregates and the inclusion of SOM within those microaggregates, resulting in physical protection from the decomposition (Merino-Martín et al., 2021; Six et al., 2004).

The breakdown of different carbon sources, especially the breakdown of recalcitrant polymers such as cellulose, hemicellulose, and lignin, the major constituents of plant cells, are dependent on the microbial enzymes.

A majority of the cellulolytic microorganisms belong to bacteria and fungi. Several researchers (Berlemont and Martiny, 2013; Wilhelm et al., 2021) have shown that cellulolytic microorganisms can establish synergistic relationships with non-cellulolytic species. Those interactions can lead to the complete degradation of cellulose to carbon dioxide and water under aerobic conditions, and carbon dioxide, methane, and water under anaerobic conditions.

Microorganisms capable of degrading cellulose produce a plethora of enzymes with different activities and specificity for different types of substrates, which complement each other. For example, cellulases hydrolyze the β-1,4-glycosidic bonds in cellulose. They are divided into two classes, endoglucanases, and cellobiohydrolases. Endoglucanases (endo-1,4-β-glucanases, EGs) hydrolyze internal bonds forming new terminal ends. Cellobiohydrolases (exo-1,4-β-glucanases, CBHs) act on the existing or endoglucanase-generated chain ends. Both classes of enzymes can degrade amorphous cellulose and CBHs can efficiently degrade crystalline cellulose as well. The end product of hydrolysis catalysed by CBHs and EGs is cellobiose. Released cellobiose is then broken down into two glucose molecules by β-glucosidases. The released glucose represents available

carbon and energy sources for cellulolytic and/or other microorganisms present in the environment where cellulose is degraded.

To function correctly, endoglucanases, cellobiohydrolases, and β-glycosidases must be stable under varying environmental conditions, including temperature and pH. For example, the cellulase systems of the mesophilic fungi *Trichoderma reesei* and *Phanerochaete chrysosporium* are glycosylated and show optimum activity at acidic pH (Liu et al., 2021). CBHs act synergistically with EGs to solubilize high molecular weight cellulose molecules. On the other hand, the EGs of thermophilic fungi are thermostable and show optimal activity between 55 and 80 °C, and at pH 5.0–5.5. β-glucosidases show optimal activity depending on their origin and are active at a wide range of pH, from pH 4.1 to 8.1, and temperatures from 35 to 71 °C (Ahmed et al., 2017). The most common and best-studied aerobic cellulolytic bacteria belong to the genera *Cellulomonas*, *Pseudomonas*, and *Streptomyces* (Kameshwar and Qin, 2016; Pathak and Navneet, 2017).

In addition to the aerobic cellulose degradation, about 5-10 % of cellulose is degraded under anaerobic conditions. The cellulose-degrading system of anaerobic microorganisms differs from that of aerobic microorganisms. It is best characterized in *Clostridium thermocellum* where the enzymes are organized into a large cell surface-bound protein complex known as cellulosome (Barth et al., 2018; Ha-Tran et al., 2021). Such organization of cellulolytic enzymes promotes the synergism between catalytic units and positions them at the interface between the cell and the substrate. However, since high temperatures are needed for the growth of these microorganisms and cellulose degradation, their contribution to cellulose degradation in most ecosystems is most likely only marginal. Although several mesophilic cellulolytic anaerobes have been isolated from different ecosystems such as soil, sediments, compost, sewage, and sludge, the majority of well-known anaerobic cellulolytic microorganisms are associated with ecosystems such as rumen where they degrade vast amounts of cellulose (Thapa et al., 2020).

Hemicellulose, another recalcitrant polymer, is a group of linear and branched heterogeneous polysaccharides that are built from different monomeric units and includes xylans, mannans, arabinans, galactans, glucuronoxylans, arabinoxylans, glucomannans, β-glucans, and xyloglucans. Thus, many different enzymes, hemicellulases, are needed to degrade hemicellulose to monomeric sugars and acetic acid (Kameshwar and Qin, 2018). Hemicellulases are classified according to their specificity to different substrates.

The main carbohydrate found in hemicellulose is xylan whose complete degradation depends on the variety of different hydrolytic enzymes including endo-1,4-β-xylanase, which cleaves the β-1,4-glycosidic bond in the xylan backbone thus producing

xylooligosaccharides, and β-xylosidase which releases xylose from xylooligosaccharides. In addition, hemicellulose degradation depends on accessory enzymes such as arabinofuranosidase which removes arabinose side chains, and acetyl xylan esterases that remove acetyl groups from the xylan backbone, and feruloyl and ferulic acid esterases which remove ferulic acid from xylan side chains (Sun et al., 2012).

The complete degradation of mannan-based hemicellulose which includes several subfamilies, linear mannan, glucomannan, galactomannan, and galactoglucomannan, also requires several different enzymes called mannanolytic enzymes. The first step in the degradation is catalysed by β-mannase (endomannases) that randomly cleaves the backbone of mannan-based hemicellulose, and liberates short β-1,4-mannooligosaccharides, such as mannobiose and mannotriose. This is followed by the hydrolysis of β-1,4 bonds in β-1,4-mannosides catalysed by β-mannosidases, during which mannose and mannan oligosaccharides are released. Further, β-glucosidases hydrolyze β-1,4 bonds of 1,4-β-D-glucopyranoses at the non-reducing ends of oligosaccharides released by β-mannase, and finally, α-galactosidases catalyse the removal of galactose residues (Malgas et al., 2015).

Xylanases, the major component of hemicellulases are isolated from many ecosystems with plant material. Also, xylanases have been described in several aerobic bacterial species and some bacteria found in the rumen (Walia et al., 2017). The optimum temperature for xylanases from bacteria and fungi varies from 40 to 60 °C. In general, fungal xylanases are less thermostable than bacterial xylanases. Thermophilic xylanases have been found in Actinobacteria such as *Thermomonospora* and *Actinomadura* (Baruah 2018; Sriyapai et al., 2011; Yu et al., 2021) and hyperthermophilic primitive bacterium *Thermotoga* (Hamid and Aftab, 2019). Xylanases from Actinobacteria are active at pH 6.0–7.0 (Corrêa et al., 2019). In addition, xylanases active at alkaline pH have been isolated from *Bacillus* sp. and *Streptomyces viridosporus* (Khusro et al., 2016; L. Liu et al., 2020b; Raj et al., 2018).

Another important structurally complex, high molecular, insoluble, and thus recalcitrant carbon polymer is lignin. The most efficient lignin degraders belong to the white-rot fungi.

The initial phase of lignin depolymerization depends on the variety of extracellular, oxidative, and unspecific enzymes. During this phase highly unstable products, which further undergo many different oxidative reactions, are released. Two major enzymatic families are involved in ligninolysis, peroxidases, and laccases. In addition, several reductive enzymes, including cellobiose oxidizing enzymes, aryl-alcohol oxidases, and aryl-alcohol dehydrogenases, are important in lignin degradation.

Peroxidases can be divided into two groups, lignin peroxidases (LiPs) and manganese-dependent peroxidases (MnPs). LiPs have a heme group in their active center thatcan catalyse the oxidation of phenolic and non-phenolic compounds, amines, aromatic ethers, and polycyclic aromatics (Singh et al., 2021). MnPs are very similar to LiPs and oxidize Mn (II) to Mn (III) which generates phenoxy-radicals that undergo different reactions, leading to depolymerization. In addition, MnPs can oxidize non-phenolic lignin compounds in the presence of Mn (II) via the peroxidation of unsaturated lipids (Datta et al., 2017). Several researchers have described a versatile peroxidase (VP) involved in lignin degradation, which shows both manganese peroxidase and lignin peroxidase activity (Datta et al., 2017; Liu et al., 2019; Moreira et al., 2007; Pérez-Boada et al., 2005). It catalyses the oxidation of hydroquinone in the absence of exogenous H_2O_2 when Mn (II) is present. Laccases are blue-copper phenoloxidases that catalyse mainly the oxidation of phenolic compounds and non-phenolics in the presence of different mediators (Datta et al., 2017; Vrsanska et al., 2015). The resulting formation of phenoxy-free radicals can lead to polymer cleavage. Laccases are mainly associated with fungi and the main producers of laccases are wood-rotting fungi. In addition, they have also been isolated from other fungi, including *Aspergillus* sp., *Myceliophthora thermophila,* and *Chaetomium thermophilium* (Chukwuma et al., 2020; Viswanath et al., 2014). Also, several researchers have found laccase in different bacterial genera such as *Azospirillum*, *Citrobacter*, *Staphylococcus*, *Bacillus*, *Streptomyces*, and *Thermus* (Abdel-Hamid et al., 2013; Baruah et al., 2018; de Gonzalo et al., 2016). Contrary, Alexandre and Zhulin (2000) have found laccases-like enzymes in bacteria, where they are involved in the polymerization of low molecular weight, water-soluble organic matter from compost, into the high molecular weight products, suggesting their involvement in humification processes.

2.2.2. Nitrogen cycle

Nitrogen (N) is an essential macronutrient without which life is not possible, and is required in the synthesis of most quintessential biological macromolecules, including proteins, nucleic acids, and chlorophyll (Elser et al., 2007). Even though it is the fourth most abundant element in biomass, bioavailable nitrogen, or fixed N, is the proximate limiting nutrient in most of Earth's surface environments (Du et al., 2020). The largest reservoirs of nitrogen on Earth are in the atmosphere in form of an inert dinitrogen gas (N_2) (Johnson and Goldblatt, 2015), followed by non-N_2 nitrogen within the crust and ocean sediments, for example, as ammonium in silicate minerals and clays and as organic N in the soil, sediments and sedimentary rocks (Li et al., 2021a; Zhang et al., 2020). The interchange of unavailable nitrogen and bioavailable nitrogen forms i.e., nitrogen compounds that support

and/or are part of the cellular metabolism is mostly controlled by microorganisms (Stein and Klotz, 2016).

In terrestrial ecosystems, generally, amount of bioavailable N is limited which results in strong competition between microorganisms and plants (Geisseler et al., 2010; Vitousek and Howarth, 1991). Microorganisms have developed different mechanisms for the acquisition, uptake, and assimilation of organic and mineral forms of N, thus enabling them to utilize a wide range of organic and mineral compounds. Here, plant and microbial residues are the two main sources of organic input, while atmospheric nitrogen gas (N_2) represents the main source of inorganic nitrogen in the soil (Kögel-Knabner, 2002; Nicolás et al., 2019). Quantitatively most important organic N-containing molecules are proteins. Proteins alone comprise 60% or more of the N found in soil, plant, and microbial cells (Geisseler et al., 2010).

Nowadays, it is considered that the nitrogen cycle consists of several nitrogen-transformation flows and includes depolymerisation/proteolysis, ammonification, nitrogen fixation, assimilatory (ANRA) and dissimilatory (DNRA) nitrate reduction to ammonia, nitrification, denitrification, anammox (coupled nitrification-denitrification), and nitrite-nitrate interconversion (Stein and Klotz 2016) (Figure 3).

At certain stages, nitrogen can be temporarily taken out of the soil, i.e., assimilated into microbial cells, where it participates in cellular metabolism and is eventually incorporated into organic cellular material, and later returned into the cycle via dissimilation (Nelson et al., 2016). Most of the N assimilation into bacterial biomass occurs via the conversion of NH_4^+ into amino acids glutamine and glutamate which are then used as a source for the synthesis of other amino acids. The conversion of NH_4^+ into glutamine is catalysed by glutamine synthetase (encoded by *glnA*) and glutamate synthase (encoded by *gltS*), whereas the conversion into glutamate is catalysed by glutamate dehydrogenase (encoded by *gudB* and *gdhA*) (Chuckran et al., 2021).

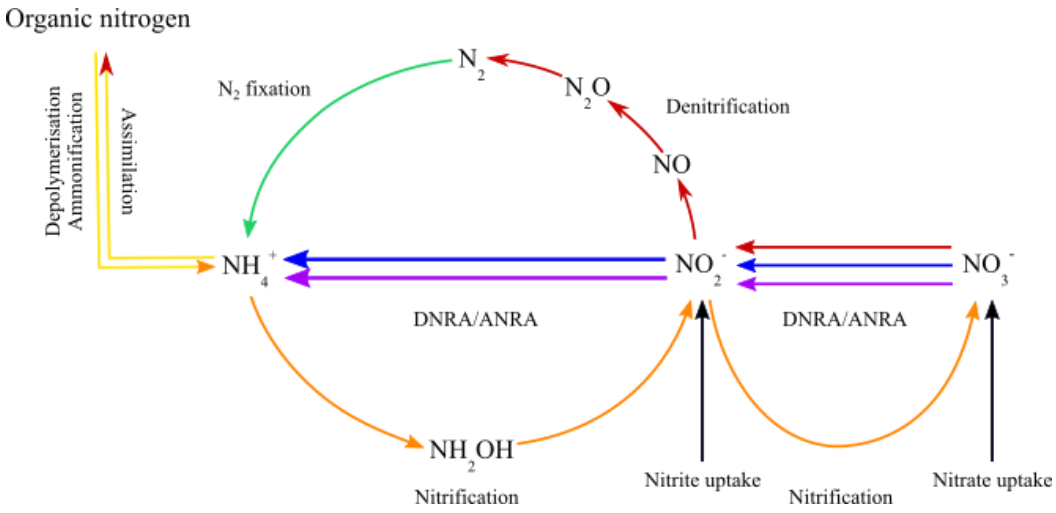

Figure 3. Representation of nitrogen cycle. Main nitrogen transformation processes are colour-coded. Green arrow – nitrogen fixation; yellow arrows – N mineralization (depolymerisation/ammonification) and assimilation; orange arrows – nitrification; purple arrows – dissimilatory nitrate reduction (DNRA), blue arrows – assimilatory nitrate reduction (ANRA); red arrows – denitrification; black arrows – nitrite/nitrate uptake.

Since most of the N in soil is in the form of organic polymers, they have to be broken down into smaller units by extracellular depolymerases (Schimel and Bennett, 2004) such as proteases, and chitinase (Chuckran et al., 2021; Geisseler et al., 2010). Proteases hydrolyse large proteins and polypeptides into peptides and amino acids by catalysing the cleavage of amino acid residues at the N-terminal position of proteins, polypeptides, and peptides. The aforementioned enzymes show wide substrate-specificities and can degrade most non-structural proteins. Also, they are widely distributed amongst prokaryotes and eukaryotes. The most important bacterial proteases include alkaline serine endopeptidase (*gdhA*), subtisilin (*sub*), alkaline (*apr*), and neutral metallopeptidase (*npr*) (Khan et al., 2010; Matkawala et al., 2021).

Chitinases, encoded by *chiA*, on the other hand, hydrolyse the links between N-acetyl-D-glucosamine molecules. They are produced by a wide range of organisms, including bacteria, fungi, and plants. Bacteria produce chitinases mainly to degrade chitin as a source of N and C, whereas in fungi they are important for cell wall development, as well (Sieradzki et al., 2020).

The small organic molecules released by the extracellular depolymerases can then be taken up directly or further mineralized to ammonia or ammonium (NH_4^+) in the process known as ammonification. Ammonification, the second step of organic N mineralization, is a

microbially mitigated process during which low molecular weight, organic molecules with amine or amide groups (-NH_2) are converted into ammonia or its ionic form, ammonium (NH_4^+) (Grzyb et al., 2021). This is mostly a biochemical process catalysed by several groups of enzymes including intracellular deaminase (*codA*, *ade*) and dehydrogenase (*GLUD1*, *GLUD2*) cell surface-bound amino acid oxidase (*aao*), and extracellular urease (*ureA*, *ureB*, *ureC*) (Deng et al., 2020; Fujii et al., 2020). Bacteria and other microorganisms involved in ammonification derive metabolically useful energy from the oxidation of organic N to ammonium. Amongst enzymes responsible for the extracellular ammonification of organic compounds in soil, only the urease has been extensively studied due to the ureas' importance as a fertilizer. Ammonium released during the ammonification is then available to be assimilated and incorporated into amino acids or used for other metabolic purposes. Ammonification is the last step of the nitrogen cycle involving organic compounds and is the intermediary step between the depolymerization of large organic molecules and the nitrification step (Bottomley and Myrold, 2015).

Nitrification, as a part of the microbial nitrogen cycle, involves the conversion of ammonia to hydroxylamine (NH_2OH) catalysed by ammonia monooxygenase (encoded by *amoABC*). NH_2OH is then converted into nitrate (NO_3^-) either directly or indirectly via nitrite (NO_2^-, catalysed by hydroxylamine oxidoreductase HAO encoded by *hao*) (Nelson et al., 2016). Indirect nitrification involves the conversion of ammonia to nitrite by ammonia-oxidizing archaea (AOA) and bacteria (AOB), after which nitrite is subsequently converted into nitrate by nitrite-oxidizing bacteria (NOB) (Francis et al., 2007). Nitrification can occur when ammonia is directly converted into nitrate without the intermediate nitrite step by certain *Nitrospira* species (Pjevac et al., 2017). Nitrate and nitrite can also be assimilated by archaea, bacteria, and fungi as cellular nutrients at these points (Nelson et al., 2016). Additionally, nitrate can be reduced back into ammonium anaerobically in a process known as dissimilarity nitrate reduction to ammonium (DNRA). Even though it was thought that DNRA is primarily performed by prokaryotes (Giblin et al., 2013) some research has shown it can also occur in fungi (Rütting et al., 2011). The final stages of the microbial nitrogen cycle involve returning nitrogen gas to the atmosphere which can be achieved through two distinct pathways, denitrification, and anammox (Francis et al., 2007; Nelson et al., 2016). The anammox pathway combines ammonia and nitrate transforming these compounds into nitrogen gas (Francis et al., 2007). Anammox can be performed by a deep branching group of five bacterial genera which belong to the phylum Planctomycetes (Van Teeseling et al., 2015). Anammox bacteria appear to be highly abundant in freshwater and marine environments (Francis et al., 2007), though the process has also been detected in agricultural soils, wetland soil, and forest ecosystems (Xi et al., 2016). Denitrification

involves the conversion of nitrate (NO_3^-) into nitrogen gas (N_2) through several intermediary steps via nitrite (NO_2-), nitric oxide (NO), and nitrous oxide (N_2O) (Francis et al., 2007) by certain chemolithoautotrophic bacteria and possibly archaea (Clark et al., 2012). The denitrification process has been found under both aerobic and anaerobic conditions (Marchant et al., 2017) in both terrestrial and aquatic environments (Seitzinger et al., 2006).

Acquisition of N from inert atmospheric nitrogen gas (N_2) is achieved via biological nitrogen fixation (BNF), and its transformation into ammonia (NH_4^+), an intensely energy-requiring and oxygen-sensitive process (Bellenger et al., 2020). This process is carried out by a small but diverse group of specialized archaea and bacteria called diazotrophs, which can be found in both terrestrial and marine environments (Boatman et al., 2017; Regan et al., 2017). Those microorganisms harbour the nitrogenase complex which catalyses the N_2 reduction to ammonia. The nitrogenase is made up of two metalloproteins, the molybdenum Mo-Fe protein (dinitrogenase) encoded by *nifD* and *nifK* genes, and Fe protein (dinitrogenase reductase) encoded by the *nifH* gene. There are three biochemically different forms of nitrogenase with different metallic-containing cofactors, either molybdenum (Mo), vanadium (V), or iron (Fe) associated with the catalytic site. Mo-nitrogenase is found in all diazotrophs. V- and Fe- nitrogenases, on the other hand, are mostly found in free-living bacteria and cyanobacteria. When N_2 reduction is catalysed by Mo-nitrogenase, two ATP molecules are needed for each electron that is transferred from nitrogenase reductase to the active site of dinitrogenase, and henceforth to the N_2 molecule. Also, N_2 reduction is tightly coupled with H_2 production from H^+ at the nitrogenase active site (Harris et al., 2020). Hence, Mo-nitrogenase requires 16 molecules of ATP, in total, to reduce one molecule of N_2 to two ammonia molecules. Alternative nitrogenase, V- and Fe- are less efficient at room temperature, and require 24 and 40 ATP molecules, respectively, to reduce a single N_2 molecule (Bottomleey and Myrold, 2015). BNF-produced ammonia becomes bioavailable and can be assimilated by plants, archaea, bacteria, and fungi, and used for the biosynthesis of amino acids and other cellular components (Nelson et al., 2016).

2.2.3. Phosphorus turnover

Phosphorus is an essential macronutrient that has a structural and functional role in all living organisms. It is a component of macromolecules such as phospholipids and nucleic acids and it plays an important role in storing and transferring biochemical energy.

Phosphorus is considered one of the most limiting and difficult to obtain macronutrients in soil, thus, together with nitrogen, it represents an element that most often limits biological productivity. Unlike nitrogen and carbon, it is primarily rock-derived. At the beginning of the pedogenesis, it is scarce and mainly depends on the composition of the underlying bedrock. With the progression of rock weathering the initial content of phosphorus in soil increases, and it mainly depends on the solubilization of inorganic phosphorus forms. In time, it is followed by the mineralization of organic phosphorus. The mineralization and solubilization of P are attributed to different microbial hydrolytic enzymes, such as non-specific phosphatases, phosphatases, and C-P lyases (Rodríguez et al., 2006), and the excretion of organic acids. In addition, microorganisms can, directly or indirectly, increase the orthophosphate ions in soil solution or mobility of organic P (Brito et al., 2020; Seeling and Zasoski, 1993).

Phosphorus can be present in the soil in several different forms depending on the soil's physical and chemical properties. Mainly, it occurs in a form of inorganic phosphates and organic phosphate derivates which vary in solubility and availability. Hence, they form different P-pools. Phosphorus transformation processes can be divided into biological and geochemical transformations (Figure 4), where the mineralogical composition and transfer between P-pools are primarily mediated by microorganisms and abiotic factors, respectively (Hou et al., 2019; Walbridge 1991).

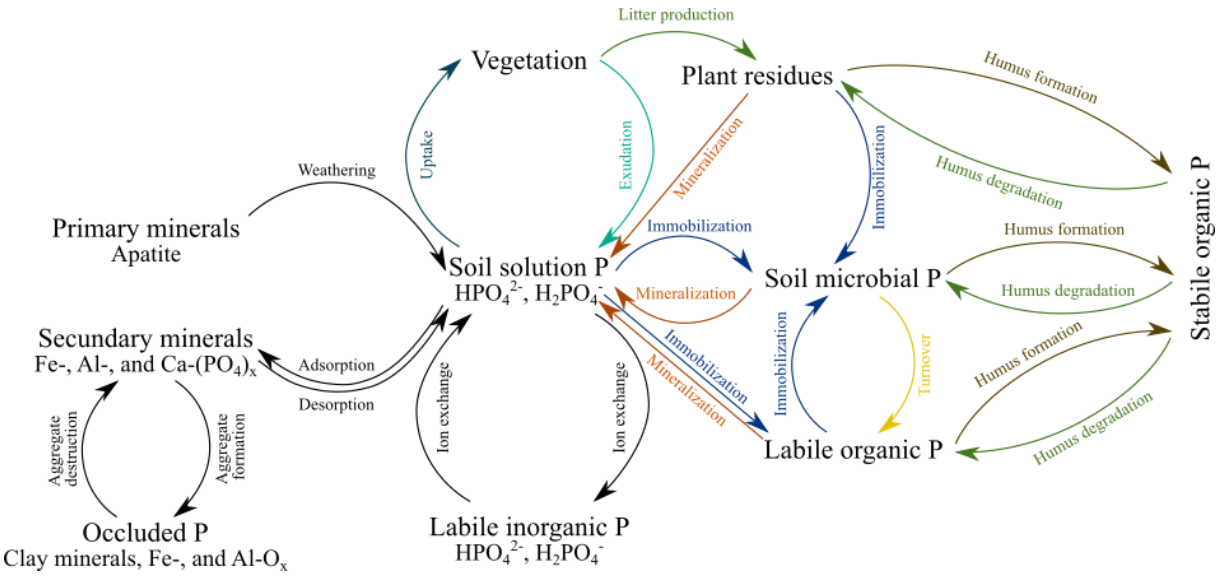

Figure 4. Representation of phosphorus turnover in soil (modified from Walbridge 1991). The P transformations (weathering, adsorption/desorption, aggregate formation/destruction, ion exchange) that are mainly mediated by abiotic factors are depicted in black, whereas the P transformations mediated by biotic factors, mainly microorganisms, are colour-coded. Dark green arrow – phosphate uptake by plants; turquoise arrow – plant exudation, green arrows – humus degradation; brown arrows – humus formation; yellow arrow – microbial P turnover; blue arrows – P immobilization; orange arrows - P mineralization.

In the early phases of soil development mineral-P represents the dominant form. Depending on the soil pH, part of the P is adsorbed to clay minerals, such as aluminum (Al) and iron (Fe) oxides, or calcium (Ca) and magnesium (Mg) carbonates. With time this leads to the increase of secondary mineral-P fraction, Al-, Fe-, Ca- and Mg-phosphates. Another significant portion of P adsorbs to the organic complexes in soil-forming an organic-P pool. Organic-P is mainly stable and highly diverse, comprising phosphoesters, phosphonates, polyphosphates, orthophosphate, inositol phosphates, etc.

Although the P levels in the soil increase with time, it remains one of the most inaccessible macronutrients in the soil. Firstly, this is because only a small part of organic-P, a fraction originating from microbial biomass, is biologically active. Microorganisms and plants can uptake only a small fraction directly after cell lysis and P release into the soil solution. The remaining organic-P released in such way is quickly stabilized in the soil matrix by adsorption on mineral components, and it becomes part of the labile, biologically unavailable, organic-P pool. Secondly, plants can uptake only soluble mineral-P from soil solution which is quickly depleted in the majority of soils. Biologically available P in soil solution can be replenished from the labile-P pool. The extent to and rate at which this is

possible depends on the size of and extent of release of P from the labile-P pool into the soil solution. At the same time, the labile-P pool depends on the mineralization of organic-P and desorption of P from oxides and release from primary and secondary P minerals (George et al., 2018; Hou et al., 2016; Shen et al., 2011). Finally, formation of occluded-P, encapsulation of P by soil minerals, makes it insoluble and hence unavailable to biological degradation and plant and microorganism uptake (Schubert et al., 2020; Vitousek et al., 2010).

During the soil development C and N content in soil increases, while P content decreases, P most often becomes the limiting step for ecosystem functions (Čapek et al., 2018; Vitousek et al., 2010). Although microorganisms compete with plants for P by incorporating it into their biomass and making it temporarily unavailable for the plants, they are indispensable in P and other macro- and micronutrient cycling processes in soil. When incorporated in microbial biomass, P is protected from adsorption to the soil minerals and other soil constituents and leaching. In addition, the microorganism can accelerate the transfer of inorganic-P into the soil solution and mobilize P from organic- and inorganic-P pools. Finally, highly dynamic microbial biomass releases P back into soil solution in response to various environmental factors. Such P is biologically active and easily available for plant uptake. Consequently, microorganisms can be considered a cornerstone for soil fertility and subsequent sustainable plant production.

The microbial role in nutrient cycling relies on the synthesis and excretion of enzymes. Microbial mobilization of P is mainly dependent on various hydrolytic enzymes that can mobilize P either from organic- or inorganic-P. The main enzymes involved in the mobilization of organic-P are classes of nonspecific acid and alkaline phosphatase (NSAPs), whereas pyrophosphatase and the exopolyphosphatase use inorganic-P as a substrate. Several nonspecific acids and alkaline phosphatase (NSAPs and ALP, respectively) are phosphodiesterases, in other words, they catalyse the breakage of ester and anhydride bonds in phosphoric acids (Nannipieri et al., 2011; Ragot et al., 2016). Three classes (A, B, C) of bacterial nonspecific acid phosphatases (NSAPs) encoded by genes *phoN*, *aphA,* and *olpA*, respectively (Ragot et al., 2016; Rossolini et al., 1998) and three families (PhoA, PhoD, PhoX) of alkaline phosphatases (ALPs), encoded by the genes *phoA*, *phoD* and *phoX* (Monds et al., 2006) are known. The occurrence of phosphatase activity depends on the soil pH, with NSAP dominating in acidic and ALP in alkaline soils.

Although NSAP and ALP are the main enzymes that continuously degrade organic-P content in soils, other types of phosphodiesterases (UgpQ, PhnP) with the same activity are known. The main substrate for UgpQ are glycerol diesters. It catalyses the hydrolysis of glycerophosphoryl diesters into glycerol-3-phosphate (G3P) and the corresponding

alcohols. On the other hand, the phosphodiesterase PhnP is part of the carbon-phosphorus (C-P) lyase which degrades various soil organophosphonates into alkanes and a phosphate group by breaking chemically inert C-P bond (McGrath et al., 2013; Stosiek et al., 2020). In addition, microorganisms mobilize P from inorganic-P species such as polyphosphate (poly-P) by inorganic pyrophosphatase (*ppa*) (Keasling et al., 1993; Müller et al., 2019).

Another major group of microorganisms important in the P cycle is phosphate-solubilizing bacteria (PSB) that convert insoluble rock phosphates into soluble forms through acidification, chelation, and exchange reactions. Illmer and Schinner (1995) suggested that organic acid production in *Aspergillus niger* may be an important mechanism for solubilizing aluminium phosphates. In contrast, they also showed that other organisms, such as *Penicillium aurantiogriseum* and *Pseudomonas* sp. effectively solubilize aluminum or calcium phosphates without the production of organic acids. They proposed ammonium assimilation as a possible mechanism. On the other hand, organic acids produced by plant roots and associated microorganisms may act as chelating agents which form complexes with Ca, Fe, or Al resulting in the release of phosphates into the soil solution. However, the exact mechanisms of phosphate solubilization remain uncertain and may be organism-dependent (Rawat et al., 2021; Rodriguez et al., 2006).

2.3. Artificial soils as a tool to study soil development

Important insights into soil development, the formation of biogeochemical interfaces, and pedogenetic processes were mostly gained by studying chronosequences in the field (Dümig et al., 2012; Mikutta et al., 2019; Qiao et al., 2021; Schaaf et al., 2011; Schurig et al., 2013; Yang et al., 2021). However, since such studies include analyses of soils in natural environments, the interpretation of results can be difficult due to the variability of climatic conditions, biotic and abiotic factors, unclear history of the soil development, and natural heterogeneity of underlying parent material and environmental conditions.

Understanding how soil biota and their abiotic environment interact and evolve, as well as the controlling factors and kinetics of various processes, is a key to understanding soil development and soils themselves (Brevik et al., 2015; Vos et al., 2013). Hence, in such studies, it is often difficult to separate the effects of specific factors, for example, mineralogy, nutrient availability, or microbiota, on soil formation and to identify and quantify their relative importance.

Therefore, simplified artificial soil-like model systems represent a valuable toolbox in studying natural soil development. Careful design of laboratory experiments with well-characterized and predefined variables performed under controlled laboratory conditions

can target and isolate specific processes in simplified systems allowing easy manipulation of the parameters of interest. Such artificial model systems were first introduced by Hallsworth and Crawford (1965) in experimental pedology.

The value of such model systems in studying and better understanding soil-forming processes for specific soil types was recognized long ago (Bockheim and Gennadiyev 2009; Egli et al., 2021; Porder, 2019). The majority of artificial soil experiments have been designed to investigate a single factor or a limited number of soil properties and functions. In addition, several artificial soil incubation experiments were specifically designed to study the formation of active biogeochemical interfaces and the interplay between physicochemical and biological processes during the early stages of pedogenesis (Pronk et al., 2012; Vogel et al., 2014). Those experiments aimed to study the effect of mineral composition on the formation of biogeochemical interface and understand the aggregate formation as well as microbial processes affecting it. Currently, it is accepted that the microaggregates and organo-mineral associations result from direct interactions between minerals, organic matter, and microbes stabilized by small-dimensioned organic compounds, whereas macroaggregates formation is affected by the roots and fungal hyphae, which act as binding agents between particles separated by greater distances or pores (Egli and Mirabella, 2021; Six et al., 2004). Therefore, experimental approaches linking micro- and macro-aggregation can help gain deeper insight and understanding of mechanisms and factors affecting the early phases of soil development.

Altogether, carefully designed artificial soils may be used as a model system, representing an early phase of soil development. Hence, a well-designed artificial soil with pre-determined mineral composition is an excellent tool for this research, allowing to study the effect of clay minerals aggregation dynamics on the availability of major macronutrients in soil, C, N, and P, and the consequent effect on bacterial abundance, diversity, and its functional potential. Furthermore, such system enables, an in-depth phylogenetic and functional study of the microbiota in relation to soil mineralogy, as well as the prediction and reconstruction of C, N, and P turnover processes prevailing in the early stages of pedogenesis.

3. MATERIALS AND METHODS

3.1. Materials

3.1.1. Chemicals

The chemicals used in this study are listed in Table 1.

Table 1. The list of chemicals used in this study.

Chemical	Manufacturer
Agarose	Biozym Scientific GmbH, Hessisch Oldendorf, Germany
Bovine serum albumin (BSA)	Sigma-Aldrich Chemie GmbH, Taufkirchen, Germany
Calcium chloride ($CaCl_2$)	Merck KgaA, Darmstadt, Germany
Chloroform/isoamyl alcohol	Carl Roth GmbH + Co, Karlsruhe, Germany
Hexadecyltrimethylammoniumbromide (CTAB)	Sigma-Aldrich Chemie GmbH, Steinheim, Germany
Diethyl pyrocarbonate (DEPC)	AppliChem GmbH, Darmstadt, Germany
Dimethyl sulfoxide (DMSO)	Sigma-Aldrich Chemie GmbH, Taufkirchen, Germany
Deoxynucleotides (dNTPs)	Fermentas, Vilnius, Lithuania
Ethanol	Merck KgaA, Darmstadt, Germany
Ethidium bromide solution	Sigma-Aldrich Chemie GmbH, Steinheim, Germany
Formamide	Fisher Scientific GmbH, Schwerte, Germany
Isopropanol	AppliChem GmbH, Darmstadt, Germany
Dipotassium hydrogen phosphate (K_2HPO_4)	Serva Electrophoresis GmbH, Heidelberg, Germany
Potassium dihydrogen phosphate (KH_2PO_4)	AppliChem GmbH, Darmstadt, Germany
β-mercaptoethanol	Sigma-Aldrich Chemie GmbH, Steinheim, Germany
Magnesium chloride ($MgCl_2$)	Fermentas, Vilnius, Lithuania
MspI and Buffer Tango with BSA	Fisher Scientific GmbH, Schwerte, Germany
Sodium chloride (NaCl)	Merck KgaA, Darmstadt, Germany
Sodium hydroxide (NaOH)	Merck KgaA, Darmstadt, Germany

Table 1. The list of chemicals used in this study – continued.

Chemical	Manufacturer
Phenol/chloroform/isoamyl alcohol	Carl Roth GmbH + Co, Karlsruhe, Germany
Polyethylene glycol 6000 (PEG 6000)	Serva Electrophoresis GmbH, Heidelberg, Germany
Sodium dodecyl sulfate (SDS)	Fisher Scientific GmbH, Schwerte, Germany
TE buffer	AppliChem GmbH, Darmstadt, Germany
Tris-HCl	Merck KgaA, Darmstadt, Germany

3.1.2. Oligonucleotides

All oligonucleotides used in this study were provided by Metabion International AG (Planegg, Germany). The primers were synthesized with a scale of 0.02 µmol, purified by HPLC and their quality was checked with mass spectrometry. The primers were acquired lyophilized, and the stock solution of each primer (100 µM) was prepared by adding sterile nuclease-free DEPC-water according to the manufacturers' instructions. The primers used in this study are listed in Table 2.

Table 2. The list of primers used in this study.

Target gene	Primer set	Sequence	Amplicon size	Reference
16S rRNA	27f	5'-6-FAM-AGAGTTTGATCCTGGCTCAG-3'	~ 1.4 kb	Lane, 1991
	1401r	5'-CGGTGTGTACAAGACCC-3'		
16S rRNA	FP 16S	5'-GGTAGTCYAYGCMSTAAACG-3'	263 bp	Bach et al., 2002
	RP 16S	5'-GACARCCATGCASCACCTG-3'		

3.1.3. Kits and master mixes

The kits and master mixes used in this study are listed in Table 3.

Table 3. The list of kits and master mixes used in this study.

Kit	Manufacturer
Agencourt AMPure XP beads	Beckman Coulter Inc., Brea, California, USA
Agilent DNA 7500 kit	Agilent Technologies GmbH & Co, Waldbronn, Germany
High Sensitivity DNA kit	Agilent Technologies GmbH & Co, Waldbronn, Germany
MapMarker 1000	Eurogentec, Köln, Germany
MiSeq Reagent Kit v3	Illumina Inc., San Diego, California, USA
NEBNext Multiple Oligos for Illumina (Index Primers Set 1)	New England BioLabs LtD., Hitchin, UK
NEBNext High Fidelity Master Mix	New England BioLabs LtD., Hitchin, UK
NEBNext Ultra DNA Library Prep kit for Illumina	New England BioLabs LtD., Hitchin, UK
NucleoSpin Gel and PCR Clean-up kit	Macherey-Nagel GmbH&Co. KG, Düren, Germany
NucleoSpin Genomic DNA from Soil Kit	Macherey-Nagel GmbH&Co. KG, Düren, Germany
Lysing Matrix E tubes	MP Biomedicals, France
Power SYBR Green PCR Master Mix	Life Technologies LTD, Warrington, UK
Quant-iT^{TM} Picogreen dsDNA assay kit	Life Technologies Corporation, Eugene, Oregon, USA
TopTaq DNA Polymerase kit	Qiagen GmbH, Hilden, Germany

3.1.4. Instruments

The instruments used in this study are listed in Table 4.

Table 4. The list of instruments used in this study.

Instrument	Manufacturer
ABI 3100 Genetic Analyzer System	Applied Biosystems Inc, Foster City, California, USA
ABI 7300 Real Time PCR System	Applied Biosystems Inc, Foster City, California, USA
Agilent 2100 Bioanalyzer	Agilent Technologies GmbH & Co. KG, Waldbronn, Germany
E220 Focused-ultrasonicator	Covaris Inc., Woburn, Massachusetts, USA
Elemental analyzer Euro EA 3000	Hekatech, Wegberg, Germany
Liquid chromatography coupled with stable isotope ratio mass spectrometry MAT 253	Thermo Fisher Scientific, Dreieich, Germany
Precellys® 24 homogenizer	Bertin technologies, Montigny-le-Bretonneux, France
MiSeq System	Illumina Inc., San Diego, California, USA
Nanodrop ND-1000 Spectrophotometer	PeqLab Biotechnologie GmbH, Erlangen, Germany
Pippin Prep	Sage Science, Beverly, Massachusetts, USA
PeqStar 96x PCR cycler	PeqLab Ltd, Fareham, UK
SpectraMax Gemini EM Spectrofluorometer	Molecular Devices GmbH, Ismaning, Germany
Total organic carbon analyzer TOC-5050	Shimadzu, Tokyo, Japan
UV-VIS spectral photometer Specord®200	Analytik Jena AG, Jena, Germany

3.2. Methods

The following experiments were the base for this research:

(i) preliminary screening of bacterial abundance and diversity in artificial soils with different mineral compositions (montmorillonite (MT), illite (IL), montmorillonite+charcoal (MT+CH), and illite+ferrihydrite (IL+FH)) based on qPCR and T-RFLP analysis

(ii) an in-depth study of microbial diversity in MT and IL based on a metagenomic shotgun approach

(iii) an in-depth study of functional genes involved in carbon, nitrogen, and phosphorus turnover, as well as major taxa driving aforementioned processes based on a metagenomic shotgun approach

This combined approach will allow a better understanding of microbial diversity and functional potential of artificial soils microbiome, a model for early stages of soil development, in relation to the type of clay minerals (MT and IL). In addition, it will enable the reconstruction of major processes and taxa involved in nutrient (C, N, and P) turnover.

3.3. Preparation of artificial soils[1] and experimental design

3.3.1. Preparation and maturation of artificial soils

Four artificial soils with different mineral compositions, containing montmorillonite (MT), illite (IL), montmorillonite+charcoal (MT+CH), and illite+ferrihydrite (IL+FH) in nine independent replicates totaling 500 g were prepared (Vogel et al., 2014). To achieve a similar texture all mixtures contained 40-42% sand-sized (>63 µm, Quartz Sand Haltern, H33), 52-54 % coarse and medium silt-sized (6.3-63 µm, Millisil W11H), and 6% fine silt and clay (<6.3 µm, Quarzwerke GmbH, Frechen, Germany).

Each mixture contained an additional component:

(i) MT – 6.3% montmorillonite (Ceratosil WG, Süd-Chemie AG, Moosburg, Germany)

(ii) IL – 8.0% illite (Inter-ILI Mérnöki Iroda, Hungary)

(iii) MT+CH – 4.3 % montmorillonite and 2.0 % charcoal, where charcoal was prepared from commercial barbeque charcoal by grounding and sieving to 63 – 200 µm

(iv) IL+FH – 7.0% illite and 1.0% ferrihydrite, where ferrihydrite was synthesized under laboratory conditions according to Schwertmann and Cornell (1991)

Detailed information on the model materials and artificial soil composition can be found in Table 5.

[1] All artificial soils preparation and treatments were performed by Dr Cordula Vogel (Chair of Soil Science, Technical University of Munich, Freising-Weihenstephan, Germany).

Table 5. Model material (modified from Pronk et al., 2012; Vogel et al., 2014) used for artificial soil preparation. For materials with an unknown particle size distribution, total content (%) is indicated for all unknown components (e.g., -100-).

Model component	Texture			CEC	C	N	SSA
	Sand (%)	Silt (%)	Clay (%)	(cmol kg^{-1})	(mg g^{-1})	(mg g^{-1})	(BET–N_2 m^2 g^{-1})
Quartz sand	100				0.05	0.01	0.1
Silt-sized quartz	6	94			0.05	0.01	1
Montmorillonite	8	25	67	85.97	2.38	0.01	71
Illite		50	50	16.65	0.18	0.16	40
Ferrihydrite		-100-			3.50	3.40	247
Charcoal	100				750	3.8	45

At the beginning of the experiment, each batch of 500 g of artificial soil was inoculated with a water-extractable inoculum from the Ap horizon of a Luvisol (from Scheyern, Germany) and dry and sterilized manure (4.5 wt %, OC content of 338.5 ± 6.9 mg g^{-1}, N content of 30.7 ± 1.6 mg g^{-1}, C/N ratio 11.0 ± 0.4) sieved to <2 mm. The manure was sterilized by repeated autoclaving at 121 °C over four weeks. The microbial inoculum was prepared by shaking soil with gravel and demineralized water (ratio 1:1:9) for 2 h. The suspension was then centrifuged for 12 min at 1000 x *g*. The supernatant was centrifuged again for 30 min at 3470 g. The obtained precipitate was resuspended in demineralized water in a ration of 1:10 and 500 g of artificial soil was inoculated with 30 ml of prepared suspension. The batches were incubated in the dark environment at 20 °C, having water content of 60% of the maximum water holding capacity for 842 days. After the initial wetting with 0.01 M $CaCl_2$ solution to provide a soil solution with an ionic strength typical for soils, artificial soils were moistened weakly with water followed by gentle mixing to ensure homogenous water distribution and to avoid disruption of micro- and macro-aggregates formed in artificial soil mixtures. To replenish depleted nutrients and overcome nutrient limitations for microbial growth, fresh organic matter in form of sterile manure (4.5 wt %, OC content of 165.4 ± 2.7 mg g^{-1}, N content of 11.5 ± 0.2 mg g^{-1}, C/N ratio 14.4 ± 0.2) sieved to <2 mm was reapplied on day 562 (Figure 5).

First, at the end of maturation, MT, IL, MT+CH, and IL+FH soils were treated and incubated with plant litter as described in Chapter 3.3.2 and used in a preliminary screening of bacterial diversity and abundance based on 16S rRNA T-RFLP (Chapter 3.5.3) and qPCR analysis (Chapter 3.5.2), respectively. In addition, the dynamics of water-extractable carbon (WEOC) and microbial biomass (C_{mic}), were determined in all soils used in the preliminary experiment as described in Chapter 3.5.1. The main goal of preliminary screening was to assess the effect of different clay minerals and to identify the clay minerals with the greatest effect on

bacterial diversity and abundance which would then be used for in-depth metagenomic analysis.

Second, the artificial soils prepared by 842 days long incubation, were stored at -20 °C until the main experiment, which included the determination of total organic carbon (OC), N, and P, and shotgun metagenomic analyses of microbial diversity, functional genes, and major taxa harbouring genes involved in carbon, nitrogen and phosphorus turnover in soils with the strongest influence as shown by preliminary screening.

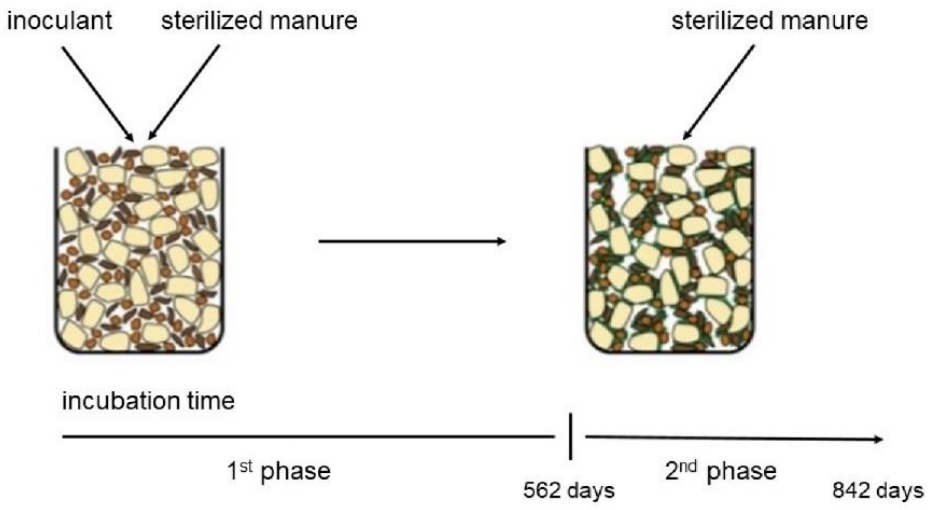

Figure 5. Schematic representation of artificial soil. The first phase represents the period between the first and second manure addition (0-562 days) and the second phase, the period between the second manure addition until the end of the maturation period (562-842 days) (modified from Vogel et al., 2015).

3.3.2. Treatment of MT, IL, MT+CH, and IL+FH soils with plant litter

To evaluate the effect of different clay minerals on the bacterial diversity and abundance, as well as on WEOC and C_{mic} dynamics, the matured MT, IL, MT+CH, and IL+FH soils were treated with plant litter, as a part of preliminary screening.

Briefly, at the end of the 842 days of incubation artificial soils were homogenized, sieved to <2 mm, and mixed with plant litter (<200 µm) derived from maize (*Zea mays*) and potato (*Solanum tuberosum*) leaves mixed in a 1:1 ratio. The plant litter was characterized by 404.2 ± 1.8 mg g^{-1} soil of organic C, 23.3 ± 0.0 mg g^{-1} soil of N, and a C/N ratio of 17.3 ± 0.1. For this experiment, 35 g of the artificial soil was homogenized with 0.350 g of plant litter in three independent replicates. The controls, soil columns without plant litter addition, were

set up in the same way as soil columns treated with plant litter. Additionally, the Ap horizon of Luvisol used to generate the microbial inoculum was used as natural soil material and was set up and treated in the same way as artificial soils. All soil columns were then incubated for 63 days at 14 °C in the dark and at 60 % maximum water-holding capacity. The soil columns were watered every 2 days with distilled water, to maintain the constant water content. For each soil, three soil columns were taken at four different time points: 2 hours directly after litter addition (day 0), and after 7, 21, and 63 days (n=24). The overview of the experimental setup is depicted in Figure 6.

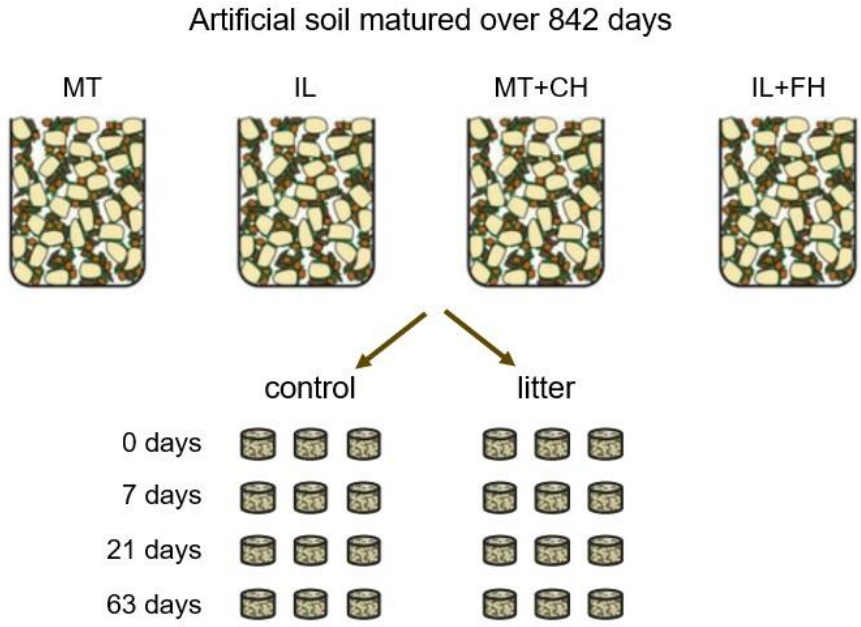

Figure 6. Design of the experiment with four artificial soils MT, IL, MT+CH, and IL+FH treated with plant litter (modified from Vogel et al., 2015).

The soil samples for the preliminary experiment were stored at -80 °C until further analysis.

3.4. Nucleic acid extraction

The MT, IL, MT+CH, and IL+FH soil samples treated with plant litter were stored at -80 °C until the DNA extraction. The total DNA/RNA from artificial soil samples treated with plant litter for preliminary screening of bacterial diversity and abundance was extracted according to the modified protocol described by Töwe et al. (2011). The composition of buffers (Solution A-E) used in the nucleic acid extraction is shown in Table 6.

Table 6. The composition of buffers used in DNA/RNA co-extraction.

Buffer	Composition	Concentration
Solution A	Hexadecyltrimethylammoniabromide (CTAB)	0.27 M
	NaCl	0.7 M
	ß-mercaptoethanol	10 ml/l
	K_2HPO_4	0.94 M
	KH_2PO_4	0.06 M
Solution B	Phenol:chloroform:isoamyl alcohol (pH 8.0)	25:24:1 (v/v/v)
Solution C	Chloroform:isoamylalkohol	24:1 (v/v)
Solution D	Polyethylene glycol 6000 (PEG 6000)	10 % (v/v)
	NaCl	1.2 M
Solution E	Ethanol	70 %

In brief, the total DNA/RNA was co-extracted from 0.35-0.50 g of a soil sample to Lysing Matrix E tubes (MP Biomedicals, France) and mixed with 0.5 ml of Solution A and 0.5 ml of Solution B. The cells were lysed in Precellys®24 Homogenizer (Bertin Technologies, Montigny-le-Bretonneux, France) by a single bead-beating step at 5.5 m s^{-1} for 30 s followed by centrifugation at 16,000 x*g* for 5 min at 4 °C. The aqueous supernatant containing nucleic acids was purified by mixing with an equal amount of Solution C and centrifugated at 16,000 x *g* for 5 min at 4 °C. The resulting aqueous supernatant was again mixed with an equal amount of Solution C. After the repeated centrifugation (16,000 x *g*, 5 min, 4 °C) the resulting aqueous phase was mixed with 1 volume of Solution D and incubated on ice for 2 h. Samples were then centrifuged at 16,000 x *g* for 10 min at 4 °C. The supernatant was discarded, and the precipitated nucleic acid pellet was centrifuged again at 16,000 x*g* for 2 min to remove all remaining supernatant. The nucleic acid pellet was washed with ice-cold Solution E, and centrifuged at 16,000 x*g* for 10 min at 4 °C. All remains of Solution E were discarded, and the nucleic acid pellet was air-dried and re-suspended in 50 µm of pure, nuclease-free DEPC-water. Afterward, the nucleic acid concentration was determined with a nanodrop ND-1000 (PeqLab Biotechnologie GmbH, Erlangen, Germany) at 260 nm and stored at -80 °C until further analysis.

Although the quality, purity, and quantity of DNA obtained by Töwe et al. (2011) were sufficient for bacterial diversity and abundance analysis it was not the case for shotgun metagenomics analysis. Therefore, DNA for the in-depth shotgun metagenomic analysis of MT and IL artificial soils was extracted by using NucleoSpin Genomic DNA from Soil Kit (Macherey-Nagel GmbH&Co. KG, Düren, Germany) according to the manufacturers' instructions, such to achieve quality, purity, and quantity of DNA needed for the sequencing.

For in-depth metagenomic analyses of microbial diversity, gene pattern, and taxa harboring genes involved in C, N, and P turnover, three randomly selected batches of each composition (MT and IL), stored at -20 °C until the DNA extraction, were selected for further analyses. Total community DNA (TC-DNA) was extracted from 0.5 g of each replicate using NucleoSpin Genomic DNA from Soil Kit (Macherey-Nagel GmbH&Co. KG, Düren, Germany) according to the manufacturers' instructions. To optimize the DNA yield 700 µl of lysis buffer SL2 and 150 µl of enhancer SX were used, and the bead beating step using Precellys® 24 Homogenizer (Bertin Technologies, Montigny-le-Bretonneux, France) was performed twice (5.5 ms^{-1}, 30 s). DNA quality was checked on the agarose gel and with a nanodrop, ND-1000 (PeqLab Biotechnologie GmbH, Erlangen, Germany) and quantified on a SpectraMax Gemini EM Spectrofluorometer (Molecular Devices GmbH, Ismaning, Germany) using the Quant-iT™ Picogreen dsDNA Assay Kit (Life Technologies Corporation, Eugene, Oregon, USA) and stored at -20 °C until further analysis.

3.5. Preliminary screening of bacterial diversity and abundance in artificial soils

To determine which soil minerals have the greatest impact on bacterial diversity and abundance the preliminary screening based on 16S rRNA T-RFLP and qPCR was performed on MT, IL, MT+CH, and IL+FH artificial soils treated with plant litter (Chapter 3.3.2). In addition, the dynamics of water-extractable carbon (WEOC) and microbial biomass (C_{mic}), were monitored.

3.5.1 Determination of microbial biomass (C_{mic}) and water-extractable carbon (WEOC) in MT, IL, MT+CH, and IL+FH artificial soils[2]

As a part of the preliminary screening experiment, microbial biomass (C_{mic}) and water-extractable carbon (WEOC) were monitored in MT, IL, MT+CH, and IL+FH artificial soils pre-incubated with plant litter. Microbial biomass (C_{mic}) was determined by the fumigation-extraction method described by Vance et al. (1987). Approximately 5 g of fresh soil was weighed into two separate glass containers. One container was fumigated in a desiccator under a chloroform atmosphere for 24 hours. Both vessels were mixed and shaken with 25

[2] The microbial biomass (C_{mic}) and water-extractable carbon (WEOC) analyses were conducted by Franz Buegger (Helmholtz Zentrum München, Germany) and the results were described in detail by Vogel et. al (2015).

ml 0.01 M $CaCl_2$ solution for 45 min. The supernatant was separated by filtration (4-7 µm, Watman 595½, Bruchsal, Germany). Supernatants were then used for the determination of water-extractable carbon (WEOC). WEOC was measured by the Total organic carbon analyzer TOC-5050 (Shimadzu, Tokyo, Japan) according to Joergensen (1996).

WEOC was calculated according to the formula (1):

$$\text{WEOC [µg g}^{-1}\text{ DM]} = \frac{\text{c (carbon) x } D_f}{\text{m (soil) DM}} \quad (1)$$

where c(carbon) corresponds to the carbon concentration of water-soluble carbon in the non-fumed extracts expressed in mg l^{-1} and Df to the dilution factor 20.

The C_{mic} was calculated according to the formula (2):

$$C_{mic}\text{[µg g}^{-1}\text{ DM]} = \frac{WEOC_f - WEOC_{nf}}{k_{EC}} \quad (2)$$

where WEOC is the total carbon in fumigated (f) and non-fumigated (nf) samples, and κ_{EC} equals 0.45 (Joergensen, 1996).

The effects of mineral composition and litter addition on the WEOC and C_{mic} values were tested by multivariate analysis of variance (MANOVA) using R package “vegan” (Oksanen et al., 2015).

3.5.2. qPCR analysis of pre-incubated artificial soil treated with plant litter[3]

To monitor the changes in bacterial abundance in artificial soils with different mineral compositions after the litter addition, 16S rRNA gene copy numbers were quantified using an ABI 7300 Real Time PCR System. The 16S rRNA gene was amplified by 16S rRNA primers FP 16S (5’-GGTAGTCYAYGCMSTAAACG-3’) and RP 16S (5’-GACARCCATGCASCACCTG-3’) described by Bach et al. (2002) and Power SYBR Green

[3] The qPCR and T-RFLP experiments were conducted by Nicolas Weithmann as a part of his Master Thesis.

PCR Master Mix (Life Technologies LTD, Warrington, UK). The final concentration of the reagents in each of the 25 µl final reaction volumes was as follows: 1x SYBR Green PCR Master Mix, 0.4 µM of each primer, 0.06 % BSA, and 2 µl of DNA. Prior to the qPCR, the DNA was diluted to 1:32 to minimize the amplification inhibition. To enable the 16S rRNA gene quantification a standard of known concentration was prepared by transforming a 16S rRNA gene originating from *Clavibacter michiganensis* into *Escherichia coli*. Samples were amplified using the following program: 95 °C for 10 min, followed by 40 cycles of 95 °C for 20 s, 57 °C for 30 s, and 72 °C for 45 s, and a final and dissociation step of 95 °C for 15 s, 60 °C for 30 s and 95 °C for 15 s. The data were collected at each elongation step (72 °C for 45 s) (Gomes et al., 2001).

The statistical analysis of qPCR was performed in the R environment version 3.0.2 (R Core Team, 2013). The impact of artificial soil mineral composition and litter addition on the bacterial abundance was tested by multivariate analysis of variance (MANOVA) using R package “vegan” (Oksanen et al., 2015).

3.5.3. Terminal Restriction Fragment Length Polymorphism (T-RFLP) analysis of pre-incubated artificial soil treated with plant litter[3]

To determine which clay mineral or combination of minerals has the greatest influence on bacterial diversity a preliminary screening based on 16S rRNA T-RFLP was performed on MT, IL, MT+CH, and IL+FH soils.

A near full-length bacterial 16S rRNA gene fragments were amplified using the universal primers 27f with a 5′ end-labeled with 6-carboxyfluorescein (6-FAM-5′-AGAGTTTGATCCTGGCTCAG-3′) and unlabelled primer 1401r (5′-CGGTGTGTACAAGACCC-3′) (Lane, 1991). The final concentration of the reagents for each 50 µl reaction was as follows: 1x Taq PCR buffer, 2.5 mM $MgCl_2$, 0.2 mM of each dNTP, 0.2 µM of each primer, 2.5 U Top*Taq* DNA polymerase (Qiagen GmbH, Hilden, Germany), 0.06 % BSA, DMSO and 20 ng of DNA template. Samples were amplified using the following program: 94 °C for 5 min, followed by 35 cycles of 94 °C for 1 min, 57 °C for 1 min and 72 °C for 1.5 min, and a final extension step at 72 °C for 10 min (Gschwendtner et al., 2015). The correct amplicon size was checked after gel electrophoresis (80 V, 60 min) on agarose gel (2%) stained with ethidium bromide. The amplification products were then purified with NucleoSpin Gel and PCR Clean-up kit (Macherey-Nagel GmbH&Co. KG, Düren, Germany) according to the manufacturer’s instructions and quantified with a nanodrop ND-1000 (PeqLab Biotechnologie GmbH, Erlangen, Germany) at 260 nm. An amount of 300 ng purified PCR products were digested with the restriction enzyme *Msp*I

(Fisher Scientific GmbH, Schwerte, Germany) in a 20 µl reaction. The digests were incubated in a water bath at 37 °C for 4 h and then in a heating block at 80 °C for 20 min to deactivate the restriction enzyme. Digested PCR products were purified using NucleoSpin Gel and PCR Clean-up kit (Macherey-Nagel, GmbH&Co. KG, Düren, Germany). Purified digests were resuspended in formamide and MapMarker 1000 standard (Eurogentec, Köln, Germany) mixed in a 500:1 ratio. The digests were then denatured by heating at 95 °C for 2 min and separated with capillary electrophoresis on an ABI 3100 Genetic Analyzer System (Applied Biosystems Inc, Foster City, California, USA) (Gschwendtner et al., 2015).

The T-RFLP profiles were evaluated using Peak Scanner Software v. 2.0 (Applied Biosystems Inc, Foster City, California, USA), where fragments smaller than 50 bp were excluded to avoid primer-induced signals. Noise removal and peak alignment were performed using the online software T-REX (Culman et al., 2009). Noisy peaks were filtered by using a standard deviation multiplier for fluor B of 0.8 and peaks were aligned across the sample using the peak aligning algorithm with a clustering threshold of 1.0 bp (Gschwendtner et al., 2015). The resulting data matrices were analysed by calculating the Bray-Curtis coefficient and principal component analysis (PCA) using “vegan” R package (Oksanen et al., 2015). Significant differences were determined by permutational multivariate analysis of variance (PERMANOVA).

Based on the T-RF fingerprints two artificial soil mixtures, MT and IL were selected for shotgun metagenomic analyses.

3.6. In-depth analyses of microbial diversity, functional genes, and microbiota involved in carbon, nitrogen, and phosphorus turnover

3.6.1. Measurements of pH, organic carbon, nitrogen, and phosphorus concentrations[4]

The pH, organic carbon (OC), total nitrogen, and different phosphorus (bioavailable phosphorus (P_{NaHCO3}), total P (P_{total}), stable inorganic P (P_i), and organic P (P_o)) concentrations were measured in artificial soil (MT and IL) at the end of the incubation period of 842 days. The pH was measured potentiometrically in the solution of soil samples and 0.01 M $CaCl_2$ mixed in a 2.5:1 ratio (Gruba and Mulder, 2015). The OC and total N

[4] OC content, total N and phosphorus concentrations were measured by Dr Cordula Vogel (Chair of Soil Science, Technical University of Munich, Freising-Weihenstephan, Germany) and the results were published by Vogel et al., 2014 and Tanuwidjaja et al., 2021, respectively.

content were measured in grinned soil samples using an elemental analyzer Euro EA 3000 (Hekatech, Wegberg, Germany) in duplicates (Zimmermann et al., 2007). The bioavailable phosphorus (P_{NaHCO3}) was extracted from 4 g of dry soil by adding 40 ml of 0.5 M $NaHCO_3$. The stable P pools, including P_{total}, $P_{i,}$ and P_o were measured by the ignition-acid extraction method as described by Saunders and Williams (1955). To determine the P_i 0.5 g of dry soil was extracted with 25 ml 0.5 M H_2SO_4 before and to determine the P_{total} after the ignition at 550 °C. In both H_2SO_4 extracts, the molybdate-reactive P was measured photometrically with UV-VIS spectral photometer Specord®200 (Analytik Jena AG, Jena, Germany) using the molybdenum-blue method. All measurements were done in technical triplicates. The P_o was calculated as the difference between P_{total} and P_i.

The significant differences in pH, OC, total N and P, bioavailable P, P_i and P_o were determined by an unpaired *t*-test, with *P*-values adjusted by the Bonferroni test.

3.6.2. Library preparation and high-throughput metagenomic sequencing

After 842 days of maturation, the total DNA was extracted from the artificial soils containing MT and IL as described in chapter 3.4. The extracted DNA was used for the preparation of shotgun metagenomic libraries as described by Michas et al. (2017).

In brief, from each sample, 2 µg of DNA were fragmented using the E220 Focused-ultrasonicator (Covaris Inc., Woburn, Massachusetts, USA) with the following settings: peak instrument power 175 W, duty factor 10 %, 200 cycles per burst, treatment time 100 s. Fragmented DNA was purified with Agencourt AMPure XP beads (Beckman Coulter Inc., Brea, California, USA) and the fragment size was assessed by Agilent Bioanalyzer 2100 (Agilent Technologies GmbH & Co. KG, Waldbronn, Germany) using Agilent DNA 7500 Kit (Agilent Technologies GmbH & Co. KG, Waldbronn, Germany). Six metagenomic libraries were prepared from 100 ng DNA per library using NEBNext Ultra DNA Library Prep Kit (New England BioLabs LtD., Hitchin, UK) according to the manufacturers' instructions with a single modification – a 10-fold dilution of NEBNext Adaptor for Illumina with a final concentration of 1.5 µM was used for adaptor ligation. In the final enrichment, PCR libraries were indexed using the NEBNext Multiplex Oligos for Illumina (Dual Index Primers Set 1; New England BioLabs LtD., Hitchin, UK). PCR reaction contained 2.5 µl of each indexed primer, 25 µl of NEBNext High-Fidelity 2x PCR master mix, and 20 µl of adapter-ligated DNA. PCR cycling consisted of initial denaturation at 98 °C for 30 s; 6 cycles of denaturation at 98 °C for 10 s, annealing at 65 °C for 30 s and extension at 72 °C for 30 s; and a final extension at 72 °C for 5 min. Metagenomic libraries were electrophoretically size-selected on Pippin Prep (Sage Science, Beverly, Massachusetts, USA) with the setting "range mode"

to select for 300-580 bp. The final libraries were checked for size using Agilent Bioanalyzer 2100 (Agilent Technologies GmbH & Co. KG, Waldbronn, Germany) and Agilent High Sensitivity DNA Kit (Agilent Technologies GmbH & Co. KG, Waldbronn, Germany) and quantified with Quant-iT™ PicoGreen dsDNA Assay Kit (Life Technologies Corporation, Eugene, Oregon, USA). Replicate libraries were diluted to 2 nM each and pooled. The pooled samples were denaturated with 0.2 N NaOH, diluted to 10 pM, and spiked with 2.5 % (v/v) PhiX.

Paired-end sequencing was performed on the MiSeq system (Illumina Inc., San Diego, California, USA), using MiSeq® 2 x 300 cycle V3 kit (Illumina Inc., San Diego, California, USA), following standard Illumina sequencing protocol. The obtained sequences were deposited to NCBI Sequence read archive (SRA) under the accession number PRJNA 556907.

3.6.3. Bioinformatics and statistical analysis[5]

Raw sequences were processed following the protocol described by Vestergaard et al. (2017) with a few modifications. Any remaining adaptor sequences read shorter than 50 bp and read with a Phred score < 15 were removed from the dataset using AdapterRemoval v2 (Schubert et al., 2016). Since an improvement in accuracy is already achieved with trimming at the Phred score > 5 a less aggressive trimming approach was chosen to avoid the unnecessary read loss (MacManes, 2014). Further processing included the removal of PhiX sequences using DeconSeq version 0.4.3 (Schmieder and Edwards, 2011).

For the taxonomic annotation, high-quality fasta sequences were aligned against the NCBI non-redundant (nr) protein sequences using DIAMOND (version 0.5.2) (Buchfink et al., 2015) with default settings. Sequences were aligned against the KEGG database (June 2011) (Kanehisa and Goto, 2000) by using DIAMOND with default settings to get the functional annotation. Blastn results were mapped and taxonomically and functionally annotated with MEGAN5 (version 5.6.5) (Huson et al., 2011). Mapping files dated October 2014 and the following parameters: Min Score = 50, Top Percent = 10, Min Support = 1, Min Complexity = 0 were used.

Sequences of enzymes with corresponding KO numbers involved in carbon, nitrogen, and phosphorus turnover were extracted from the functionally annotated dataset obtained from

[5] The pipelines for bioinformatic analyses of the shotgun metagenomic sequencing were developed by Dr Gisle Vestergaard (Department of Biology, University of Copenhagen, Denmark).

the KEGG database and taxonomically annotated by using DIAMOND against NCBI non-redundant (nr) protein sequences database.

In total, 45 predicted genes involved in C, 82 in N, and 42 in P turnover were investigated. The investigated genes, together with corresponding enzymes and genes and KO numbers are shown in figures 7-9.

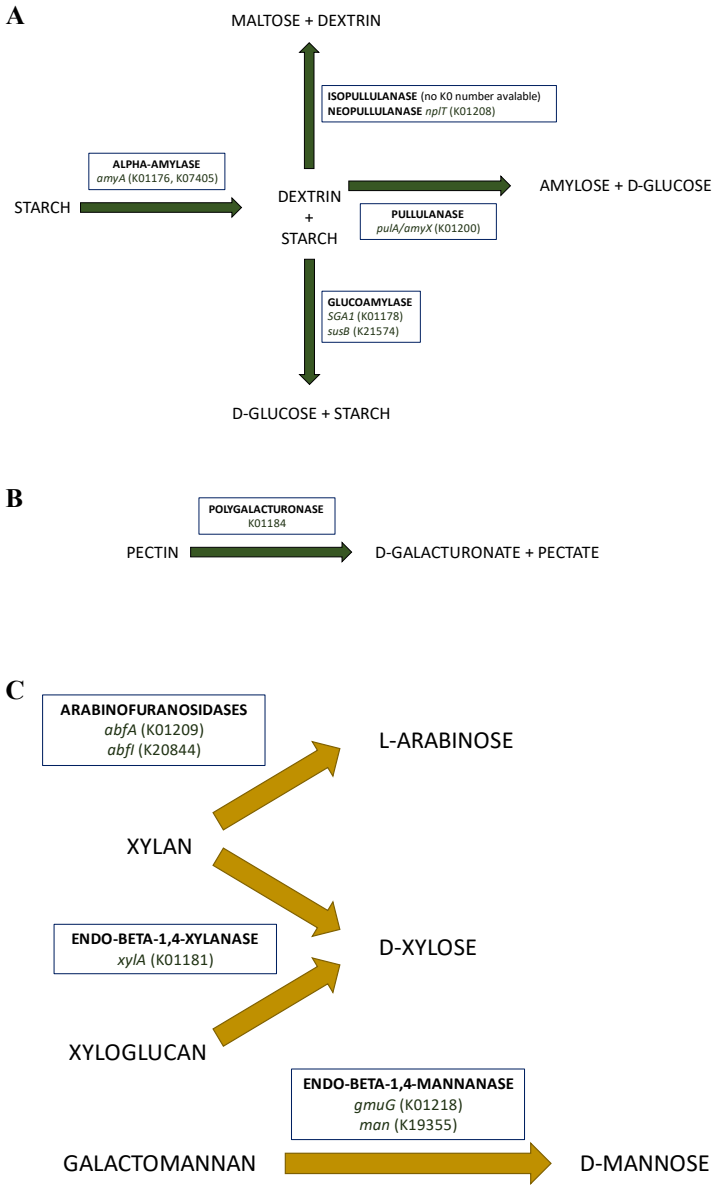

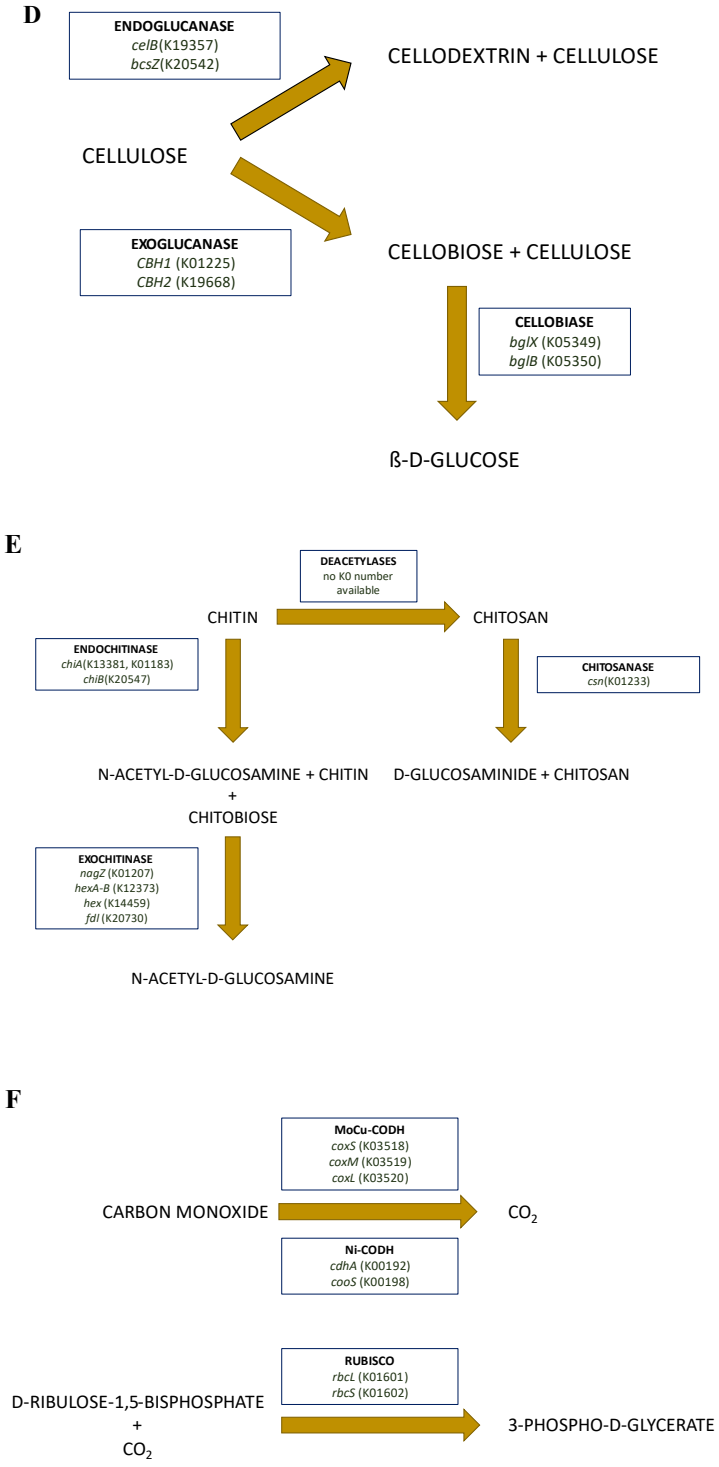

Figure 7. The predicted genes involved in the microbial C cycle with corresponding enzymes and KEGG KO numbers. Depicted are the enzymes involved in (A) starch metabolism; (B) pectin metabolism; (C) hemicellulose metabolism; (D) cellulose metabolism; (E) chitin metabolism, and (F) carbon fixation.

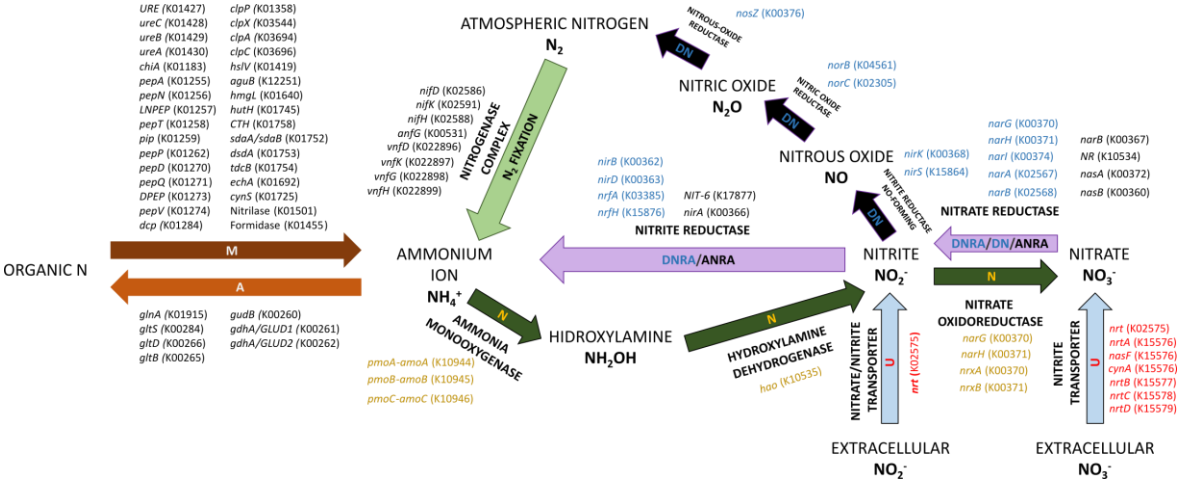

Figure 8. The predicted genes involved in the N cycle with corresponding enzymes and KEGG KO numbers. Different processes involved in the N cycle are colour-coded. Orange arrow – N mineralization and assimilation; light green arrow – N_2 fixation; dark green arrows – nitrification; black arrows – denitrification; purple arrows – dissimilatory and assimilatory nitrate reduction; light blue arrows – uptake of extracellular nitrite and nitrate.

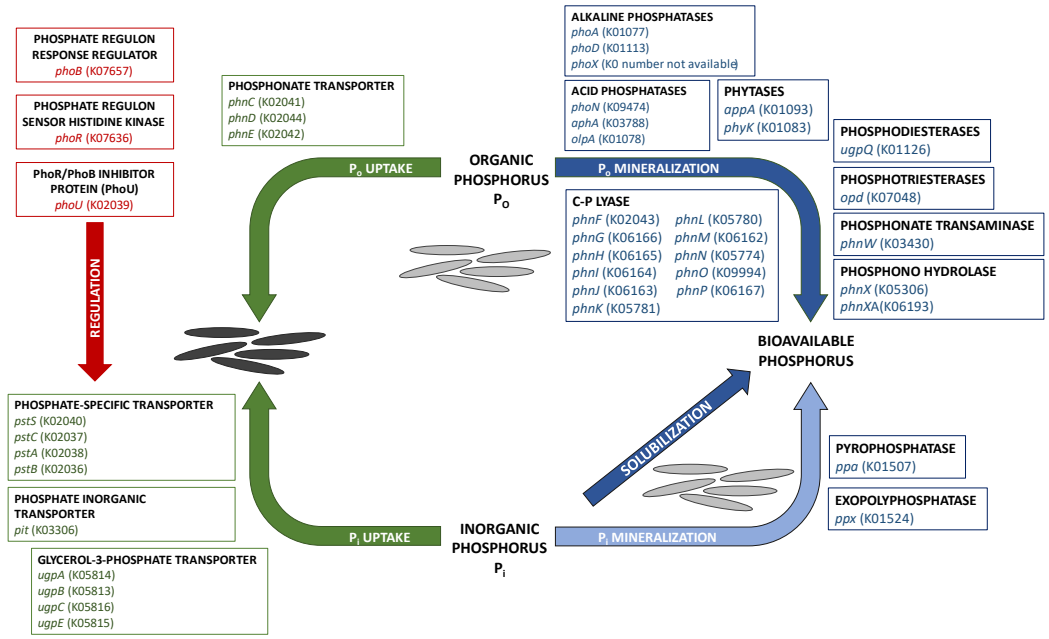

Figure 9. The predicted genes involved in microbial P turnover with corresponding enzymes and KEGG KO numbers. Different processes involved in P turnover are colour-coded. Dark blue arrow – organic P mineralization and solubilization; light blue arrow – inorganic P mineralization; green arrow – uptake of organic and inorganic P; red arrow – regulation of P turnover.

Prior to statistical analyses, the absolute counts of the metagenomic datasets were subsampled to the lowest number of reads per sample using the rarefy function from "GUniFrac" (Chen, 2012). Statistical analyses were performed on randomly subsampled data and computed in the R environment version 3.0.2 (R Core Team, 2013). Packages "stats", "graphics", "grDevices" (R Core Team 2013), "vegan" (Oksanen et al., 2015), "GUniFrac" (Chen, 2012), "gridExtra" (Auguie and Antonov, 2015), "cluster" (Maechler et al., 2015), "calibrate" (Graffelman, 2013), "RColorBrewer" (Neuwirth, 2014), "gplots" (Warnes et al., 2013), and "vcd" (Meyer et al., 2014) were used. Before the principal component analysis (PCA), all sequences with an abundance of less than 3.0 % in all samples were excluded, the abundance data was Hellinger-transformed (Ramette, 2007), and significant differences were determined by permutational multivariate analysis of variance (PERMANOVA). The significant differences in the diversity indices between the metagenomes were determined by Welch's *t*-test, whereas significant differences in the relative abundance of prokaryotic taxa, function, functional genes, and families involved in C and N cycle and P turnover were determined by unpaired *t*-test, where *P*-values were adjusted by the Bonferroni test. The correlation between the pH, OC, total N, and P, bioavailable P, inorganic and organic P, C:N:P ratios, and gene abundance involved in C, N, and P turnover, was determined by Spearman correlation by using the "Hmisc" package (Harrel and Dupont, 2020).

4. RESULTS

4.1. Effect of clay minerals on bacterial diversity and abundance as shown by preliminary screening

To identify which clay minerals or the combination of clay minerals (MT, IL, MT+CH, and IL+FH) has the strongest influence on bacterial diversity and abundance, the water-extractable carbon (WEOC) and microbial biomass (C_{mic}), as well as bacterial diversity and abundance, were monitored at days 0, 7, 21, and 63.

4.1.1. Water-extractable carbon (WEOC) and microbial biomass (C_{mic})

In all soil samples, including one natural and all artificial soils, WEOC content was always higher in soils treated with litter than in untreated soils where it never exceeded 200.0 µg g^{-1} DM (Figure 10). The WEOC values showed a similar trend in both natural soil and all artificial soils treated with litter: during the first incubation period, until day 7, the WEOC content decreased rapidly in all soils treated with litter, and then slowly continued to decrease over the remaining incubation time until day 63. The only exceptions were natural and MT soil, where the WEOC value increased between days 21 and 63.

Contrary to the treated soils, in untreated soils, the WEOC values increased at the beginning of the incubation until day 7. Afterward, the WEOC values decreased until day 21 in all untreated soils. This decrease was followed by increase of WEOC values until day 63 in all soils, apart from in MT+CH soil.

The lowest initial WEOC value in all treated soils was detected in the natural soil (164.6 ± 3.1 µg g^{-1} DM, Figure 10A) which further decreased until day 7 to 33.1 ± 27.3 µg g^{-1} DM. Until the end of incubation, the WEOC values in natural soil soils were similar and varied between 20.3 ± 3.5 µg g^{-1} DM (day 21) and 23.8 ± 2.1 µg g^{-1} DM (day 63). The WEOC value in untreated natural soil was even lower at the beginning of the experiment than in treated natural soil, 19.5 ± 1.3 µg g^{-1} DM. Until day 7 it increased to 35.3 ± 3.6 µg g^{-1} DM at day 7. This increase in WEOC was then followed by a steady decrease until the end of the incubation period (16.9 ± 2.1 µg g^{-1} DM). The WEOC values differed significantly between treated and untreated natural soil only on day 0 ($P < 0.01$).

Although the artificial soils treated with plant litter (Figure 10B-E) showed a similar trend as natural soil, the WEOC values were always higher when compared to the natural soil. On day 0, the lowest WEOC values were measured in MT (520.7 ± 8.5 µg g^{-1} DM), while the highest were measured in IL (725.3 ± 36.8 µg g^{-1} DM) and MT+CH (736.0 ± 47.1 µg g^{-1}

DM). The WEOC values then rapidly decreased by more than two-fold until day 7, followed by a steady decrease until the end of incubation in all artificial soils except MT. At the end of incubation, the lowest WEOC values were detected in MT+CH (127.9 ± 16.7 µg g^{-1} DM), followed by IL+FH (189.5 ± 14.0 µg g^{-1} DM). Slightly higher WEOC values were detected in simple artificial mixtures with only one component MT (201.2 ± 12.2 µg g^{-1} DM) and IL (213.5 ± 7.4 µg g^{-1} DM).

In general, the WEOC values were significantly higher ($P < 0.05$) in all artificial soils treated with litter at all time points than in untreated artificial soils, with exception of MT+CH on day 21 (Figure 10D).

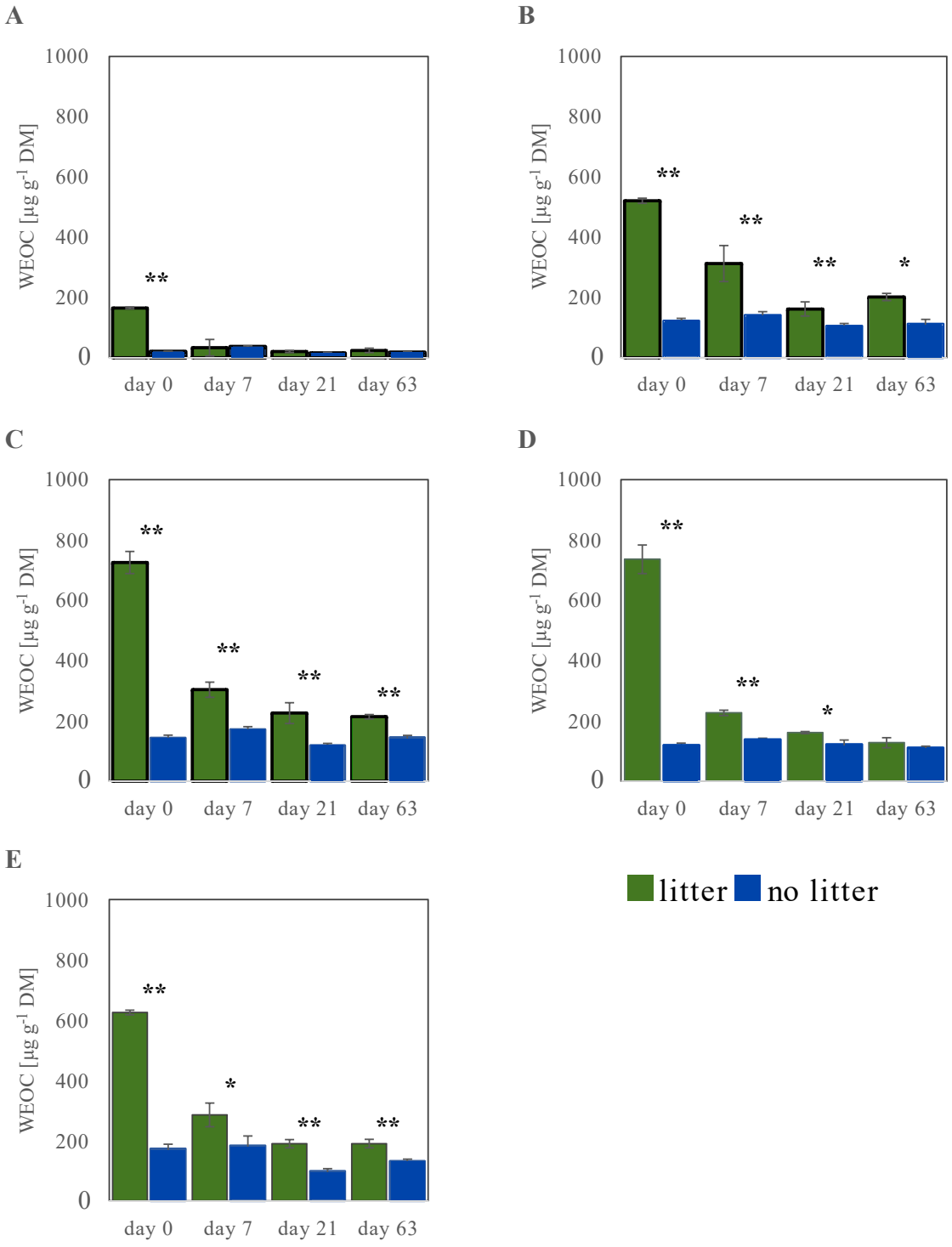

Figure 10. Share of water extractable organic carbon (WEOC) in natural and artificial soils given as mean values (n = 3) and standard deviation at different time points (day 0, day 7, day 21, and day 63) in (A) natural soil, (B) MT, (C) IL, (D) MT+CH, and (E) IL+FH. Green bars represent soil samples treated with plant litter and blue bars untreated soil samples. Asterisks indicate significant differences in WEOC values where *$P < 0.05$ and **$P < 0.01$.

The changes in microbial biomass (C_{mic}) with incubation time in both natural and artificial soils are shown in Figure 11. In all untreated soils, natural and artificial, the C_{mic} values were always lower than in the treated soils and showed similar dynamics. First, microbial biomass decreased slightly between day 0 and day 7, followed by a steady increase until the end of the incubation period (day 63).

In general, the highest C_{mic} values were observed in natural soil sample (Figure 11A), and this was the only soil where microbial biomass was always above 250 µg g^{-1} DM, regardless of plant litter addition. The high initial C_{mic} value (818.5 µg g^{-1} DM) in natural soil treated with plant litter increased even further and reached the maximum value on day 7 (890.2 µg g^{-1} DM). As the incubation continued, the C_{mic} decreased to 493.8 µg g^{-1} DM (day 21) and finally increased to 778.9 µg g^{-1} DM (day 63) in treated natural soil. In contrast, the initial C_{mic} value in untreated natural soil was three times lower than in treated natural soil. There, the C_{mic} slightly decreased and reached the minimum value of 255.0 µg g^{-1} DM on day 21, and then constantly increased until day 63 when it reached 547.7 µg g^{-1} DM. With exception of day 63, C_{mic} concentrations were significantly higher ($P < 0.01$) in natural soil treated with plant litter at all sampling points.

In all artificial soils treated with litter, higher C_{mic} concentrations were detected when compared to the controls. The C_{mic} values ranged between 408.8 and 691.9 µg g^{-1} DM in MT, 655.9 and 957.9 µg g^{-1} DM in IL, 529.2 and 805.5 µg g^{-1} DM in MT+CH, and 459.4 and 713.9 µg g^{-1} DM in IL+FH. There was no specific trend in how C_{mic} changes with incubation time in artificial soils treated with plant litter. However, slight similarities in C_{mic} dynamics were detected in two-component artificial soils (MT+CH, IL+FH), where in both treated and untreated soils, the initial increase in C_{mic} value between day 0 (MT+CH: 529.2 µg g^{-1} DM, IL+FH: 459.4 µg g^{-1} DM) and 7 (MT+CH: 805.5 µg g^{-1} DM, IL+FH: 713.9 µg g^{-1} DM) was followed by a slight decrease until day 21 (MT+CH: 742.7 µg g^{-1} DM, IL+FH: 664.1 µg g^{-1} DM). Afterward, the C_{mic} remained nearly constant until the end of incubation (MT+CH: 735.2 µg g^{-1} DM, IL+FH: 617.8 µg g^{-1} DM) (Figure 11 D-E).

As for untreated artificial soils, the C_{mic} values ranged between 89.4 and 319.9 µg g^{-1} DM in MT, 84.0 and 288.8 µg g^{-1} DM in IL, 111.2 and 313.2 µg g^{-1} DM in MT+CH, and 75.2 and 307.3 µg g^{-1} DM in IL+FH. In all untreated artificial soils, the same C_{mic} dynamics were detected, where the initial c_{mic} value decreased until day 7, and then steadily increased until the end of incubation. Overall, the C_{mic} values were significantly higher in treated artificial soils with few exceptions (day 21 in MT, day 0 in MT+CH, and day 0 in IL+FH) (Figure 11B-E).

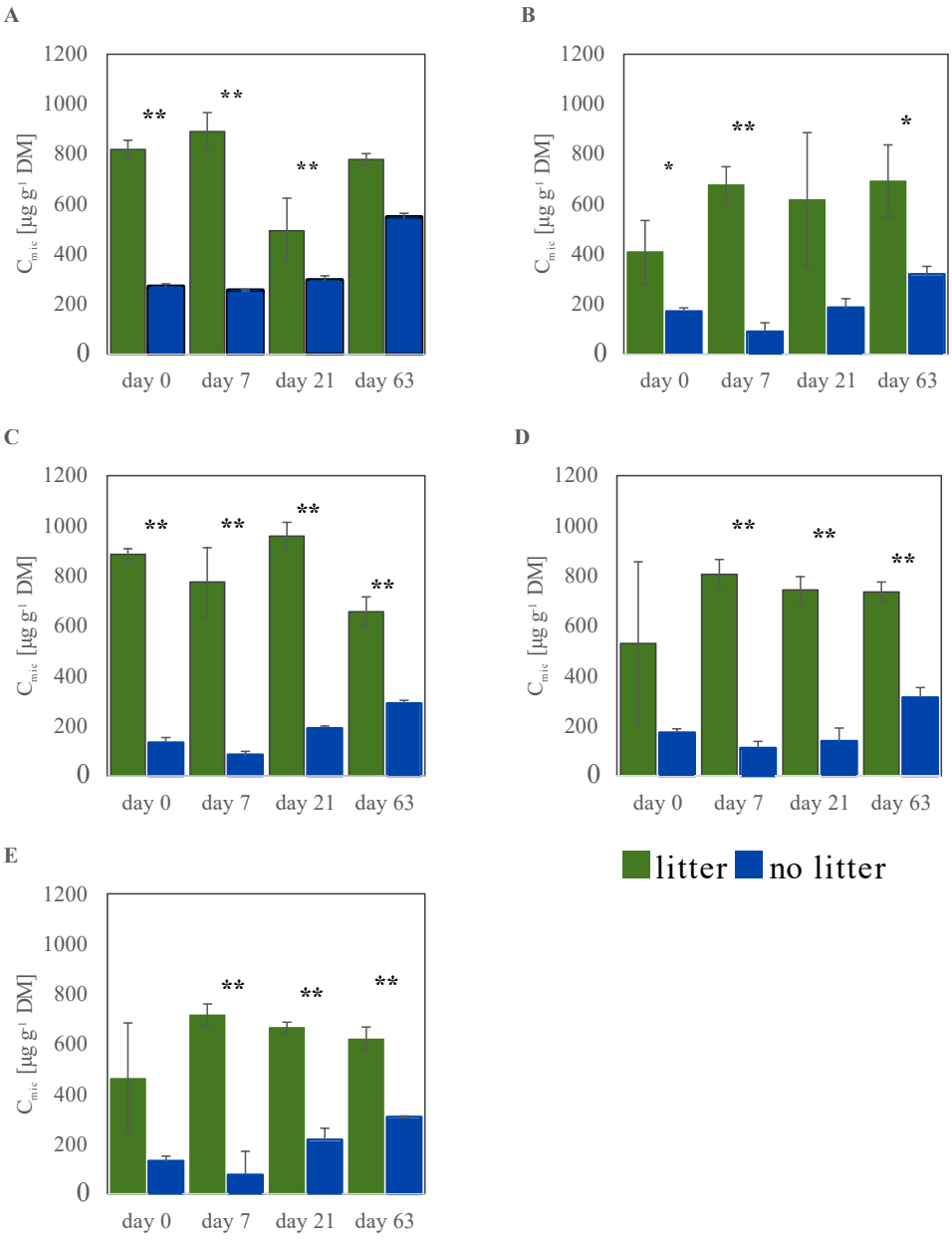

Figure 11. C_{mic} values in natural and artificial soils. Green bars represent C_{mic} in soils treated with litter and blue bars C_{mic} in untreated soils. C_{mic} mean values (n = 3) with standard deviation are shown for different time points (day 0, day 7, day 21, and day 63) in (A) natural soil, (B) MT, (C) IL, (D) MT+CH, and (E) IL+FH. Asterisks indicate significant differences in C_{mic} values where $^{*}P < 0.05$ and $^{**}P < 0.01$.

4.1.2. qPCR analysis of pre-incubated artificial soil treated with plant litter

To compare the relative bacterial abundance in natural and artificial soils a qPCR of 16S rRNA genes was performed. The 16S rRNA gene copy numbers in natural (Luvisol) and artificial soils varied between 10^6 and 10^{10} copies g^{-1} DM (Figure 12A-E).

In the untreated natural soil, the gene copy number between day 0 and day 7 remained almost constant (day 0: 2.1 x 10^7 copies g^{-1} DM; day 7: 2.3 x 10^7 copies g^{-1} DM) followed by a continuous increase in copy number over the incubation time, with a maximum value at day 63 (1.9 x 10^8 copies g^{-1} DM. The increase between day 0 and day 63 was approximately one order of magnitude (Figure 12A).

Except for IL (Figure 12B-E), untreated artificial soils initially show a decrease between day 0 and day 7, followed by a constant increase until the end of the incubation period, when maximum values of copy numbers were reached. A relatively large decrease between day 0 and day 7 was detected in MT, where the 16S rRNA gene copy number gene decreased from 8.3 x 10^8 to approximately 2.7 x 10^6 copies g^{-1} DM (Figure 12B).

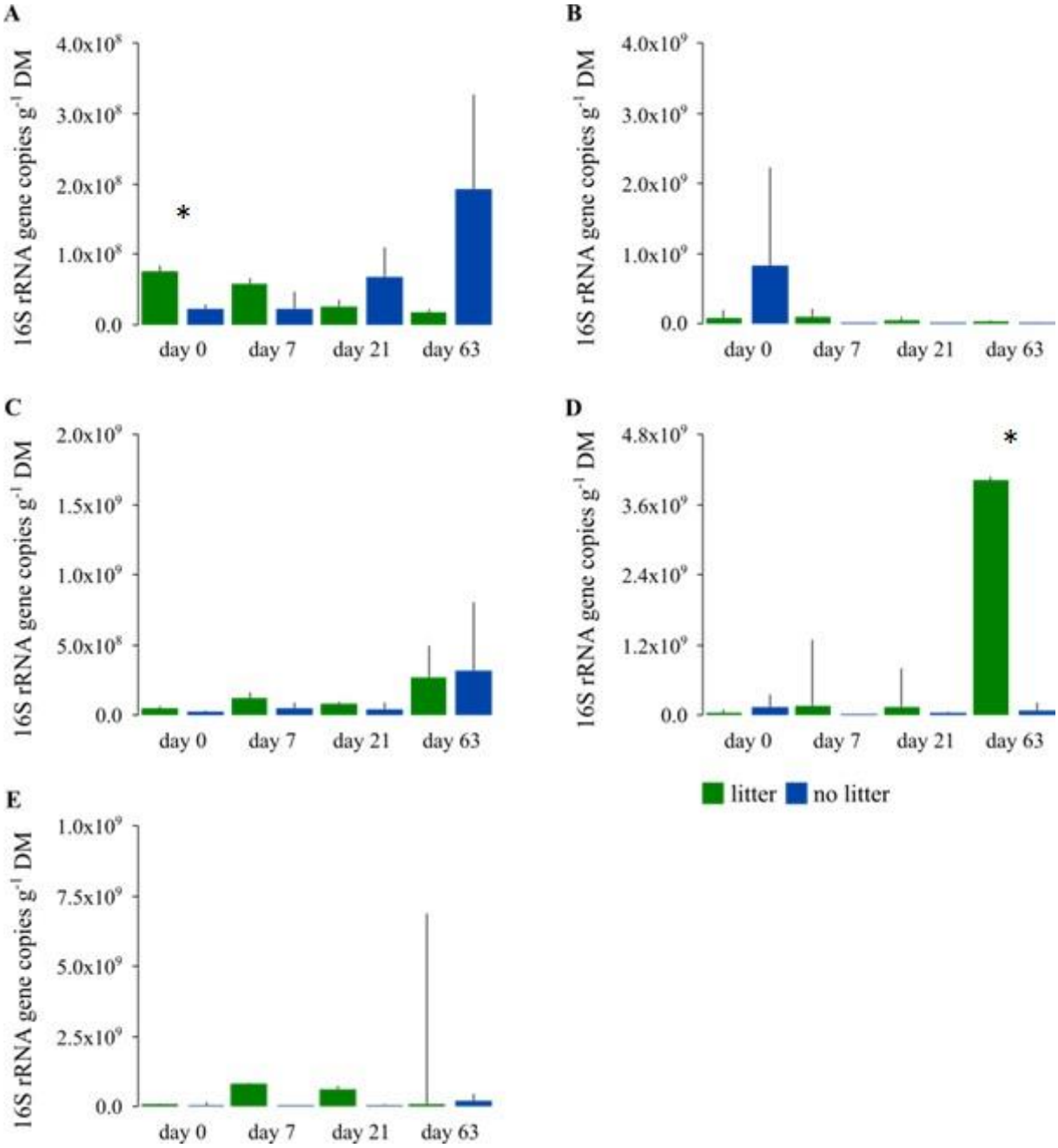

Figure 12. Number of copies of 16S rRNA gene in natural and artificial soils. Green bars represent number of copies of 16S rRNA gene per gram of dry soil in soils treated with litter, while blue bars represent number of copies of 16S rRNA gene in untreated soils. Mean values (n = 3) of number of copies of 16S rRNA gene with standard deviation are shown for different time points (day 0, day 7, day 21, and day 63) in (A) natural soil, (B) MT, (C) IL, (D) MT+CH, and (E) IL+FH. Asterisks indicate significant differences in 16S rRNA copy number where *$P < 0.05$.

In the soils treated with litter, the artificial soils initially showed an increase of gene copy number between day 0 and day 7 (Figure 12B-E). The largest increase was observed for IL+FH, where the gene copy number increased from 1.0 x 10^8 to 8.5 x 10^8 copies g^{-1} DM (Figure 12E). The treated samples of the artificial soils showed a consistent pattern between day 0 and day 21. Here, bacterial abundance increased from day 0 to day 7 and then decreased on day 21. Subsequently, the bacterial abundance in MT+CH (MANOVA, $P < 0.05$) and IL increased again on day 63, while bacterial abundance in MT and IL+FH decreased after day 21 (Figure 7B-E).

The natural soil, however, showed a continuous decrease in bacterial abundance from the beginning (7.5 x 10^7 copies g^{-1} DM) until the end of incubation (1.0 x 10^7 copies g^{-1} DM, Figure 7A).

4.1.3. Terminal Restriction Fragment Length Polymorphism (T-RFLP) analysis of pre-incubated artificial soil treated with plant litter

To determine the potential differences in the composition of microbial communities with respect to different mineral compositions of artificial soils, a model for the early stages of soil development, a T-RFLP of partial 16S rRNA gene was run.

The T-RFLP profiles for each sample were composed of on average 67 terminal restriction fragments (T-RFs). T-RFLP profiles of natural soil (64 T-RFs in treated and 69 T-RFs in untreated soil), MT (57 T-RFs in treated and 60 T-RFs in untreated soil), and MT+CH (71 T-RFs in treated and 76 T-RFs in untreated soil) showed similar complexity, whereas soils containing illite (IL: 62 T-RFs in treated and 82 T-RFs in untreated soil; IL+FH: 60 T-RFs in treated and 72 T-RFs in untreated soil) were more complex. Only, the number of T-RFs in untreated IL soil was significantly lower than in treated IL ($P < 0.01$). In general, more T-RFs were found in untreated than in treated soils indicating that litter addition is an important factor in selecting specific bacterial groups, thus, inducing changes in bacterial community composition.

Figure 13 shows the results of the principal component analysis (PCA) performed on a dataset that included all fragments that accounted for more than 1% of the total relative abundance in at least one sample.

Figure 13A shows the results of the PCA where natural and all artificial soils (MT, IL, MT+CH, IL+FH) were included. All samples that originate from the natural soil were grouped in the upper left quarter of the graph. The samples from natural soil, regardless of the treatment and the time of sampling, are clustered together and clearly differ from the artificial

soils. Within this cluster, untreated and treated natural soil formed separate groups. Also, samples from day 7 and day 21 were grouped separately from days 0 and 63.

The samples originating from the artificial soils, on the other hand, form several clusters, which are dispersed around the center of the remaining quadrants. Samples from artificial soils treated with litter at day 0 form a single cluster, and the samples from the later timepoint form another cluster. Also, there is a clear distinction between treated and untreated samples, which are grouped into two separate clusters.

Another PCA, in which only the artificial soil clusters are shown (Figure 13B) further increases the resolution, showing that the samples from treated and untreated soils form two clusters according to the clay mineral type present. All soils that contain MT (MT and MT+CH) form a cluster in the upper two quadrants, whereas soils that contain IL (IL and IL+FH) form a cluster in the lower two quadrants, thus highlighting the role of the MT and IL on the establishment of distinct microbial communities.

Considering all T-RFs that accounted for more than 1% of the total relative abundance in at least one sample, the most pronounced differences were found when different clay minerals were compared. (PERMANOVA, P = 0.001). However, significant differences were also detected when treatment with litter (PERMANOVA, P = 0.001), and sampling time (PERMANOVA, P = 0.001) were analysed.

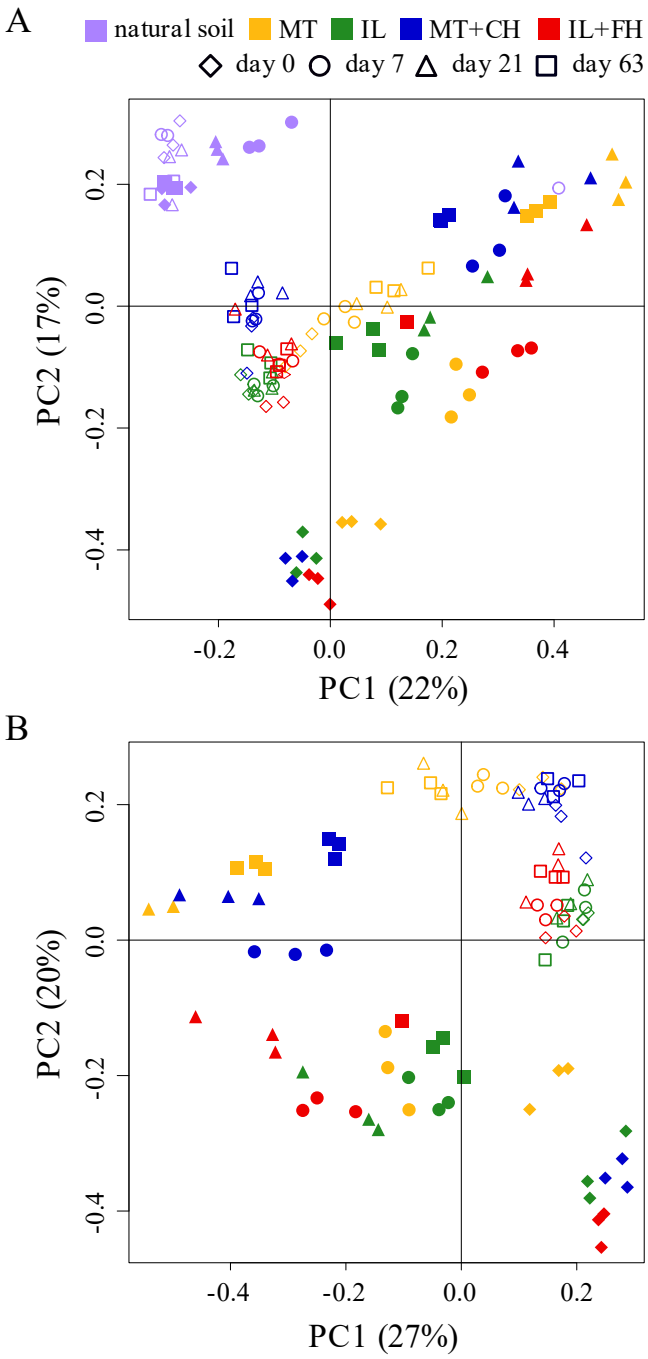

Figure 13. Results of PCA analysis of T-RF profiles of microbial communities originating from natural soil (Luvisol, from Scheyern, Germany) and artificial soils. T-RFLP was performed on all soils in triplicates (n = 3). (A) natural soil and all artificial soils, and (B) artificial soils. Natural soil and artificial soils with different compositions are depicted with different colours (purple – natural soil, yellow – MT, green – IL, blue – MT+CH, and red – IL+FH), different sampling times with distinct shapes (rhomb – day 0, circle – day 7, triangle – day 21 and square – day 63), and samples treated with litter are depicted with open symbols and untreated with closed symbols.

Even though the WEOC, $C_{mic,}$ and 16S rRNA gene values were similar in both MT and IL-containing soils, the T-RFLP showed a clear distinction in bacterial diversity depending on the type of clay minerals present, i.e., the distinct clusters were formed for MT and IL containing soils. Therefore, based on the T-RFLP fingerprinting analysis, two artificial soils, MT and IL, were selected for further metagenomic shotgun analysis.

4.2. The influence of different types of clay minerals on phylogenetic and functional diversity and major processes involved in carbon, nitrogen, and phosphorus turnover as shown by metagenomic shotgun sequencing

The preliminary screening has shown that the development of distinct bacterial communities is dependent on the type of minerals present, i.e., different bacterial communities were found in MT and IL. Hence, to understand the impact of different types of clay minerals on the establishment and development of a distinct MT and IL microbiome, and consequent functional potential, major processes, and taxa that drive the turnover of most important macronutrients (C, N, and P), a shotgun metagenomic sequencing of MT and IL soils was performed.

4.2.1. The properties of MT and IL soils

The artificial soils investigated in this study (MT and IL) were prepared as described by Pronk et al. (2012) and Vogel et al. (2014) (Chapter 3.2.1.) and incubated for 842 days. Since Vogel et al. (2014) have detected a decline in the respiration rates soon after the first manure addition, the additional external nutrient input, in a form of second manure addition, was added to overcome the nutrient depletion. At end of incubation soil pH, OC, total N, total P, P_{NaHCO3}, and inorganic and organic P were measured. In addition, C:N, C:P, N:P, and C:N:P ratios were calculated.

The properties of artificial soils determined after 842 days of incubation, as well as the manure, which was added to the artificial soils, are summarised in Table 7.

Table 7. The properties of artificial soils (MT and IL) after 842 days of incubation. The manure was added twice. The first addition took place at the beginning of the experiment and the second after 562 days of incubation. The values are shown as mean with a standard deviation of three independent replicates (n = 3). Asterisks indicate significant differences in soil properties between MT and IL as shown by the *t*-test ($P < 0.05$).

	MT	IL	1st manure	2nd manure
pH	7.2 ± 0.2	7. 6 ± 0.3	n.a.	n.a.
OC [mg g^{-1}]	13.5 ± 0.9	11.6 ± 0.7	338.5 ± 6.9	165.4 ± 2.7
N_{total} [mg g^{-1}]	1.5 ± 0.1	1.3 ± 0.2	30.7 ± 1.6	11.5 ± 0.2
P_{total} [mg g^{-1}]	0.40 ± 0.02	0.38 ± 0.03	10.5 ± 0.2	2.8 ± 0.1
P_{NaHCO3}[mg g^{-1}]	0.15 ± 0.01*	0.13 ± 0.01*	0.87 ± 0.03	0.39 ± 0.02
P_i [mg g^{-1}]	0.30 ± 0.04*	0.26 ± 0.01*	8.5 ± 0.1	2.0 ± 0.0
P_o [mg g^{-1}]	0.09 ± 0.04	0.12 ± 0.03	2.0 ± 0.3	0.78 ± 0.13
C:N ratio	9.3 ± 0.3	9.3 ± 0.6	11.0 ± 0.4	14.4 ± 0.2
C:P ratio	34.6 ± 4.6	30.8 ± 1.6	32.2 ± 0.5	60.1 ± 2.4
N:P ratio	3.7 ± 0.5	3.3 ± 0.3	2.9 ± 0.0	4.2 ± 0.2
C:N:P	9.3 : 3.7 : 1.0	9.3 : 3.3 : 1.0	32.2 : 2.9 : 1.0	60.0 : 4.2 : 1.0

In general, the pH value, OC, total N, and total P concentrations were similar in both soils. The pH value was slightly lower in MT (7.2 ± 0.2) than in IL (7.6 ± 0.3), whereas the OC and total N concentrations were higher in MT (OC: 13.5 ± 0.9 mg g^{-1}, total N: 1.5 ± 0.1 mg g^{-1}) than in IL (OC: 11.6 ± 0.7 mg g^{-1}, total N: 1.3 ± 0.2 mg g^{-1}). However, the detected differences were not significant (Vogel et al., 2014).

The P-pools concentrations differed between MT and IL, where total P, $P_{NaHCO3,}$ and P_i were higher in MT (total P: 0.40 ± 0.02 mg g^{-1}, P_{NaHCO3}: 0.15 ± 0.01 mg g^{-1}, P_i: 0.30 ± 0.04 mg g^{-1}), and organic P was slightly higher in IL (0.12 ± 0.03 mg g^{-1}). Only P_{NaHCO3} and P_i were significantly higher in MT when compared to IL.

Even though main macronutrients (C, N, and P) were added to artificial soils with two manure additions, C:N:P ratios were very low in both soils. C:N, C:P, and N:P ratios in MT were 9.3 ± 0.3, 34.6 ± 4.6, and 3.7 ± 0.5 respectively. Furthermore, they were comparable with C:N:P ratios in IL (C:N 9.3 ± 0.6, C:P 30.8 ± 1.6, and N:P 3.3 ± 0.3).

4.2.2. Taxonomic and functional differences in MT and IL microbiomes

To assess the impact of different clay minerals on the establishment and the structure of microbial communities, two model artificial soils, one containing montmorillonite and the other illite were used for metagenomic shotgun sequencing. The used approach resulted in

35,583,862 raw sequences with an average length of 300 bp. After data trimming and removal of contaminant sequences, a total of 35,583,824 high-quality sequences with an average length of 296 bp was obtained. The details of the sequencing run are shown in Table 8. To minimize the impact of varied sequencing depth and to compare the alpha diversity, all samples were randomly subsampled to the common depth that corresponded to 3,074,662 reads per sample by using the rarefy function from the “GUniFrac” package.

Table 8. The number of reads and average fragment length per replicate before and after quality trimming and removal of contaminant sequences are shown for both forward and reverse reads.

			MT1	MT2	MT3	IL1	IL2	IL3
Forward reads	Number of reads	Raw reads	5,162,677	3,293,551	1,646,829	4,097,160	1,537,332	2,054,382
		Trimmed reads	5,162,677	3,293,550	1,646,829	4,097,159	1,537,332	2,054,382
		Filtered reads	5,162,669	3,293,544	1,646,829	4,097,159	1,537,331	2,054,382
	Average read length (bp)	Raw reads	300.59	300.60	300.58	300.60	300.58	300.59
		Trimmed reads	294.24	298.21	295.75	299.04	299.58	297.08
		Filtered reads	294.24	298.21	295.75	299.04	299.58	297.08
Reverse reads	Number of reads	Raw reads	5,162,677	3,293,551	1,646,829	4,097,160	1,537,332	2,054,382
		Trimmed reads	5,162,675	3,293,550	1,646,827	4,097,158	1,537,331	2,054,382
		Filtered reads	5,162,669	3,293,543	1,646,827	4,097,158	1,537,331	2,054,382
	Average read length (bp)	Raw reads	300.62	300.62	300.60	300.61	300.57	300.60
		Trimmed reads	293.38	297.49	294.75	298.28	298.46	296.12
		Filtered reads	293.38	297.49	294.75	298.28	298.46	296.12

The artificial soil metagenomes coverage based on the read redundancy was calculated by the Nonpareil algorithm and it ranged between 0.657 and 0.773.

The richness and diversity of detected bacterial families, for all samples were estimated by the number of detected phyla and families, Pielou evenness, and standard diversity indices, including Shannon-Wiener, Simpson, and inverse Simpson index (Table 9).

In the whole genome, the number of detected phyla (MT: 66 ± 1; IL: 66 ± 2) and families (MT: 462 ± 1; IL: 463 ± 3) were similar. Detected phyla and families were evenly distributed across both MT (Pielou evenness on phylum: 0.50 ± 0.03, and family level: 0.66 ± 0.02) and IL (Pielou evenness on phylum: 0.48 ± 0.05, and family level: 0.65 ± 0.05). Although no

significant differences were observed, the diversity was slightly higher in MT, both on phylum (Shannon-Wiener index: MT - 2.08 ± 0.13, IL -2.00 ± 0.21; Simpson index: MT - 0.79 ± 0.03, IL - 0.76 ± 0.06; inverse Simpson index: MT - 4.77 ± 0.78, IL - 4.29 ± 1.05) and family (Shannon-Wiener index: MT - 4.04 ± 0.09, IL - 3.97 ± 0.31; Simpson index: MT - 0.96 ± 0.00, IL - 0.95 ± 0.02; inverse Simpson index: MT - 24.03 ± 2.06, IL - 22.73 ± 7.70) level then in IL, with respect to all diversity indices calculated.

The number of detected phyla involved in C (MT: 18 ± 2; IL: 18 ± 2) and N (MT: 15 ± 2; IL: 15 ± 2) turnover were similar, whereas slightly more phyla were involved in P turnover (MT: 23 ± 3; IL: 21 ± 2). The number of families involved in C, N, and P turnover was similar in both soils. In total, the smallest number of families was involved in N turnover (MT: 53 ± 12; IL: 56 ± 16). Furthermore, almost twice as many families were involved in C (MT: 103 ± 20; IL: 95 ± 7) and thrice as many in P (MT: 151 ± 26; IL: 148 ± 28) than in N turnover.

The phyla diversity was similar in both MT and IL soils for all phyla involved in C, N, and P turnover (Table 9).

Table 9. Diversity indices based on the phyla and families found in the montmorillonite and illite. All values are shown as mean with a standard deviation of three independent replicates (n = 3).

	Phylum			Family		
	MT	**IL**	***P*-value[f]**	**MT**	**IL**	***P*-value[f]**
Index	**Microbiome in montmorillonite (MT) and illite (IL)**					
Richness (S)[a]	66 ± 0	66 ± 2	1.000	462 ± 1	463 ± 3	0.599
Pielou evenness (J)[b]	0.50 ± 0.03	0.48 ± 0.05	0.606	0.66 ± 0.02	0.65 ± 0.05	0.754
Shannon - Wiener index (H')[c]	2.08 ± 0.13	2.00 ± 0.21	0.610	4.04 ± 0.09	3.97 ± 0.31	0.746
Simpson index (λ)[d]	0.79 ± 0.03	0.76 ± 0.06	0.498	0.96 ± 0.00	0.95 ± 0.02	0.616
Inverse Simpson index (1/λ)[e]	4.77 ± 0.78	4.29 ± 1.05	0.558	24.03 ± 2.06	22.73 ± 7.70	0.802
Index	**Microbiome involved in C turnover in montmorillonite (MT) and illite (IL)**					
Richness (S)[a]	18 ± 2	18 ± 2	0.842	103 ± 20	95 ± 7	0.541
Pielou evenness (J)[b]	0.56 ± 0.04	0.55 ± 0.02	0.963	0.69 ± 0.04	0.70 ± 0.03	0.866
Shannon - Wiener index (H')[c]	1.60 ± 0.10	1.59 ± 0.11	0.892	3.19 ± 0.09	3.16 ± 0.14	0.801
Simpson index (λ)[d]	0.69 ± 0.02	0.67 ± 0.04	0.387	0.92 ± 0.01	0.91 ± 0.01	0.099
Inverse Simpson index (1/λ)[e]	3.29 ± 0.26	3.02 ± 0.40	0.403	12.64 ± 1.38	10.77 ± 0.81	0.130
Index	**Microbiome involved in N turnover in montmorillonite (MT) and illite (IL)**					
Richness (S)[a]	15 ± 1	15 ± 2	0.538	53 ± 12	56 ± 16	0.812
Pielou evenness (J)[b]	0.51 ± 0.04	0.57 ± 0.06	0.254	0.57 ± 0.10	0.67 ± 0.06	0.247
Shannon - Wiener index (H')[c]	1.37 ± 0.10	1.55 ± 0.21	0.281	2.25 ± 0.30	2.68 ± 0.36	0.188
Simpson index (λ)[d]	0.67 ± 0.06	0.70 ± 0.06	0.480	0.77 ± 0.10	0.87 ± 0.04	0.206
Inverse Simpson index (1/λ)[e]	3.06 ± 0.52	3.47 ± 0.64	0.437	4.90 ± 1.74	8.85 ± 3.77	0.203
Index	**Microbiome involved in P turnover in montmorillonite (MT) and illite (IL)**					
Richness (S)[a]	23 ± 3	21 ± 2	0.233	151 ± 26	148 ± 28	0.897
Pielou evenness (J)[b]	0.69 ± 0.03	0.71 ± 0.04	0.644	0.69 ± 0.03	0.71 ± 0.04	0.590
Shannon - Wiener index (H')[c]	2.17 ± 0.07	2.14 ± 0.16	0.751	3.45 ± 0.07	3.52 ± 0.27	0.703
Simpson index (λ)[d]	0.85 ± 0.01	0.83 ± 0.04	0.454	0.94 ± 0.00	0.94 ± 0.02	0.993
Inverse Simpson index (1/λ)[e]	6.87 ± 0.58	6.21 ± 1.71	0.579	16.93 ± 1.39	17.63 ± 4.27	0.809

(S)[a] represents the number of phyla or families observed in the sample. (J)[b] was calculated as follows (Hill et al., 2003): $J = H'/H_{max}$ where H' is Shannon - Wiener index and $H_{max} = \ln(S)$. (H')[c] was calculated as follows (Hill et al., 2003): $H' = -\Sigma(p_i)(\ln p_i)$ where p_i is a proportion of the *i*th phylum or family in the total number of observed taxa. (λ)[d] was calculated as follows (Hill et al., 2003): $\lambda = 1 - (\Sigma n_i(n_i - 1))/(N(N - 1))$ where n_i is the number of entities belonging to the *i*th taxa observed in the sample and N is the total number of taxa. (1/λ)[e] was calculated as follows (Hill et al., 2003): 1/λ where λ is Simpson index. P-value[f] significant differences between the two metagenomes were ascertained by Welch's *t*-test.

Generally, the diversity of families involved in C and P turnover, was slightly higher than the family diversity involved in N turnover. Only the diversity of families involved in C turnover (Shannon-Wiener index: MT - 3.19 ± 0.09, IL - 3.16 ± 0.14; Simpson index: MT - 0.92 ± 0.01, IL - 0.91 ± 0.01; inverse Simpson index: MT - 12.64 ± 1.38, IL - 10.77 ± 0.81) was slightly higher in MT than in IL. In contrast, the diversity of families involved in and N (Shannon-Wiener index: MT - 2.25 ± 0.30, IL - 2.68 ± 0.36; Simpson index: MT - 0.77 ± 0.10, IL - 0.87 ± 0.04; inverse Simpson index: MT - 4.90 ± 1.74, IL - 8.85 ± 3.77) and P (Shannon-Wiener index: MT - 3.45 ± 0.07, IL - 3.52 ± 0.27; Simpson index: MT - 0.94 ± 0.00, IL - 0.94 ± 0.02; inverse Simpson index: MT - 16.93 ± 1.39, IL - 17.63 ± 4.27) turnover was higher in IL than in MT.

In addition, the PCA analysis of all families detected in MT and IL metagenomes, and families involved in C, N, and P turnover was performed. Clear separation and differences within the family community structure between MT and IL metagenome, and families involved in C, N, and P turnover were detected (Figure 14). Also, all MT and IL replicates showed similar variations. Although clear separation of metagenomes was detected no significant differences (PERMANOVA, C: $P = 0.1$, N: $P = 0.1$ and P: $P = 0.2$) were observed.

For all families found in MT and IL metagenomes, PC1 explained 51.5% and PC2 23.1% of the total variance (Figure 11A). On the other hand, smaller percentages accounted for the total variance of microbiome involved in C (PCA1: 38.4%; PCA2: 21.3%), N (PCA1: 43.5%; PCA2: 22.0%), and P (PCA1: 44.6%; PCA2: 19.6%) turnover.

Different taxa were responsible for the separation of MT and IL metagenome. Phylum Microgenomates, and families *Microchaetaceae,* and *Ignavibacteriaceae* had the greatest influence on the total MT and IL metagenome separation (Figure 14A). Interestingly, Microgenomates, the phylum with the greatest influence on the metagenome separation was the only low abundant taxa (< 2 %).

Different families, with exception of *Bacillaceae*, had the greatest influence on the separation of the microbiome involved in a major nutrient turnover. In detail, *Bacillaceae*, *Rhodothermaceae*, and *Microchaetaceae* had the greatest influence on the separation of microbiome involved in C turnover (Figure 14B), *Bacillaceae*, *Chitinophagaceae*, and *Flavobacteriaceae* on N turnover (Figure 14C), and *Melioribacteraceae*, *Microchaetaceae*, and *Bacillaceae* on P turnover (Figure 14D). Unlike the taxa responsible for the separation of total MT and IL metagenome, only the highly abundant families influenced the separation of microbiome involved in a major nutrient turnover.

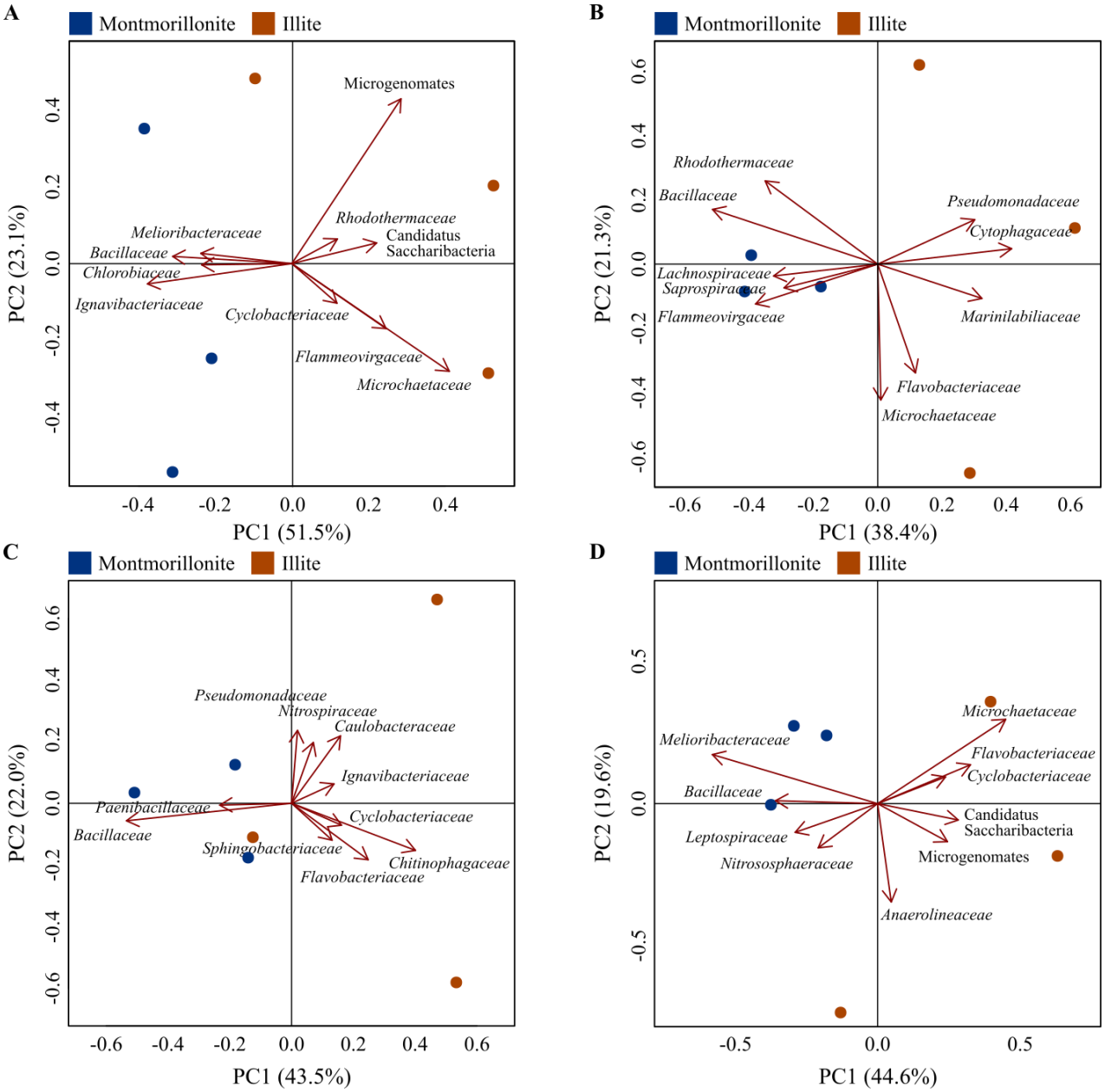

Figure 14. Principal component analysis (PCA) of montmorillonite (MT, n = 3) and illite (IL, n = 3) soil metagenomes (A) and microbiota harbouring genes involved in C (B), N (C), and P turnover (D). (A-D) the first two components based on relative, Hellinger transformed abundance on the family level are shown. Arrows represent families that have the largest influence on metagenome separation. No significant changes between the MT and IL were detected.

4.2.3. Phylogenetic annotation of MT and IL metagenomes

To determine the microbial community structure in MT and IL and to analyse the response of microbial communities to different mineralogy, a shotgun sequencing approach was used. Phylogenetic annotation of the metagenomes was performed by comparing sequences with the NCBI non-redundant (nr) protein sequence database.

In total, 55.84% of all reads were annotated by using the NCBI-nr sequence database. Bacterial reads comprised 93.72%, eukaryotic 4.21%, and archaeal 2.07% of all annotated reads. A total of 68 phyla and 477 families was detected. Only 5 phyla and 7 families showed a relative abundance >1.0%. The majority of phyla (54 phyla; 98.2% of all annotated reads) and families (346 families; 97.4% of all annotated reads) were found in both metagenomes.

Both metagenomes were dominated by Bacteroidetes (29.17%), followed by Proteobacteria (10.56%), Firmicutes (8.30%), and Cyanobacteria (5.58%). At the family level *Microchaetaceae* (4.50%), *Bacillaceae* (3.51%), *Cytophagaceae* (2.95%), *Flavobacteriaceae* (2.57%), *Flammeovirgaceae* (2.48%), *Ignavibacteriaceae* (1.96%), and *Chitinophagaceae* (1.81%) were the most abundant (Figure 15). Besides previously mentioned families, an additional 339 families were found in both soils but in lower abundances.

Firmicutes, Ignavibacteriae, Chlorobi, and Planctomycetes were prevalent in MT, whilst Bacteroidetes, Proteobacteria, Cyanobacteria, and Microgenomates in IL. The same abundance trend dependent on the mineral composition was observed also on the family level, with *Bacillaceae*, *Paenibacillaceae*, *Ignavibacteriaceae,* and *Chlorobiaceae* dominating in MT, and *Microchaetaceae*, *Cytophagaceae,* and *Flammeovirgaceae* in IL.

To detect significant differences between the prokaryotic communities in MT and IL the abundance of all annotated phyla and families was compared. To be more stringent, only taxa with an abundance of at least 0.005 % in one of the samples related to the total number of assigned sequences were included. On the phylum level, 8 and the family 54 taxa differed significantly in the number of assigned reads. Ignavibacteriae and Chlorobi were significantly higher in montmorillonite (Bonferroni adjusted unpaired *t*-test, $P = 0.020$ and $P = 0.049$, respectively). The families belonging to the previously mentioned phyla were significantly more abundant in MT with *Ignavibacteriaceae*, *Bacillaceae,* and *Paenibacillaceae* showing a significant difference (Bonferroni adjusted unpaired *t*-test; $P = 0.010$, $P = 0.045$, and $P = 0.003$, respectively), whilst no bacterial family was significantly more abundant in IL.

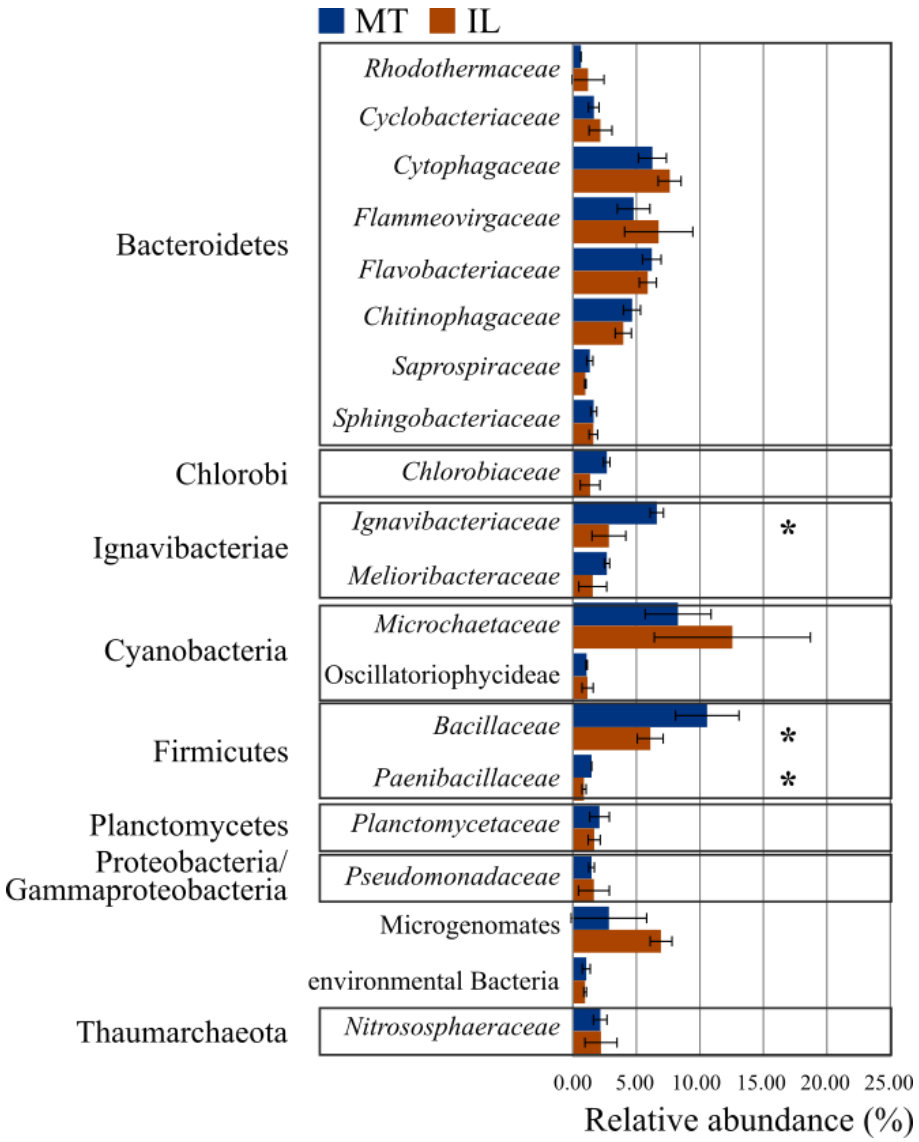

Figure 15. Relative abundance of prokaryotic families in artificial soils containing MT and IL. Sequences were aligned against the NCBI-nr database and annotated with MEGAN5. Relative abundance was calculated based on the number of all assigned reads. The mean relative abundance with standard deviations (n = 3) of the twenty most abundant taxa is shown. Asterisks indicate significant differences in prokaryotic families between two metagenomes ($P < 0.05$).

Even though the number of phyla and families involved in C turnover was threefold lower than the number of phyla and families found in MT and IL metagenome, the microbiota involved in C turnover showed a similar abundance trend. A total of 23 phyla and 161 families involved in C turnover was detected in MT and IL containing soils. Of that, 10 phyla and 16 families had a relative abundance above 1.0%. 20 phyla (87.0%) and 113 families (70.2%) were common among microbiota involved in C turnover.

Bacteroidetes (50.48%), Firmicutes (21.14%), Proteobacteria (9.04%), and Cyanobacteria (6.38%) were the most abundant phyla, and *Cytophagaceae* (19.44%), *Bacillaceae* (13.67%), *Flammeovirgaceae* (7.00%), *Rhodothermaceae* (6.91%), *Flavobacteriaceae* (6.46%), and *Microchaetaceae* (6.35%) were the most abundant families involved in C turnover (Figure 16). Besides those families, an additional 155 families were found in both soils with abundances lower than 5%.

Firmicutes, Cyanobacteria, Actinobacteria, and Ignavibacteriae were prevalent in MT, and Bacteroidetes, Chloroflexi, Verrucomicrobia, and Chlorobi in IL. At the same time, Proteobacteria were equally abundant in both MT and IL. On the family level, *Bacillaceae*, *Flammeovirgaceae*, *Rhodothermaceae*, and *Microchaetaceae* were dominant in MT, and *Cytophagaceae*, *Flavobacteriaceae*, *Alteromonadaceae*, and *Cyclobacteriaceae* in IL.

The abundance of 2 phyla and 4 families differed significantly between MT and IL. Firmicutes and Euryarchaeota were significantly higher in MT (Bonferroni adjusted unpaired *t*-test, $P = 0.011$, and $P = 0.014$, respectively). *Bacillaceae* (Bonferroni adjusted unpaired *t*-test, $P = 0.020$), and *Planococcaceae* (Bonferroni adjusted unpaired *t*-test, $P = 0.023$) were significantly higher in MT, and *Paenibacillaceae* (Bonferroni adjusted unpaired *t*-test, $P = 0.008$) and *Halobacteriaceae* (Bonferroni adjusted unpaired *t*-test, $P = 0.014$) in IL.

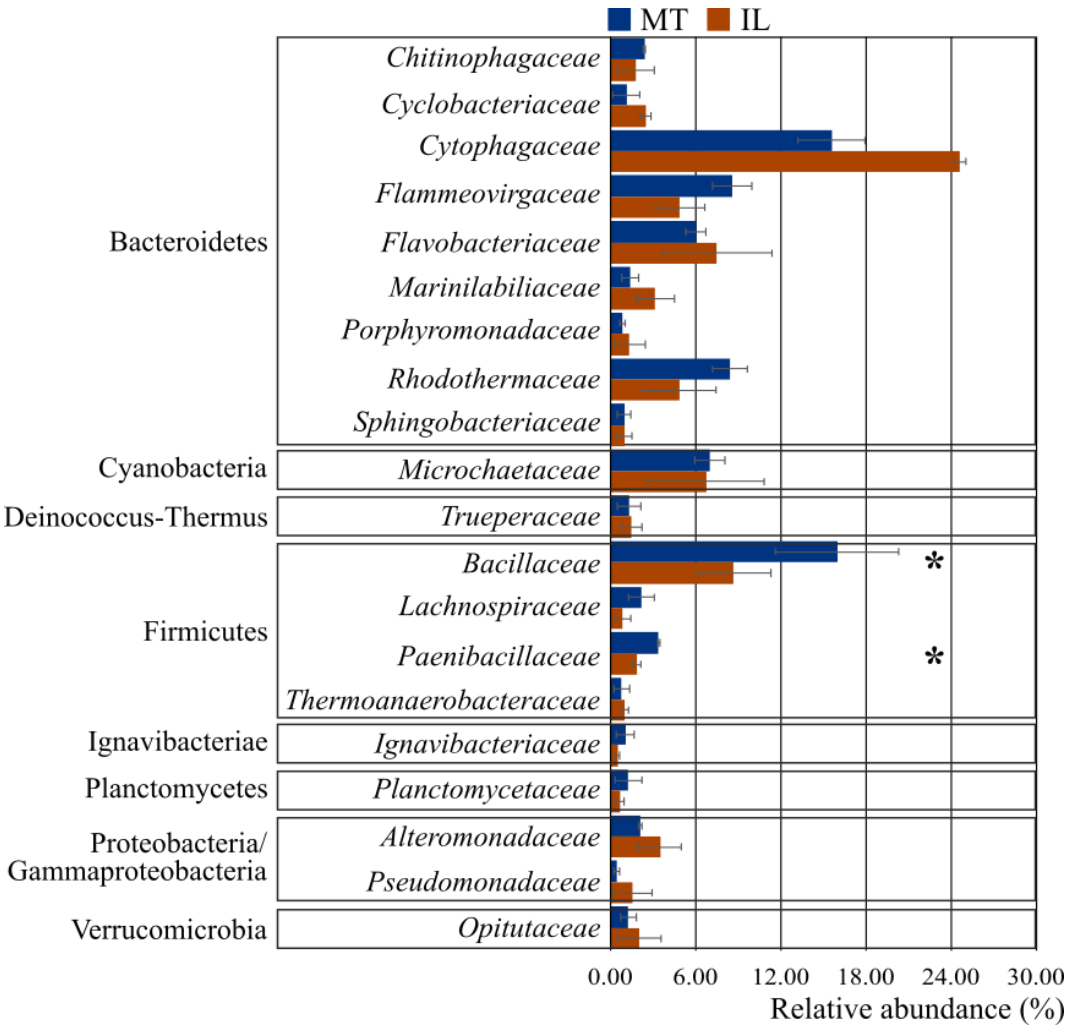

Figure 16. Relative abundance of prokaryotic families involved in C turnover in artificial soils containing MT and IL. Sequences were aligned against the NCBI-nr database and annotated with MEGAN5. Relative abundance was calculated based on the number of all assigned reads. The mean relative abundance with standard deviations (n = 3) of the twenty most abundant taxa is shown. Asterisks indicate significant differences in prokaryotic families involved in C turnover in artificial soils ($P < 0.05$).

The number of phyla and families involved in N turnover was somewhat lower than the number of phyla and families involved in C turnover. A total of 20 phyla and 112 families involved in N turnover was detected in MT and IL containing soils. Of that, 7 phyla and 13 families had a relative abundance above 1.0%. 15 phyla (75.0%) and only 61 families (54.5%) involved in N turnover were common, i.e., found in both MT and IL.

Among microbiota involved in N turnover, Firmicutes (31.45%), Bacteroidetes (25.06%), Cyanobacteria (15.83%), Proteobacteria (14.16%), Thaumarchaeota (5.29%), and Ignavibacteriae (2.63%) were the most abundant phyla, and *Chitinophagaceae* (9.34%),

Cytophagaceae (8.49%), *Flavobacteriaceae* (3.10%), *Flammeovirgaceae* (1.69%), *Cyclobacteriacea* (1.11%), and *Polyangiaceae* (1.02%) the most abundant families involved in N turnover (Figure 17). In addition, 13 phyla with an abundance of less than 2% and 59 families with an abundance of less than 1% were involved in N turnover.

Firmicutes, Proteobacteria, Thaumarchaeota, and Ignavibacteriae were prevalent in MT, Cyanobacteria, Fusobacteria, Nitrospirae, and Euryarchaeota in IL, whereas the abundance of Bacteroidetes was comparable in both MT and IL. On the family level, amongst the most abundant families, *Bacillaceae*, *Chitinophagaceae*, *Nitrososphaeraceae*, *Ectothiorhodospiraceae*, and *Clostridiaceae* were more abundant in MT, and *Microchaetaceae*, *Cytophagaceae*, *Flavobacteriaceae* in IL.

Even though the differences on the phylum level were detected, none of them were significant, whereas, on the family level, significant differences between MT and IL were detected only amongst low abundant families such as *Bradyrhizobiaceae* (Bonferroni adjusted unpaired *t*-test, $P = 0.044$), *Alcaligenaceae* (Bonferroni adjusted unpaired *t*-test, $P = 0.041$), *Lentisphaeraceae* (Bonferroni adjusted unpaired *t*-test, $P = 0.020$), and *Gemmatimonadaceae* (Bonferroni adjusted unpaired *t*-test, $P = 0.038$).

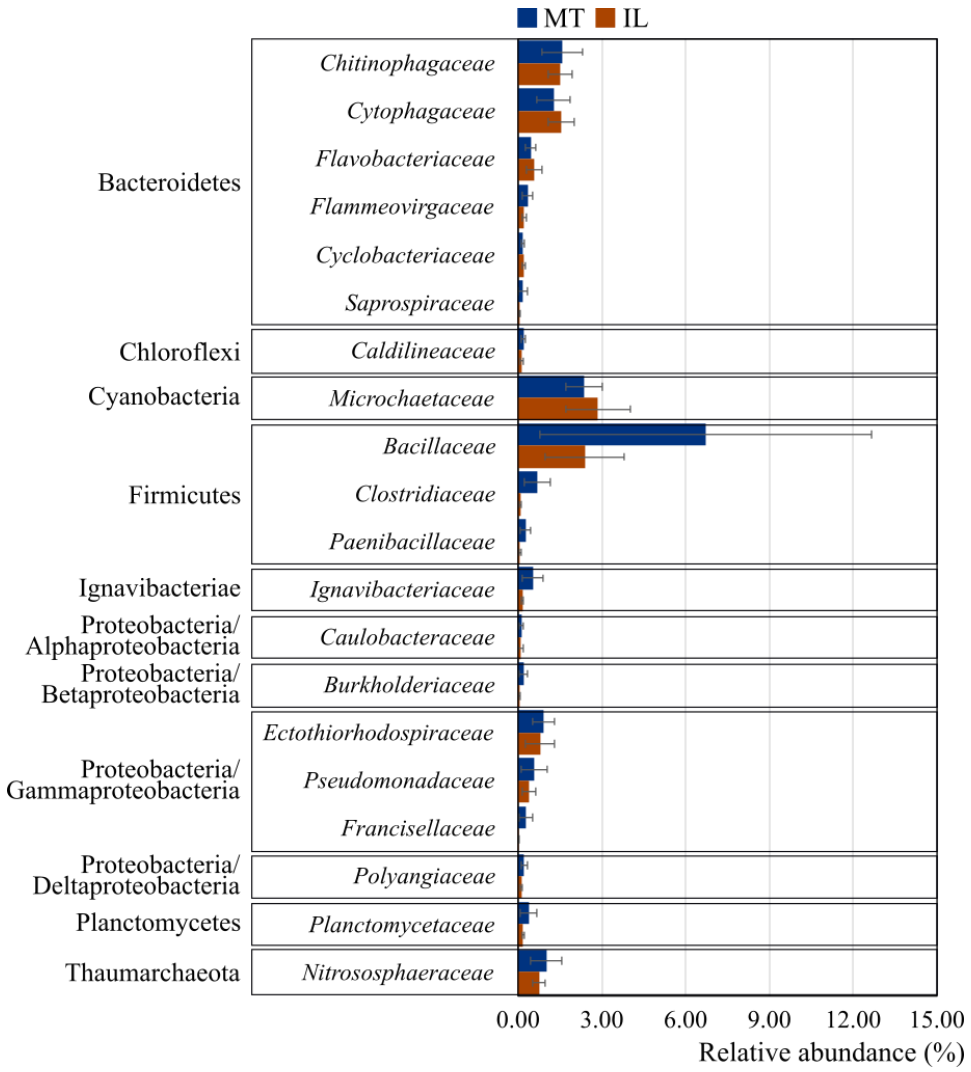

Figure 17. Relative abundance of prokaryotic families involved in N turnover in artificial soils containing MT and IL. Sequences were aligned against the NCBI-nr database and annotated with MEGAN5. Relative abundance was calculated based on the number of all assigned reads. The mean relative abundance with standard deviations (n = 3) of the twenty most abundant taxa is shown.

A total of 27 phyla and 249 families involved in P turnover was detected in MT and IL soils. Of that, 17 phyla and 232 families had a relative abundance above 1.0%. 24 phyla (88.9%) and 172 families (69.1%) were common among microbiota involved in P turnover.

Bacteroidetes (25.23%), Firmicutes (16.49%), Ignavibacteriae (12.15%), and Cyanobacteria (9.44%) were the most abundant phyla, and *Bacillaceae* (11.18%), *Microchaetaceae* (8.89%), *Melioribacteraceae* (8.51%), *Nitrososphaeraceae* (7.50%), *Leptospiraceae* (7.07%), and *Cytophagaceae* (6.17%) were the most abundant families involved in P turnover (Figure 18). Additionally, 6 phyla with abundance above 1%, 17 phyla

with abundance below 1%, and 243 families with abundance lower than 5% were involved in P turnover.

Ignavibacteriae, Firmicutes, Planctomycetes, and Spirochetes were prevalent in MT, and, Bacteroidetes, Chloroflexi, Cyanobacteria, and Thaumarchaeota in IL. On the family level, *Ignavibacteriaceae*, *Melioribacteraceae*, *Bacillaceae*, and *Leptospiraceae* were more abundant in MT, and *Cytophagaceae*, *Flammeovirgaceae*, *Flavobacteriaceae*, *Microchaetaceae*, and *Nitrososphaeraceae* in IL.

Only the abundance of 3 phyla involved in P turnover differed significantly between MT and IL. Firmicutes (Bonferroni adjusted unpaired *t*-test, $P = 0.021$), Ignavibacteriae (Bonferroni adjusted unpaired *t*-test, $P = 0.009$), and Spirochetes (Bonferroni adjusted unpaired *t*-test, $P = 0.013$) were significantly higher in MT. Furthermore, the relative abundance of *Melioribacteraceae* (Bonferroni adjusted unpaired *t*-test, $P = 0.011$) and *Paenibacillaceae* (Bonferroni adjusted unpaired *t*-test, $P = 0.030$) was significantly higher in MT than in IL.

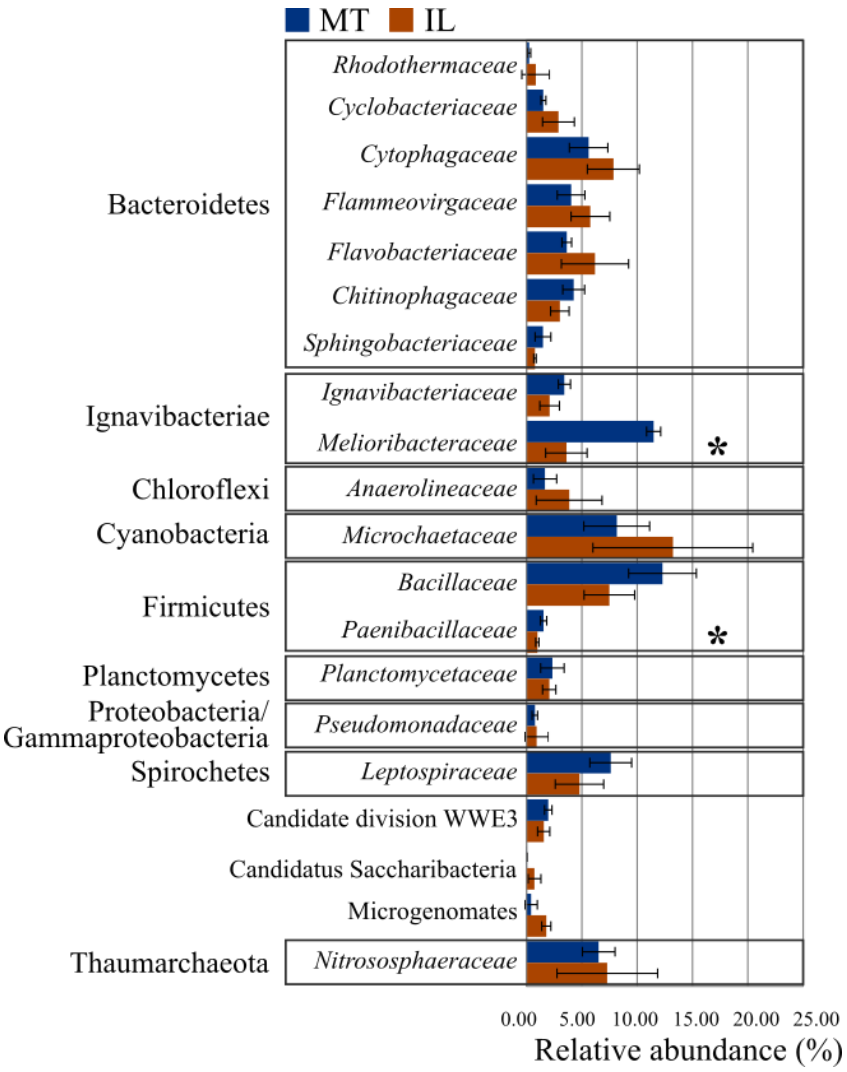

Figure 18. Relative abundance of prokaryotic families involved in P turnover in artificial soils containing MT and IL. Sequences were aligned against the NCBI-nr database and annotated with MEGAN5. Relative abundance was calculated based on the number of all assigned reads. The mean relative abundance with standard deviations (n = 3) of the twenty most abundant taxa is shown. Asterisks indicate significant differences in prokaryotic families involved in P turnover in artificial soils ($P < 0.05$).

4.2.4. Functional analysis of artificial soil

The functional annotation of reads from soils containing montmorillonite and illite was performed by aligning the subsampled dataset against the KEGG database (Kanehisa and Goto, 2000) and visualizing the results with MEGAN5 (Huson et al., 2011). In total 843,312 sequences were assigned.

A rarefaction analysis based on KO identifiers revealed the similar functional richness of both metagenomes (Figure 19).

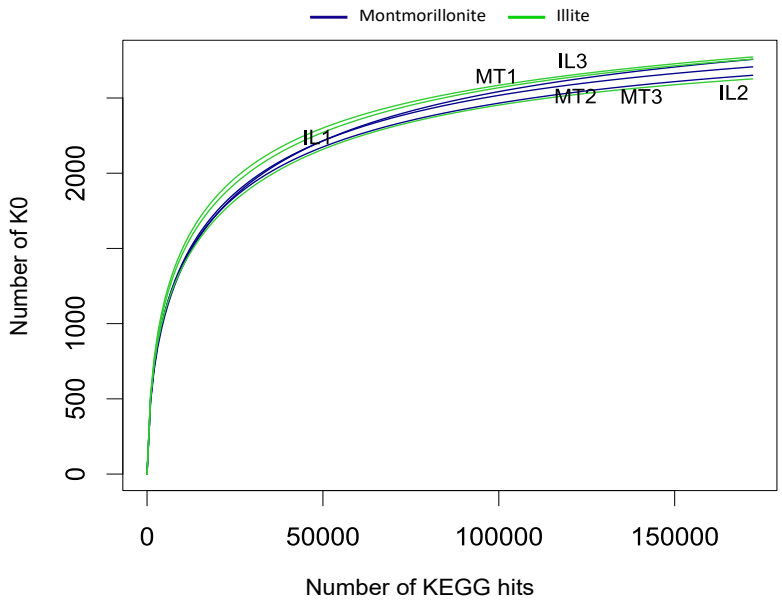

Figure 19. Rarefaction curves based on KO-Ids identified in montmorillonite and illite-containing artificial soils. Depicted is the number of observed KO ID of subsampled KEGG hits where the amount of KEGG hits was randomly chosen from the metagenome for each replicate.

The analysis of level 2 revealed that 68.08% of reads could be assigned. From assigned reads, the majority of the reads belonged to the global metabolism (35.66%), genetic (12.69%), and environmental information processes (6.73%) where only nucleotide metabolism was significantly higher in MT (Bonferroni adjusted unpaired *t*-test, $P < 0.01$) (Figure 20). Further analysis was focused on the genes involved in global metabolism. Most of the metabolic pathways were present in both artificial soils. The functional Shannon diversity index calculated for the detected genes involved in the global metabolism was higher for illite throughout all KEGG levels. However, a significant difference was observed only on level 5 (6.652 ± 0.050 and 6.537 ± 0.033 in montmorillonite and illite, respectively; $P = 0.036$).

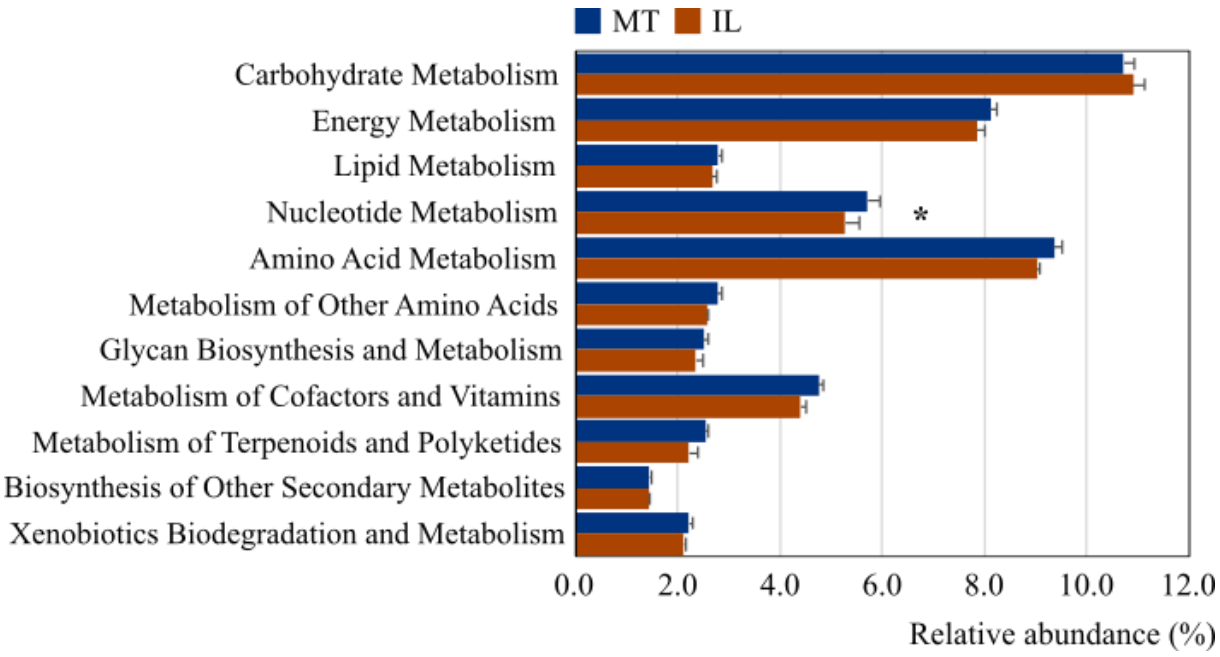

Figure 20. Metabolic and functional diversity in artificial soils containing montmorillonite (MT) and illite (IL). Sequences were aligned against the KEGG database and annotated with MEGAN5. Relative abundance was calculated based on the number of all assigned KEGG reads. The mean relative abundance with standard deviations (n = 3) is shown. Asterisks indicate significant differences in metabolic and functional diversity in artificial soils ($P < 0.05$).

Although none of the metabolic pathways and genes was unique for a certain mineral composition the analysis of KEGG level 5 revealed several significant differences that indicated that microbial communities inhabiting both artificial soils were well adapted to the degradation of easily available carbon substrates through different pathways. The relative abundance of genes related to the glycolysis and pentose-phosphate pathway was significantly higher in montmorillonite, and that involved in fructose, mannose, galactose, starch, and sucrose metabolism in illite. Furthermore, genes involved in the carbon fixation, fatty acid, glycerolipid, and amino acid (e.g., glycine, serine, threonine, etc.) metabolism, were significantly more abundant in montmorillonite. In contrast, energy metabolism in illite is maintained, in addition to the already mentioned pathways, through methane and other amino acids (e.g., alanine, aspartate, glutamate) metabolism. Genes involved in nutrient cycles that are normally energy consuming (e.g., N cycle) were detected in very low abundance.

Further analysis focused on the genes involved in microbial carbon, nitrogen, and phosphorus turnover.

4.2.5. Gene abundance and microbial groups harbouring genes involved in the carbon turnover

To assess the potential and identify major processes involved in carbon turnover in early phases of soil development with different types of clay minerals genes involved in C degradation, C fixation, and methane metabolism were investigated. In total, 13,149 reads were assigned to the genes predicted to encode enzymes involved in the C cycle. Of 37 investigated genes, 22 genes were detected in both MT and IL (Figure 21). The majority of reads were assigned to the genes involved in the C degradation (12,404), followed by the C fixation (733), whereas methane metabolism (2) can be considered undetectable.

Amongst all detected genes, only *amyA* encoding alpha-amylase was significantly higher in IL (Bonferroni adjusted unpaired *t*-test, P=0.03). In addition, *nagZ/hexA-B/hex* genes encoding exochitinase, *nplT* encoding neopullulanase, and polygalacturonase were more abundant in MT. All other detected genes were more abundant in IL and encoded enzymes involved in cellulose, hemicellulose, chitin, and starch degradation, i.e. endoglucanase (*celB*) and cellobiohydrolase (*CBH1*); arabinofuranosidases (*abfA*); endochitinase (*chiA/CHIT1*); and glucoamylase (*SGA1*). However, none of those differences in abundance were significant. Lastly, genes associated with C fixation (*aclA/aclB, coxL/coxM/coxS, cooS, rbcL/rbcS*) were found in nearly the same relative abundance in both MT and IL.

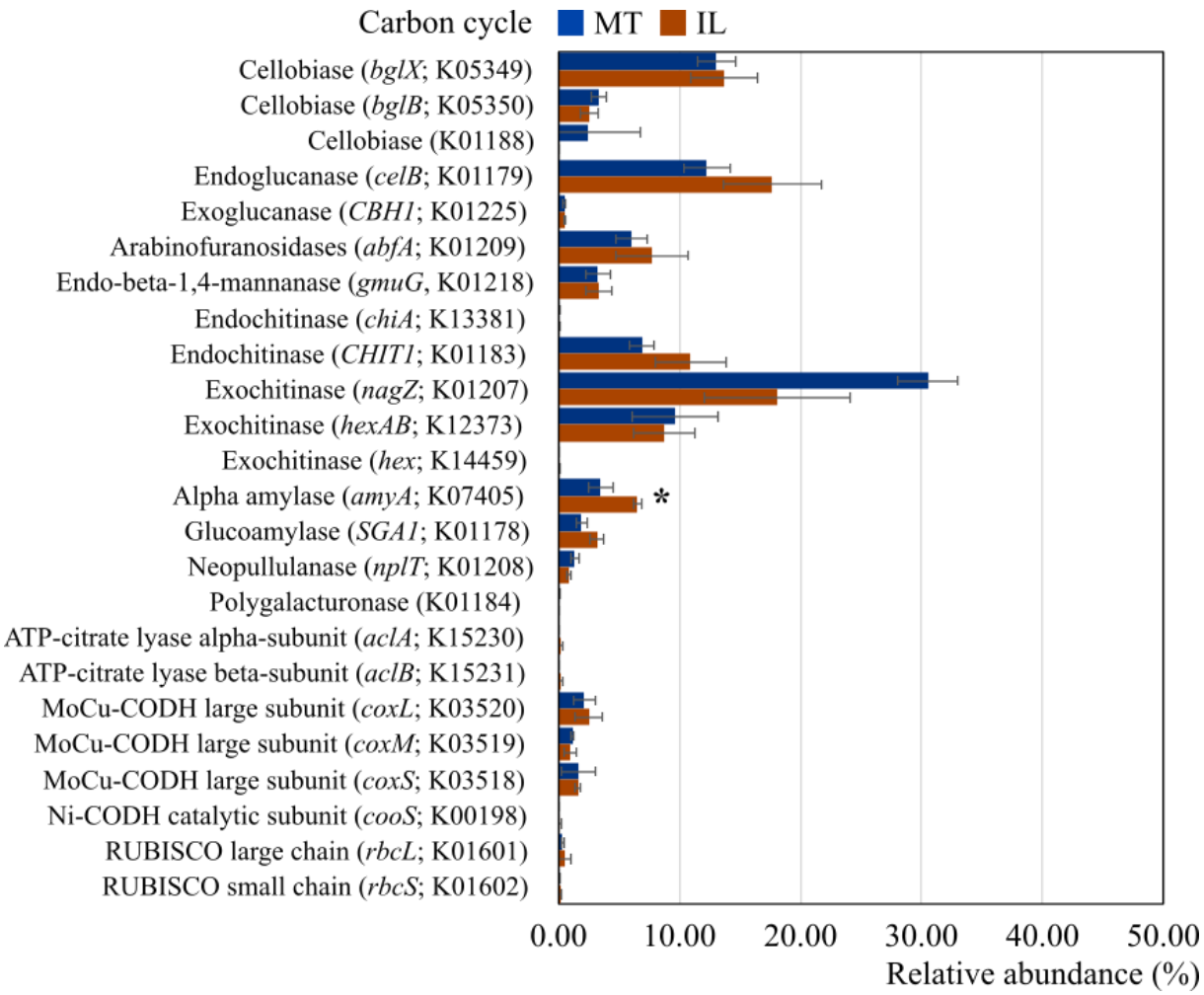

Figure 21. Relative abundance of enzymes involved in carbon turnover in artificial soils containing MT and IL. Obtained sequences were aligned against the KEGG database and annotated with MEGAN5. Relative abundance was calculated based on the number of reads assigned to the C cycle. The mean relative abundance with standard deviations (n = 3) of predicted genes involved in (A) cellulose, (B) hemicellulose, (C) chitin, (D) starch, and (E) pectin metabolism, and (F) C fixation is shown. Asterisks indicate significantly different ($P < 0.05$) annotated reads in the artificial soils containing MT and IL.

To identify a possible correlation between the abundance of genes involved in C cycling, and pH and C:N:P stoichiometry in MT and IL, a Spearman correlation analysis was performed.

In MT and IL the abundance of genes involved in the C cycle was correlated to both pH, and the C:N:P stoichiometry, including OC, total N, and P, P_{NaHCO3}, P_i, P_o, and all C:N:P ratios (Figure 22).

pH showed mostly negative relationships in MT, and mostly positive in IL with genes involved in the C cycle. In MT, pH was positively correlated only with predicted genes involved in hemicellulose (*abfA, gmuG*), chitin degradation (*chiA/CHIT1, nagZ/hexA-B, hex*), starch (*nplT*), and C fixation (*coxL/coxM/coxS*), and negatively with genes involved in cellulose (*bglX/bglB, celB, CBH1*), starch (*amyA, SGA1*), and pectin degradation (polygalacturonase), and genes encoding RUBISCO (*rbcL/rbcS*). Contrary, in IL all genes involved in cellulose degradation (*bglX/bglB, celB, CBH1*), and C fixation (*aclA/aclB, coxL/coxM/ coxS, rbcL/rbcS*) were positively correlated to the pH. Furthermore, some genes involved in hemicellulose (*gmuG*), chitin (*chiA/CHIT1*), and starch (*amyA, nplT*) degradation were also positively correlated to the pH. Other genes were negatively correlated with pH in IL.

In MT the impact of total C, N, and P contents was similar to the impact of C:N:P ratios on the abundance of genes involved in the C cycle, and they showed a mostly positive relationship, whereas in IL the impact of total C, N, and P contents was stronger than the impact of C:N:P ratios, and mostly negative. In MT soil C:N ratio showed a negative relationship with cellulose, starch, and pectin degradation, and with the abundance of genes encoding RUBISCO, whereas C:P and N:P ratios showed the opposite trend. In IL, on the other hand, the C:N ratio positively influenced the abundance of all genes involved in cellulose degradation, and C fixation, and some genes involved in hemicellulose (*gmuG*), and starch degradation (*chiA/CHIT1*). C:P, and N:P showed mostly opposite trend with exception of *bglx/bglB*, *abfA*, *amyA*, *SGA1*, *nplT*, and *coxL/ coxM/coxS*. Both in MT and IL, pH, total C, N, and P contents, and their ratios showed significant relationships with the abundance of genes involved in the C cycle ($P < 0.05$) with few exceptions.

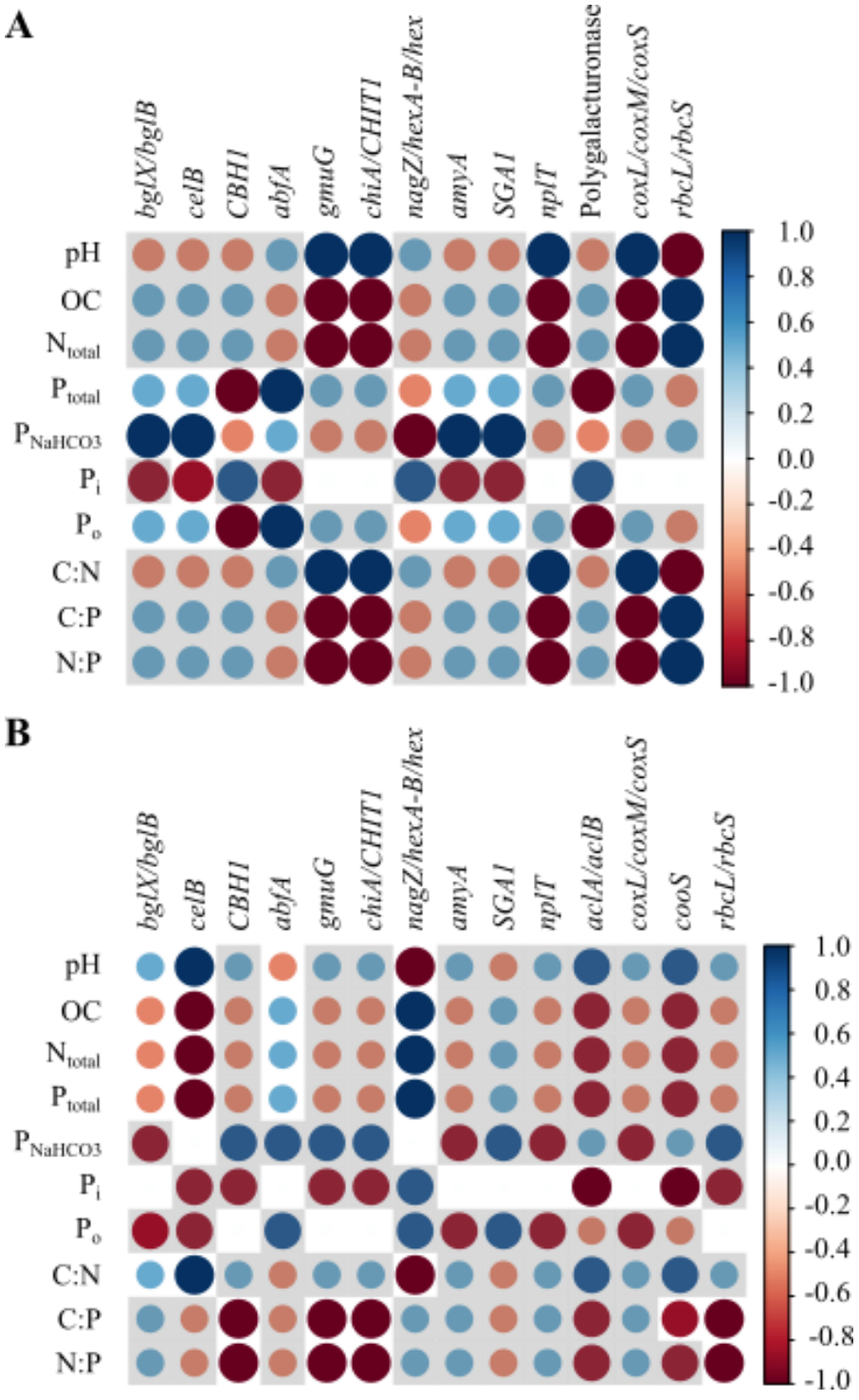

Figure 22. Correlation between the abundance of genes involved in cellulose (*bglX/bglB*, *celB*, *CBH1*), hemicellulose (*abfA*, *gmuG*), chitin (*chiA/CHIT1*, *nagZ/hexA-B/hex*), starch (*amyA*, *SGA1*, *nplT*), and pectin (polygalacturonase) degradation, and carbon fixation (*aclA/aclB*, *coxL/coxM/coxS*, *cooS*, *rbcL/rbcS*), and soil pH, and C:N:P stoichiometry in artificial soils containing (A) MT and (B) IL. Blue colours represent the positive, and red negative correlation. Darker colour and larger circle diameter indicate a stronger correlation. White squares indicate the absence of correlation. Grey squares indicate significant correlation ($P < 0.05$).

In order to identify key microbial drivers of carbon turnover in artificial soils (MT and IL), the 22 detected genes associated with the C cycle were extracted from the KEGG annotated dataset. Those reads were then taxonomically annotated with the DIAMOND and NCBI-nr protein sequence database. The most abundant families involved in C cyle, in both soils, belonged to the most abundant families in general, such as *Cytophagaceae* (19.45%), *Bacillaceae* (13.67%), *Flammeovirgaceae* (7.01%), *Rhodothermaceae* (6.91%), *Flavobacteriaceae* (6.47%), and *Microchaetaceae* (6.35%) (Figure 16, Figure 23). Microbiota from both artificial soils had a potential for the degradation of recalcitrant carbon sources such as hemicellulose, cellulose, and chitin, and a labile carbon source such as starch. The potential for pectin degradation and methane metabolism was detected only in MT-containing soil. Several families, including *Cytophagaceae*, *Bacillaceae*, *Flammeovirgaceae*, *Paenibacillaceae*, and *Streptomycetaceae*, could potentially cover almost all processes, with exception of pectin degradation and methane metabolism.

In detail, in MT the cellulose degradation was driven by *Bacillaceae, Cytophagaceae*, *Microchaetaceae*, *Flavobacteriaceae*, and *Alteromonadaceae*; hemicellulose degradation by *Bacillaceae*, *Trueperaceae*, *Paenibacillaceae*, *Alteromonadaceae*, and *Opitutaceae*; chitin degradation by *Rhodothermaceae*, *Cytophagaceae*, *Flammeovirgaceae*, and *Bacillaceae*; starch degradation by *Cytophagaceae*, *Bacillaceae*, and *Cyclobacteriaceae*; and pectin degradation by *Acidobacteriaceae* and *Burkholderiaceae*.

Similar families were involved in the C cycle in IL. For example, *Cytophagaceae, Bacillaceae, Marinilabiliaceae*, *Alteromonadaceae,* and *Microchaetaceae* showed the cellulose degradation potential; *Flavobacteriaceae*, *Alteromonadaceae*, *Trueperaceae*, *Flammeovirgaceae*, and *Paenibacillaceae* hemicellulose degradation potential; *Cytophagaceae* chitin degradation potential; and *Cytophagaceae* and *Cyclobacteriaceae* starch degradation potential.

The potential for C fixation was detected in similar families in both MT and IL. *Bacillaceae* and *Anaerolineaceae* harboured predicted genes that encode RUBISCO.

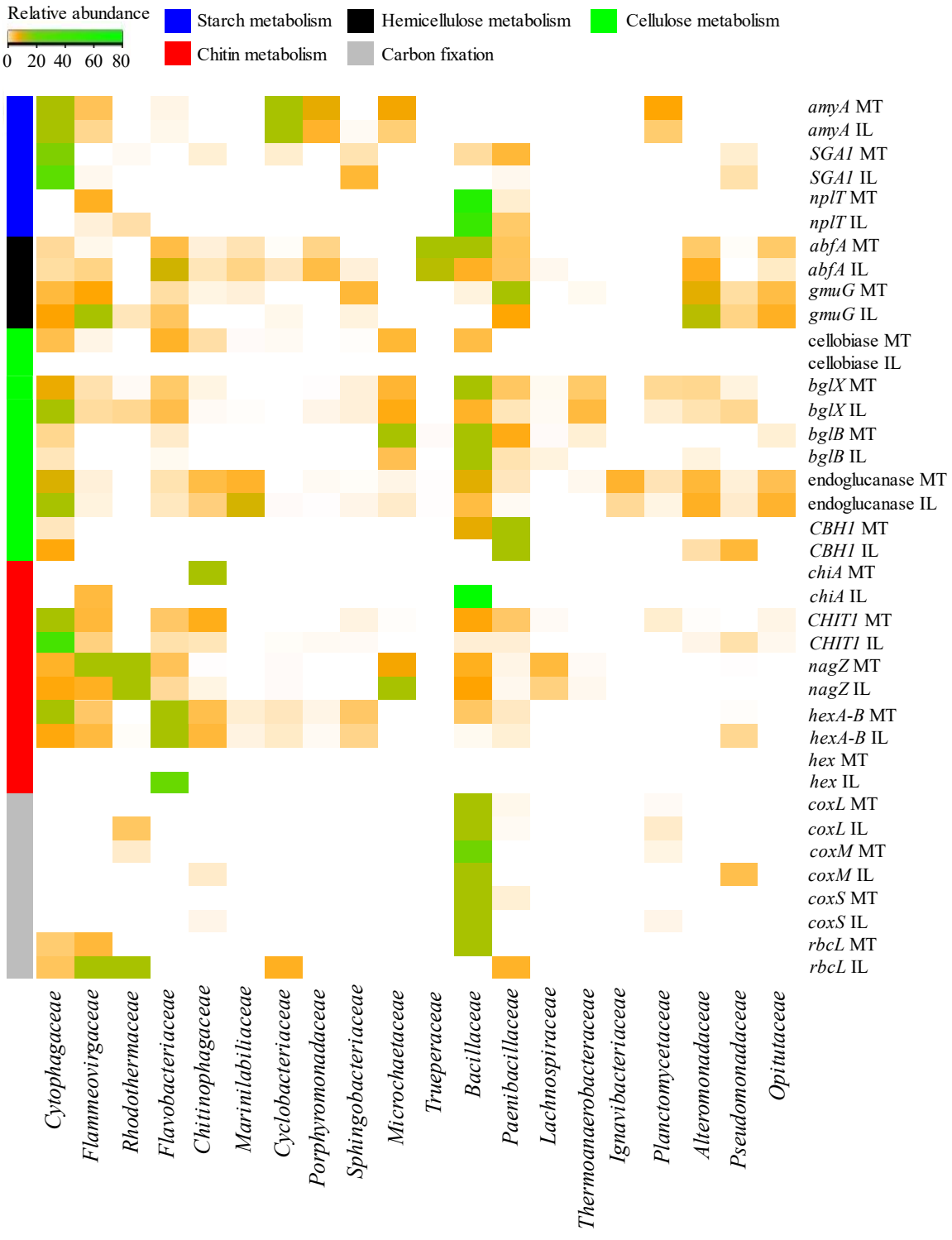

Figure 23. Relative abundance of prokaryotic families involved in the carbon cycle in the artificial soils containing MT and IL. Obtained sequences were assigned on the functional level by aligning against KEGG, and on the taxonomic level against the NCBI-nr database. Relative abundances were calculated based on the number of reads assigned to the C cycle. The colour intensity in the heatmap represents the relative abundance of families associated with a C cycle in montmorillonite and illite. Twenty most abundant families are depicted.

Predicted genes involved in the C cycle were found in 160 different families. Most of the families predicted to be involved in C turnover were common for both MT and IL (Figures 24 and 25).

Amongst the 50 most abundant families, 43 families were involved in cellulose degradation, 30 in hemicellulose degradation, 37 in chitin degradation, and 22 in starch degradation in both MT and IL. In addition, 18 families predicted to be involved in carbon fixation were shared between MT and IL.

In general, the relative abundance of unique families was very low, and similar diversity of unique families was found in both MT and IL. Unique families were involved in the same processes of C turnover as the shared families, namely recalcitrant and more easily degradable C compounds, and C fixation.

Unique families potentially involved in cellulose degradation in MT belonged to the families *Saprospiraceae*, *Amoebophilaceae*, *Gemmatimonadaceae*, and *Vibrionaceae*, whilst none were found in IL. Unique families predicted to be involved in hemicellulose degradation included *Micromonosporaceae*, *Thermoanaerobacteraceae*, *Melioribacteraceae*, and *Vibrionaceae* in MT, and *Pseudonocardiaceae*, *Rhodothermaceae*, *Rikenellaceae*, *Lachnospiraceae*, and *Phyllobacteriaceae* in IL. Finally, *Amoebophilaceae*, *Anaerolineaceae*, *Planctomycetaceae*, *Burkholderiaceae*, and *Desulfovibrionaceae* in MT, and *Caldilineaceae*, *Roseiflexaceae*, *Bradyrhizobiaceae*, *Xanthomonadaceae*, and *Thermotogaceae* in IL were unique families predicted to be involved in chitin degradation (Figure 24).

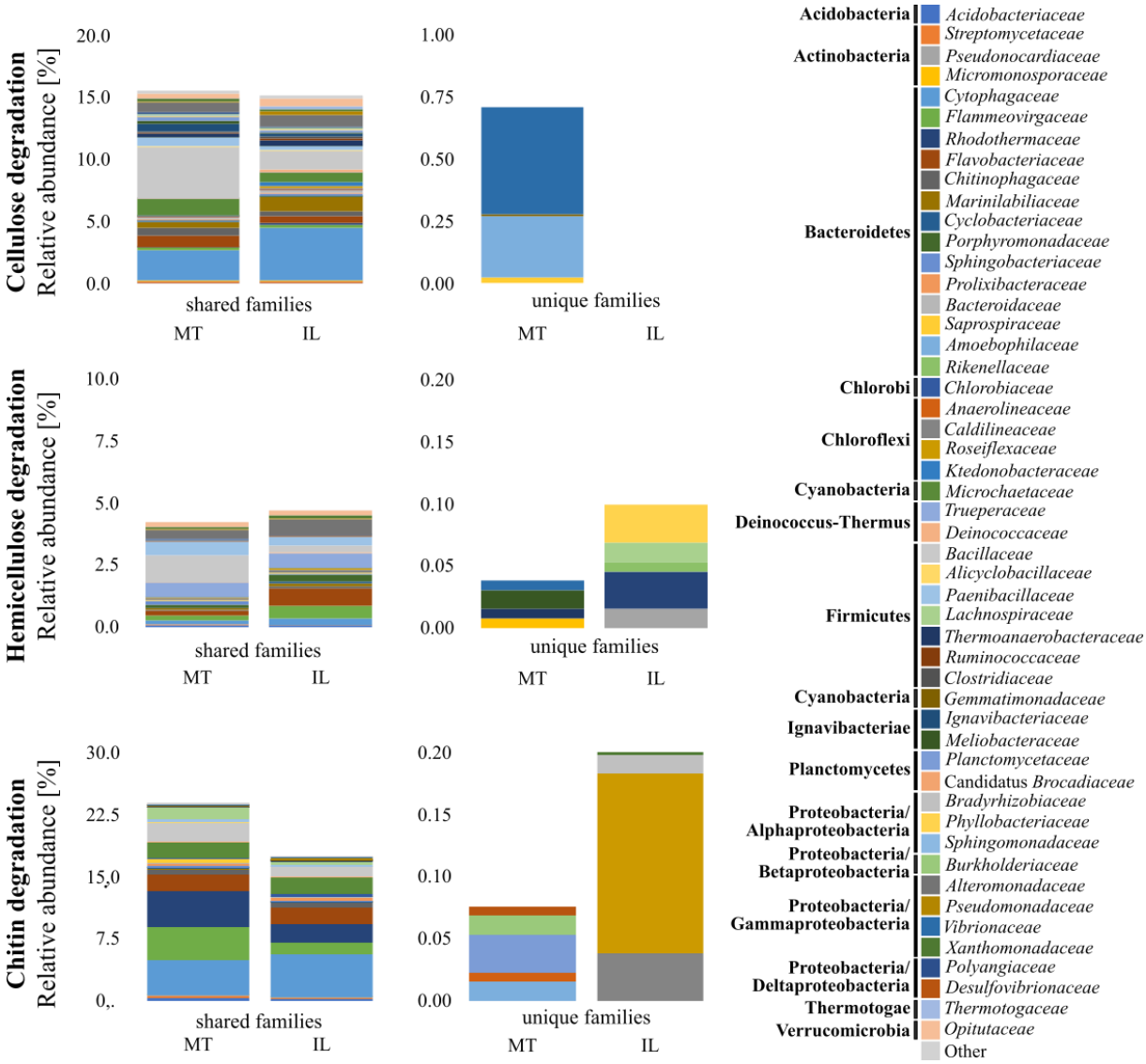

Figure 24. Distribution of shared and unique families involved in the C cycle in the artificial soils containing montmorillonite (MT) and (IL). The reads were functionally assigned with KEGG and taxonomically with the NCBI-nr database. Shown are the mean values of the most abundant families involved in cellulose, hemicellulose, and chitin degradation. Relative abundances were based on the number of all reads assigned to the C cycle.

Unique families predicted to be involved in the degradation of more easily degradable C compounds, such as starch included *Pseudonocardiaceae*, *Chitinophagaceae*, *Burkholderiaceae*, and *Xanthomonadaceae* in MT, and *Acidobacteriaceae*, *Bacteroidaceae*, *Ruminococcaceae*, and *Vibrionaceae* in IL. Predicted families (*Acidobacteriaceae* and *Burkholderiaceae*) involved in pectin degradation were only detected in MT. In MT unique families predicted to be involved in C fixation included only

Roseiflexaceae, and in IL *Chitinophagaceae*, *Cyclobacteriaceae*, *Ktedonobacteraceae*, *Ruminococcaceae*, and *Pseudomonadaceae*. Only one family, which belonged to low abundant taxa, *Mycobacteriaceae*, predicted to be involved in methane metabolism was found in MT (Figure 25).

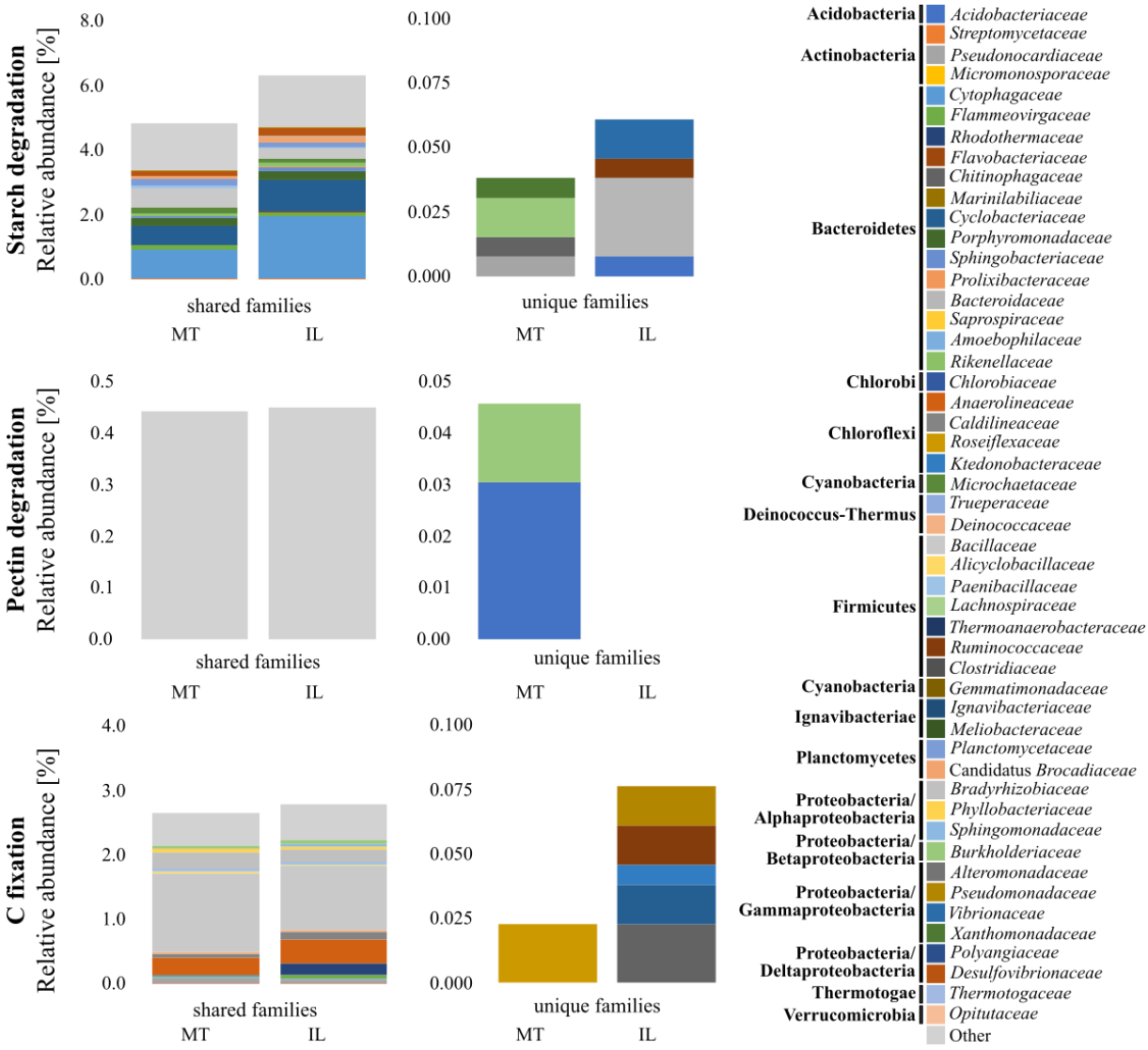

Figure 25. Distribution of shared and unique families involved in the C cycle in the artificial soils containing montmorillonite (MT) and (IL). The reads were functionally assigned with KEGG and taxonomically with the NCBI-nr database. Shown are the mean values of the most abundant families involved in starch, and pectin degradation, and C fixation. Relative abundances were based on the number of all reads assigned to the C cycle.

Although families predicted to be involved in C turnover were very diverse only 9 families predicted to be involved in C turnover were significantly different, with *Cytophagaceae* (*P* = 0.044), *Sphingobacteriaceae* (*P* = 0.028), *Bacillaceae* (*P* = 0.045), and *Paenibacillaceae* (*P* = 0.006) belonging to the twenty most abundant families.

4.2.6. Gene abundance and microbial groups harbouring genes involved in the nitrogen cycle

To assess the potential and identify major processes involved in the nitrogen cycle in early phases of soil development with different types of clay minerals genes involved in N mineralization (depolymerisation/ammonification), immobilization, denitrification, dissimilatory (DNRA), and assimilatory (ANRA) nitrate reduction, nitrification, N_2 fixation, and nitrite and nitrate uptake were investigated. In total, 27,168 reads were assigned to the genes predicted to encode enzymes involved in the N cycle. Of 82 investigated genes, 49 genes were detected in both MT and IL (Figure 26). Most of the reads were assigned to the genes involved in the N mineralization (10,666), followed by the N immobilization (9,506), denitrification (4,649), DNRA (1,686), ANRA (763), and nitrate/nitrite uptake (450), whereas the abundance of genes involved in nitrification (33) was very low.

The relative abundance of all predicted genes involved in N transformations are shown in the Figure 26.

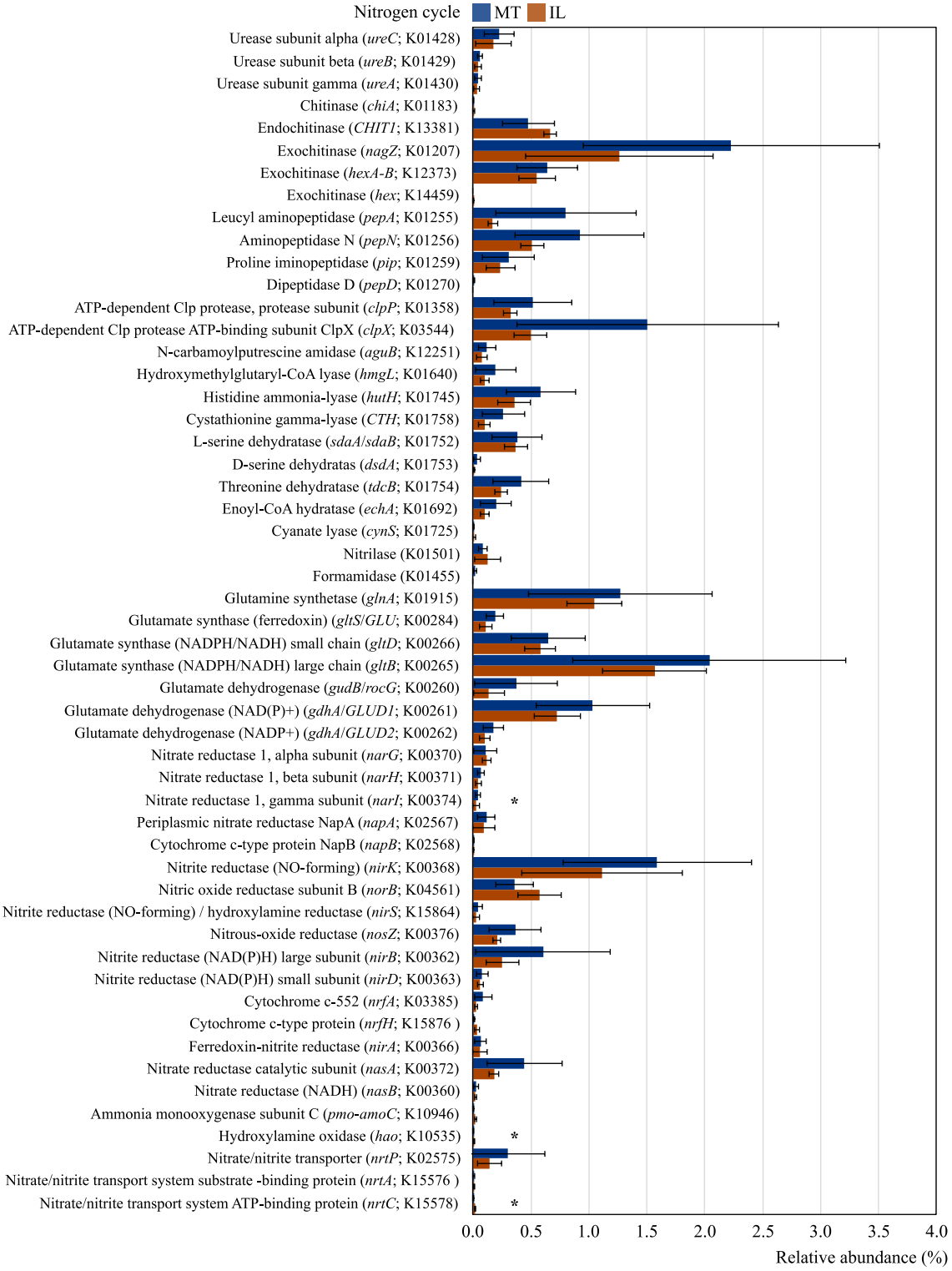

Figure 26. Relative abundance of predicted prokaryotic genes encoding enzymes involved in the nitrogen cycle in artificial soils containing MT and IL. Obtained sequences were aligned against the KEGG database and annotated with MEGAN5. Relative abundance was calculated based on the number of all assigned KEGG reads. Values are shown as the mean with standard deviation (n = 3). Asterisks indicate significant differences (P<0.05) in the number of annotated reads between the MT and IL soils.

In general, all N transformations, with exception of nitrification, were more pronounced in MT than in IL. For example, the abundance of all genes encoding proteolytic (*pepA, pepN, pepD, pip, clpP, clpX, aguB, hmgL, hutH, CTH, sdaA/sdaB, dsdA, tdcB*,) and ureolytic enzymes (*urea, ureB*, and *ureC*) were always higher in MT, and only predicted genes encoding mineralization of alternative organic N sources, such as chitin (*chiA*, *CHIT1*) and nitrile were dominant in IL. Furthermore, the abundance of predicted genes encoding enzymes involved in denitrification (nitrate reductase - *narH*; periplasmatic nitrate reductase - *napA/napB*; nitrite reductase – *nirK/nirS*; and nitrous-oxide reductase - *nosZ*), DNRA nitrate reduction (nitrite reductase - *nirB/nirD*; cytochrome c-522 - *nfrA*), ANRA nitrate reduction (ferredoxin-nitrite reductase – *nirA*; nitrate reductase - *nasA/nasB*), and nitrite/nitrate uptake (nitrate/nitrite transporter - *nrtP*) was always higher in MT. However, none of these predicted genes differed significantly at the significance level of 5%. Contrary, the abundance of predicted genes encoding enzymes involved in denitrification (nitrate reductase - *narI*), nitrification (ammonia monooxygenase - *amoC*; hydroxylamine oxidase - *hao*), and nitrite/nitrate uptake (nitrate transporter – *nrtA/nrtC*) was significantly higher in IL containing soil (Bonferroni adjusted *t*-test, P=0.04, P=0.01, and P=0.03, respectively). Finally, N assimilation was dominant in MT, where all predicted genes encoding enzymes involved in glutamate synthesis, glutamate synthetase (*glnA*), glutamate synthase (*gltS, gltD, gltB*), and glutamate dehydrogenase (*gudB/rocG, gdhA/GLUD1, gdhA/GLUD2*) were more abundant in MT than in IL.

To identify a possible correlation between the abundance of genes involved in N cycling, and pH and C:N:P stoichiometry in MT and IL, a Spearman correlation analysis was performed.

In MT and IL the abundance of genes involved in the N cycle was correlated to both pH, and the C:N:P stoichiometry, including total OC, N, and P, P_{NaHCO3}, P_i, P_o, and all C:N:P ratios. In general, the impact of pH and C:N:P stoichiometry on gene abundance was stronger in MT than in IL. In MT, pH showed negative relationships with all genes involved in the N cycle in MT, and mostly positive in IL. Only with few genes involved in the N cycle showed a negative relationship with pH (*nirK/nirS, norB/norC, nasA/nasB*) in IL. C:N:P stoichiometry showed opposite relationships in MT and IL. C:N showed the same trend as pH in both soils, with a strong negative relationship with all genes involved in the N cycle in MT, and a mostly positive relationship with few exceptions (*chiA*, *nirK/nirS, norB/norC, nasA/nasB*) in IL. C:P and N:P were positively related to all genes involved in the N cycle in MT. In IL, C:N and N:P showed the same effect on N cycling genes, where negative relationships were predominant. C:N and N:P were positively correlated only with *pepA, pepN, pip, pepD, clpP, clpX, nirK/nirS, nosZ, nirB/nirD, nirA*, and *nrt* in IL.

Both in MT and IL, pH, total C, N, and P contents, and their ratios showed significant relationships with the abundance of genes involved in the N cycle ($P < 0.05$) with few exceptions (Figure 27).

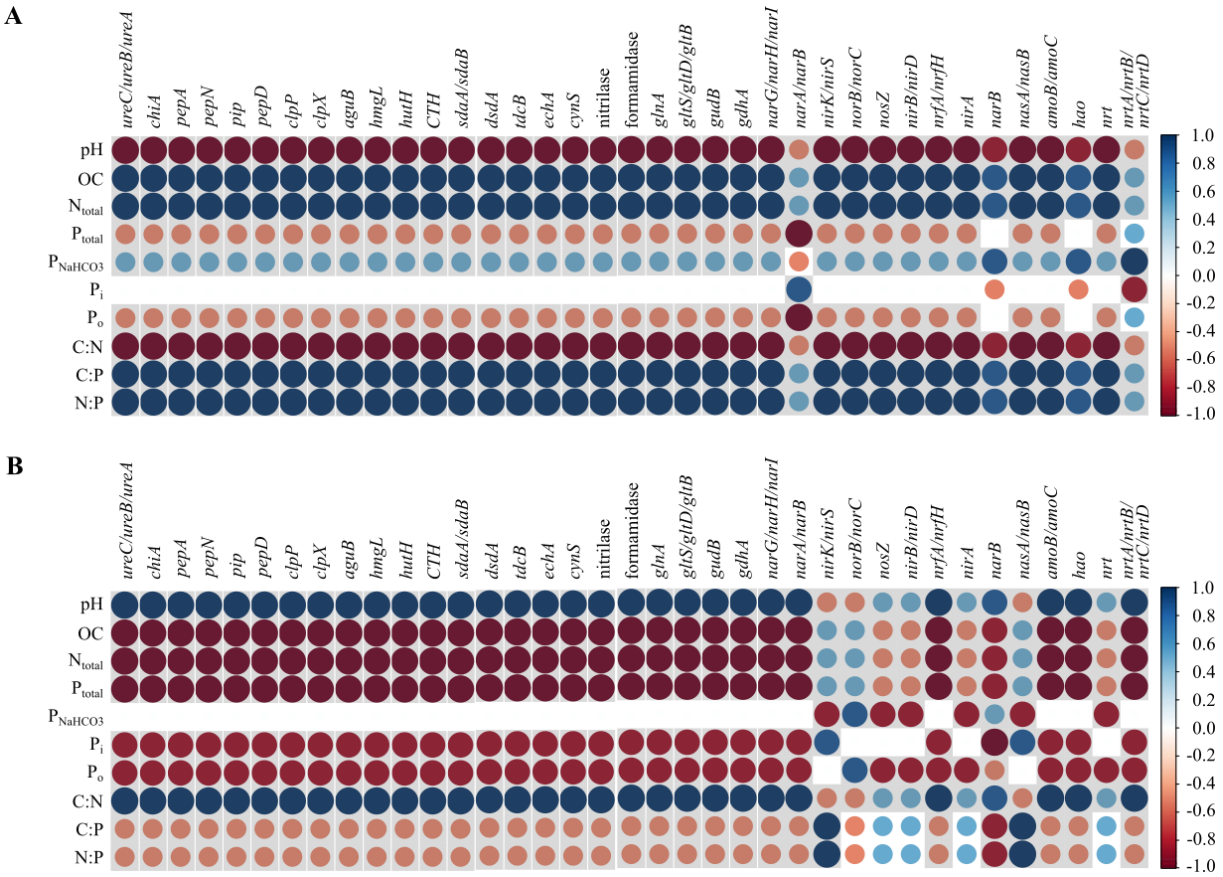

Figure 27. Correlation between the abundance of genes involved in depolymerisation/ammonification (*ureC/ureB/urea, chiA, pepA, pepN, pip, pepD, clpP, clpX, aguB, hmgL, hutH, CTH, sdaA/sdaB, dsdA, tdcB, echA, cynS,* nitrilase, formamidase), N assimilation (*glnA, gltS/gltD/gltB, gudB, gdhA*), denitrification (*narG/narH/narI*, *narA/narB*, *nirK/nirS*, *norB/norC*, *nosZ*), dissimilatory nitrate reduction (*nirB/nirD*, nrfA/nrfH), assimilatory nitrate reduction (*nirA*, *narB*, *nasA/nasB*), nitrification (*amoB/amoC*, *hao*), and nitrite and nitrate uptake (*nrt*, *nrtA/nrtB/nrtC/nrtD*), and soil pH, and C:N:P stoichiometry in artificial soil containing (A) MT and (B) IL. Blue colours represent the positive, and red negative correlation. Darker colour and larger circle diameter indicate a stronger correlation. White squares indicate the absence of correlation. Grey squares indicate significant correlation ($P < 0.05$).

To identify key microbial drivers of N turnover in MT and IL, the 82 detected genes associated with the N turnover were extracted from the KEGG annotated dataset and taxonomically annotated with DIAMOND and NCBI-nr protein sequence database.

The most abundant families involved in N turnover, in MT and IL, belonged to the most abundant families, including *Bacillaceae* (35.78%), *Ectothiorhodospiraceae* (16.86%), *Chitinophagaceae* (9.40%), *Flavobacteriaceae* (5.16%), *Pseudomonadaceae* (4.68%), *Cytophagaceae* (2.69%), *Nitrososphaeraceae* (2.66%), and *Caulobacteraceae* (2.25%). Additional 5 families involved in N turnover with relative abundance > 1% were detected (Figure 17, Figure 28). Microbiota in both artificial soils had a potential for denitrification, DNRA, ANRA, nitrification, and nitrate/nitrite uptake.

Unlike the microbiota that drove C turnover, in MT and IL the N turnover was driven by very similar families. The denitrification was driven by *Bacillaceae, Ectothiorhodospiraceae*, *Chitinophagaceae*, *Flavobacteriaceae*, and *Pseudomonadaceae* in MT and IL. In MT the DNRA was driven by *Bacillaceae*, *Flavobacteriaceae*, *Pseudomonadaceae*, *Nitrososphaeraceae*, and *Planctomycetaceae*, and in IL by *Bacillaceae*, *Flavobacteriaceae*, *Pseudomonadaceae*, *Cytophagaceae*, and *Planctomycetaceae*. ANRA was driven by *Bacillaceae*, *Flavobacteriaceae*, *Nitrososphaeraceae*, and *Planctomycetaceae* in MT and IL. Additional taxa that drove ANRA in MT, belonged to the family *Cytophagaceae*, and in IL to *Cyclobacteriaceae*. Only three families, *Flavobacteriaceae*, *Nitrososphaeraceae*, and *Nitrosomonadaceae* drove nitrification in MT and IL. Finally, *Bacillaceae*, *Pseudomonadaceae*, *Cytophagaceae*, *Paenibacillaceae*, and *Flammeovirgaceae* drove nitrate/nitrite uptake in MT, and *Bacillaceae*, *Ectothiorhodospiraceae*, *Pseudomonadaceae*, *Cytophagaceae*, and *Flammeovirgaceae* drove nitrate/nitrite uptake in IL.

Flavobacteriaceae, *Paenibacillaceae*, and *Flammeovirgaceae* could potentially cover all processes involved in N turnover.

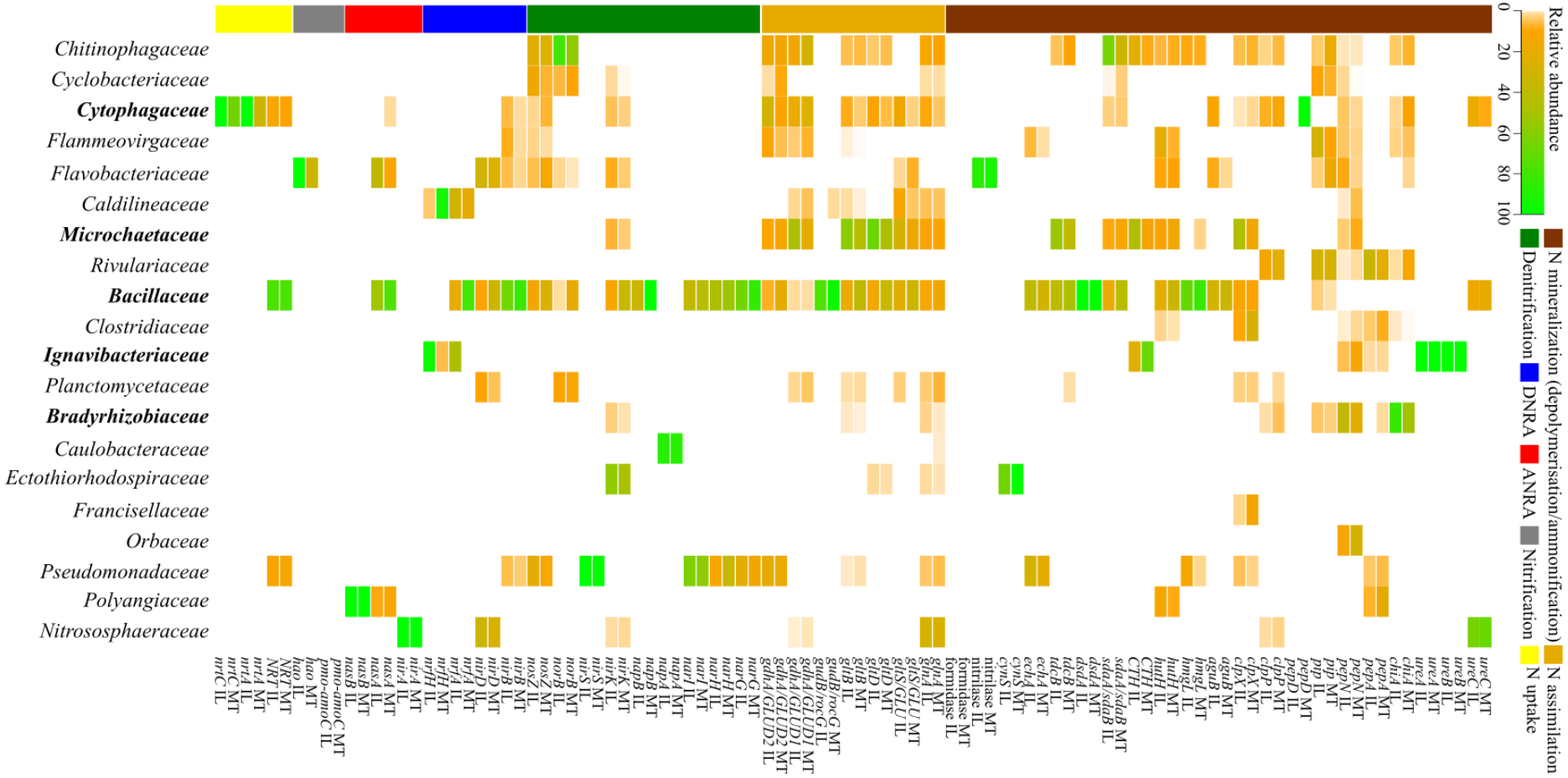

Figure 28. Relative abundance of prokaryotic families involved in the nitrogen cycle in the artificial soils containing MT and IL. Obtained sequences were assigned on the functional level by aligning against the KEGG database, and on the taxonomic level against the NCBI-nr database. Relative abundances were calculated based on the number of reads assigned to the N cycle. The colour intensity in the heatmap represents the relative abundance of families associated with the N cycle in montmorillonite and illite. Twenty most abundant families are depicted.

Predicted genes involved in the N turnover were found in 73 different families. Most of the families predicted to be involved in N turnover were found in both MT and IL (Figure 29).

Amongst the 50 most abundant families, 41 families were involved in depolymerisation/ammonification, 27 in N assimilation, 20 in denitrification, 16 in DNRA, 4 in ANRA, 2 in nitrification, and 3 in nitrate/nitrite uptake in both MT and IL. In MT and IL, all N transformations were driven mostly by *Bacillaceae*, *Cytophagaceae*, *Microchaetaceae*, and *Nitrosomonadaceae.*

As the abundance of unique families involved in C and P turnover, the relative abundance of unique families involved in N turnover was very low. The unique families involved in N turnover were only found in MT (number of unique families involved in mineralization: 1; N assimilation: 3; denitrification: 1; ANRA: 1), and none in IL. Amongst the 50 most abundant families, nitrification, DNRA, and N uptake were driven only by shared families.

Unique families potentially involved in N mineralization in MT belonged to the families *Alcaligenaceae*, *Amoebophilaceae*, *Anaerolineaceae*, *Planctomycetaceae*, *Burkholderiaceae*, and *Desulfovibrionaceae*, and in IL to families *Caldilineaceae*, *Roseiflexaceae*, *Bradyrhizobiaceae*, *Xanthomonadaceae*, and *Thermotogaceae*. Furthermore, *Caulobacteraceae*, *Alcaligenaceae*, and *Moraxellaceae* were the unique families that drove N assimilation, and *Cytophagaceae* ANRA in MT, whereas only denitrification was driven by a rare family *Gemmatimonadaceae*. (Figure 29).

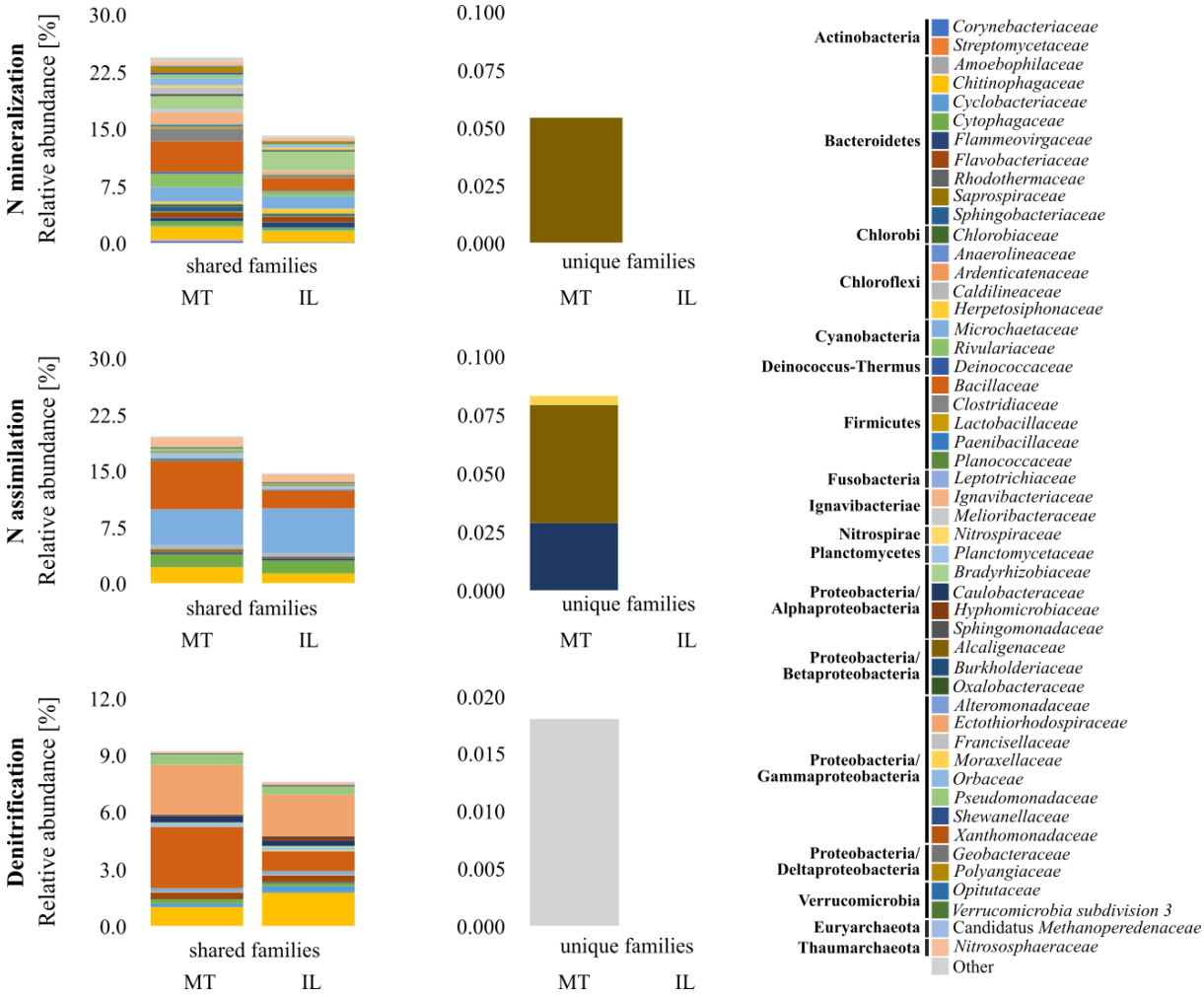
N mineralization
Relative abundance [%]
30.0
22.5
15.0
7.5
0.0
shared families
MT
IL
0.100
0.075
0.050
0.025
0.000
unique families
MT
IL
N assimilation
Relative abundance [%]
30.0
22.5
15.0
7.5
0.0
shared families
MT
IL
0.100
0.075
0.050
0.025
0.000
unique families
MT
IL
Denitrification
Relative abundance [%]
12.0
9.0
6.0
3.0
0.0
shared families
MT
IL
0.020
0.015
0.010
0.005
0.000
unique families
MT
IL
Actinobacteria
Corynebacteriaceae
Streptomycetaceae
Bacteroidetes
Amoebophilaceae
Chitinophagaceae
Cyclobacteriaceae
Cytophagaceae
Flammeovirgaceae
Flavobacteriaceae
Rhodothermaceae
Saprospiraceae
Sphingobacteriaceae
Chlorobi
Chlorobiaceae
Chloroflexi
Anaerolineaceae
Ardenticatenaceae
Caldilineaceae
Herpetosiphonaceae
Cyanobacteria
Microchaetaceae
Rivulariaceae
Deinococcus-Thermus
Deinococcaceae
Firmicutes
Bacillaceae
Clostridiaceae
Lactobacillaceae
Paenibacillaceae
Planococcaceae
Fusobacteria
Leptotrichiaceae
Ignavibacteriae
Ignavibacteriaceae
Melioribacteraceae
Nitrospirae
Nitrospiraceae
Planctomycetes
Planctomycetaceae
Proteobacteria/ Alphaproteobacteria
Bradyrhizobiaceae
Caulobacteraceae
Hyphomicrobiaceae
Sphingomonadaceae
Proteobacteria/ Betaproteobacteria
Alcaligenaceae
Burkholderiaceae
Oxalobacteraceae
Proteobacteria/ Gammaproteobacteria
Alteromonadaceae
Ectothiorhodospiraceae
Francisellaceae
Moraxellaceae
Orbaceae
Pseudomonadaceae
Shewanellaceae
Xanthomonadaceae
Proteobacteria/ Deltaproteobacteria
Geobacteraceae
Polyangiaceae
Verrucomicrobia
Opitutaceae
Verrucomicrobia subdivision 3
Euryarchaeota
Candidatus Methanoperedenaceae
Thaumarchaeota
Nitrososphaeraceae
Other

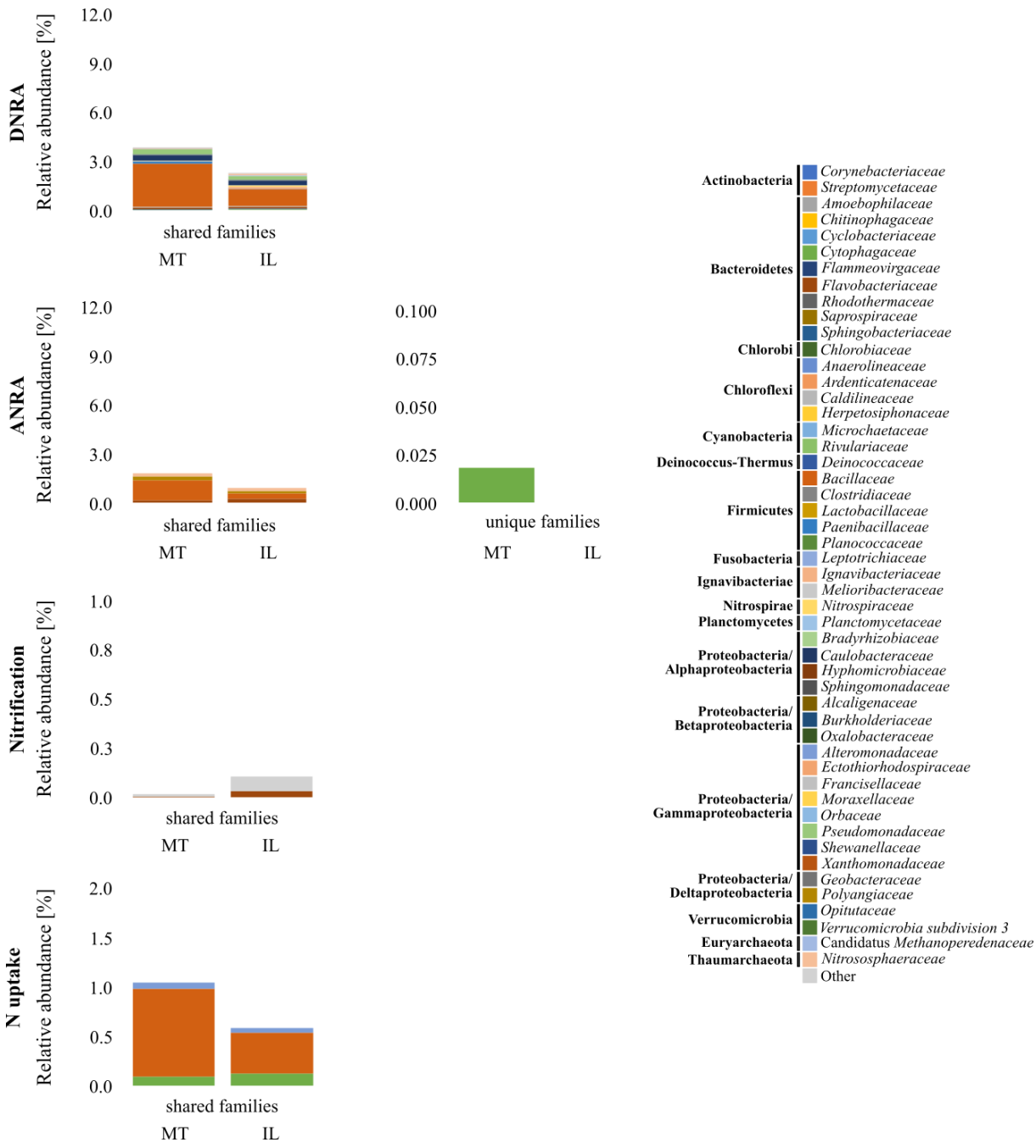

Figure 29. Distribution of shared and unique families involved in the N cycle in the artificial soils containing montmorillonite (MT) and (IL). The reads were functionally assigned using KEGG and taxonomically with the NCBI-nr database. Shown are the mean values of the most abundant families involved in N mineralization, N assimilation, denitrification, DNRA, ANRA, nitrification, and N uptake. Relative abundances were based on the number of all reads assigned to the N cycle.

4.2.7. Gene abundance and microbial groups harbouring genes involved in phosphorus transformation

In order to identify major processes that take place in the early phases of soil development genes that code for enzymes involved in solubilization, mineralization, and phosphorus transport and uptake were investigated. A total of 92,430 reads of all functionally annotated reads was related to the phosphorus turnover. The majority of reads were assigned to the genes involved in phosphorus transport and uptake (33,720), followed by mineralization (26,461), regulation systems (18,774), and solubilization (13,525) (Figure 30).

In total, 29 genes from 42 investigated were detected in both MT and IL. Among all predicted genes, only three were significantly more abundant in MT, *phnX* (encodes phosphonoacetaldehyde hydrolase), *phnK* (C-P lyase subunit), and *pstC* (phosphate-specific transport system subunit). Interestingly, different genes involved in P transport and mineralization were more abundant in MT when compared to IL. However, none of those predicted genes differed significantly at the significance level of 5 %. The more abundant genes involved in P transport and mineralization in MT included other subunits of the phosphate-specific transport system (*pstSCAB*), inorganic pyrophosphatase (*ppa*), and exopolyphosphatase (*ppx*). In contrast, genes encoding the glycerol-3-phosphatase transport system (*ugpBAEC*), alkaline phosphatases (*phoA*, *phoD*), glycerophosphoryl diester phosphodiesterase (*ugpQ*), and quinoprotein glucose dehydrogenase (*gcd*) were more abundant in IL, although these differences were also not significant. Lastly, genes associated with P regulation (*phoR*, *phoB*) showed almost the same relative abundances in both soils.

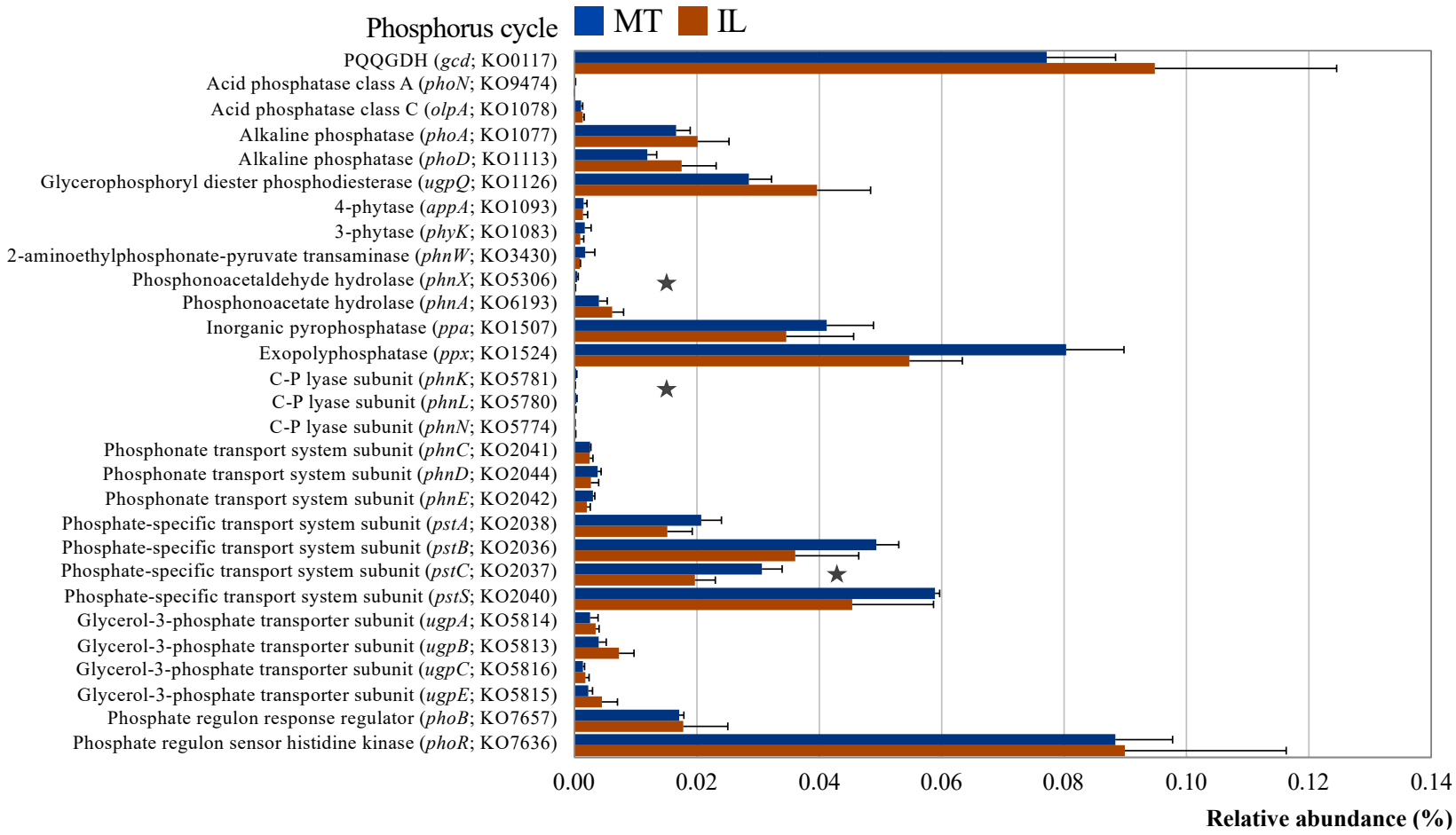

Figure 30. Relative abundance of predicted prokaryotic genes encoding enzymes involved in phosphorus turnover in artificial soils containing MT and IL. Obtained sequences were aligned against the KEGG database and annotated with MEGAN5. Relative abundance was calculated based on the number of all assigned KEGG hits and values were shown as mean with standard deviation (n = 3). Asterisks indicate significant differences ($P < 0.05$) in the number of annotated reads between the investigated soils.

To identify a possible correlation between the abundance of genes involved in P turnover, and pH and C:N:P stoichiometry in MT and IL, a Spearman correlation analysis was performed.

In MT and IL the abundance of genes involved in the P turnover was correlated to both pH, and the C:N:P stoichiometry, including total OC, N, and P, PNaHCO3, Pi, Po, and all C:N:P ratios. Relationships between abiotic factors and genes involved in P turnover showed a similar trend as N cycling genes, where the impact of pH and C:N:P stoichiometry on gene abundance was stronger in MT than in IL. In MT, pH showed both positive and negative relationships with genes involved in the P turnover in MT (positive: *phoB, phoR, phoN, olpA, phoD, ugpQ, appA*, 3-phytase, *phnW, phone, ugpA, ugpB, ugpC, ugpE, pstS, gcd*; negative: *phoA, phnX, phnA, ppa, ppx, phnK, phnL, phnN, phnC, phnD, pstA, pstB, pstC)* and IL (positive: *phoB, phoR, phoN, olpA, ugpQ, appA*, 3-phytase, *ppa, phnN, phnD, phone, ugpC, ugpE, ugpC, ugpE, pstA, pstC, pstS*; negative: *phoA, phoD, phnX, phnA, ppx, phnC, ugpA, ugpB, pstB, gcd*). In MT C:N showed a positive relationship with genes involved in P regulation and genes involved in P_o mineralization and uptake, and negative with P_i mineralization and uptake, whereas the C:P and N:P showed an opposite effect on the same N genes. In IL, on the other hand, C:N, C:P, and N:P were positively correlated with the abundance of genes involved in P turnover, and negatively correlated with P_o. C:N, C:P, and N:P had the same effect on the rest of the genes involved in P turnover as in MT. In MT and IL, pH, total C, N, and P contents, and their ratios showed significant relationships with the abundance of genes involved in the P turnover ($P < 0.05$) with few exceptions (Figure 31).

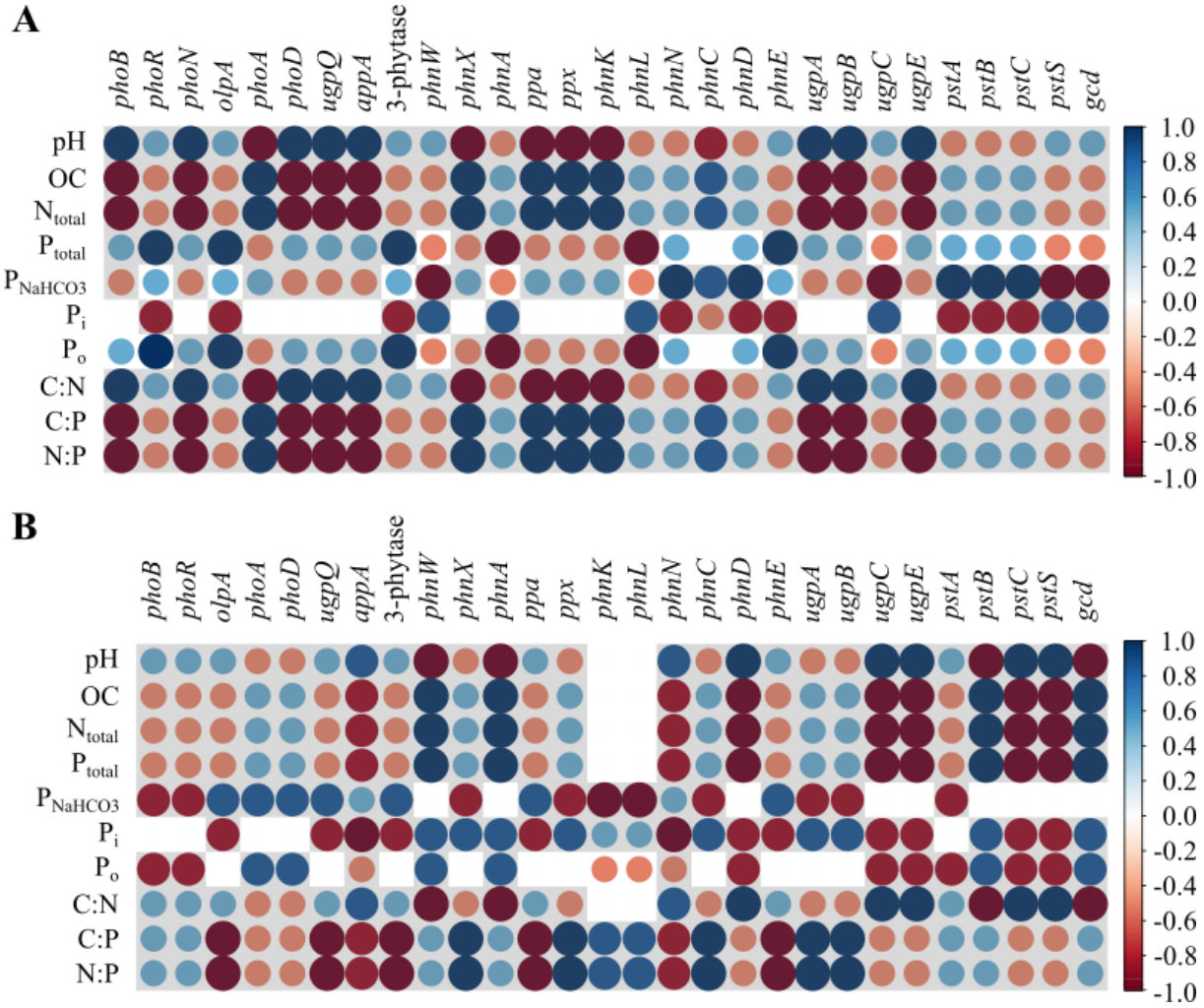

Figure 31. Correlation between the abundance of genes involved in P regulation (*phoB*, *phoR*), P mineralization (*phoN*, *olpA*, *phoA, phoD, ugpQ, appA,* 3-phytase, *phnW, phnX, phnA, ppa, ppx, phnK, phnL, phnN*), organic P uptake (*phnC, phnD, phone, ugpA, ugpB, ugpC, ugpE*), inorganic P uptake (*pstA*, *pstB*, *pstC*, *pstS*), and P solubilization (*gcd*), and soil pH, and C:N:P stoichiometry in artificial soils containing (A) MT and (B) IL. Blue colours represent the positive, and red negative correlation. Darker colour and larger circle diameter indicate a stronger correlation. White squares indicate the absence of correlation. Grey squares indicate significant correlation ($P < 0.05$).

To identify the key drivers of phosphorus turnover in MT and IL sequences of enzymes involved in phosphorus turnover were extracted from the KEGG annotated dataset, and taxonomically annotated by using DIAMOND against NCBI non-redundant (nr) protein sequences database. Microbiota belonging to phyla Bacteroidetes (42.55 %), Firmicutes (17.84 %), Proteobacteria (11.64 %), and Planctomycetes (1.22 %) were involved in all P turnover processes in both soils.

In MT P solubilization was driven by Bacteroidetes (14.67 %), mineralization by Bacteroidetes (11.43 %), Firmicutes (8.27 %), Proteobacteria (4.47 %) and Cyanobacteria (3.15 %) and uptake by Bacteroidetes (7.61 %), Firmicutes (9.26 %), Proteobacteria (4.00 %) and Ignavibacteriae (0.40 %). Similar phyla were the drivers of P turnover in IL, except for Ignavibacteriae in P uptake, where members of phylum Chloroflexi (2.08 %) were more abundant. Most of the genes involved in the P turnover were harboured by Bacteroidetes, whilst *ugpBAEC* was specific for Firmicutes and Proteobacteria, and *ppx* was dominant in Cyanobacteria and *ppa* in Proteobacteria. In addition, different families belonging to the same phyla were the drivers of P turnover in MT in comparison to the IL (Figure 32).

In general, families predicted to be involved in most P turnover processes in both soils mostly belonged to the highly abundant families, such as *Nitrososphaeraceae*, *Cytophagaceae*, *Bacillaceae*, *Chitinophagaceae*, and *Flammeovirgaceae*. (Figure 18, Figure 32). More specifically, it was predicted that P solubilization in MT was driven by *Ignavibacteriaceae*, *Cytophagaceae*, *Chitinophagaceae*, candidate division WWE3, and *Nitrososphaeraceae*. The mineralization of P was predicted to be dominated by *Bacillaceae* and *Microchaetaceae* and uptake by *Anaerolinaceae*, *Bacillaceae*, and *Meliobacteriaceae* in MT. Similar families were potentially involved in P turnover in IL.

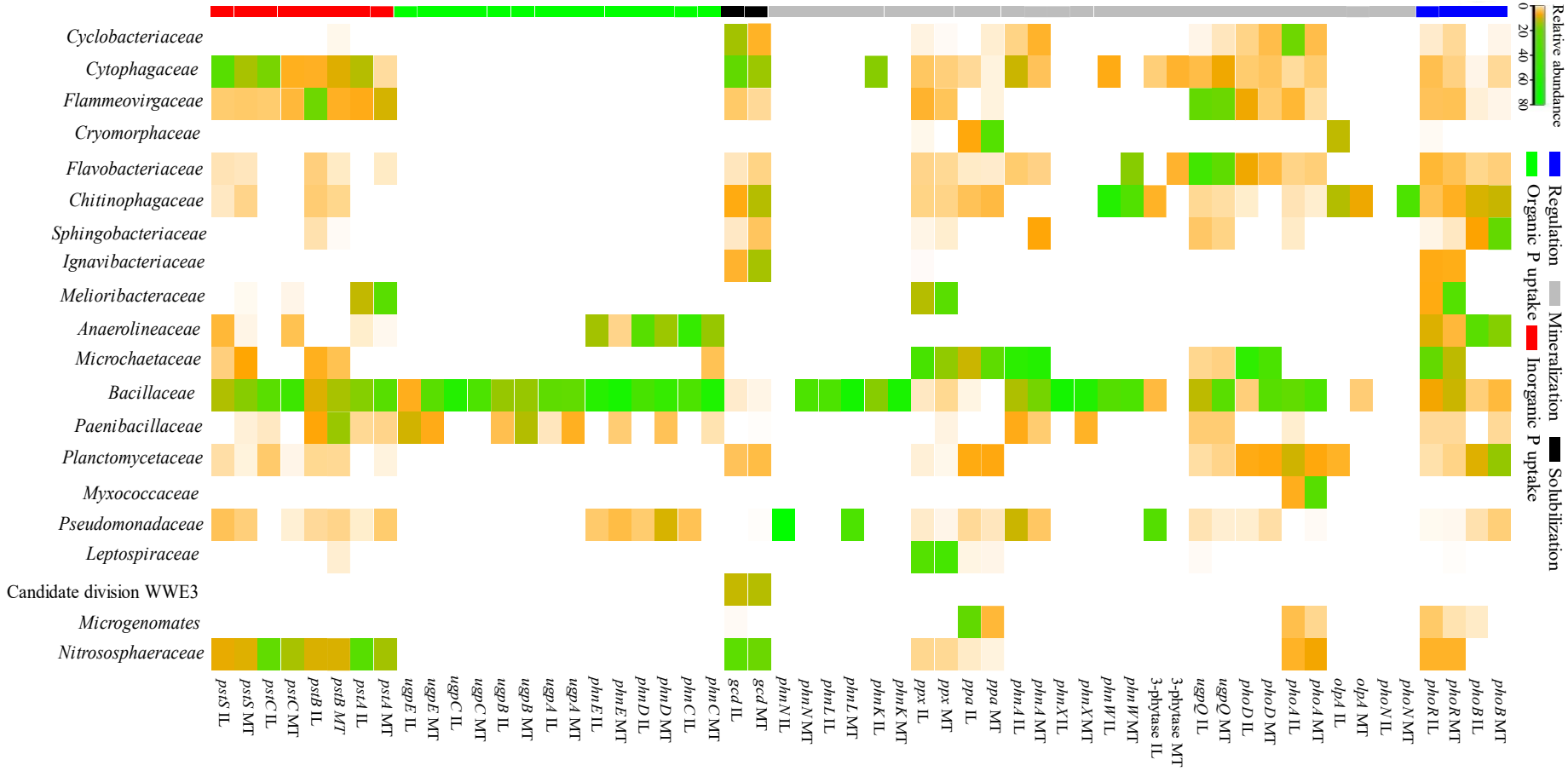

Figure 32. Relative abundance of prokaryotic families involved in phosphorus turnover in the artificial soils containing MT and IL. Obtained sequences were assigned on the functional level by aligning against the KEGG database, and on the taxonomic level against the NCBI-nr database. Relative abundances were calculated based on the number of reads assigned to the microbial P turnover. The colour intensity in the heatmap represents the relative abundance of families associated with a P turnover in montmorillonite and illite. Twenty most abundant families are depicted.

Interestingly, most of the families predicted to be involved in P turnover were shared between the two soils (Figure 33). Among the 50 most abundant families, 17 were similar in IL and MT for solubilization, 41 for mineralization, and 43 for the uptake of P. The relative abundance of unique families was generally very low. In IL, unique families potentially involved in P solubilization were assigned to *Prolixybacteraceae* and *Halobacteriaceae*, and for P mineralization to *Ignavibacteriaceae* and *Sphaerobacteraceae*. Unique families in MT predicted to be involved in P solubilization (*Streptomycetaceae*, *Saprospiraceae*, *Deinococcaceae*, *Thermaceae*, *Paenibacillaceae*, and *Pseudomonadaceae*) and P mineralization (*Chlamydiaceae*, *Herpetosiphonaceae*, *Thermaceae*, *Syntrophaceae*, and *Thermotogaceae*) were slightly more diverse when compared to IL. Regarding P uptake, only one family per soil was predicted to be unique, namely *Leptospiraceae* in MT and *Cryomorphaceae* in IL. Although both soils had many families in common, the relative abundance of 13 bacterial families that were predicted to be involved in P turnover was significantly different, with only *Meliobacteriaceae* (P = 0.002) and *Paenibacillaceae* (P = 0.042) belonging to the 20 most abundant families. Only *Bacillaceae* potentially covered all processes in both soils, while the other families were predicted to drive specific transformation steps in P turnover (Figure 33).

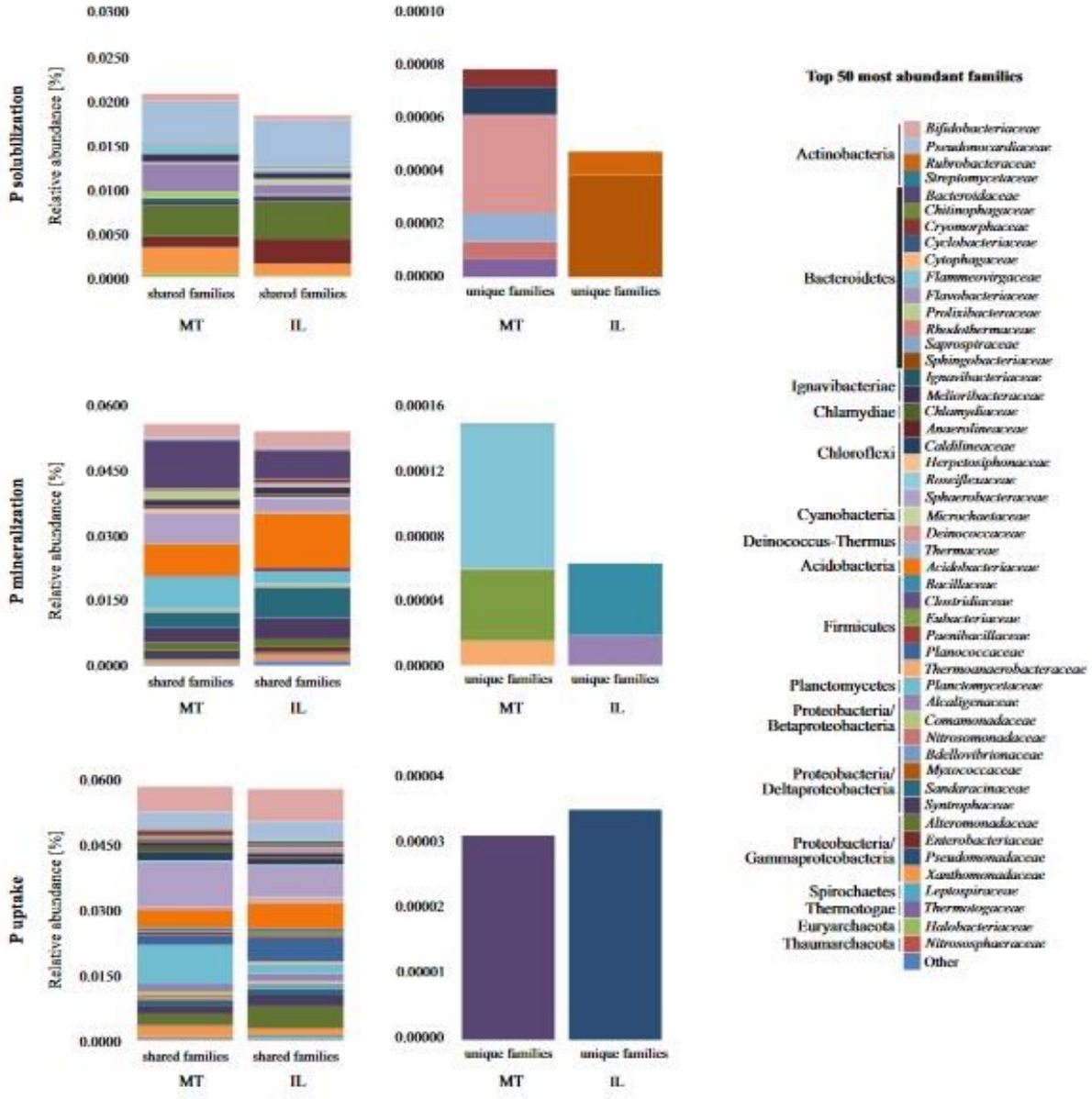

Figure 33. Distribution of shared and unique families involved in the P turnover in the artificial soils containing montmorillonite (MT) and (IL). The reads were functionally assigned with KEGG and taxonomically using the NCBI-nr database. Shown are the mean values of the fifty most abundant families involved in P solubilization, mineralization, and uptake. Relative abundances were based on the number of all reads assigned reads.

5. DISCUSSION

5.1. Influence of clay minerals on the establishment of the microbiome in the early phases of soil development

One of the aims of this research was to investigate the influence of clay minerals on the establishment of the microbiome in the early phases of soil development. To test the hypothesis (**H1**) that clay minerals with different physicochemical characteristics select for distinct microbial communities, two approaches were used.

In the first approach, artificial soils with different mineralogy (montmorillonite (MT), illite (IL), montmorillonite+charcoal (MT+CH), and illite+ferrihydrite (IL+FH)) were treated with litter after prolonged maturation. The use of such pristine mineral surfaces in combination with organic litter allowed us to investigate the dynamics of nutrient release from minerals, the impact of nutrient bioavailability on the microbial community establishment and the influence of the established microbiome on overall nutrient turnover, focusing in particular on the drivers of microbial C, N, and P turnover in the early stages of soil development.

5.1.1. The influence of clay minerals on the dynamics of water-extractable carbon in natural and artificial soils

The addition of litter to the artificial soils initially caused increase of water-extractable carbon (WEOC) indicating a quick release of bioavailable, easily degradable carbon that represents a potential substrate that soil microorganisms can easily utilise, followed by a steady decrease in WEOC values until the end of the experiment. A previous experiment with the same soils has shown that biogeochemical interfaces are rapidly forming in artificial soils leading to complex, aggregated systems which is in line with other studies (Totsche et al., 2018). However, a quick release of low molecular weight molecules, i.e., rapidly degradable carbon compounds from the litter at the beginning of the experiment can also be attributed to the high microporosity and the hydrophobic surface structure of the clay minerals (Egli and Mirabella, 2021; Prost and Yaron, 2001). Furthermore, as only a small amount of minerals was present in the artificial soils, it is possible that during the two years of preincubation already a large part of the mineral surfaces were covered with organic carbon. Hence, a large part of the water-soluble organic compounds could not be bound to the mineral surfaces. For example, Pronk et al. (2012) using similar artificial soils, showed that deposition of organic matter through interactions with minerals took place at the specific surface of the soils directly after the start of the incubation. This has led to a significant

decrease in the available specific surface area of the minerals. All aforementioned parameters, together with the low specific surface area of the main components, sand, and quartz, could have limited the binding of water-soluble organic compounds in artificial soils at the beginning of the experiment, thus explaining the high initial concentrations of easily degradable carbon.

Contrary to the artificial soils, the initial increase of easily degradable carbon in natural soil was significantly lower. Following the initial increase, the WEOC values decreased in the natural soil and reached the level of the soil without litter as early as day 7 which confirms that unbound water-soluble carbon compounds from the litter were either completely degraded by microorganisms or bound to the aggregates and SOM within the first week. The much more effective retention of water-soluble organic compounds in natural soil, when compared to the artificial soils, could be explained by the presence of better-developed structures in the natural soil, which bind nutrients released from the litter more effectively. Such structures are often present in older soils, and their formation is promoted by the input of external carbon sources, the more complex external influences that promote the soil aggregation, and the formation of organo-mineral complexes during the natural soil formation process. While the artificial soils were pre-incubated under constant conditions, the natural soil was exposed to fluctuations such as cycles of freezing/thawing and heat, dry/humid periods, as well as soil plant and animal influences, and several previous studies have shown that changing environmental conditions have a positive effect on aggregation in the soil (Denef et al., 2002; Egli and Mirabella, 2021; Six et al., 2004).

5.1.2. The release of easily degradable carbon and microbial activity

The levels of easily degradable carbon compounds in artificial and natural soils are a direct reflection of the microbial activity, thus allowing additional testing of the hypothesis that clay minerals select specific microbial communities and thus shape microbial activity (**H1**).

All artificial soils in this study reacted to the readily available carbon sources with an immediate decrease in WEOC values that correspond to the increase in microbial metabolic activity. Although a similar trend was detected in all artificial soils, slightly lower WEOC values were detected in all MT-containing soils when compared to IL-containing soils. This might be attributed to the higher microbial respiration rates in MT, thus indicating that the microbial activity is dependent on different minerals present in the soils. However, these differences were not pronounced. Similarly, the addition of external OM after long-term incubation, but before the litter addition, to the soils used in this study, also resulted only in slight differences in microbial activity, as was already described by Vogel et al. (2015).

Contrary to results of this study, Pronk et al. (2012) detected no differences in microbial activity as shown by CO_2 respiration rates over 18 months with a consistent supply of nutrients between artificial soils with similar mineralogy.

In contrast to artificial soils, in natural soil, the increase of microbial activity was delayed between day 7 and day 21, rather than between day 0 and day 7 as in artificial soils. This could also be due to the better-developed structure of the natural soil, which, as shown by the significantly lower WEOC value, binds nutrients from the litter more effectively. The significant increase in activity at day 21 in natural soil indicates that the readily degradable carbon was finally mobilized by the microorganisms even when it was bound to mineral surfaces. It might be that the microorganisms in the natural soil had to move the bound nutrients, which is in concurrence with the time delay, whilst in the artificial soils, the nutrients are readily available to the microorganisms, thus resulting in an earlier increase in activity. In general, a similar trend in WEOC dynamics was detected in all artificial soils, thus for artificial soils, the **H1** hypothesis could not be fully resolved based on WEOC results.

5.1.3. The influence of clay minerals on the microbial biomass and bacterial abundance

In all soils, artificial and natural, treated with litter, the C_{mic} values increased significantly at day 7 when compared to the controls without litter addition. An analysis of C_{mic} value in added litter showed that no microbial carbon was present, which indicates that the buildup of microbial biomass started immediately after the homogenization of the soil and the litter most likely due to the microbial consumption of easily available carbon present in the litter. Since the microbial carbon was analysed in the chloroform fumigation extracts (CFE), the lower initial value could be explained by the fact that the lysis under a chloroform atmosphere does not immediately detect all microorganisms (DeLuca et al., 2019). Since both C_{mic} and bacterial abundance are a measure of the microbial biomass, a correlation between these values could be expected. However, a correlation could only be recognized in rare cases, which could be due to the presence of fungi and archaea, in addition to the bacteria, in the soils. Hence, they are also lysed in CFE and thus contribute to biomass (Alessi et al., 2011). However, the abundance of fungi and archaea is not reflected by the 16S rRNA gene.

Furthermore, the correlation between C_{mic} values and 16S rRNA gene abundance could be affected by multiple heterogeneous copies of 16S genes occurring within a genome (Louca et al., 2018; Větrovský and Baldrian, 2013). Depending on the bacterial species present, it

can lead to variations in the number of copies and thus to the imprecise prediction of an actual microbial community abundance.

The bacterial abundance, as shown by 16S rRNA gene abundance, in natural soil did not increase over time despite the addition of litter. The abundance of the 16S rRNA gene in MT, MT+CH, and IL+FH initially decreased in untreated soils, followed by an increase at later incubation time. In the soils treated with litter, such a decrease did not occur. The initial decline in abundance could be a result of the disturbance of aggregate structures during the soil transfer in experimental preparation. This could have initially made it difficult for microorganisms to access the nutrients from the soil. One possible consequence would be the resolution of microbial hotspots. The increase in bacterial abundance throughout the experiment indicates a reformation of interfaces and microbial communities. Similarly, Denef et al. (2002) showed that aggregate structures in sieved soils can be regenerated after a few weeks. The increase in bacterial abundance in the soils with litter could be explained by the fact that the partial destruction of the aggregates was compensated by the easily accessible carbon. Due to the methodological limitation in linking bacterial biomass and activity directly to soil mineralogy, we tried to account for this limitation by evaluating the establishment of bacterial communities in artificial soils with different clay content by T-RFLP analysis.

5.1.4. Linkage between bacterial community structure and clay minerals

The composition of the bacterial community of natural soil was distinctly different when compared to the artificial soils. As shown in the PCA, the T-RF fragments from the natural soil, independent of the litter treatment, formed a distinct group, which was clearly separated from the artificial soils. Even though the artificial soils were inoculated with an inoculum originating from the natural Luvisol, the differences between artificial and natural soils could be explained by the selection of specific microbes dependent on mineral composition, and, thus, distinct microbial communities in artificial soils have developed. In a previous experiment, using soils of the same composition, significant similarities in the microbial community could be identified when the same clay minerals were added to the soils (Kögel-Knabner et al., 2010; Totsche et al., 2018). However, in the said experiment, the soils were not preincubated, the samples were taken at different intervals over 90 days and the 16S rRNA gene was analysed by temperature gradient gel electrophoresis. Here, the Unweighted Pair Group Methodology with Arithmetic Mean (UPGMA) showed that communities from soils with montmorillonite differed from samples with illite, and a clear clustering of the community was observed in soils containing charcoal. Similarly, in the

present research, the microbial communities differed depending on the MT and IL content as shown by the PCA analysis of T-RFs from artificial soils. However, the bacterial community did not cluster with respect to charcoal or oxide presence in artificial soil. This could be attributed to the loss of the formative properties of the soil components over time. For example, it may be possible for charcoal to lose its porous structure and thus reactive surface over time as it is degraded by microorganisms (Kolb et al., 2009, Kome et al., 2019; Totsche et al., 2018). Besides, the differences in the active microbial community between respective soils may be too small to achieve the formation of distinct groups.

PCA based on T-RFs which included only artificial soils showed that they form groups according to the clay mineral present. In addition, the microbial community was exposed to the same incubation conditions, such as water content, nutrient intake, and temperature, during preincubation for two years, indicating that the diversity of the microbial community in the long term is not only determined by environmental conditions and food supply, but also by the soil components. Müller-Stöver et al. (2012) made a similar observation in natural soils. In this experiment, the soils were of similar composition but of different ages. While the soils at the time of sampling still showed significant differences in the microbial community, a steady adjustment process could be observed over the test duration of 100 days due to the same incubation conditions.

In general, our findings could not entirely confirm the hypothesis (**H1**) that different clay minerals select for specific microorganisms and thus shape distinct microbial communities and activity. Only artificial soils containing clay minerals montmorillonite and illite supported the differentiation of the bacterial community composition after prolonged soil development thus indicating that properties of MT and IL might regulate the establishment of the bacterial community via the formation of microbial habitats in soil.

5.2. Microbial diversity and establishment of microbial communities after a prolonged artificial soil incubation as affected by soil mineralogy

The simplified model artificial soils with comparable and well-defined physicochemical characteristics were used to test hypothesis (**H1**) that nutrient depletion after a prolonged soil incubation, as well as clay minerals affect microbial diversity, microbial establishment and development, and consequent functional diversity in dependence of clay minerals (montmorillonite and illite).

Confirming hypothesis (**H1**), results of PCA analysis of MT and IL metagenome revealed distinct prokaryotic communities that have developed in the two selected artificial soils. Variations within prokaryotic communities were similar in both respective artificial soils, suggesting that macro-aggregation in both soils (Vogel et al., 2015) resulted in the spatial formation of nutrient and activity hotspots. As special care was taken during the watering, and mixing of the artificial soils, so as not to disturb the formed macro-aggregates and to limit the outside disturbance of the systems, spatial heterogeneity and niche development may have increased and contributed to the observed variation (Vogel et al., 2015).

The effect of the mineral composition on the establishment of different microbial communities was observed in several short-term (Babin et al., 2013; Ding et al., 2013) and long-term artificial soil incubation experiments (Vogel et al., 2014). Clay minerals show different physical and chemical properties, for example, size, porosity, specific surface area (SSA), and cation exchange capacity (CEC) (Kome et al., 2019; Ouyang et al., 2021; Stotzky, 1986). It is assumed that they can directly interact with microbes, thereby altering the rate of microbial metabolism, modifying the environment, and binding extracellular enzymes (Olagoke et al., 2019; Stotzky, 1986; Stotzky and Rem, 1967). Several studies have indicated that montmorillonite stimulates microbial activity due to its buffering capacity (Kunc and Stotzky, 1974; Stotzky and Rem, 1966). In this study, the differences in bacterial community structures depended on clay mineralogy, which is in line with the findings of several other experiments, thus confirming hypothesis H1. Ding et al. (2013) and Vogel et al. (2014) showed that clay minerals (montmorillonite and illite) have a strong influence on the bacterial community structure only after prolonged incubation of artificial soils, after 90 and 862 days, respectively. This has been confirmed in the present study.

Sequence analysis revealed that the microbial communities established in both montmorillonite and illite had high richness and evenness, especially at the family level. However, microbial diversity was slightly lower in illite when compared to montmorillonite. This could be due to the lower specific surface area of illite that could result in decreased availability of microhabitats and consequently in the decrease of microbial diversity.

Furthermore, sequence analysis revealed several taxa with higher abundance in montmorillonite than in illite-containing soil, for example, Firmicutes, Ignavibacteriae, Chlorobi, and Planctomycetes were prevalent in montmorillonite, whilst Bacteroidetes, Proteobacteria, Cyanobacteria, and Microgenomates in illite. Similarly, Ding et al. (2013) found that the genera belonging to the phyla Proteobacteria, Firmicutes, Actinobacteria, and Bacteroidetes were significantly more common in illite. Together, this suggests that certain bacterial taxa favour different types of minerals.

Different clay mineral characteristics, their interaction with organic matter, and consequently nutrient availability could have caused the establishment of different microbial communities. For instance, the protective influence of SSA on organic matter and consequent lower mineralization rate leads to the decrease in the nutrient availability in montmorillonite. We assume that this could have selected for the members of Firmicutes, Ignavibacteriae, and Chlorobi that can utilize recalcitrant compounds from organic matter. Higher mineralization rates in illite, on the other hand, could account for the higher nutrient availability that could explain the higher abundance of Bacteroidetes and Proteobacteria, whose members are typically found in copiotrophic environments (Fierer et al., 2007). Altogether, this confirms the hypothesis that different types of clay select for distinct microorganisms (**H1**).

5.3. Microbial nutrient turnover in montmorillonite and illite containing artificial soils

In addition to studying the effects of clay minerals on the microbial diversity and structure, simplified matured model artificial soils represent a good system for studying the effects of nutrients, such as C, N, and P depletion on microbiota and expression of different compensation mechanisms by simulating a developing soil system where C, N, and P are limiting factors due to the elimination of their input and other external disturbance, as well as the elimination of plant competition for C, N, and P (Vitousek et al., 2010; Walker and Syers, 1976). With the metagenomic approach, we tested several hypotheses including that prolonged incubation will lead to the consumption of easily degradable carbon compounds, organic N and P that will lead to the depletion of bioavailable forms of C, N, and P (**H2**) thus leading to the microbial adaptation to the nutrient shortage which will be reflected in genes involved in C, N, and P turnover (**H3**, **H4**) as well as in the development of functional microbiota (**H5**).

5.3.1. Nutrient limitation in artificial soils

Since the last nutrient addition occurred more than 300 days before the sampling, a carbon, nitrogen, and phosphorus depletion were detected which is underlined by low OC, N_{total}, and P_{total}, and a very low C:N, C:P, and N:P ratios of less than 9.3, 3.8 and 34.6 respectively. The calculated ratios were lower than normally found in grassland and forests (Cleveland and Liptzin, 2007). However, they were comparable to severely nutrient-depleted systems such as glacial and mountain regions (Krauze et al., 2021). The C and N limitation found in our system was not surprising given that plants, which were excluded from our experiment,

are the major source of both C and N in the soils (Daly et al., 2021; Jiling et al., 2018). Surprisingly, high concentrations of available inorganic P, similar to forest soils (Lang et al., 2017) were found in both soils. This might be linked to the low microbial respiration rates at the time of sampling (Vogel et al., 2014) indicating low microbial activity and highly efficient strategies for the remobilization of P from the microbial biomass, as the community composition significantly changed since the last manure addition (Vogel et al., 2014). Furthermore, the limitation of other nutrients like nitrogen and carbon might have caused high remaining P concentrations, which is underlined by very low C:P and N:P ratios of less than 3.8 and 34.6, respectively. These values are much lower than those observed by Cleveland and Liptzin (2007), who postulated a well-constrained C:P ratio of 186:1 and N:P ratios of 13:1. This is also in line with the findings of Heuck et al. (2015), who demonstrated that under C limitation, organic P resources are mineralized with the aim to take up the released C first, which explains higher C:P ratios in our experiment. Thus, our findings confirm hypothesis (**H2**) that after a prolonged maturation an easily available C, N, and P compounds will be depleted with only recalcitrant forms of macronutrients remaining in artificial soils.

5.3.2. Carbon transformations and functional microbiota involved in overcoming carbon depletion

Due to the severe C depletion, underlined by low C:N, and C:P ratios, in both MT and IL soil, the C transformation processes were mainly directed towards the degradation of remaining organic recalcitrant C compounds as a source of C needed for the microbial metabolism, rather than C fixation and methane metabolism. Similar findings come from biological soil crusts on bare land (Li et al., 2021b; Su et al., 2013; Wang et al., 2021), which are very limited in C content. Even though it is known that in the early stages of soil development archaea and bacteria mainly use C sources provided by autotrophic CO_2 fixing bacteria (Wang et al., 2021), such a pattern was not detected in our MT and IL artificial soils. This may indicate that at the studied timepoint, after manure addition, available C sources supported an establishment of stable heterotrophic, degrading communities rather than autotrophic communities. Also, the low abundance of predicted genes involved in C fixation and methane metabolism could be explained by the artificial soil incubation conditions, such as prolonged soil incubation in dark and aerobic conditions which do not favour the aforementioned processes (Evans et al., 2019; Foster et al., 2022; Masuda et al., 2018; Morales et al., 2018).

Furthermore, several different genes encoding for cellulose, hemicellulose, and chitin degradation were detected in both MT and IL, which is comparable to other ecosystems (Berlemont and Martiny, 2013; Luo et al., 2020) confirming that complete polymer degradation comprises ubiquitous and complex processes that involve several different steps catalysed by several enzymes in many bacterial taxa. The prevalence of genes predicted to encode enzymes involved in polymer degradation found in both MT and IL is in line with several other studies that have shown that the degradation of polymers originating mostly from plant cell walls is mostly driven by soil microorganisms, and it is considered a key step in carbon cycling in many ecosystems, including soil (Aanderud et al., 2018; Buchkowski et al., 2019; Wei et al., 2020). However, not all microorganisms can degrade recalcitrant polymers and are dependent on polymer degrading bacteria, to release short-chain molecules, which they can then hydrolyse and utilize. Such bacteria are known as “cheaters” and they are mostly associated with Bacteroidetes (Schimel and Schaeffer, 2012) which were also highly abundant in our soils, further underlining the complexity of processes and the diversity of microorganisms included in complete polymer degradation.

The abundance of main genes involved in C cycling in both soils was mainly governed by soil C:N:P stoichiometry, and to a lesser extent by other abiotic factors including pH, and OC, N, and P content. This is consistent with previous studies which showed that multiple edaphic factors, including soil stoichiometry, physicochemical properties, temperature, and moisture, either together or individually influence microbially driven processes (Luo et al., 2020; Wei et al., 2020). For example, Luo et al. (2020) have shown that the C:N:P stoichiometry imparted a greater effect on the abundance of microbial groups associated with the main C, N, and P transformation processes than mean annual temperature and precipitation, whereas Wei et al. (2020) identified that N:P ratios are critical for the regulation of soil C mineralization.

As the soil development progresses, the development is characterized by ever-frequent external C input suggesting a need for diverse C sources including autotrophic C originating from primary producers (i.e., plants, algae, cyanobacteria), photo- and chemolito-autotrophs (Wang et al., 2021; Wei et al., 2020). Contrary, to this study, C input is partially restricted due to the experimental design which excludes the effect of plants and photoautotrophs. However, the detection of Cyanobacteria and genes coding for enzymes involved in C fixation, indicate that C fixation is an additional albeit marginal, C source in MT and IL soils. Even though soil microbes preferentially use readily available substrates rather than recalcitrant C sources (Wei et al., 2020), only the genes predicted to code for enzymes involved in the degradation of more readily available substrates such as pectin, and starch were detected in MT, and IL, respectively. This together with a substantial

decrease in the diversity of taxa involved in C turnover in comparison to the overall diversity in both MT and IL, indicates that the microbes became increasingly C-limited as the soil incubation proceeds. We speculate that this leads to the death of microorganisms that are poorly adapted to the utilization of recalcitrant C forms, and a consequent increase in microbial necromass, with a shift towards prokaryotic taxa capable of utilizing remaining necromass and recalcitrant C sources. This is in line with studies that showed that the addition of easily available substrates such as low molecular weight organic sugars, acids, and necromass provide a C source and energy for soil microorganisms, inducing rapid mineralization of easily available C compounds, and increasing microbial diversity, growth, and activity followed by a decrease in microbial activity due to the C limitation (Gunina and Kuzyakov, 2015). Contrary, other studies (Qiao et al., 2019) have shown that the C limitation leads to the decrease in degradation of recalcitrant SOM, due to the protective influence of microbial necromass which might cover the soil surface, thus physically protecting the SOM and decreasing the accessibility of SOM for microbial decomposition. A similar discrepancy in microbial activity was detected, as reported by Vogel et al. (2015), in our soils, where lower microbially-assisted OM degradation was detected in MT than in IL, probably due to the differences in clay physical properties. For example, the higher SSA and CEC in MT when compared to the IL, might lead to the sorption of SOM to the MT, thus protecting SOM from decomposition and subsequently reducing mineralization and the metabolic activity of the microbiota (Saidy et al., 2015).

To our knowledge, the phylogenetic distribution of genes encoding enzymes involved in polymer degradation is still largely unknown. Moreover, since genes encoding processes involved in C cycling are ubiquitous and present in all life forms, it is often difficult to differentiate the true origin of those genes (Berlemont and Martiny, 2013).

In this study, the bacterial phyla that dominated the C cycle included Bacteroidetes, Firmicutes, Actinobacteria, and Verrucomicrobia. A higher abundance of members of phyla Verrucomicrobia found in our soils was not surprising as they are normally associated with oligotrophic environments characterized by low carbon availability (Cederlund et al., 2014; Yao et al., 2017; Zhang et al., 2015). However, the response of Actinobacteria to the nutrient availability and its trophic characterization, on the other hand, is still not clear. Our findings are consistent with the study of Wang et al. (2021) where Actinobacteria, together with Proteobacteria, were the dominant bacterial taxa involved in C cycling during the biological soil crusts development. Contrary, several studies have documented an increase in the relative abundance of Actinobacteria in response to nutrient additions (Pan et al., 2014; Ramirez et al., 2012). Surprisingly, we have also detected a high abundance of Bacteroidetes and Firmicutes which are normally associated with copiotrophic ecosystems

(Francioli et al., 2016). However, more and more studies have indicated that the dominant bacterial communities in soils, including Acidobacteria, Actinobacteria, Proteobacteria, and Bacteroidetes, are similar in various ecosystems and the bacterial community composition does not vary significantly across different biomes (Fierer et al., 2007). Furthermore, since C is one of the essential macronutrients in energy metabolism, enzymes related to the degradation of C sources are harboured by a wide range of microorganisms (Nannipieri et al., 2011), which was also demonstrated in this study.

Various studies have shown that dominant phyla (Bacteroidetes, Firmicutes, Actinobacteria, and Verrucomicrobia) found in our soils are also dominant during the decomposition of plant residues which often comprise recalcitrant C compounds, such as cellulose (Bernard et al., 2007). In addition, these bacteria can often also metabolize hemicellulose and cleave glycosidic bonds present in xylan (Flint et al., 2012).

At the family level, functional microbiota involved in C cycling was highly diverse, and mainly shared between both MT and IL, with exception of a few families unique for each soil, however, those were only marginal. In both soils, cellulose and hemicellulose degradation was assigned to the several families, amongst them the *Bacillaceae* and *Paenibacillaceae* whose members, such as *Bacillus* spp. and *Paenibacillus* spp., respectively, are known to produce exogenous cellulases located on the surface of bacterial cells called cellulosomes (Górska et al., 2015; Pason et al., 2006). Moreover, not only were different families involved in chitin degradation, but the diversity of chitin degrading community was also smaller than the diversity of cellulose and hemicellulose degrading community, indicating that more microorganisms can decompose less recalcitrant organic forms of C, while a smaller number of individual microorganisms can decompose recalcitrant organic C such as chitin. Our results are in line with a study by Dai et al. (2021) who investigated soil microbial communities involved in carbon cycling along elevation climosequences. Interestingly, C fixation was additionally driven exclusively by *Roseiflexaceae* in MT, and *Ktedonobacteraceae* in IL, the members of Chloroflexi. However, those families were detected only in low abundance. Similarly, Zhou et al. (2018) have shown that vegetation cover plays an important role in the distribution of microorganisms, in particular, photosynthetic microorganisms. This is further supported by the increased abundance of Chloroflexi in the highest elevations without vegetation cover (Dai et al., 2021). Even though in our experiment the vegetation cover was omitted, we could tentatively argue that the incubation of soils in dark has to some extent mimicked the vegetation cover concerning the light availability, thus affecting the Chloroflexi abundance. Furthermore, Crouzet et al. (2019) have shown that soil photosynthetic microbial biomass is negatively affected by exposure to the dark periods.

Altogether our results confirm the hypothesis that with prolonged incubation following the last organic matter input mostly recalcitrant C forms remain in the system (**H2**) which is also reflected in the adaptation of carbon-associated genes (**H3**). In addition to mineralization of recalcitrant C forms, our results indicate mineralization of microbial necromass and C fixation as an additional C source in the early phases of soil development is independent of soil mineralogy. Furthermore, our findings indicate that the degradation of C compounds is the main function of microbiota found in both MT and IL and that all the dominant species participate in the C cycle which is consistent with previous studies (Liu et al., 2017; Wang et al., 2021) which confirms our hypothesis that functional microbiota involved in C cycle consists of generalists and highly abundant taxa (**H5**).

5.3.3. Nitrogen transformation and microbiota driving the nitrogen remobilization

In both MT and IL soils, N inputs are generally dependent on N depolymerisation, even though the depolymerisation of complex organic N compounds to oligomers or monomers is considered to be the rate-limiting step in terrestrial N cycling (Daly et al., 2021). In this study, most of the detected genes encoded enzymes associated with the degradation of microbial residues such as cell walls and proteins identifying the microbial necromass as an important source of organic N which is confirmed by other studies. For example, Hu et al. (2020) have found that the microbial cell walls represent a primary input to soil organic matter (SOM), that soil microorganisms can readily utilize. Also, Séneca et al. (2021) detected a high transcription level of genes encoding enzymes involved in the breakdown and recycling of microbial residues. Furthermore, it was shown that the depolymerisation is influenced by soil mineral composition, in particular by soil physicochemical properties that influence substrate bioavailability by entrapping substrate in small pores and aggregate structures, thus regulating the breakdown of N polymers into bioavailable N (Daly et al., 2021; Jilling et al., 2018; Noll et al., 2019). In addition, other studies have shown that the organic N depolymerisation is dependent, as well, on other abiotic factors, such as substrate availability, pH, elevated temperature, etc. (Noll et al., 2019; Z. Wang et al., 2021).

Even though no significant differences were detected in N depolymerisation between MT and IL, detected gene abundances indicate that microorganisms in MT and IL may utilize different organic N sources. For example, in MT, the elevated abundance of predicted genes involved in N depolymerisation and mineralization which encode proteases and ureases indicates that the N acquisition in MT mainly depends on the decomposition of organic N compounds originating from organic litter and dead microbial biomass which is in

line with above mentioned studies (Daly et al., 2021; Jansson and Hofmockel, 2020; Séneca et al., 2021). Contrary, the microbiome in IL was mainly dependent on alternative organic N sources, such as chitin which was underlined by a higher abundance of predicted genes encoding chitinase, in particular, *CHIT1* which not only increases the availability of N but also C. This is in line with the study of Brankatschk et al. (2011) who found that the mineralization in glacier forefield with scarce vegetation cover which is characterized by nutrient depletion was dependent on simultaneous chitinolysis and proteolysis. Furthermore, we could argue that fungal cell walls are contributing more to the microbial necromass in IL than in MT. However, as the fungal abundance was extremely low, this conclusion is speculative at best.

Unlike N depolymerisation, biological N fixation was only marginal in both MT and IL, which is contrary to other research that showed that ecosystems characterized by low nutrient content and scarce vegetation are mainly dependent on N fixation (Levy-Booth et al., 2019; Luo et al., 2020). This, further confirms that the added plant litter, as well as the microbial necromass, were the main source of N in this study.

Inorganic N transformation processes were also detected in both the MT and IL with DNRA, and ANRA prevailing in MT, and nitrification in IL. On the other hand, denitrification and nitrogen uptake was detected in both soils, however, different genes encoding enzymes involved in denitrification and N uptake were more abundant in MT (*narI*, *napA*/*napB*, *nirK*/*nirS*, *nosZ*, and nitrite/nitrate transporter *nrtP*), and IL (*narH*, and *nrtA/nrtC*).

Those results further underline that different, effective microbial strategies for N recycling, and preventing additional N loss in an already N depleted system, have developed depending on the clay mineral composition of artificial soils which is in line with several other studies (Malik et al., 2018; Yarwood et al., 2015). Furthermore, N assimilation was dominant in MT, where all predicted genes encoding enzymes involved in glutamate synthesis, glutamate synthetase (*glnA*), glutamate synthase (*gltS, gltD, gltB*), and glutamate dehydrogenase (*gudB/rocG, ghhA/GLUD1, gdhA/GLUD2*) were more abundant than in IL. Similar was found in the study by Chuckran et al. (2021) where under low-to-moderate intracellular concentrations of NH_4^+, the enzymes glutamine synthetase (GS) (encoded by *glnA*) and glutamate synthase (GOGAT) (*gltS*) convert NH_4^+ to glutamate in a two-step reaction known as the GS-GOGAT pathway.

Even though the N fixation was only marginal in both MT and IL, the elevated abundance of *nosZ* and *nirS*, and detection of the N-fixing bacteria belonging to the genera *Microchaetacea* and *Bradyrhizobium* in MT and IL, respectively, indicate a potential relationship between biological N fixation and denitrification in both soils (Rösch and Meier,

2009). In addition, nitrification which leads to the conversion of ammonium to nitrate, and loss of nitrate via denitrification indicates a dependence on the energy provided by carbon decomposers (Forbes et al., 2009; Levy-Booth et al., 2019; Luo et al., 2020). Thus, a broader understanding of N biogeochemical cycling in all ecosystems can be attained only by simultaneous analyses of all the genes and the microbial populations harbouring not only the N but also C cycling genes.

Both MT and IL soils were characterized by a highly diverse community dominated by Bacteroidetes, Firmicutes, Proteobacteria, Actinobacteria, Gemmatimonadetes, Cyanobacteria, and Chloroflexi. This is in line with the observations in other nutrient-poor habitats (Bajerski and Wagner, 2013; Ganzert et al., 2011; Meier et al., 2019). Higher abundances of Firmicutes, especially *Bacillaceae*, and Bacteroidetes, especially *Flavobacteriaceae*, were observed in both MT and IL. Said families are known for resilience to adverse abiotic factors due to the sporulation ability, and pH resistance, respectively, allowing them to survive unfavourable conditions. In addition, the detected members of Bacteroidetes could prefer the distinct clay minerals (Meier et al., 2019). Even though predicted genes involved in C and N fixation were only marginal, Cyanobacteria and Chloroflexi, known for N fixation, were found in MT and IL indicating the potential for alternative pathways in N acquisition. Due to the low diversity and abundance of chemoautotrophic organisms, in general, in MT and IL, organic and inorganic N compounds and metabolic pathways utilizing those may have a more pronounced role in sustaining the initial stage of the soil development (Meier et al., 2019). Also, among detected prokaryotic families, the *Thaumarchaeota* were found in relatively high abundance in both MT and IL. These oligotrophic, chemoautotrophic archaea are known to oxidize ammonia aerobically to nitrite thus contributing to the increasing N in its habitat.

Since the C, N, and P requirements of microbial biomass differ among species and are not homeostatic through time it is expected that ecosystems' nutrient stoichiometry will govern the development of microbial community structure, and consequently function (Buchkowski et al., 2019; Cleveland and Liptzin, 2007). As expected, the majority of N cycling gene abundances were related to soil C, N, and P contents and C:P and N:P ratios. For example, the abundance of the *nifH* gene was correlated with soil total C and N contents because fixed N can drive the coupling of N and C cycling processes, as seen in litter decomposition (Wei et al., 2020). Thus, resource allocation processes may balance C and N acquisition, and restore stoichiometric balance. The abundances of genes involved in soil C, N, and P cycling were differentially induced in MT and IL. These idiosyncrasies may stem from different chemical and physical properties of MT and IL clay minerals, likely affecting the microbial community structure. Therefore, selecting for different functional groups (Uroz et

al., 2015) and with different mechanisms for surviving nutrient depletion, thus reflecting complex macronutrient cycling processes within the soil-microorganism system. For example, both bacteria and fungi are known to induce survival strategies against unfavourable conditions, including nutrient depletion, desiccation, and rewetting, which include the accumulation of easily available C, and N when in abundance, in streptomycetes (Schimel and Bennet, 2004), exopolysaccharide production studied in *Pseudomonas* and Acidobacteria (Chang et al., 2007), and the induction of dormant phases such as spore production in *Bacillaceae* (Barnard et al., 2013). Therefore, microbial functional groups may select for characteristic patterns in responding to nutrient depletion by implementing varied physiological strategies that enable survival in unfavourable conditions such as C and N depletion.

Overall, our results showed the increased metabolic investment towards the production of depolymerizing enzymes that act on the microbial necromass and the remaining insoluble high-molecular organic N sources, thus confirming our hypothesis (**H4**) that recycling of organic N, together with increased nitrogen uptake, is likely a key strategy for microorganisms in overcoming the N limitation in the early stages of soil development. Furthermore, we detected differences in dominant genes involved in different processes of the nitrogen cycle, but only a few to no changes in the structure of the microbial communities responsible for nitrogen transformations between MT and IL soils. This suggests that physiological changes rather than major changes in community composition were responsible for adaptations to nitrogen limitation, especially since the ability to produce and secrete enzymes involved in the nitrogen cycle is widespread among soil microorganisms thus confirming our hypothesis (**H5**) that functional microbiota involved in N transformations consist of generalists and highly abundant taxa.

5.3.4. Microbial phosphorus turnover and microbiota involved in phosphorus recycling

Similar to the C and N cycling, our data have shown that the P turnover in MT and IL mainly relied on the utilization of remaining inorganic Pi or Po, respectively, which was paired with highly effective P uptake systems. In both soils, genes predicted to encode the phosphate-specific transport system (*pst*) were highly abundant, while no reads were assigned to the phosphate inorganic transporter (*pitA*). This suggests that P is a highly competitive nutrient in those soils, as this transporter is typically expressed under P starvation (Santos-Beneit, 2015). It is not surprising that bacterial families predicted to be involved in P cycling belonged to the most abundant families, as P mobilization and uptake are of high importance in nutrient-limited soils. Members of *Bacillaceae* were among the most abundant bacteria in both soils and have the potential to perform all processes of P turnover. These results are consistent with previous data from cultivation studies of *Bacillaceae* family members. For example, *Bacillus* spp. include well-known phosphorus-solubilizing bacteria (PSB). They harbour a variety of P-solubilizing mechanisms including changing pH, excretion of organic acids, siderophores, and phosphatase (Oliveira et al., 2009). In addition, members of the *Bacillaceae* family can sporulate under unfavorable conditions, which helps them to survive and outcompete other microbiota in MT and IL soils (Mandic-Mulec et al., 2015). Since P is one of the most important macronutrients, essential in energy metabolism and other cellular processes, enzymes related to the use of external P sources are harboured by a wide range of microorganisms (Richardson and Simpson, 2011), which we also show in this study. Genes predicted to be involved in external P turnover were assigned to microbiota belonging to Bacteroidetes, Firmicutes, Proteobacteria, and Planctomycetes in both soils, which is comparable to findings of Grafe et al. (2018) in mature agricultural soils. This is not surprising, as the artificial soils had been inoculated with a microbial community extracted from agricultural soil at the beginning of the maturation phase. In contrast, Bergkemper et al. (2016) found that most reads assigned to P turnover in metagenomes from P-depleted forest soils belonged to the Acidobacteria (Acidobacteriales, Solibacterales), Actinobacteria (Actinomycetales), and Proteobacteria (Rhodospirillales, Burkholderiales). This difference could be due to the complexity of forest soil and the resulting differences in physicochemical properties, as well as to the different mineral composition, which selects for different families. In the MT, the most abundant predicted gene associated with P mineralization were *ppa* and *ppx*; the respective enzymes are predominantly involved in the utilization of inorganic P. The *ppa* gene codes for an inorganic pyrophosphatase, an enzyme that hydrolyzes polyphosphate compounds (poly-P), and *ppx* for an exopolyphosphatase which in turn releases inorganic P from poly-P

chains (Keasling et al., 1993) in prokaryotes under the condition of P starvation (Adams et al., 2008). Thus, a first mechanism in overcoming P starvation might be the use of internal P storage pools like acidocalcisomes, which might have been developed after the addition of manure. Acidocalcisomes are well known and widespread both in prokaryotes and eukaryotes (Docampo et al., 2005). Moreover, MT has a higher storage capacity than IL due to its bigger soil surface area. Thus, inorganic P from external sources like manure might persist longer. Interestingly, in MT, the reads predicted to code for the *ppx* gene (exopolyphosphatase) were exclusively assigned to members of Cyanobacteria. Adams et al. (2008) have shown that the expression of the *ppx* gene allows Cyanobacteria to adapt to the environmental fluctuation of P and C. Additionally, it has been demonstrated that exopolysaccharides can be used to solubilize P. As Cyanobacteria are well known as exopolysaccharide producers, it might be an advantage in MT soils where more reaction sites are available (Sharma et al., 2013). An additional advantage of some Cyanobacteria could be their potential capability to fix nitrogen and CO_2 (Rai et al., 1992). In contrast, the relative abundance of predicted genes involved in P mineralization did not significantly differ in the two soils. This was further accompanied by comparable P_o concentrations. This included genes coding for alkaline phosphatases (ALP), namely *phoA* and *phoD*, and *ugpQ*, which coded for a glycerophosphoryl diester phosphodiesterase. While PhoA includes mainly phosphomonoesterase, PhoD shows phosphodiesterase activity as well (Rodriguez et al., 2014). UgpQ has phosphodiesterase activity and hydrolyzes glycerophosphoryldiesters to glycerol-3-phosphate (G3P). In line with that, we also detected reads, which were assigned to all four subunits of the glycerol-3-phosphate transporter system (*ugpBAEC*), whose relative abundance exceeded those detected in other studies (Bergkemper et al., 2016; Grafe et al., 2018). This could allow the utilization of organic P sources in nutrient-depleted systems. The detection of predicted ALP genes was higher than that of the predicted acid phosphatase genes in both soils. However, this was not surprising as both soils had a pH of 7.7 at the beginning of the experiment (Pronk et al., 2012) and of 7.2 (MT) and 7.6 (IL) after 842 days of incubation (Vogel et al., 2014), which is still above the optimal pH for acid phosphatase activities (Nannipieri et al., 2011). Moreover, Fraser et al. (2015) demonstrated that the addition of manure might increase the abundance of the *phoD* community as well as the ALP activity. Genes coding for the Pho regulon (Rodriguez at al., 2014) that controls *phoA* and *phoD* gene expression were also highly abundant in both soils, which was in line with the high abundance of *pstS*, underlining again the need for a strict control of P utilization. Interestingly, the predicted quinoprotein glucose dehydrogenase (*PQQGDH*), potentially involved in P solubilization, was among the top three abundant genes in both soils. Its relative abundance was even higher compared to a study on agricultural soils (Grafe et al., 2018), which regularly obtained organic

fertilizers. Solubilization processes so far have been mostly described for P-rich systems (Bergkemper et al., 2016, Frkova et al., 2021). However, the P_{NaHCO3} concentration and the total P_i concentration suggest that there is still a high potential to solubilize P from the stable inorganic fraction.

Our results have shown that microorganisms in MT rely on the effective P uptake and use of internal poly-P stores, whereas in IL on organic P sources thus confirming our hypothesis (**H4**) that microbiota in the two soils will develop different strategies to overcome P depletion. Furthermore, same as in C and N cycle, the P turnover was driven by highly abundant taxa, where only a few unique taxa were detected in very low abundance, which is in line with our **H5** hypothesis.

Altogether, our results have shown, that the abundance of main functional genes involved in the biogeochemical cycling of C (cellulose, hemicellulose, chitin, starch, and pectin degradation), N (mineralization, assimilation, denitrification, DNRA, ANRA, nitrification, nitrite, and nitrate uptake), and P (P mineralization, solubilization, and P uptake) were dependent not only on the type of clay mineral present but also on C:N:P stoichiometry. Several studies have shown multiple edaphic factors, including soil physicochemical properties, temperature, and moisture, either together or individually to influence the processes driven by microorganisms (Luo et al., 2020; Wei et al., 2020). Since the microbial C, N, and P requirements differ among different species and are not constant through time (Aanderud et al., 2018), the hypotheses (**H3**, **H4**) have confirmed that the abundance of the majority of predicted C, N, and P cycling genes was related to total C and total N content, and with Po and Pi in MT and IL. In addition, the aforementioned genes were also related to C:N:P ratios which in turn depend on the physical and chemical properties of clay minerals (Kome et al., 2019).

5.4. Artificial soil systems as a model for unraveling soil processes

The soil development, including the formation of biogeochemical interfaces and pedogenetic processes, was extensively studied in different soils in both natural and anthropogenically influenced environments. In particular, the studies of chronosequences have provided important insights into soil development (Dümig et al., 2011; Mikutta et al., 2019; Schurig et al., 2013). However, the interpretation of the results obtained through those studies can be difficult or even impossible due to the unavailability of data about the soil development through time, natural heterogeneity of parental material, and the varying climatic conditions. Also, it is often difficult to separate the effects of specific factors such

as mineral composition, nutrient availability, or microbiota, on soil formation and to identify their relative importance since they are inherently related. Furthermore, a resident microbial community is present before the initial stages of soil development, making it difficult to determine their exact role in the subsequent development and maturation of the soil. Lastly, most studies include soils whose' development spans over a long period of time and are thus not suited to study processes that occur during the initial phase of soil development.

Hence, carefully designed laboratory experiments with simplified artificial soil systems that eliminate the effect of plant roots, fauna, and varying environmental conditions, performed under predefined and controlled conditions, can be considered a valuable tool in studying and pinpointing the effect of a limited number or even a single parameter on the soil development and avoiding ambiguities which arise when studying natural and more complex soils (Barré et al., 2014). A clear advantage of such systems is that they can be easily tailored according to the specific hypothesis, needs, and aims of the experiment, that the experimental conditions can be controlled, and parameters of interest can be easily manipulated. Despite such a long history of use in experimental pedology (Bockheim and Gennadiyev, 2009; Hallsworth and Crawford, 1965; Madhok, 1937) artificial soils are still recognized as a valuable resource in studying the processes involved in soil formation, including the microbial dynamics, formation of OM, macro-, and micro-aggregation (Guenet et al., 2011; Lamparter et al., 2014).

The soil development as shown by artificial soils containing MT or IL was influenced, exclusively, by the direct interactions between fine clay particles and microbes. Although the effects of plant roots, soil fauna, and varying environmental conditions which are essential for many soil-forming processes, were excluded from the experiment, the micro- and macro- aggregates formed in the artificial soils within 28 months. In addition, the OC mineralization after the addition of litter to the 28-month matured artificial soils was similar to natural soil (Vogel et al., 2015). The development of organo-mineral associations and aggregates and the mineralization of OC in the artificial soils were comparable with natural soils, stressing the suitability of artificial soils as a model for studying the processes in soil. However, it must be taken into account that the investigated MT or IL soils were provided with a larger amount of mineral surfaces than natural initial soils and that the soil development normally takes a much longer period of time than in this study. Furthermore, the artificial soils went through a cycle in which structural associations and macroaggregates were established followed by their decline as soil microorganisms colonized mineral and organic surfaces and substrate availability became reduced (Ding et al., 2013; Pronk et al., 2012; Vogel et al., 2014). Aggregation could be reactivated by the addition of manure and/or plant litter (Vogel et al., 2015) creating new, more variable niches

which could result in succession and diversification of microbial communities with subsequent increase in biodiversity (Or et al., 2007). This general trend in the formation and decline of soil systems must be taken into account whilst designing the experiments and choosing the sampling times since it can greatly affect the study outcomes.

As various materials in the formation of artificial soils can be added and different parameters can be varied independently, artificial soil systems can thus be used in a wide range of experiments. Such an approach may help avoid the ambiguities encountered when studying complex natural soils (Barré et al., 2014). Altogether, artificial soils with carefully selected model clay minerals, as was the case in this study, is an invaluable tool that allowed us to isolate and investigate the effect of clay minerals on the establishment of soil microbiota, the main processes involved in C, N and P transformations, as well as the microbial drivers of aforementioned processes during early phases of soil formation. Thus, allowing us to investigate the proposed hypotheses (**H1-H5**).

5.5. Potentials and drawbacks of the shotgun metagenomic approach

Soils are the most diverse ecosystems on micro- and macroscale, that consist of a vast mixture of niche and microhabitat with different physicochemical properties, hence, selecting different microbial communities. It is estimated that several thousand different bacterial species are present in only 1 g of soil (Nannipieri et al., 2003), which translates to approximately 1,000 Gbp of microbial genome sequences per gram of soil (Vogel et al., 2009). In addition, the soils are not only three-dimensional structures but are also highly dynamic and change with time, and in response to abiotic and anthropogenic influences (Nannipieri et al., 2020). Hence, it is extremely difficult to assess microbiological diversity, community structure, and activity, as well as to link taxa to specific soil functions. In that aspect, several approaches, including cultivation-based and cultivation-independent, were used with varying success, leaving the comprehensive assessment of soil microbiome and understanding of soil processes as one of the biggest unsolved challenges.

Since our knowledge of microbial requirements (e.g., nutrients, growth factors, temperature, pH, the combination of, etc.) is incomplete, the majority of soil microorganisms cannot be cultivated under laboratory conditions (Torsvik et al., 1990). It is estimated that less than 0.5 % of soil microorganisms have been cultivated *in vitro* (Guazzaroni et al., 2009; Vogel et al., 2009). Hence, cultivation-based methods can introduce bias by selecting only the cultivable part of the soil microbiome (Torsvik and Øvreås, 2002).

Thus, coupled with ever-decreasing sequencing prices and high-throughput bioinformatic analyses, in the last couple of decades, the studies of soil microbiome are more and more directed towards the cultivation-independent methods. There are two main cultivation-independent techniques, molecular barcoding and amplification of target genes, and shotgun sequencing. The molecular barcoding and amplification of target genes do not provide any information on soil microbiota function and are likely to introduce bias in the microbial community composition due to the amplification step (Bergmann et al., 2011; Schöler et al., 2017).

Hence, the next-generation shotgun sequencing of the soil metagenome was used in this study to gain an insight into the microbiota involved in the early stages of soil development and to test the hypotheses **H2-H5**. Namely, shotgun sequencing of the microbial community DNA can provide a piece of comprehensive information not only about the community structure but also about the genetic potential and the role of soil microorganisms in various soil processes, including different biogeochemical cycles. The detection of specific genes can enable the detection and reconstruction of metabolic pathways (Myrold et al., 2014). Also, taxonomy can be linked to the function by annotating the reads belonging to studied genes, thus predicting and identifying the soil microorganisms, and linking them to a certain process. This can reveal different ecological patterns, and indicate a relationship between microorganisms and function (Thomas et al., 2012). Finally, comparing metagenomes from different environments can provide powerful indications of a core- and biome-specific genetic potential in microbial communities. For example, Howe et al. (2016) identified the "core" set of C associated genes widely spread in multiple soil metagenomes from fertilized prairie (n=20), whereas Berlemont and Martiny (2013) showed that, in around 2,000 metagenomes collected from different biomes, the potential for utilization of carbohydrates differed according to the type of biome.

However, several drawbacks that can undermine the importance of shotgun metagenomic data need to be taken into account. Even though the NGS capacity is several terabases, it is still impossible to reconstruct the genomes of all microorganisms in a single gram of soil (Nannipieri et al., 2020). In addition, due to the heterogeneity of soil microbiota and dynamic changes in microbial communities with time (Penton et al., 2016; Schöler et al., 2017; Vestergaard et al., 2017), such analysis would give only limited information about the overall soil functionality in a given ecosystem. Also, soils are three-dimensional structures that differ not only on the macro- but also on the microscale. Besides, 1 gram of soil can contain a large number of niches with different physicochemical properties and consequently, different microbial communities, which questions if such a sample is adequate.

DNA extraction is another potential step that can introduce bias since the quality and quantity of DNA are heavily dependent on the soil type and extraction method (Bakken and Frostegård, 2006). Simultaneously with DNA extraction, humic substances are often coextracted. Since they can limit or even inhibit downstream analyses, DNA purification is advised. However, purification can result in DNA loss. Several studies have shown that during DNA extraction certain microorganisms such as active microbial communities can be favored, thus influencing the amount and proportion of DNA extracted from soil (Delmont et al., 2012). In addition, DNA extraction can lead to DNA shearing, which can influence the shotgun metagenomic sequencing which requires higher amounts of quality, high-molecular weight DNA (Vestergaard et al., 2017).

The sequencing library preparation is not only laborious and time-consuming but it is also prone to the selection of DNA sequences with higher stability which are resistant to mechanical shearing, and size selection steps which can lead to artificial exponential amplification during the PCR, and a false representation of sequence frequency in a dataset.

In the last decades, different bioinformatics tools and pipelines have become available. Since different pipelines often involve different quality filtering and de-noising steps, and comparison with different databases, results of the metagenome or amplicon analyses may vary depending on the pipeline used (Vestergaard et al., 2017). Also, considering the sequencing depth the sequencing efforts are still questionable. In the majority of soil sequencing projects, based on the rarefaction analysis it was shown that the metagenomic data covered less than 20 % of total diversity. In addition, to reconstruct and identify genes involved in major nutrient cycles at least 5-10 Gb per sample is needed (Vestergaard et al., 2017).

Furthermore, the conclusions in metagenomic sequencing projects are mostly based on taxonomy and predicted gene relative abundances acquired by reads annotation and comparison with publicly available databases. Often, those predictions for a metagenome are not reliable, since read annotation is normally given as “best hits” or are considered “unknown”. The publicly available databases (e.g., National Center for Biotechnology Information - NCBI, Kyoto Encyclopedia of Genes and Genomes - KEGG, SEED, and Clusters of Orthologous Groups - COG) differ greatly, once again stressing the fact that analyses results depend on the pipelines and databases used. However, such annotations are not indicative of absolute abundances, as the annotation is dependent on several factors, including the previously mentioned sequencing depth.

Firstly, annotation quality is highly dependent on the read length, and for short reads, it increases with the assembly of contigs. Secondly, only the fraction of sequencing reads can be both taxonomically and functionally annotated when reference sequences from publicly available databases are used for comparison (Wooley et al., 2010). The sequences in previously mentioned databases contain mostly sequences that originate from cultivation studies, gene isolation and expression, and biochemical characterization studies. However, lately, an increasing number of sequences in databases originate from high-throughput sequencing studies of DNA from various environments (Benson et al., 2013). Such sequences are only putative and not as reliable as sequences that originate from cultivation and biochemical characterization studies, since the microorganisms which harbour those sequences were never cultivated and characterized.

The majority of genomic databases are not representative of the soil microbiome (Choi et al., 2017). However, numerous reliable reference sequences are still available. For example, Pruitt et al. (2012) estimated that in 2012, the curated NCBI Reference Sequence (RefSeq) database contained around 18,000 species from which 64 % belonged to the microbes, where bacterial and archaeal sequences (approx. 59 %) dominate, whereas only around 7 % of all accessions belong to the fungi and Pruesse et al. (2007) that the SILVA database contained nearly 6 million small-subunit ribosomal sequences which corresponded to approximately 700,000 non-redundant sequences. Keeping in mind that less than 0.5 % of soil microorganisms (Guazzaroni et al., 2009; Vogel et al., 2009) and around 1% of bacteria, in general, have been cultivated under the laboratory conditions (Amann, 1995) the true extent of microbial diversity and related functions in different ecosystems are still largely unknown. The underrepresentation of fungal sequences in particular, in publicly available databases may be contributed to even greater cultivation difficulties (Collado et al., 2007) in comparison to other microorganisms. Due to this underrepresentation, fungi are often detected in soil metagenomes in low abundance 0.2-1.6 % (Noronha et al., 2017), despite their high abundance and diversity estimation in different soils (Buée et al., 2009).

Furthermore, despite the increasing number of studies and soil sequencing datasets available a soil-specific database is still missing. To bridge this gap Choi et al. (2017) have curated the RefSoil database, a subset of NCBI's database of sequenced genomes, RefSeq (release 74). This database consists of sequenced genomes of organisms originating from soil. In total it contains 922 genomes, of which 888 belong to bacteria and 34 to archaea. Whilst it contains similar dominant microorganisms (e.g., Proteobacteria, Firmicutes, and Actinobacteria) as RefSeq, it also contains higher proportions of Armatimonadetes,

Germmatimonadetes, Thermodesulfobacteria, Acidobacteria, Nitrospirae, and Chloroflexi which are underrepresented in RefSeq, whilst they are associated with different soil.

In the artificial soil metagenomes analyzed here, the percentage of reads which could be taxonomically assigned using the NCBI non-redundant protein sequence database (NCBI-nr) was approximately 56 %. Of those annotated sequences approximately 94 % were bacterial, 4 % eukaryotic, 2 % archaeal, and only up to 0.4 % fungal reads.

Generally, the annotation success is higher for taxonomic than for functional reads. In this study, 35 % and 22 % of all sequences from the MT and IL metagenome, respectively, were functionally annotated. This is in line with other previously published soil metagenomes, where successful functional annotation varies from 10-35 % of reads (Delmont et al., 2011; Fierer et al., 2012). The lower functional annotations might be contributed to a large number and high diversity of genes encoding proteins and enzymes found in microbial genomes. For example, the average bacterial genome consists of 5,000 protein-coding regions. *Escherichia coli* contains more than 60,000 unique and only approximately 3,000 core gene families (Land et al., 2015). Although the gene-coding regions in microbial genomes are well predicted, the functional annotation of such a variety of genes is still not fully successful. Even though according to Kanehisa et al. (2016) KEGG database comprises approximately 25 million gene sequences obtained mainly from the Genbank and Refseq databases, divided into approximately 21,000 orthologous groups, it, apparently, still does not cover the estimated diversity of genes encoding proteins.

All considering, it is not surprising that a significant portion of metagenome sequences cannot be taxonomically or functionally assigned. Altogether, the above-mentioned factors may limit the overall taxonomic and functional annotation of the metagenomes, as well as the linkage between function and taxonomy. However, besides all potential drawbacks, shotgun metagenomics represents one of the best tools for a comprehensive study of microbial diversity, the complexity of microbially driven processes in soil, and linking the studied process with microbial taxa driving them, at the moment. Finally, this was an invaluable approach that allowed us to test and confirm the hypotheses **H2-H5**.

6. CONCLUSIONS AND OUTLOOK

Since the artificial soil allows the use of pristine mineral surfaces, it represents a strong foundation for mechanistic inference. Despite the simplification inherent in such approach, particularly with respect to the biological and physical processes involved in aggregation, the limited maturation times, and the absence of other biotic factors such as flora and fauna, it provides a valuable insight into soil dynamics in the early stage of soil development. The present study focused on the effect of different clay minerals, montmorillonite (MT) and illite (IL), on the establishment and development of a distinct microbiome and henceforth the soil activities in the initial stages of soil development characterized by main nutrients, such as C, N and P depletion.

Our results confirmed that physicochemical properties of clay minerals MT and IL, such as variable surface area, and charge, in particular, dictate the bioavailability of nutrients thus, shaping the microbial communities, and activities later on. Furthermore, they gave us insight into the processes involved in C, N, and P transformations during the initial phase of soil formation, as well as into the functional groups that drive said processes, thus, enabling us to predict the main processes involved in nutrient cycling and turnover depending on the soil stoichiometry.

In addition, this research has shown that the predicted key players involved in C, N, and P transformation were among the dominant taxa, which underlines the importance of main nutrient acquisition in both artificial soil mixtures, with only a few taxa with the potential for driving all processes involved in C, N, or P cycling. Families unique for a single artificial soil type with the potential to drive a specific process were found in a very low abundance. The dominant families predicted to be involved in C, N, and P turnover like *Bacillaceae*, *Microchaetaceae,* and *Thaumarchaeota* are perfectly adapted to harsh environments with the ability to rest as spores or acquire additional nutrients like C and N by fixation.

Since the bioavailability of carbon, nitrogen, and phosphorus was limited after a prolonged maturation, our results have shown that microorganisms have developed new strategies, such as recycling of mineral and organic C, N, and P, as well as an increase in N and P uptake, in order to adapt and survive. For example, our data indicate that mainly recalcitrant C compounds, organic N compounds, and organic P are an important source in both artificial soil mixtures, as many reads were assigned to genes potentially involved in the recalcitrant C compounds degradation, N mineralization, and assimilation, as well as effective use of organic P sources, including different cellulolytic, proteolytic, ureolytic enzymes, and different alkaline phosphatases and glycerophosphoryl diester phosphodiesterase, respectively. These might be involved in the mineralization of still

available C polymers, organic N, and organic P introduced with the manure or released from the dead microbial biomass, whose composition significantly changed in more than 300 days after the last manure addition.

Furthermore, our data has shown that in MT, which has a larger soil surface area, the relative abundance of the predicted *gltDB* and *pstC* gene was higher when compared to IL. These genes encode highly effective enzymes involved in the assimilation of N into microbial biomass under N depleted conditions, and the high-affinity phosphate-specific transporter (*pstSCAB*) system acting under P starvation, respectively, thus allowing effective recycling of N and P, and overcoming nutrient depletion.

However, since our observations were based on DNA sequencing, they represent the system’s potential, which allowed us to investigate the general potential of the microbial communities but doesn't provide information about the activity of the microbiomes. In order to deepen the insight into nutrient turnover mechanisms and to identify active microbial communities involved in the processes, RNA and proteome-based studies and additional experiments should be employed.

7. LITERATURE

Aanderud Z.T., Saurey S., Ball B.A., Wall D.H., Barrett J.E., Muscarella M.E., Griffin N.A., Virginia R.A., Barberán A., Adams B.J. (2018). Stoichiometric Shifts in Soil C:N:P Promote Bacterial Taxa Dominance, Maintain Biodiversity, and Deconstruct Community Assemblages. Front Microbiol 9: 1401. doi:10.3389/fmicb.2018.01401

Abdel-Hamid A.M., Solbiati J.O., Cann I.K.O. (2013). Insights into Lignin Degradation and its Potential Industrial Applications. In: Advances in Applied Microbiology (Sariaslani S., Gadd G., eds), Academic Press Inc Elsevier Science, San Diego, California, USA, pp. 1–28. doi:10.1016/B978-0-12-407679-2.00001-6

Abdulla H. (2009). Bioweathering and Biotransformation of Granitic Rock Minerals by Actinomycetes. Microb Ecol 58 (4): 753–761. doi:10.1007/s00248-009-9549-1

Adams M.M., Gómez-García M.R., Grossman A.R., Bhaya D. (2008). Phosphorus Deprivation Responses and Phosphonate Utilization in a Thermophilic Synechococcus sp. from Microbial Mats. J Bacteriol 190 (24): 8171–8184. doi:10.1128/JB.01011-08

Ahmed A., Aslam M., Ashraf M., ul-Hassan Nasim F., Batool K., Bibi A. (2017). Microbial β-Glucosidases: Screening, Characterization, Cloning and Applications. J Appl Environ Microbiol 5 (2): 57–73. doi:10.12691/jaem-5-2-2

Alessi D.S., Walsh D.M., Fein J.B. (2011). Uncertainties in determining microbial biomass C using the chloroform fumigation-extraction method. Chem Geol 280 (1–2): 58–64. doi:10.1016/j.chemgeo.2010.10.014

Alexandre G., Zhulin I.B. (2000). Laccases are widespread in bacteria. Trends Biotechnol 18 (2): 41–42. doi:10.1016/S0167-7799(99)01406-7

Amann R.I., Ludwig W., Schleifer K.H. (1995). Phylogenetic identification and in situ detection of individual microbial cells without cultivation. Microbiol Rev 59 (1): 143–169. doi:10.1128/mmbr.59.1.143-169.1995

Auguie B., Antonov A. (2015). gridExtra: Miscellaneous functions for “grid” graphics: R Package version 2.0.0. Available at: http://cran.r-project.org/package=gridExtra [Accessed: 22 November 2015]

Babin D., Ding G.-C., Pronk G.J., Heister K., Kögel-Knabner I., Smalla K. (2013). Metal oxides, clay minerals and charcoal determine the composition of microbial communities in matured artificial soils and their response to phenanthrene. FEMS Microbiol Ecol 86 (1): 3–14. doi:10.1111/1574-6941.12058

Bach H.J., Tomanova J., Schloter M., Munch J.C. (2002). Enumeration of total bacteria and bacteria with genes for proteolytic activity in pure cultures and in environmental samples by quantitative PCR mediated amplification. J Microbiol Methods 49 (3): 235–245. doi:10.1016/S0167-7012(01)00370-0

Bajerski F., Wagner D. (2013). Bacterial succession in Antarctic soils of two glacier forefields on Larsemann Hills, East Antarctica. FEMS Microbiol Ecol 85 (1): 128–142. doi:10.1111/1574-6941.12105

Bakken L.R., Frostegård Å. (2006). Nucleic acid extraction from soil. In: Nucleic acids and proteins in soil (Nannipieri P., Smalla K., eds), Springer, Berlin, Heidelberg, pp. 49–73. doi:10.1007/3-540-29449-X_3

Baldock J.A. (2002). Interactions of organic materials and microorganisms with minerals in the stabilization of soil structure. In: Interactions between Soil Particles and Microorganisms: Impact on the Terrestrial Ecosystem (Huang P.M., Bollag J.-M., Senesi N., eds), John Wiley & Sons Ltd, New York, NY, USA, pp. 85–131

Bardgett R.D., Caruso T. (2020). Soil microbial community responses to climate extremes: resistance, resilience and transitions to alternative states. Philos Trans R Soc B Biol Sci 375 (1794): 20190112. doi:10.1098/rstb.2019.0112

Bardgett R.D., van der Putten W.H. (2014). Belowground biodiversity and ecosystem functioning. Nature 515 (7528): 505–511. doi:10.1038/nature13855

Barnard R.L., Osborne C.A., Firestone M.K. (2013). Responses of soil bacterial and fungal communities to extreme desiccation and rewetting. ISME J 7 (11): 2229–2241. doi:10.1038/ismej.2013.104

Barré P., Fernandez-Ugalde O., Virto I., Velde B., Chenu C. (2014). Impact of phyllosilicate mineralogy on organic carbon stabilization in soils: Incomplete knowledge and exciting prospects. Geoderma 382–395. doi:10.1016/j.geoderma.2014.07.029

Barth A., Hendrix J., Fried D., Barak Y., Bayer E.A., Lamb D.C. (2018). Dynamic interactions of type I cohesin modules fine-tune the structure of the cellulosome of Clostridium thermocellum. Proc Natl Acad Sci USA 115 (48): E11274–E11283. doi:10.1073/pnas.1809283115

Baruah J., Nath B.K., Sharma R., Kumar S., Deka R.C., Baruah D.C., Kalita E. (2018). Recent Trends in the Pretreatment of Lignocellulosic Biomass for Value-Added Products. Front Energy Res 6: 141. doi:10.3389/fenrg.2018.00141

Baveye P.C., Otten W., Kravchenko A., Balseiro-Romero M., Beckers É., Chalhoub M., Darnault C., Eickhorst T., Garnier P., Hapca S., Kiranyaz S., Monga O., Mueller C.W., Nunan N., Pot V., Schlüter S., Schmidt H., Vogel H.J. (2018). Emergent Properties of Microbial Activity in Heterogeneous Soil Microenvironments: Different Research Approaches Are Slowly Converging, Yet Major Challenges Remain. Front Microbiol 9: 1929. doi:10.3389/fmicb.2018.01929

Bellenger J.P., Darnajoux R., Zhang X., Kraepiel A.M.L. (2020). Biological nitrogen fixation by alternative nitrogenases in terrestrial ecosystems: a review. Biogeochemistry 149 (1): 53–73. doi:10.1007/s10533-020-00666-7

Bender S.F., Wagg C., van der Heijden M.G.A. (2016). An Underground Revolution: Biodiversity and Soil Ecological Engineering for Agricultural Sustainability. Trends Ecol Evol 31 (6): 440–452. doi:10.1016/j.tree.2016.02.016

Benson D.A., Cavanaugh M., Clark K., Karsch-Mizrachi I., Lipman D.J., Ostell J., Sayers E.W. (2013). GenBank. Nucleic Acids Res 41 (D1): D36–D42. doi:10.1093/nar/gks1195

Bergkemper F., Schöler A., Engel M., Lang F., Krüger J., Schloter M., Schulz S. (2016). Phosphorus depletion in forest soils shapes bacterial communities towards phosphorus recycling systems. Environ Microbiol 18 (6): 1988–2000. doi:10.1111/1462-2920.13188

Bergmann G.T., Bates S.T., Eilers K.G., Lauber C.L., Caporaso J.G., Walters W.A., Knight R., Fierer N. (2011). The under-recognized dominance of Verrucomicrobia in soil bacterial communities. Soil Biol Biochem 43 (7): 1450–1455. doi:10.1016/j.soilbio.2011.03.012

Berlemont R., Martiny A.C. (2013). Phylogenetic Distribution of Potential Cellulases in Bacteria. Appl Environ Microbiol 79 (5): 1545–1554. doi:10.1128/AEM.03305-12

Bernard L., Mougel C., Maron P.A., Nowak V., Lévêque J., Henault C., Haichar F.E.Z., Berge O., Marol C., Balesdent J., Gibiat F., Lemanceau P., Ranjard L. (2007). Dynamics and identification of soil microbial populations actively assimilating carbon from 13C-labelled wheat residue as estimated by DNA- and RNA-SIP techniques. Environ Microbiol 9 (3): 752–764. doi:10.1111/j.1462-2920.2006.01197.x

Boatman T.G., Lawson T., Geider R.J. (2017). A Key Marine Diazotroph in a Changing Ocean: The Interacting Effects of Temperature, CO2 and Light on the Growth of Trichodesmium erythraeum IMS101. PLoS One 12 (1): E0168796. doi:10.1371/journal.pone.0168796

Bockheim J.G., Gennadiyev A.N. (2009). The value of controlled experiments in studying soil-forming processes: A review. Geoderma 152 (3–4): 208–217. doi:10.1016/j.geoderma.2009.06.019

Boeddinghaus R.S., Marhan S., Gebala A., Haslwimmer H., Vieira S., Sikorski J., Overmann J., Soares M., Rousk J., Rennert T., Kandeler E. (2021). The mineralosphere—interactive zone of microbial colonization and carbon use in grassland soils. Biol Fertil Soils 57 (5): 587–601. doi:10.1007/s00374-021-01551-7

Bottomley P.J., Myrold D.D. (2015). Biological N inputs. In: Soil Microbiology, Ecology and Biochemistry (Paul E.A., ed), Academic Press, San Diego, CA, San Diego, California, USA, pp. 447–470. doi:10.1016/B978-0-12-415955-6.00015-3

Boyd E.S., Cummings D.E., Geesey G.G. (2007). Mineralogy Influences Structure and Diversity of Bacterial Communities Associated with Geological Substrata in a Pristine Aquifer. Microb Ecol 54 (1): 170–182. doi:10.1007/s00248-006-9187-9

Brankatschk R., Töwe S., Kleineidam K., Schloter M., Zeyer J. (2011). Abundances and potential activities of nitrogen cycling microbial communities along a chronosequence of a glacier forefield. ISME J 5 (6): 1025–1037. doi:10.1038/ismej.2010.184

Brevik E.C., Cerdà A., Mataix-Solera J., Pereg L., Quinton J.N., Six J., Van Oost K. (2015). The interdisciplinary nature of SOIL. SOIL 1 (1): 117–129. doi:10.5194/soil-1-117-2015

Brito L.F., López M.G., Straube L., Passaglia L.M.P., Wendisch V.F. (2020). Inorganic Phosphate Solubilization by Rhizosphere Bacterium Paenibacillus sonchi: Gene Expression and Physiological Functions. Front Microbiol 11: 588605. doi:10.3389/fmicb.2020.588605

Buchfink B., Xie C., Huson D.H. (2015). Fast and sensitive protein alignment using DIAMOND. Nat Methods 12 (1): 59–60. doi:10.1038/nmeth.3176

Buchkowski R.W., Shaw A.N., Sihi D., Smith G.R., Keiser A.D. (2019). Constraining Carbon and Nutrient Flows in Soil With Ecological Stoichiometry. Front Ecol Evol 7: 382. doi:10.3389/fevo.2019.00382

Buée M., Reich M., Murat C., Morin E., Nilsson R.H., Uroz S., Martin F. (2009). 454 Pyrosequencing analyses of forest soils reveal an unexpectedly high fungal diversity. New Phytol 184 (2): 449–456. doi:10.1111/j.1469-8137.2009.03003.x

Čapek P.T., Manzoni S., Kaštovská E., Wild B., Diáková K., Bárta J., Schnecker J., Biasi C., Martikainen P.J., Alves R.J.E., Guggenberger G., Gentsch N., Hugelius G., Palmtag J., Mikutta R., Shibistova O., Urich T., Schleper C., Richter A., Šantrůčková H. (2018). A plant–microbe interaction framework explaining nutrient effects on primary production. Nat Ecol Evol 2 (10): 1588–1596. doi:10.1038/s41559-018-0662-8

Cederlund H., Wessén E., Enwall K., Jones C.M., Juhanson J., Pell M., Philippot L., Hallin S. (2014). Soil carbon quality and nitrogen fertilization structure bacterial communities with predictable responses of major bacterial phyla. Appl Soil Ecol 84: 62–68. doi:10.1016/j.apsoil.2014.06.003

Certini G., Campbell C.D., Edwards A.C. (2004). Rock fragments in soil support a different microbial community from the fine earth. Soil Biol Biochem 36 (7): 1119–1128. doi:10.1016/j.soilbio.2004.02.022

Chaerun S.K., Tazaki K., Asada R., Kogure K. (2005). Interaction between clay minerals and hydrocarbon-utilizing indigenous microorganisms in high concentrations of heavy oil: implications for bioremediation. Clay Miner 40 (1): 105–114. doi:10.1180/0009855054010159

Chan Y., Lacap D.C., Lau M.C.Y., Ha K.Y., Warren-Rhodes K.A., Cockell C.S., Cowan D.A., Mckay C.P., Pointing S.B. (2012). Hypolithic microbial communities: Between a rock and a hard place. Environ Microbiol 14 (9): 2272–2282. doi:10.1111/j.1462-2920.2012.02821.x

Chang W.S., van de Mortel M., Nielsen L., de Guzman G.N., Li X., Halverson L.J. (2007). Alginate production by Pseudomonas putida creates a hydrated microenvironment and contributes to biofilm architecture and stress tolerance under water-limiting conditions. J Bacteriol 189 (22): 8290–8299. doi:10.1128/JB.00727-07

Chen J. (2012). GUniFrac: generalized UniFrac distances. R Package version 1.0. Available at: http://cran.r-project.org/package=GUniFrac [Accessed: 22 November 2015]

Chen R., Senbayram M., Blagodatsky S., Myachina O., Dittert K., Lin X., Blagodatskaya E., Kuzyakov Y. (2014). Soil C and N availability determine the priming effect: microbial N mining and stoichiometric decomposition theories. Glob Chang Biol 20 (7): 2356–2367. doi:10.1111/gcb.12475

Choi J., Yang F., Stepanauskas R., Cardenas E., Garoutte A., Williams R., Flater J., Tiedje J.M., Hofmockel K.S., Gelder B., Howe A. (2017). Strategies to improve reference databases for soil microbiomes. ISME J 11 (4): 829–834. doi:10.1038/ismej.2016.168

Chuckran P.F., Fofanov V., Hungate B.A., Morrissey E.M., Schwartz E., Walkup J., Dijkstra P. (2021). Rapid Response of Nitrogen Cycling Gene Transcription to Labile Carbon Amendments in a Soil Microbial Community. mSystems 6 (3): e00161-21. doi:10.1128/msystems.00161-21

Chukwuma O.B., Rafatullah M., Tajarudin H.A., Ismail N. (2020). Lignocellulolytic Enzymes in Biotechnological and Industrial Processes: A Review. Sustainability 12 (18): 7282. doi:10.3390/su12187282

Clark I.M., Buchkina N., Jhurreea D., Goulding K.W.T., Hirsch P.R. (2012). Impacts of nitrogen application rates on the activity and diversity of denitrifying bacteria in the Broadbalk Wheat Experiment. Philos Trans R Soc B Biol Sci 367 (1593): 1235–1244. doi:10.1098/rstb.2011.0314

Cleveland C.C., Liptzin D. (2007). C:N:P stoichiometry in soil: Is there a 'Redfield ratio' for the microbial biomass? Biogeochemistry 85 (3): 235–252. doi:10.1007/s10533-007-9132-0

Collado J., Platas G., Paulus B., Bills G.F. (2007). High-throughput culturing of fungi from plant litter by a dilution-to-extinction technique. FEMS Microbiol Ecol 60 (3): 521–533. doi:10.1111/j.1574-6941.2007.00294.x

Corrêa T.L.R., Júnior A.T., Wolf L.D., Buckeridge M.S., dos Santos L.V., Murakami M.T. (2019). An actinobacteria lytic polysaccharide monooxygenase acts on both cellulose and xylan to boost biomass saccharification. Biotechnol Biofuels. doi:10.1186/s13068-019-1449-0

Crouzet O., Consentino L., Pétraud J.P., Marrauld C., Aguer J.P., Bureau S., Le Bourvellec C., Touloumet L., Bérard A. (2019). Soil Photosynthetic Microbial Communities Mediate Aggregate Stability: Influence of Cropping Systems and Herbicide Use in an Agricultural Soil. Front Microbiol 10: 1319. doi:10.3389/fmicb.2019.01319

Cuadros J. (2017). Clay minerals interaction with microorganisms: a review. Clay Miner 52 (2): 235–261. doi:10.1180/claymin.2017.052.2.05

Cui J., Zhu Z., Xu X., Liu S., Jones D.L., Kuzyakov Y., Shibistova O., Wu J., Ge T. (2020a). Carbon and nitrogen recycling from microbial necromass to cope with C:N stoichiometric imbalance by priming. Soil Biol Biochem 142 (2019): 107720. doi:10.1016/j.soilbio.2020.107720

Cui Y., Fang L., Guo X., Wang X., Zhang Y., Li P., Zhang X. (2018). Ecoenzymatic stoichiometry and microbial nutrient limitation in rhizosphere soil in the arid area of the northern Loess Plateau, China. Soil Biol Biochem 116: 11–21. doi:10.1016/j.soilbio.2017.09.025

Cui Y., Zhang Y., Duan C., Wang X., Zhang X., Ju W., Chen H., Yue S., Wang Y., Li S., Fang L. (2020b). Ecoenzymatic stoichiometry reveals microbial phosphorus limitation decreases the nitrogen cycling potential of soils in semi-arid agricultural ecosystems. Soil Tillage Res 197: 104463. doi:10.1016/j.still.2019.104463

Culman S.W., Bukowski R., Gauch H.G., Cadillo-Quiroz H., Buckley D.H. (2009). T-REX: Software for the processing and analysis of T-RFLP data. BMC Bioinformatics 10: 171.

doi:10.1186/1471-2105-10-171

Dai Z., Zang H., Chen J., Fu Y., Wang X., Liu H., Shen C., Wang J., Kuzyakov Y., Becker J.N., Hemp A., Barberán A., Gunina A., Chen H., Luo Y., Xu J. (2021). Metagenomic insights into soil microbial communities involved in carbon cycling along an elevation climosequences. Environ Microbiol 23 (8): 4631–4645. doi:10.1111/1462-2920.15655

Daly A.B., Jilling A., Bowles T.M., Buchkowski R.W., Frey S.D., Kallenbach C.M., Keiluweit M., Mooshammer M., Schimel J.P., Grandy A.S. (2021). A holistic framework integrating plant-microbe-mineral regulation of soil bioavailable nitrogen. Biogeochemistry 154 (2): 211–229. doi:10.1007/s10533-021-00793-9

Datta R., Kelkar A., Baraniya D., Molaei A., Moulick A., Meena R.S., Formanek P. (2017). Enzymatic Degradation of Lignin in Soil: A Review. Sustainability 9 (7): 1163. doi:10.3390/su9071163

Davidson E.A., Janssens I.A. (2006). Temperature sensitivity of soil carbon decomposition and feedbacks to climate change. Nature 440 (7081): 165–173. doi:10.1038/nature04514

de Gonzalo G., Colpa D.I., Habib M.H.M., Fraaije M.W. (2016). Bacterial enzymes involved in lignin degradation. J Biotechnol 236: 110–119. doi:10.1016/j.jbiotec.2016.08.011

Delgado-Baquerizo M., Giaramida L., Reich P.B., Khachane A.N., Hamonts K., Edwards C., Lawton L.A., Singh B.K. (2016). Lack of functional redundancy in the relationship between microbial diversity and ecosystem functioning. J Ecol 104 (4): 936–946. doi:10.1111/1365-2745.12585

Delmont T.O., Robe P., Clark I., Simonet P., Vogel T.M. (2011). Metagenomic comparison of direct and indirect soil DNA extraction approaches. J Microbiol Methods 86 (3): 397–400. doi:10.1016/j.mimet.2011.06.013

DeLuca T.H., Pingree M.R.A., Gao S. (2019). Assessing soil biological health in forest soils. In: Developments in Soil Science (Busse M., Giardina C.P., Morris D.M., PageDumroese D., eds), Elsevier, Amsterdam, Netherlands, pp. 397–426. doi:10.1016/B978-0-444-63998-1.00016-1

Denef K., Six J., Merckx R., Paustian K. (2002). Short-term effects of biological and physical forces on aggregate formation in soils with different clay mineralogy. Plant Soil 246 (2): 185–200. doi:10.1023/A:1020668013524

Deng M., Hou J., Song K., Chen J., Gou J., Li D., He X. (2020). Community metagenomic assembly reveals microbes that contribute to the vertical stratification of nitrogen cycling in an aquaculture pond. Aquaculture 520: 734911. doi:10.1016/j.aquaculture.2019.734911

Ding G.-C., Pronk G.J., Babin D., Heuer H., Heister K., Kögel-Knabner I., Smalla K. (2013). Mineral composition and charcoal determine the bacterial community structure in artificial soils. FEMS Microbiol Ecol 86 (1): 15–25. doi:10.1111/1574-6941.12070

Docampo R., de Souza W., Miranda K., Rohloff P., Moreno S.N.J. (2005). Acidocalcisomes - Conserved from bacteria to man. Nat Rev Microbiol 3 (3): 251–261.

doi:10.1038/nrmicro1097

Donhauser J., Frey B. (2018). Alpine soil microbial ecology in a changing world. FEMS Microbiol Ecol 94 (9): fiy099. doi:10.1093/femsec/fiy099

Drigo B., Pijl A.S., Duyts H., Kielak A.M., Gamper H.A., Houtekamer M.J., Boschker H.T.S., Bodelier P.L.E., Whiteley A.S., van Veen J.A., Kowalchuk G.A. (2010). Shifting carbon flow from roots into associated microbial communities in response to elevated atmospheric CO2. Proc Natl Acad Sci U S A 107 (24): 10938–10942. doi:10.1073/pnas.0912421107

Du E., Terrer C., Pellegrini A.F.A., Ahlström A., van Lissa C.J., Zhao X., Xia N., Wu X., Jackson R.B. (2020). Global patterns of terrestrial nitrogen and phosphorus limitation. Nat Geosci 13 (3): 221–228. doi:10.1038/s41561-019-0530-4

Ducat D.C., Silver P.A. (2012). Improving carbon fixation pathways. Curr Opin Chem Biol 16 (3–4): 337–344. doi:10.1016/j.cbpa.2012.05.002

Duiker S.W., Rhoton F.E., Torrent J., Smeck N.E., Lal R. (2003). Iron (Hydr)Oxide Crystallinity Effects on Soil Aggregation. Soil Sci Soc Am J 67 (2): 606–611. doi:10.2136/sssaj2003.0606

Dümig A., Häusler W., Steffens M., Kögel-Knabner I. (2012). Clay fractions from a soil chronosequence after glacier retreat reveal the initial evolution of organo-mineral associations. Geochim Cosmochim Acta 85: 1–18. doi:10.1016/j.gca.2012.01.046

Dungait J.A.J., Hopkins D.W., Gregory A.S., Whitmore A.P. (2012). Soil organic matter turnover is governed by accessibility not recalcitrance. Glob Chang Biol 18 (6): 1781–1796. doi:10.1111/j.1365-2486.2012.02665.x

Egli M., Bösiger M., Lamorski K., Cezary S., Wiesenberg G.L.B., Tikhomirov D., Musso A., Hsu S.-Y., Raimondi S. (2021). Pedogenesis and carbon sequestration in transformed agricultural soils of Sicily. Geoderma 402 (115355). doi:10.1016/j.geoderma.2021.115355

Egli M., Hunt A.G., Dahms D., Raab G., Derungs C., Raimondi S., Yu F. (2018). Prediction of Soil Formation as a Function of Age Using the Percolation Theory Approach. Front Environ Sci 6: 108. doi:10.3389/fenvs.2018.00108

Egli M., Mirabella A. (2021). The origin and formation of clay minerals in alpine soils. In: Hydrogeology, Chemical Weathering, and Soil Formation (Hunt A, Egli M., Faybishenko B., eds), Wiley, New York, NY, USA, pp. 121–137

Egli M., Wernli M., Burga C., Kneisel C., Mavris C., Valboa G., Mirabella A., Plötze M., Haeberli W. (2011). Fast but spatially scattered smectite-formation in the proglacial area Morteratsch: An evaluation using GIS. Geoderma 164 (1–2): 11–21. doi:10.1016/j.geoderma.2011.05.001

Elser J.J., Acharya K., Kyle M., Cotner J., Makino W., Markow T., Watts T., Hobbie S., Fagan W., Schade J., Hood J., Sterner R.W. (2003). Growth rate-stoichiometry couplings in diverse biota. Ecol Lett 6 (10): 936–943. doi:10.1046/j.1461-0248.2003.00518.x

Elser J.J., Bracken M.E.S., Cleland E.E., Gruner D.S., Harpole W.S., Hillebrand H., Ngai J.T., Seabloom E.W., Shurin J.B., Smith J.E. (2007). Global analysis of nitrogen and phosphorus limitation of primary producers in freshwater, marine and terrestrial ecosystems. Ecol Lett 10 (12): 1135–1142. doi:10.1111/j.1461-0248.2007.01113.x

Evans P.N., Boyd J.A., Leu A.O., Woodcroft B.J., Parks D.H., Hugenholtz P., Tyson G.W. (2019). An evolving view of methane metabolism in the Archaea. Nat Rev Microbiol 17 (4): 219–232. doi:10.1038/s41579-018-0136-7

Evans S.E., Wallenstein M.D., Burke I.C. (2014). Is bacterial moisture niche a good predictor of shifts in community composition under long-term drought? Ecology 95 (1): 110–122. doi:10.1890/13-0500.1

Fang Y., Nazaries L., Singh B.K., Singh B.P. (2018). Microbial mechanisms of carbon priming effects revealed during the interaction of crop residue and nutrient inputs in contrasting soils. Glob Chang Biol 24 (7): 2775–2790. doi:10.1111/gcb.14154

Fierer N., Bradford M.A., Jackson R.B. (2007). Toward an ecological classification of soil bacteria. Ecology 88 (6): 1354–1364

Fierer N., Leff J.W., Adams B.J., Nielsen U.N., Bates S.T., Lauber C.L., Owens S., Gilbert J.A., Wall D.H., Caporaso J.G. (2012). Cross-biome metagenomic analyses of soil microbial communities and their functional attributes. Proc Natl Acad Sci USA 109 (52): 21390–21395. doi:10.1073/pnas.1215210110

Flint H.J., Scott K.P., Duncan S.H., Louis P., Forano E. (2012). Microbial degradation of complex carbohydrates in the gut. Gut Microbes 3 (4): 289–306. doi:10.4161/gmic.19897

Fontaine S., Mariotti A., Abbadie L. (2003). The priming effect of organic matter: a question of microbial competition? Soil Biol Biochem 35 (6): 837–843. doi:10.1016/S0038-0717(03)00123-8

Forbes M.S., Broos K., Baldock J.A., Gregg A.L., Wakelin S.A. (2009). Environmental and edaphic drivers of bacterial communities involved in soil N-cycling. Aust J Soil Res 47 (4): 380–388. doi:10.1071/SR08126

Foster R.A., Tienken D., Littmann S., Whitehouse M.J., Kuypers M.M.M., White A.E. (2022). The rate and fate of N2 and C fixation by marine diatom-diazotroph symbioses. ISME J 16 (2): 477–487. doi:10.1038/s41396-021-01086-7

Francioli D., Schulz E., Lentendu G., Wubet T., Buscot F., Reitz T. (2016). Mineral vs. Organic Amendments: Microbial Community Structure, Activity and Abundance of Agriculturally Relevant Microbes Are Driven by Long-Term Fertilization Strategies. Front Microbiol 7: 1446. doi:10.3389/fmicb.2016.01446

Francis C.A., Beman J.M., Kuypers M.M.M. (2007). New processes and players in the nitrogen cycle: the microbial ecology of anaerobic and archaeal ammonia oxidation. ISME J 1 (1): 19–27. doi:10.1038/ismej.2007.8

Fraser T.D., Lynch D.H., Bent E., Entz M.H., Dunfield K.E. (2015). Soil bacterial phoD gene abundance and expression in response toapplied phosphorus and long-term

management. Soil Biol Biochem 88: 137–147. doi:10.1016/j.soilbio.2015.04.014

Frkova Z., Pistocchi C., Vystavna Y., Capkova K., Dolezal J., Tamburini F. (2022). Phosphorus dynamics during early soil development in a cold desert: Insights from oxygen isotopes in phosphate. Soil 8 (1): 1–15. doi:10.5194/soil-8-1-2022

Frost P.C., Evans-White M.A., Finkel Z. V, Jensen T.C., Matzek V. (2005). Are you what you eat? Physiological constraints on organismal stoichiometry in an elementally imbalanced world. Oikos 109: 18–28. doi:10.1111/j.0030-1299.2005.14049.x

Fujii K., Yamada T., Hayakawa C., Nakanishi A., Funakawa S. (2020). Decoupling of protein depolymerization and ammonification in nitrogen mineralization of acidic forest soils. Appl Soil Ecol 153: 103572. doi:10.1016/j.apsoil.2020.103572

Ganzert L., Lipski A., Hubberten H.W., Wagner D. (2011). The impact of different soil parameters on the community structure of dominant bacteria from nine different soils located on Livingston Island, South Shetland Archipelago, Antarctica. FEMS Microbiol Ecol 76 (3): 476–491. doi:10.1111/j.1574-6941.2011.01068.x

Geisseler D., Horwath W.R., Joergensen R.G., Ludwig B. (2010). Pathways of nitrogen utilization by soil microorganisms - A review. Soil Biol Biochem 42 (12): 2058–2067. doi:10.1016/j.soilbio.2010.08.021

George T.S., Giles C.D., Menezes-Blackburn D., Condron L.M., Gama-Rodrigues A.C., Jaisi D., Lang F., Neal A.L., Stutter M.I., Almeida D.S., Bol R., Cabugao K.G., Celi L., Cotner J.B., Feng G., Goll D.S., Hallama M., Krueger J., Plassard C., Rosling A., Darch T., Fraser T., Giesler R., Richardson A.E., Tamburini F., Shand C.A., Lumsdon D.G., Zhang H., Blackwell M.S.A., Wearing C., Mezeli M.M., Almås R., Audette Y., Bertrand I., Beyhaut E., Boitt G., Bradshaw N., Brearley C.A., Bruulsema T.W., Ciais P., Cozzolino V., Duran P.C., Mora M.L., de Menezes A.B., Dodd R.J., Dunfield K., Engl C., Frazão J.J., Garland G., González Jiménez J.L., Graca J., Granger S.J., Harrison A.F., Heuck C., Hou E.Q., Johnes P.J., Kaiser K., Kjær H.A., Klumpp E., Lamb A.L., Macintosh K.A., Mackay E.B., McGrath J., McIntyre C., McLaren T., Mészáros E., Missong A., Mooshammer M., Negrón C.P., Nelson L.A., Pfahler V., Poblete-Grant P., Randall M., Seguel A., Seth K., Smith A.C., Smits M.M., Sobarzo J.A., Spohn M., Tawaraya K., Tibbett M., Voroney P., Wallander H., Wang L., Wasaki J., Haygarth P.M. (2018). Organic phosphorus in the terrestrial environment: a perspective on the state of the art and future priorities. Plant Soil 427 (1–2): 191–208. doi:10.1007/s11104-017-3391-x

Giblin A.E., Tobias C.R., Song B., Weston N., Banta G.T., Rivera-Monroy V.H. (2013). The importance of Dissimilatory Nitrate Reduction to Ammonium (DNRA) in the Nitrogen Cycle of Coastal Ecosystems. Oceanography 26 (3): 124–131. doi:10.5670/oceanog.2013.54

Gomes N.C.M., Heuer H., Schönfeld J., Costa R., Mendonça-Hagler L., Smalla K. (2001). Bacterial diversity of the rhizosphere of maize (Zea mays) grown in tropical soil studied by temperature gradient gel electrophoresis. Plant Soil 232 (1–2): 167–180. doi:10.1023/A:1010350406708

Gong F., Zhu H., Zhang Y., Li Y. (2018). Biological carbon fixation: From natural to synthetic.

J CO2 Util 28: 221–227. doi:10.1016/j.jcou.2018.09.014

Górska E.B., Dobrzyński J., Jankiewicz U., Kwasowski W., Russel S., Pietkiewicz S., Kalaji H., Gozdowski D., Pińkowski R., Kowalczyk P. (2015). Degradation and Colonization of Cellulose by Diazotrophic Strains of Paenibacillus polymyxa Isolated from Soil. J Bioremediation Biodegrad 6 (2): 1000271. doi:10.4172/2155-6199.1000271

Grafe M., Goers M., von Tucher S., Baum C., Zimmer D., Leinweber P., Vestergaard G., Kublik S., Schloter M., Schulz S. (2018). Bacterial potentials for uptake, solubilization and mineralization of extracellular phosphorus in agricultural soils are highly stable under different fertilization regimes. Environ Microbiol Rep 10 (3): 320–327. doi:10.1111/1758-2229.12651

Graffelman J. (2013). calibrate: calibration of scatterplot and biplot axes.R Package version 1.7.2. Available at: http://cran.r-project.org/package=calibrate [Accessed: 22 November 2015]

Gruba P., Mulder J. (2015). Tree species affect cation exchange capacity (CEC) and cation binding properties of organic matter in acid forest soils. Sci Total Environ 511: 655–662. doi:10.1016/j.scitotenv.2015.01.013

Grzyb A., Wolna-Maruwka A., Niewiadomska A. (2021). The Significance of Microbial Transformation of Nitrogen Compounds in the Light of Integrated Crop Management. Agronomy 11 (7): 1415. doi:10.3390/agronomy11071415

Gschwendtner S., Leberecht M., Engel M., Kublik S., Dannenmann M., Polle A., Schloter M. (2015). Effects of Elevated Atmospheric CO2 on Microbial Community Structure at the Plant-Soil Interface of Young Beech Trees (Fagus sylvatica L.) Grown at Two Sites with Contrasting Climatic Conditions. Microb Ecol 69 (4): 867–878. doi:10.1007/s00248-014-0527-x

Guazzaroni M.E., Beloqui A., Golyshin P.N., Ferrer M. (2009). Metagenomics as a new technological tool to gain scientific knowledge. World J Microbiol Biotechnol 25 (6): 945–954. doi:10.1007/s11274-009-9971-z

Guenet B., Leloup J., Hartmann C., Barot S., Abbadie L. (2011). A new protocol for an artificial soil to analyse soil microbiological processes. Appl Soil Ecol 48 (2): 243–246. doi:10.1016/j.apsoil.2011.04.002

Gunina A., Kuzyakov Y. (2015). Sugars in soil and sweets for microorganisms: Review of origin, content, composition and fate. Soil Biol Biochem 90: 87–100. doi:10.1016/j.soilbio.2015.07.021

Ha-Tran D.M., Nguyen T.T.M., Huang C.-C. (2021). Clostridium thermocellum as a Promising Source of Genetic Material for Designer Cellulosomes : An Overview. Cata 11 (8): 996. doi:10.3390/catal11080996

Habig J., Swanepoel C. (2015). Effects of Conservation Agriculture and Fertilization on Soil Microbial Diversity and Activity. Environments 2 (3): 358–384. doi:10.3390/environments2030358

Hallsworth E.G., Crawford D. V. (1965). Experimental Pedology. In: Proceedings of the 11th

Easter School in Agricultural Science (Hallsworth E.G., Crawford D. V, eds), Butterworths, London, UK

Hamid A., Aftab M.N. (2019). Cloning, Purification, and Characterization of Recombinant Thermostable β-Xylanase Tnap_0700 from Thermotoga naphthophila. Appl Biochem Biotechnol 189 (4): 1274–1290. doi:10.1007/s12010-019-03068-0

Harrell F.E., Dupont C. (2020). Hmisc: Harrell Miscellaneous. R Package version 4.1-1. Available at: http://cran.r-project.org/package=Hmisc [Accessed: 21 September 2020]

Harris D.F., Jimenez-Vicente E., Yang Z.Y., Hoffman B.M., Dean D.R., Seefeldt L.C. (2020). CO as a substrate and inhibitor of H+ reduction for the Mo-, V-, and Fe-nitrogenase isozymes. J Inorg Biochem 213: 111278. doi:10.1016/j.jinorgbio.2020.111278

Haygarth P.M., Ritz K. (2009). The future of soils and land use in the UK: Soil systems for the provision of land-based ecosystem services. Land use policy 26S: S187–S197. doi:10.1016/j.landusepol.2009.09.016

Heuck C., Weig A., Spohn M. (2015). Soil microbial biomass C: N: P stoichiometry and microbial use oforganic phosphorus. Soil Biol Biochem 85: 119–129. doi:10.1016/j.soilbio.2015.02.029

Hill T.C.J., Walsh K.A., Harris J.A., Moffett B.F. (2003). Using ecological diversity measures with bacterial communities. FEMS Microbiol Ecol 43 (1): 1–11. doi:10.1016/S0168-6496(02)00449-X

Ho A., Di Lonardo D.P., Bodelier P.L.E. (2017). Revisiting life strategy concepts in environmental microbial ecology. FEMS Microbiol Ecol 93 (3): fix006. doi:10.1093/femsec/fix006

Hodkinson I.D., Coulson S.J., Webb N.R. (2003). Community assembly along proglacial chronosequences in the high Arctic: vegetation and soil development in north-west Svalbard. J Ecol 91 (4): 651–663. doi:10.1046/j.1365-2745.2003.00786.x

Hou E., Chen C., Kuang Y., Zhang Y., Heenan M., Wen D. (2016). A structural equation model analysis of phosphorus transformations in global unfertilized and uncultivated soils. Global Biogeochem Cycles 30 (9): 1300–1309. doi:10.1002/2016GB005371

Hou E., Lu X., Jiang L., Wen D., Luo Y. (2019). Quantifying Soil Phosphorus Dynamics: A Data Assimilation Approach. J Geophys Res Biogeosciences 124 (7): 2159–2173. doi:10.1029/2018JG004903

Howe A., Yang F., Williams R.J., Meyer F., Hofmockel K.S. (2016). Identification of the core set of carbon-associated genes in a bioenergy grassland soil. PLoS One 11 (11): e0166578. doi:10.1371/journal.pone.0166578

Hu Y., Zheng Q., Noll L., Zhang S., Wanek W. (2020). Direct measurement of the in situ decomposition of microbial-derived soil organic matter. Soil Biol Biochem 141: 107660. doi:10.1016/j.soilbio.2019.107660

Huang P.-M., Wang M.-K., Chiu C.-Y. (2005). Soil mineral-organic matter-microbe interactions: Impacts on biogeochemical processes and biodiversity in soils. Pedobiologia (Jena) 49 (6): 609–635. doi:10.1016/j.pedobi.2005.06.006

Hunt A., Egli Markus, Faybishenko Boris. (2021). Where are we and where are we going? Pedogenesis through chemical weathering, hydrologic fluxes, and bioturbation. In: Hydrogeology, Chemical Weathering, and Soil Formation (Hunt A.G., Egli M, Faybishenko B, eds), John Wiley & Sons Inc., Hoboken, New Jersey, USA, pp. 253–269. doi:10.1002/9781119563952.ch14

Huson D.H., Mitra S., Ruscheweyh H.J., Weber N., Schuster S.C. (2011). Integrative analysis of environmental sequences using MEGAN4. Genome Res 21 (9): 1552–1560. doi:10.1101/gr.120618.111

Illmer P., Schinner F. (1995). Solubilization of inorganic calcium phosphates-Solubilization mechanisms. Soil Biol Biochem 27 (3): 257–263. doi:10.1016/0038-0717(94)00190-C

Jansson J.K., Hofmockel K.S. (2020). Soil microbiomes and climate change. Nat Rev Microbiol 18 (1): 35–46. doi:10.1038/s41579-019-0265-7

Jilling A., Keiluweit M., Contosta A.R., Frey S., Schimel J., Schnecker J., Smith R.G., Tiemann L., Grandy A.S. (2018). Minerals in the rhizosphere: overlooked mediators of soil nitrogen availability to plants and microbes. Biogeochemistry 139 (2): 103–122. doi:10.1007/s10533-018-0459-5

Joergensen R.G. (1996). The fumigation-extraction method to estimate soil microbial biomass: Calibration of the kEC value. Soil Biol Biochem 28 (1): 25–31. doi:10.1016/0038-0717(95)00102-6

Johnson B., Goldblatt C. (2015). The Nitrogen Budget of Earth. Earth-Science Rev 148: 150–173. doi:10.1016/j.earscirev.2015.05.006

Johnson M.P. (2016). Photosynthesis. Essays Biochem 60 (3): 255–273. doi:10.1042/EBC20160016

Kaiser C., Franklin O., Dieckmann U., Richter A. (2014). Microbial community dynamics alleviate stoichiometric constraints during litter decay. Ecol Lett 17 (6): 680–690. doi:10.1111/ele.12269

Kaiser C., Kilburn M.R., Clode P.L., Fuchslueger L., Koranda M., Cliff J.B., Solaiman Z.M., Murphy D. V. (2015). Exploring the transfer of recent plant photosynthates to soil microbes: mycorrhizal pathway vs direct root exudation. New Phytol 205 (4): 1537–1551. doi:10.1111/nph.13138

Kameshwar A.K.S., Qin W. (2018). Understanding the structural and functional properties of carbohydrate esterases with a special focus on hemicellulose deacetylating acetyl xylan esterases. Mycology 9 (4): 273–295. doi:10.1080/21501203.2018.1492979

Kameshwar A.K.S., Qin W. (2016). Recent Developments in Using Advanced Sequencing Technologies for the Genomic Studies of Lignin and Cellulose Degrading Microorganisms. Int J Biol Sci 12 (2): 156–171. doi:10.7150/ijbs.13537

Kanehisa M., Goto S. (2000). KEGG: Kyoto Encyclopedia of Genes and Genomes. Nucleic Acids Res 28 (1): 27–30. doi:10.1016/j.meegid.2016.07.022

Kanehisa M., Sato Y., Kawashima M., Furumichi M., Tanabe M. (2016). KEGG as a reference resource for gene and protein annotation. Nucleic Acids Res 44 (D1): D457–

D462. doi:10.1093/nar/gkv1070

Keasling J.D., Bertsch L., Kornberg A. (1993). Guanosine pentaphosphate phosphohydrolase of Escherichia coli is a long-chain exopolyphosphatase. Proc Natl Acad Sci U S A 90 (15): 7029–7033. doi:10.1073/pnas.90.15.7029

Khan H., Ali I., Khan A.U., Ahmed M., Shah Z., Saeed A., Naz R., Mustafa M.R., Abbasi A. (2010). Purification and Biochemical Characterization of Alkaline Serine Protease from Caesalpinia bonducella. Nat Prod Commun 5 (6): 931–934. doi:10.1177/1934578x1000500625

Khusro A., Kaliyan B.K., Al-Dhabi N.A., Arasu M.V., Agastian P. (2016). Statistical optimization of thermo-alkali stable xylanase production from Bacillus tequilensis strain ARMATI. Electron J Biotechnol 22: 16–25. doi:10.1016/j.ejbt.2016.04.002

Kögel-Knabner I. (2002). The macromolecular organic composition of plant and microbial residues as inputs to soil organic matter. Soil Biol Biochem 34 (2): 139–162. doi:10.1016/S0038-0717(01)00158-4

Kögel-Knabner I., Ding G.-C., Heister K., Pronk G.J., Schaumann G.E., Schloter M., Schulz S., Schwarz J., Smalla K. (2010). Formation of biogeochemical interfaces in soils as controlled by mineral and organic components. In: 19th World Congress of Soil Science, Soil Solutions for a Changing World, 1 - 6 August 2010, Brisbane, Australia, pp. 74–77

Kögel-Knabner I., Guggenberger G., Kleber M., Kandeler E., Kalbitz K., Scheu S., Eusterhues K., Leinweber P. (2008). Organo-mineral associations in temperate soils: Integrating biology, mineralogy, and organic matter chemistry. J Plant Nutr Soil Sci 171 (1): 61–82. doi:10.1002/jpln.200700048

Kolb S.E., Fermanich K.J., Dornbush M.E. (2009). Effect of Charcoal Quantity on Microbial Biomass and Activity in Temperate Soils. Soil Sci Soc Am J 73 (4): 1173–1181. doi:10.2136/sssaj2008.0232

Kome G.K., Enang R.K., Tabi F.O., Yerima B.P.K. (2019). Influence of Clay Minerals on Some Soil Fertility Attributes: A Review. Open J Soil Sci 9: 155–188. doi:10.4236/ojss.2019.99010

Kono T., Mehrotra S., Endo C., Kizu N., Matusda M., Kimura H., Mizohata E., Inoue T., Hasunuma T., Yokota A., Matsumura H., Ashida H. (2017). A RuBisCO-mediated carbon metabolic pathway in methanogenic archaea. Nat Commun 8: 14007. doi:10.1038/ncomms14007

Krauze P., Wagner D., Yang S., Spinola D., Kühn P. (2021). Influence of prokaryotic microorganisms on initial soil formation along a glacier forefield on King George Island, maritime Antarctica. Sci Rep 11 (1): 13135. doi:10.1038/s41598-021-92205-z

Kunc F., Stotzky G. (1974). Effect of clay minerals on heterotrophic microbial activity in soil. Soil Sci 118 (3): 186–195. doi:10.1097/00010694-197409000-00009

Lamparter A., Bachmann J., Woche S.K., Goebel M.-O. (2014). Biogeochemical Interface Formation: Wettability Affected by Organic Matter Sorption and Microbial Activity.

Vadose Zo J 13 (7): 1–8. doi:10.2136/vzj2013.10.0175

Land M., Hauser L., Jun S.R., Nookaew I., Leuze M.R., Ahn T.H., Karpinets T., Lund O., Kora G., Wassenaar T., Poudel S., Ussery D.W. (2015). Insights from 20 years of bacterial genome sequencing. Funct Integr Genomics 15 (2): 141–161. doi:10.1007/s10142-015-0433-4

Lane D.J. (1991). 16S/23S rRNA sequencing. In: Nucleic Acid Techniques in Bacterial Systematics (Stackebrandt E., Goodfellow M., eds), John Wiley & Sons, New York, NY, USA, pp. 115–175

Lang F., Krüger J., Amelung W., Willbold S., Frossard E., Bünemann E.K., Bauhus J., Nitschke R., Kandeler E., Marhan S., Schulz S., Bergkemper F., Schloter M., Luster J., Guggisberg F., Kaiser K., Mikutta R., Guggenberger G., Polle A., Pena R., Prietzel J., Rodionov A., Talkner U., Meesenburg H., von Wilpert K., Hölscher A., Dietrich H.P., Chmara I. (2017). Soil phosphorus supply controls P nutrition strategies of beech forest ecosystems in Central Europe. Biogeochemistry 136 (1): 5–29. doi:10.1007/s10533-017-0375-0

Lavallee J.M., Soong J.L., Cotrufo M.F. (2020). Conceptualizing soil organic matter into particulate and mineral-associated forms to address global change in the 21st century. Glob Chang Biol 26 (1): 261–273. doi:10.1111/gcb.14859

Leff J.W., Jones S.E., Prober S.M., Barberán A., Borer E.T., Firn J.L., Harpole W.S., Hobbie S.E., Hofmockel K.S., Knops J.M.H., McCulley R.L., La Pierre K., Risch A.C., Seabloom E.W., Schütz M., Steenbock C., Stevens C.J., Fierer N. (2015). Consistent responses of soil microbial communities to elevated nutrient inputs in grasslands across the globe. Proc Natl Acad Sci U S A 112 (35): 10967–10972. doi:10.1073/pnas.1508382112

Leinemann T., Preusser S., Mikutta R., Kalbitz K., Cerli C., Höschen C., Mueller C.W., Kandeler E., Guggenberger G. (2018). Multiple exchange processes on mineral surfaces control the transport of dissolved organic matter through soil profiles. Soil Biol Biochem 118: 79–90. doi:10.1016/j.soilbio.2017.12.006

Levy-Booth D.J., Giesbrecht I.J.W., Kellogg C.T.E., Heger T.J., D'Amore D. V., Keeling P.J., Hallam S.J., Mohn W.W. (2019). Seasonal and ecohydrological regulation of active microbial populations involved in DOC, CO2 , and CH4 fluxes in temperate rainforest soil. ISME J 13 (4): 950–963. doi:10.1038/s41396-018-0334-3

Li H., Xu Z., Yang S., Li X., Top E.M., Wang R., Zhang Y., Cai J., Yao F., Han X., Jiang Y. (2016a). Responses of Soil Bacterial Communities to Nitrogen Deposition and Precipitation Increment Are Closely Linked with Aboveground Community Variation. Microb Ecol 71 (4): 974–989. doi:10.1007/s00248-016-0730-z

Li X., Hui R., Tan H., Zhao Y., Liu R., Song N. (2021b). Biocrust Research in China: Recent Progress and Application in Land Degradation Control. Front Plant Sci 12: 751521. doi:10.3389/fpls.2021.751521

Li Y., Li L., Wu Z. (2021a). First-principles calculations of equilibrium nitrogen isotope fractionations among aqueous ammonium, silicate minerals and salts. Geochim Cosmochim Acta 297: 220–232. doi:10.1016/j.gca.2021.01.019

Li Y., Niu S., Yu G. (2016b). Aggravated phosphorus limitation on biomass production under increasing nitrogen loading: a meta-analysis. Glob Chang Biol 22 (2): 934–943. doi:10.1111/gcb.13125

Liang C., Balser T.C. (2011). Microbial production of recalcitrant organic matter in global soils: implications for productivity and climate policy. Nat Rev Microbiol 9 (1): 75. doi:10.1038/nrmicro2386-c1

Liu J., Zhang S., Shi Q., Wang L., Kong W., Yu H., Ma F. (2019). Highly efficient oxidation of synthetic and natural lignin-related compounds by Physisporinus vitreus versatile peroxidase. Int Biodeterior Biodegrad 136: 41–48. doi:10.1016/j.ibiod.2018.10.009

Liu L., Huang W.C., Liu Y., Li M. (2021). Diversity of cellulolytic microorganisms and microbial cellulases. Int Biodeterior Biodegrad 163: 105277. doi:10.1016/j.ibiod.2021.105277

Liu L., Xu Mingyuan, Cao Y., Wang H., Shao J., Xu Meiqing, Zhang Y., Wang Y., Zhang W., Meng X., Liu W. (2020b). Biochemical characterization of xylanases from Streptomyces sp. B6 and their application in the xylooligosaccharide production from viscose fiber production waste. J Agric Food Chem 68 (10): 3184–3194. doi:10.1021/acs.jafc.9b06704

Liu X.-J.A., Sun J., Mau R.L., Finley B.K., Compson Z.G., van Gestel N., Brown J.R., Schwartz E., Dijkstra P., Hungate B.A. (2017). Labile carbon input determines the direction and magnitude of the priming effect. Appl Soil Ecol 109: 7–13. doi:10.1016/j.apsoil.2016.10.002

Liu X., Lamb E.G., Zhang S. (2020a). Nitrogen addition impacts on soil microbial stoichiometry are driven by changes in plant resource stoichiometry not by the composition of main microbial groups in an alpine meadow. Biol Fertil Soils 56 (2): 261–271. doi:10.1007/s00374-019-01423-1

Lombard N., Prestat E., van Elsas J.D., Simonet P. (2011). Soil-specific limitations for access and analysis of soil microbial communities by metagenomics. FEMS Microbiol Ecol 78 (1): 31–49. doi:10.1111/j.1574-6941.2011.01140.x

Louca S., Polz M.F., Mazel F., Albright M.B.N., Huber J.A., O'Connor M.I., Ackermann M., Hahn A.S., Srivastava D.S., Crowe S.A., Doebeli M., Parfrey L.W. (2018). Function and functional redundancy in microbial systems. Nat Ecol Evol 2 (6): 936–943. doi:10.1038/s41559-018-0519-1

Luo G., Xue C., Jiang Q., Xiao Y., Zhang F., Guo S., Shen Q. (2020). Soil Carbon, Nitrogen, and Phosphorus Cycling Microbial Populations and Their Resistance to Global Change Depend on Soil C:N:P Stoichiometry. mSystems 5 (3): e00162-20. doi:10.1128/mSystems.00162-20

Lynn T.M., Ge T., Yuan H., Wei X., Wu X., Xiao K., Kumaresan D., Yu S.S., Wu J., Whiteley A.S. (2017). Soil Carbon-Fixation Rates and Associated Bacterial Diversity and Abundance in Three Natural Ecosystems. Microb Ecol 73 (3): 645–657. doi:10.1007/s00248-016-0890-x

Lyu Z., Shao N., Akinyemi T., Whitman W.B. (2018). Methanogenesis. Curr Biol 28 (13):

R727–R732. doi:10.1016/j.cub.2018.05.021

Maaroufi N.I., De Long J.R. (2020). Global Change Impacts on Forest Soils: Linkage Between Soil Biota and Carbon-Nitrogen-Phosphorus Stoichiometry. Front For Glob Chang 3: 16. doi:10.3389/ffgc.2020.00016

Maaroufi N.I., Palmqvist K., Bach L.H., Bokhorst S., Liess A., Gundale M.J., Kardol P., Nordin A., Meunier C.L. (2018). Nutrient optimization of tree growth alters structure and function of boreal soil food webs. For Ecol Manage 428: 46–56. doi:10.1016/j.foreco.2018.06.034

Mackelprang R., Grube A.M., Lamendella R., Jesus E. da C., Copeland A., Liang C., Jackson R.D., Rice C.W., Kapucija S., Parsa B., Tringe S.G., Tiedje J.M., Jansson J.K. (2018). Microbial Community Structure and Functional Potential in Cultivated and Native Tallgrass Prairie Soils of the Midwestern United States. Front Microbiol 9: 1775. doi:10.3389/fmicb.2018.01775

MacManes M.D. (2014). On the optimal trimming of high-throughput mRNA sequence data. Front Genet 5: 13. doi:10.3389/fgene.2014.00013

Madhok M.R. (1937). Synthetic soil as a medium for the study of certain microbiological processes. Soil Sci 44 (4): 319–322

Maechler M., Rousseeuw P., Struyf A., Hubert M., Hornik K., Studer M., Roudier P. (2015). cluster: “Finding Groups in Data”: Cluster Analysis Extended Rousseeuw et al. R Package version 2.0.3. Available at: http://cran.r-project.org/package=cluster [Accessed: 22 November 2015]

Malgas S., van Dyk J.S., Pletschke B.I. (2015). A review of the enzymatic hydrolysis of mannans and synergistic interactions between β-mannanase, β-mannosidase and α-galactosidase. World J Microbiol Biotechnol 31 (8): 1167–1175. doi:10.1007/s11274-015-1878-2

Malik A.A., Puissant J., Buckeridge K.M., Goodall T., Jehmlich N., Chowdhury S., Gweon H.S., Peyton J.M., Mason K.E., van Agtmaal M., Blaud A., Clark I.M., Whitaker J., Pywell R.F., Ostle N., Gleixner G., Griffiths R.I. (2018). Land use driven change in soil pH affects microbial carbon cycling processes. Nat Commun 9 (1): 3591. doi:10.1038/s41467-018-05980-1

Mander C., Wakelin S., Young S., Condron L., Callaghan M.O. (2012). Incidence and diversity of phosphate-solubilising bacteria are linked to phosphorus status in grassland soils. Soil Biol Biochem 44 (1): 93–101. doi:10.1016/j.soilbio.2011.09.009

Mandic-Mulec I., Stefanic P., van Elsas J.D. (2015). Ecology of Bacillaceae. Microbiol Spectr 3 (2): TBS-0017-2013

Masuda Y., Itoh H., Shiratori Y., Senoo K. (2018). Metatranscriptomic insights into microbial consortia driving methane metabolism in paddy soils. Soil Sci Plant Nutr 64 (4): 455–464. doi:10.1080/00380768.2018.1457409

Matkawala F., Nighojkar S., Kumar A., Nighojkar A. (2021). Microbial alkaline serine proteases: Production, properties and applications. World J Microbiol Biotechnol 37

(4): 63. doi:10.1007/s11274-021-03036-z

Mauck B.S., Roberts J.A. (2007). Mineralogic Control on Abundance and Diversity of Surface-Adherent Microbial Communities. Geomicrobiol J 24 (3–4): 167–177. doi:10.1080/01490450701457162

Mavris C., Egli M., Plötze M., Blum J.D., Mirabella A., Giaccai D., Haeberli W. (2010). Initial stages of weathering and soil formation in the Morteratsch proglacial area (Upper Engadine, Switzerland). Geoderma 155 (3–4): 359–371. doi:10.1016/j.geoderma.2009.12.019

McGrath J.W., Chin J.P., Quinn J.P. (2013). Organophosphonates revealed: new insights into the microbial metabolism of ancient molecules. Nat Rev Microbiol 11 (6): 412–419. doi:10.1038/nrmicro3011

Medina-Sauza R.M., Álvarez-Jiménez M., Delhal A., Reverchon F., Blouin M., Guerrero-Analco J.A., Cerdán C.R., Guevara R., Villain L., Barois I. (2019). Earthworms Building Up Soil Microbiota, a Review. Front Environ Sci 7: 81. doi:10.3389/fenvs.2019.00081

Meier L.A., Krauze P., Prater I., Horn F., Schaefer C.E.G.R., Scholten T., Wagner D., Mueller C.W., Kühn P. (2019). Pedogenic and microbial interrelation in initial soils under semiarid climate on James Ross Island, Antarctic Peninsula region. Biogeosciences 16 (12): 2481–2499. doi:10.5194/bg-16-2481-2019

Merino-Martín L., Stokes A., Gweon H., Moragues-Saitua L., Staunton S., Plassard C., Oliver A., Le Bissonnais Y., Griffiths R.I. (2021). Interacting effects of land use type, microbes and plant traits on soil aggregate stability. Soil Biol Biochem 154: 108072. doi:10.1016/j.soilbio.2020.108072

Meyer D., Zeileis A., Hornik K., Gerber F., Friendly M. (2014). vcd: Visualizing categorical data. R Package version 1.3-2. Available at: http://cran.r-project.org/package=vcd [Accessed: 22 November 2015]

Michas A., Vestergaard G., Trautwein K., Avramidis P., Hatzinikolaou D.G., Vorgias C.E., Wilkes H., Rabus R., Schloter M., Schöler A. (2017). More than 2500 years of oil exposure shape sediment microbiomes with the potential for syntrophic degradation of hydrocarbons linked to methanogenesis. Microbiome 5: 118. doi:10.1186/s40168-017-0337-8

Mikutta R., Turner S., Schippers A., Gentsc N., Meyer-Stüve S., Condron L.M., Peltzer D.A., Richardson S.J., Eger A., Hempel G., Kaiser K., Klotzbücher T., Guggenberger G. (2019). Microbial and abiotic controls on mineral-associated organic matter in soil profiles along an ecosystem gradient. Sci Rep 9: 10294. doi:10.1038/s41598-019-46501-4

Monds R.D., Newell P.D., Schwartzman J.A., O'Toole G.A. (2006). Conservation of the Pho regulon in Pseudomonas fluorescens Pf0-1. Appl Environ Microbiol 72 (3): 1910–1924. doi:10.1128/AEM.72.3.1910-1924.2006

Morales M., Sánchez L., Revah S. (2018). The impact of environmental factors on carbon dioxide fixation by microalgae. FEMS Microbiol Lett 365 (3): fnx262. doi:10.1093/femsle/fnx262

Moreira P.R., Almeida-Vara E., Malcata F.X., Duarte J.C. (2007). Lignin transformation by a versatile peroxidase from a novel Bjerkandera sp. strain. Int Biodeterior Biodegradation 59 (3): 234–238. doi:10.1016/j.ibiod.2006.11.002

Müller-Stöver D., Hauggaard-Nielsen H., Eriksen J., Ambus P., Johansen A. (2012). Microbial biomass, microbial diversity, soil carbon storage, and stability after incubation of soil from grass-clover pastures of different age. Biol Fertil Soils 48 (4): 371–383. doi:10.1007/s00374-011-0633-6

Müller W.E.G., Schröder H.C., Wang X. (2019). Inorganic Polyphosphates As Storage for and Generator of Metabolic Energy in the Extracellular Matrix. Chem Rev 119 (24): 12337–12374. doi:10.1021/acs.chemrev.9b00460

Myrold D.D., Zeglin L.H., Jansson J.K. (2014). The Potential of Metagenomic Approaches for Understanding Soil Microbial Processes. Soil Sci Soc Am J 78 (1): 3–10. doi:10.2136/sssaj2013.07.0287dgs

Nannipieri P., Ascher-Jenull J., Ceccherini M.T., Pietramellara G., Renella G., Schloter M. (2020). Beyond microbial diversity for predicting soil functions: A mini review. Pedosphere 30 (1): 5–17. doi:10.1016/S1002-0160(19)60824-6

Nannipieri P., Ascher J., Ceccherini M.T., Landi L., Pietramellara G., Renella G. (2003). Microbial diversity and soil functions. Eur J Soil Sci 54 (4): 655–670. doi:10.1046/j.1351-0754.2003.0556.x

Nannipieri P., Giagnoni L., Landi L., Renella G. (2011). Role of Phosphatase Enzymes in Soil. In: Phosphorus in Action Biological Processes in Soil Phosphorus Cycling (Bünemann E., Oberson A., Frossard E., eds), Springer, Berlin, Heidelberg, Berlin, pp. 215–243. doi:10.1007/978-3-642-15271-9

Napieralski S.A., Roden E.E. (2020). The Weathering Microbiome of an Outcropping Granodiorite. Front Microbiol 11: 601907. doi:10.3389/fmicb.2020.601907

Nelson M.B., Martiny A.C., Martiny J.B.H. (2016). Global biogeography of microbial nitrogen-cycling traits in soil. Proc Natl Acad Sci U S A 113 (29): 8033–8040. doi:10.1073/pnas.1601070113

Neuwirth E. (2014). RColorBrewer: ColorBrewer palettes. R Package version 1.1-2. Available at: http://cran.r-project.org/package=RColorBrewer [Accessed: 22 November 2015]. Color Palettes

Nicolás C., Martin-Bertelsen T., Floudas D., Bentzer J., Smits M., Johansson T., Troein C., Persson P., Tunlid A. (2019). The soil organic matter decomposition mechanisms in ectomycorrhizal fungi are tuned for liberating soil organic nitrogen. ISME J 13 (4): 977–988. doi:10.1038/s41396-018-0331-6

Noll L., Zhang S., Zheng Q., Hu Y., Wanek W. (2019). Wide-spread limitation of soil organic nitrogen transformations by substrate availability and not by extracellular enzyme content. Soil Biol Biochem 133: 37–49. doi:10.1016/j.soilbio.2019.02.016

Noronha M.F., Lacerda Júnior G.V., Gilbert J.A., de Oliveira V.M. (2017). Taxonomic and functional patterns across soil microbial communities of global biomes. Sci Total

Environ 609: 1064–1074. doi:10.1016/j.scitotenv.2017.07.159

Ochoa-Hueso R., Plaza C., Moreno-Jiménez E., Delgado-Baquerizo M. (2021). Soil element coupling is driven by ecological context and atomic mass. Ecol Lett 24 (2): 319–326. doi:10.1111/ele.13648

Oksanen J., Blanchet F.G., Kindt R., Legendre P., Minchin P., O'Hara R.B. (2015). vegan: Community ecology package. R Package Version 2.2-1. Available at: http://cran.r-project.org/package=vegan [Accessed: 22 November 2015]

Olagoke F.K., Kalbitz K., Vogel C. (2019). Control of Soil Extracellular Enzyme Activities by Clay Minerals—Perspectives on Microbial Responses. Soil Syst 3 (4): 64. doi:10.3390/soilsystems3040064

Oliveira C.A., Alves V.M.C., Marriel I.E., Gomes E.A., Scotti M.R., Carneiro N.P., Guimarães C.T., Schaffert R.E., Sá N.M.H. (2009). Phosphate solubilizing microorganisms isolated from rhizosphere of maize cultivated in an oxisol of the Brazilian Cerrado Biome. Soil Biol Biochem 41 (9): 1782–1787. doi:10.1016/j.soilbio.2008.01.012

Or D., Smets B.F., Wraith J.M., Dechesne A., Friedman S.P. (2007). Physical constraints affecting bacterial habitats and activity in unsaturated porous media - a review. Adv Water Resour 30 (6–7): 1505–1527. doi:10.1016/j.advwatres.2006.05.025

Ouyang N., Zhang Y., Sheng H., Zhou Q., Huang Y., Yu Z. (2021). Clay mineral composition of upland soils and its implication for pedogenesis and soil taxonomy in subtropical China. Sci Rep 11 (1): 9707. doi:10.1038/s41598-021-89049-y

Pan Y., Cassman N., de Hollander M., Mendes L.W., Korevaar H., Geerts R.H.E.M., van Veen J.A., Kuramae E.E. (2014). Impact of long-term N, P, K, and NPK fertilization on the composition and potential functions of the bacterial community in grassland soil. FEMS Microbiol Ecol 90 (1): 195–205. doi:10.1111/1574-6941.12384

Pason P., Kyu K.L., Ratanakhanokchai K. (2006). Paenibacillus curdlanolyticus Strain B-6 Xylanolytic-Cellulolytic Enzyme System That Degrades Insoluble Polysaccharides. Appl Environ Microbiol 72 (4): 2483–2490. doi:10.1128/AEM.72.4.2483-2490.2006

Pathak V.M., Navneet. (2017). Review on the current status of polymer degradation: a microbial approach. Bioresour Bioprocess 4: 15. doi:10.1186/s40643-017-0145-9

Paul C., Kuhn K., Steinhoff-Knopp B., Weißhuhn P., Helming K. (2021). Towards a standardization of soil-related ecosystem service assessments. Eur J Soil Sci 72 (4): 1543–1558. doi:10.1111/ejss.13022

Penton C.R., Gupta V.V.S.R., Yu J., Tiedje J.M. (2016). Size matters: Assessing optimum soil sample size for fungal and bacterial community structure analyses using high throughput sequencing of rRNA gene amplicons. Front Microbiol 7: 824. doi:10.3389/fmicb.2016.00824

Pérez-Boada M., Ruiz-Dueñas F.J., Pogni R., Basosi R., Choinowski T., Martínez M.J., Piontek K., Martínez A.T. (2005). Versatile Peroxidase Oxidation of High Redox Potential Aromatic Compounds: Site-directed Mutagenesis, Spectroscopic and

Crystallographic Investigation of Three Long-range Electron Transfer Pathways. J Mol Biol 354 (2): 385–402. doi:10.1016/j.jmb.2005.09.047

Pjevac P., Schauberger C., Poghosyan L., Herbold C.W., van Kessel M.A.H.J., Daebeler A., Steinberger M., Jetten M.S.M., Lücker S., Wagner M., Daims H. (2017). AmoA-Targeted Polymerase Chain Reaction Primers for the Specific Detection and Quantification of Comammox Nitrospira in the Environment. Front Microbiol 8: 1508. doi:10.3389/fmicb.2017.01508

Poll C., Marhan S., Ingwersen J., Kandeler E. (2008). Dynamics of litter carbon turnover and microbial abundance in a rye detritusphere. Soil Biol Biochem 40 (6): 1306–1321. doi:10.1016/j.soilbio.2007.04.002

Porder S. (2019). How Plants Enhance Weathering and How Weathering is Important to Plants. Elements 15 (4): 241–246. doi:10.2138/gselements.15.4.241

Pronk G.J., Heister K., Ding G.-C., Smalla K., Kögel-Knabner I. (2012). Development of biogeochemical interfaces in an artificial soil incubation experiment; aggregation and formation of organo-mineral associations. Geoderma 189: 585–594. doi:10.1016/j.geoderma.2012.05.020

Pronk G.J., Heister K., Kögel-Knabner I. (2013). Is turnover and development of organic matter controlled by mineral composition? Soil Biol Biochem 67: 235–244. doi:10.1016/j.soilbio.2013.09.006

Prost R., Yaron B. (2001). Use of modified clays for controlling soil environmental quality. Soil Sci 166 (12): 880–895. doi:10.1097/00010694-200112000-00003

Pruesse E., Quast C., Knittel K., Fuchs B.M., Ludwig W., Peplies J., Glöckner F.O. (2007). SILVA: A comprehensive online resource for quality checked and aligned ribosomal RNA sequence data compatible with ARB. Nucleic Acids Res 35 (21): 7188–7196. doi:10.1093/nar/gkm864

Pruitt K.D., Tatusova T., Brown G.R., Maglott D.R. (2012). NCBI Reference Sequences (RefSeq): Current status, new features and genome annotation policy. Nucleic Acids Res 40 (D1): D130–D135. doi:10.1093/nar/gkr1079

Qiao C., Penton C.R., Liu C., Shen Z., Ou Y., Liu Z., Xu X., Li R., Shen Q. (2019). Key extracellular enzymes triggered high-efficiency composting associated with bacterial community succession. Bioresour Technol 288: 121576. doi:10.1016/j.biortech.2019.121576

Qiao H., Chen L., Hu Y., Deng C., Sun Q., Deng S., Chen X., Mei L., Wu J., Su Y. (2021). Soil Microbial Resource Limitations and Community Assembly Along a Camellia oleifera Plantation Chronosequence. Front Microbiol 12: 736165. doi:10.3389/fmicb.2021.736165

R Core Team. (2013). R: A language and environment for statistical computing. R Foundation for Statistical Computing, Vienna, Austria. Available at: https://www.R-project.org [Accessed: 22 November 2015]

Ragot S.A., Huguenin-Elie O., Kertesz M.A., Frossard E., Bünemann E.K. (2016). Total and

active microbial communities and phoD as affected by phosphate depletion and pH in soil. Plant Soil 408 (1–2): 15–30. doi:10.1007/s11104-016-2902-5

Rai A.N., Borthakur M., Bergman B. (1992). Nitrogenase derepresssion, its regulation and metabolic changes associated with diazotrophy in the non-heterocystous cyanobacterium Plectonema boryanum PCC 73110. J Gen Microbiol 138 (3): 481–491. doi:10.1099/00221287-138-3-481

Raj A., Kumar S., Singh S.K., Prakash J. (2018). Production and purification of xylanase from alkaliphilic Bacillus licheniformis and its pretreatment of eucalyptus kraft pulp. Biocatal Agric Biotechnol 15: 199–209. doi:10.1016/j.bcab.2018.06.018

Ramette A. (2007). Multivariate analyses in microbial ecology. FEMS Microbiol Ecol 62 (2): 142–160. doi:10.1111/j.1574-6941.2007.00375.x

Ramirez K.S., Craine J.M., Fierer N. (2012). Consistent effects of nitrogen amendments on soil microbial communities and processes across biomes. Glob Chang Biol 18 (6): 1918–1927. doi:10.1111/j.1365-2486.2012.02639.x

Rawat P., Das S., Shankhdhar D., Shankhdhar S.C. (2021). Phosphate-Solubilizing Microorganisms: Mechanism and Their Role in Phosphate Solubilization and Uptake. J Soil Sci Plant Nutr 21 (1): 49–68. doi:10.1007/s42729-020-00342-7

Regan K., Stempfhuber B., Schloter M., Rasche F., Prati D., Philippot L., Boeddinghaus R.S., Kandeler E., Marhan S. (2017). Spatial and temporal dynamics of nitrogen fixing, nitrifying and denitrifying microbes in an unfertilized grassland soil. Soil Biol Biochem 109: 214–226. doi:10.1016/j.soilbio.2016.11.011

Richardson A.E., Simpson R.J. (2011). Soil Microorganisms Mediating Phosphorus Availability. Plant Physiol 156 (3): 989–996. doi:10.1104/pp.111.175448

Rodriguez F., Lillington J., Johnson S., Timmel C.R., Lea S.M., Berks B.C. (2014). Crystal structure of the Bacillus subtilis phosphodiesterase PhoD reveals an iron and calcium-containing active site. J Biol Chem 289 (45): 30889–30899. doi:10.1074/jbc.M114.604892

Rodríguez H., Fraga R., Gonzalez T., Bashan Y. (2006). Genetics of phosphate solubilization and its potential applications for improving plant growth-promoting bacteria. Plant Soil 287 (1–2): 15–21. doi:10.1007/s11104-006-9056-9

Rösch C., Bothe H. (2009). Diversity of total, nitrogen-fixing and denitrifying bacteria in an acid forest soil. Eur J Soil Sci 60 (6): 883–894. doi:10.1111/j.1365-2389.2009.01167.x

Rossolini G.M., Schippa S., Riccio M.L., Berlutti F., Macaskie L.E., Thaller M.C. (1998). Bacterial nonspecific acid phosphohydrolases: physiology, evolution and use as tools in microbial biotechnology. Cell Mol Life Sci 54 (8): 833–850. doi:10.1007/s000180050212

Rütting T., Boeckx P., Müller C., Klemedtsson L. (2011). Assessment of the importance of dissimilatory nitrate reduction to ammonium for the terrestrial nitrogen cycle. Biogeosciences 8 (7): 1779–1791. doi:10.5194/bg-8-1779-2011

Saidy A.R., Smernik R.J., Baldock J.A., Kaiser K., Sanderman J. (2015). Microbial

degradation of organic carbon sorbed to phyllosilicate clays with and without hydrous iron oxide coating. Eur J Soil Sci 66 (1): 83–94. doi:10.1111/ejss.12180

Santos-Beneit F. (2015). The Pho regulon: a huge regulatory network in bacteria. Front Microbiol 6: 402. doi:10.3389/fmicb.2015.00402

Saunders W.M.H., Williams E.G. (1955). Observation on the determination of total organic phosphorus in soil. J Soil Sci 6 (2): 254–267. doi:10.1111/j.1365-2389.1955.tb00849.x

Schaaf W., Bens O., Fischer A., Gerke H.H., Gerwin W., Grünewald U., Holländer H.M., Kögel-Knabner I., Mutz M., Schloter M., Schulin R., Veste M., Winter S., Hüttl R.F. (2011). Patterns and processes of initial terrestrial-ecosystem development. J Plant Nutr Soil Sci 174 (2): 229–239. doi:10.1002/jpln.201000158

Schimel J.P., Bennet J. (2004). Nitrogen mineralization: Challenges of a changing paradigm. Ecology 85 (3): 591–602. doi:10.1890/03-8002

Schimel J.P., Schaeffer S.M. (2012). Microbial control over carbon cycling in soil. Front Microbiol 3: 348. doi:10.3389/fmicb.2012.00348

Schmieder R., Edwards R. (2011). Fast Identification and Removal of Sequence Contamination from Genomic and Metagenomic Datasets. PLoS One 6 (3). doi:10.1371/journal.pone.0017288

Schöler A., Jacquiod S., Vestergaard G., Schulz S., Schloter M. (2017). Analysis of soil microbial communities based on amplicon sequencing of marker genes. Biol Fertil Soils 53 (5): 485–489. doi:10.1007/s00374-017-1205-1

Scholl M.A., Mills A.L., Herman J.S., Hornberger G.M. (1990). The influence of mineralogy and solution chemistry on the attachment of bacteria to representative aquifer materials. J Contam Hydrol 6 (4): 321–336. doi:10.1016/0169-7722(90)90032-C

Schubert M., Lindgreen S., Orlando L. (2016). AdapterRemoval v2: rapid adapter trimming, identification, and read merging. BMC Res Notes 9 (1): 88. doi:10.1186/s13104-016-1900-2

Schubert S., Steffens D., Ashraf I. (2020). Is occluded phosphate plant-available? J Plant Nutr Soil Sci 183 (3): 338–344. doi:10.1002/jpln.201900402

Schulz S., Brankatschk R., Dümig A., Kögel-Knabner I., Schloter M., Zeyer J. (2013). The role of microorganisms at different stages of ecosystem development for soil formation. Biogeosciences 10 (6): 3983–3996. doi:10.5194/bg-10-3983-2013

Schurig C., Smittenberg R.H., Berger J., Kraft F., Woche S.K., Goebel M.O., Heipieper H.J., Miltner A., Kaestner M. (2013). Microbial cell-envelope fragments and the formation of soil organic matter: A case study from a glacier forefield. Biogeochemistry 113 (1–3): 595–612. doi:10.1007/s10533-012-9791-3

Schwertmann U., Cornell R.M. (1991). Iron oxides in the laboratory: preparation and characterization. John Wiley & Sons, Hoboken, New Jersey, USA. doi:10.1002/9783527613229

Seeling B., Zasoski R.J. (1993). Microbial effects in maintaining organic and inorganic

solution phosphorus concentrations in a grassland topsoil. Plant Soil 148 (2): 277–284. doi:10.1007/BF00012865

Seitzinger S., Harrison J.A., Böhlke J.K., Bouwman A.F., Lowrance R., Peterson B., Tobias C., Van Drecht G. (2006). Denitrification across landscapes and waterscapes: A synthesis. Ecol Appl 16 (6): 2064–2090. doi:10.1890/1051-0761(2006)016[2064:DALAWA]2.0.CO;2

Séneca J., Söllinger A., Herbold C.W., Pjevac P., Prommer J., Verbruggen E., Sigurdsson B.D., Peñuelas J., Janssens I.A., Urich T., Tveit A.T., Richter A. (2021). Increased microbial expression of organic nitrogen cycling genes in long-term warmed grassland soils. ISME Commun 1 (1): 69. doi:10.1038/s43705-021-00073-5

Shahbaz M., Kumar A., Kuzyakov Y., Börjesson G., Blagodatskaya E. (2018). Interactive priming effect of labile carbon and crop residues on SOM depends on residue decomposition stage: Three-source partitioning to evaluate mechanisms. Soil Biol Biochem 126: 179–190. doi:10.1016/j.soilbio.2018.08.023

Sharma S.B., Sayyed R.Z., Trivedi M.H., Gobi T.A. (2013). Phosphate solubilizing microbes: Sustainable approach for managing phosphorus deficiency in agricultural soils. Springerplus 2 (1): 587. doi:10.1186/2193-1801-2-587

Shen J., Yuan L., Zhang J., Li H., Bai Z., Chen X., Zhang W., Zhang F. (2011). Phosphorus Dynamics: From Soil to Plant. Plant Physiol 156 (3): 997–1005. doi:10.1104/pp.111.175232

Sieradzki E.T., Nuccio E.E., Pett-Ridge J., Firestone M.K. (2020). Transcription of protease and chitinase genes provides a window onto macromolecular organic nitrogen decomposition in soil. bioRXiv 2020.12.14.422732. doi:10.1101/2020.12.14.422732

Simon C., Daniel R. (2011). Metagenomic analyses: Past and future trends. Appl Environ Microbiol 77 (4): 1153–1161. doi:10.1128/AEM.02345-10

Singh A.K., Bilal M., Iqbal H.M.N., Raj A. (2021). Lignin peroxidase in focus for catalytic elimination of contaminants — A critical review on recent progress and perspectives. Int J Biol Macromol 177: 58–82. doi:10.1016/j.ijbiomac.2021.02.032

Six J., Bossuyt H., Degryze S., Denef K. (2004). A history of research on the link between (micro)aggregates, soil biota, and soil organic matter dynamics. Soil Tillage Res 79 (1): 7–31. doi:10.1016/j.still.2004.03.008

Sriyapai T., Somyoonsap P., Matsui K., Kawai F., Chansiri K. (2011). Cloning of a thermostable xylanase from Actinomadura sp. S14 and its expression in Escherichia coli and Pichia pastoris. J Biosci Bioeng 111 (5): 528–536. doi:10.1016/j.jbiosc.2010.12.024

Stein L.Y., Klotz M.G. (2016). The nitrogen cycle. Curr Biol 26 (3): R94–R98. doi:10.1016/j.cub.2015.12.021

Steinbach A., Schulz Stefanie, Giebler J., Schulz Stephan, Pronk G.J., Kögel-Knabner I., Harms H., Wick L.Y., Schloter M. (2015). Clay minerals and metal oxides strongly influence the structure of alkane-degrading microbial communities during soil

maturation. ISME J 9 (7): 1687–1691. doi:10.1038/ismej.2014.243

Stibal M., Tranter M., Benning L.G., Řehák J. (2008). Microbial primary production on an Arctic glacier is insignificant in comparison with allochthonous organic carbon input. Environ Microbiol 10 (8): 2172–2178. doi:10.1111/j.1462-2920.2008.01620.x

Stosiek N., Talma M., Klimek-Ochab M. (2020). Carbon-Phosphorus Lyase — the State of the Art. Appl Biochem Biotechnol 190 (4): 1525–1552. doi:10.1007/s12010-019-03161-4

Stotzky G. (1997). Soil as an environment for microbial life. In: Modern Soil Microbiology (van Elsas J.D., Trevors J.T., Wellington E.M.H., eds), Marcel Dekker Inc, New York, NY, USA, pp. 1–20

Stotzky G. (1986). Influence of soil mineral colloids on metabolic processes, growth, adhesion, and ecology of microbes and viruses. In: Interactions of Soil Minerals with Natural Organics and Microbes (Huang P.M., Schnitzer M., eds), Soil Science Society Of America Special Publication, Madison, WI, USA, pp. 305–428. doi:10.2136/sssaspecpub17.c10

Stotzky G., Rem L.T. (1967). Influence of clay minerals on microorganisms: IV. Montmorillonite and kaolinite on fungi. Can J Microbiol 13 (11): 1535–1550. doi:10.1139/m67-202

Štyriaková I., Štyriak I., Oberhänsli H. (2012). Rock weathering by indigenous heterotrophic bacteria of Bacillus spp. at different temperature: a laboratory experiment. Mineral Petrol 105 (3–4): 135–144. doi:10.1007/s00710-012-0201-2

Su Y.G., Wu L., Zhou Z.B., Liu Y.B., Zhang Y.M. (2013). Carbon flux in deserts depends on soil cover type: A case study in the Gurbantunggute desert, North China. Soil Biol Biochem 58: 332–340. doi:10.1016/j.soilbio.2012.12.006

Sun J., Tian C., Diamond S., Glassa N.L. (2012). Deciphering Transcriptional Regulatory Mechanisms Associated with Hemicellulose Degradation in Neurospora crassa. Eukaryot Cell 11 (4): 482–493. doi:10.1128/EC.05327-11

Sun Q., Liu X., Wang S., Lian B. (2020). Effects of mineral substrate on ectomycorrhizal fungal colonization and bacterial community structure. Sci Total Environ 721: 137663. doi:10.1016/j.scitotenv.2020.137663

Tanuwidjaja I., Vogel C., Pronk G.J., Schöler A., Kublik S., Vestergaard G., Kögel-Knabner I., Mrkonjic Fuka M., Schloter M., Schulz S. (2021). Microbial Key Players Involved in P Turnover Differ in Artificial Soil Mixtures Depending on Clay Mineral Composition. Microb Ecol 81 (4): 897–907. doi:10.1007/s00248-020-01635-1

Tarnocai C., Canadell J.G., Schuur E.A.G., Kuhry P., Mazhitova G., Zimov S. (2009). Soil organic carbon pools in the northern circumpolar permafrost region. Global Biogeochem Cycles 23: GB2023. doi:10.1029/2008GB003327

Thapa S., Mishra J., Arora N., Mishra P., Li H., O′Hair J., Bhatti S., Zhou S. (2020). Microbial cellulolytic enzymes: diversity and biotechnology with reference to lignocellulosic biomass degradation. Rev Environ Sci Biotechnol 19 (3): 621–648.

doi:10.1007/s11157-020-09536-y

Thirkell T.J., Pastok D., Field K.J. (2020). Carbon for nutrient exchange between arbuscular mycorrhizal fungi and wheat varies according to cultivar and changes in atmospheric carbon dioxide concentration. Glob Chang Biol 26 (3): 1725–1738. doi:10.1111/gcb.14851

Thomas T., Gilbert J., Meyer F. (2012). Metagenomics - a guide from sampling to data analysis. Microb Inform Exp 2 (1): 3. doi:10.1186/2042-5783-2-3

Torsvik V., Goksoyr J., Daae F.L. (1990). High diversity in DNA of soil bacteria. Appl Environ Microbiol 56 (3): 782–787. doi:10.1128/aem.56.3.782-787.1990

Torsvik V., Øvreås L. (2002). Microbial diversity and function in soil: from genes to ecosystems. Curr Opin Microbiol 5 (3): 240–245. doi:10.1016/S1369-5274(02)00324-7

Totsche K.U., Amelung W., Gerzabek M.H., Guggenberger G., Klumpp E., Knief C., Lehndorff E., Mikutta R., Peth S., Prechtel A., Ray N., Kögel-Knabner I. (2018). Microaggregates in soils. J Plant Nutr Soil Sci 181 (1): 104–136. doi:10.1002/jpln.201600451

Töwe S., Wallisch S., Bannert A., Fischer D., Hai B., Haesler F., Kleineidam K., Schloter M. (2011). Improved protocol for the simultaneous extraction and column-based separation of DNA and RNA from different soils. J Microbiol Methods 84 (3): 406–412. doi:10.1016/j.mimet.2010.12.028

Trumbore S. (2006). Carbon respired by terrestrial ecosystems - recent progress and challenges. Glob Chang Biol 12 (2): 141–153. doi:10.1111/j.1365-2486.2006.01067.x

Turner S., Schippers A., Meyer-Stüve S., Guggenberger G., Gentsch N., Dohrmann R., Condron L.M., Eger A., Almond P.C., Peltzer D.A., Richardson S.J., Mikutta R. (2014). Mineralogical impact on long-term patterns of soil nitrogen and phosphorus enzyme activities. Soil Biol Biochem 68: 31–43. doi:10.1016/j.soilbio.2013.09.016

Uroz S., Kelly L.C., Turpault M.P., Lepleux C., Frey-Klett P. (2015). The Mineralosphere Concept: Mineralogical Control of the Distribution and Function of Mineral-associated Bacterial Communities. Trends Microbiol 23 (12): 751–762. doi:10.1016/j.tim.2015.10.004

Uroz S., Tech J.J., Sawaya N.A., Frey-Klett P., Leveau J.H.J. (2014). Structure and function of bacterial communities in ageing soils : Insights from the Mendocino ecological staircase. Soil Biol Biochem 69: 265–274. doi:10.1016/j.soilbio.2013.11.002

Van Teeseling M.C.F., Mesman R.J., Kuru E., Espaillat A., Cava F., Brun Y. V., VanNieuwenhze M.S., Kartal B., van Niftrik L. (2015). Anammox Planctomycetes have a peptidoglycan cell wall. Nat Commun 6: 6878. doi:10.1038/ncomms7878

Vestergaard G., Schulz S., Schöler A., Schloter M. (2017). Making big data smart—how to use metagenomics to understand soil quality. Biol Fertil Soils 53 (5): 479–484. doi:10.1007/s00374-017-1191-3

Větrovský T., Baldrian P. (2013). The Variability of the 16S rRNA Gene in Bacterial

Genomes and Its Consequences for Bacterial Community Analyses. PLoS One 8 (2): e57923. doi:10.1371/journal.pone.0057923

Viswanath B., Rajesh B., Janardhan A., Kumar A.P., Narasimha G. (2014). Fungal Laccases and Their Applications in Bioremediation. Enzyme Res 2014: 163242. doi:10.1155/2014/163242

Vitousek P.M., Howarth R.W. (1991). Nitrogen limitation on land and in the sea: How can it occur? Biogeochemistry 13 (2): 87–115

Vitousek P.M., Porder S., Houlton B.Z., Chadwick O.A. (2010). Terrestrial phosphorus limitation: mechanisms, implications, and nitrogen-phosphorus interactions. Ecol Appl 20 (1): 5–15. doi:10.1890/08-0127.1

Vogel C., Babin D., Pronk G.J., Heister K., Smalla K., Kögel-Knabner I. (2014). Establishment of macro-aggregates and organic matter turnover by microbial communities in long-term incubated artificial soils. Soil Biol Biochem 79: S46–S47. doi:10.1016/j.soilbio.2014.07.012

Vogel C., Heister K., Buegger F., Tanuwidjaja I., Haug S., Schloter M., Kögel-Knabner I. (2015). Clay mineral composition modifies decomposition and sequestration of organic carbon and nitrogen in fine soil fractions. Biol Fertil Soils 51 (4): 427–442. doi:10.1007/s00374-014-0987-7

Vogel H.J., Balseiro-Romero M., Kravchenko A., Otten W., Pot V., Schlüter S., Weller U., Baveye P.C. (2022). A holistic perspective on soil architecture is needed as a key to soil functions. Eur J Soil Sci 73 (1): e13152. doi:10.1111/ejss.13152

Vogel T.M., Simonet P., Jansson J.K., Hirsch P.R., Tiedje J.M., van Elsas J.D., Bailey M.J., Nalin R., Philippot L. (2009). TerraGenome: a consortium for the sequencing of a soil metagenome. Nat Rev Microbiol 7 (April): 252–252. doi:10.1038/nrmicro2119

Vos M., Wolf A.B., Jennings S.J., Kowalchuk G.A. (2013). Micro-scale determinants of bacterial diversity in soil. FEMS Microbiol Rev 37 (6): 936–954. doi:10.1111/1574-6976.12023

Vrsanska M., Buresova A., Damborsky P., Adam V. (2015). Influence of Different Inducers on Ligninolytic Enzyme Activities. J Met Nanotechnologies 3: 64–70

Wagg C., Bender S.F., Widmer F., van der Heijden M.G.A. (2014). Soil biodiversity and soil community composition determine ecosystem multifunctionality. Proc Natl Acad Sci U S A 111 (14): 5266–5270. doi:10.1073/pnas.1320054111

Walbridge M.R. (1991). Phosphorus availability in acid organic soils of the lower North Carolina Coastal Plain. Ecology 72 (6): 2083–2100. doi:10.2307/1941561

Walia A., Guleria S., Mehta P., Chauhan A., Parkash J. (2017). Microbial xylanases and their industrial application in pulp and paper biobleaching: a review. 3 Biotech 7: 11. doi:10.1007/s13205-016-0584-6

Walker T.W., Syers J.K. (1976). The fate of phosphorus during pedogenesis. Geoderma 15 (1): 1–19. doi:10.1016/0016-7061(76)90066-5

Wang T., Tian Z., Bengtson P., Tunlid A., Persson P. (2017). Mineral-surface-reactive metabolites secreted during fungal decomposition contribute to the formation of soil organic matter. Environ Microbiol 19 (12): 5117–5129. doi:10.1111/1462-2920.13990

Wang X., Cui Y., Wang Y., Duan C., Niu Y., Sun R., Shen Y., Guo X., Fang L. (2022). Ecoenzymatic stoichiometry reveals phosphorus addition alleviates microbial nutrient limitation and promotes soil carbon sequestration in agricultural ecosystems. J Soils Sediments 22 (2): 536–546. doi:10.1007/s11368-021-03094-8

Wang X.G., Lü X.T., Zhang H.Y., Dijkstra F.A., Jiang Y.G., Wang X.B., Lu J.Y., Wuyunna, Wang Z.W., Han X.G. (2020). Changes in soil C:N:P stoichiometry along an aridity gradient in drylands of northern China. Geoderma 361: 114087. doi:10.1016/j.geoderma.2019.114087

Wang Zengru, Wang Y., Zhang W., Liu Y., Gao T. (2021). Potential complementary functions among bacteria, fungi, and archaea involved in carbon cycle during reversal of desertification. L Degrad Dev 32 (3): 1581–1587. doi:10.1002/ldr.3804

Wang Zhihui, Wang Zhirui, Li T., Wang C., Dang N., Wang R., Jiang Y., Wang H., Li H. (2021). N and P fertilization enhanced carbon decomposition function by shifting microbes towards an r-selected community in meadow grassland soils. Ecol Indic 132: 108306. doi:10.1016/j.ecolind.2021.108306

Warnes G.R., Bolker B., Bonebakker L., Gentleman R., Huber W., Liaw A., Lumley T., Maechler M., Magnusson A., Moeller S. (2013). gplots: Various R programming tools for plotting data. R Package version 2.12.1. Available at: http://cran.r-project.org/package=gplots [Accessed: 22 November 2015]

Wei X., Zhu Z., Liu Y., Luo Y., Deng Y., Xu X., Liu S., Richter A., Shibistova O., Guggenberger G., Wu J., Ge T. (2020). C:N:P stoichiometry regulates soil organic carbon mineralization and concomitant shifts in microbial community composition in paddy soil. Biol Fertil Soils 56 (8): 1093–1107. doi:10.1007/s00374-020-01468-7

Wei X., Zhu Z., Wei L., Wu J., Ge T. (2019). Biogeochemical cycles of key elements in the paddy-rice rhizosphere: Microbial mechanisms and coupling processes. Rhizosphere 10: 100145. doi:10.1016/j.rhisph.2019.100145

Wierzchos J., de los Ríos A., Ascaso C. (2012). Microorganisms in desert rocks: the edge of life on Earth. Int Microbiol 15 (4): 171–181. doi:10.2436/20.1501.01.170

Wilhelm R.C., Pepe-Ranney C., Weisenhorn P., Lipton M., Buckley D.H. (2021). Competitive exclusion and metabolic dependency among microorganisms structure the cellulose economy of an agricultural soil. MBio 12 (1): e03099-20. doi:10.1128/mBio.03099-20

Wilpiszeski R.L., Aufrecht J.A., Retterer S.T., Sullivan M.B., Graham D.E., Pierce E.M., Zablocki O.D., Palumbo A. V., Elias D.A. (2019). Soil Aggregate Microbial Communities: Towards Understanding Microbiome Interactions at Biologically Relevant Scales. Appl Environ Microbiol 85 (14): e00324-19. doi:10.1128/AEM.00324-19

Witzgall K., Vidal A., Schubert D.I., Höschen C., Schweizer S.A., Buegger F., Pouteau V.,

Chenu C., Mueller C.W. (2021). Particulate organic matter as a functional soil component for persistent soil organic carbon. Nat Commun 12 (1): 4115. doi:10.1038/s41467-021-24192-8

Wooley J.C., Godzik A., Friedberg I. (2010). A Primer on Metagenomics. PLoS Comput Biol 6 (2): e1000667. doi:10.1371/journal.pcbi.1000667

Wu J., Zhao Y., Qi H., Zhao X., Yang T., Du Y., Zhang H., Wei Z. (2017). Identifying the key factors that affect the formation of humic substance during different materials composting. Bioresour Technol 244: 1193–1196. doi:10.1016/j.biortech.2017.08.100

Xi D., Bai R., Zhang L., Fanga Y. (2016). Contribution of anammox to nitrogen removal in two temperate forest soils. Appl Environ Microbiol 82 (15): 4602–4612. doi:10.1128/AEM.00888-16

Yang D., Luo J., Peng P., Li W., Shi W., Jia L., He Y. (2021). Dynamics of nitrogen and phosphorus accumulation and their stoichiometry along a chronosequence of forest primary succession in the Hailuogou Glacier retreat area, eastern Tibetan Plateau. PLoS One 16 (2): e0246433. doi:10.1371/journal.pone.0246433

Yao F., Yang S., Wang Z., Wang Xue, Ye J., Wang Xugao, DeBruyn J.M., Feng X., Jiang Y., Li H. (2017). Microbial Taxa Distribution is Associated with Ecological Trophic Cascades along an Elevation Gradient. Front Microbiol 8: 2071. doi:10.3389/fmicb.2017.02071

Yarwood S., Wick A., Williams M., Daniels W.L. (2015). Parent Material and Vegetation Influence Soil Microbial Community Structure Following 30-Years of Rock Weathering and Pedogenesis. Microb Ecol 69 (2): 383–394. doi:10.1007/s00248-014-0523-1

Yu J., Liu X., Guan L., Jiang Z., Yan Q., Yang S. (2021). High–level expression and enzymatic properties of a novel thermostable xylanase with high arabinoxylan degradation ability from Chaetomium sp. suitable for beer mashing. Int J Biol Macromol 168: 223–232. doi:10.1016/j.ijbiomac.2020.12.040

Yuan Z.Y., Chen H.Y.H. (2015). Decoupling of nitrogen and phosphorus in terrestrial plants associated with global changes. Nat Clim Chang 5 (5): 465–469. doi:10.1038/nclimate2549

Zaharescu D.G., Burghelea C.I., Dontsova Katerina, Reinhard C.T., Chorover J., Lybrand R. (2020). Biological Weathering in the Terrestrial System: An Evolutionary Perspective. In: Biogeochemical Cycles: Ecological Drivers and Environmental Impact (Dontsova K, Balogh-Brunstad Z., Le Roux G., eds), John Wiley & Sons, Hoboken, New Jersey, pp. 3–32

Zechmeister-Boltenstern S., Keiblinger K.M., Mooshammer M., Penuelas J., Richter A., Sardans J., Wanek W. (2015). The application of ecological stoichiometry to plant–microbial–soil organic matter transformations. Ecol Monogr 85 (2): 133–155. doi:doi.org/10.1890/14-0777.1

Zeng J., Liu X., Song L., Lin X., Zhang H., Shen C., Chu H. (2016). Nitrogen fertilization directly affects soil bacterial diversity and indirectly affects bacterial community composition. Soil Biol Biochem 92: 41–49. doi:10.1016/j.soilbio.2015.09.018

Zhang L., Hu Y., Han F., Wu Y., Tian D., Su M., Wang S., Li Z., Hu S. (2019). Influences of multiple clay minerals on the phosphorus transport driven by Aspergillus niger. Appl Clay Sci 177: 12–18. doi:10.1016/j.clay.2019.04.026

Zhang X., Ward B.B., Sigman D.M. (2020). Global Nitrogen Cycle: Critical Enzymes, Organisms, and Processes for Nitrogen Budgets and Dynamics. Chem Rev 120 (12): 5308–5351. doi:10.1021/acs.chemrev.9b00613

Zhang X., Wei H., Chen Q., Han X. (2014). The counteractive effects of nitrogen addition and watering on soil bacterial communities in a steppe ecosystem. Soil Biol Biochem 72: 26–34. doi:10.1016/j.soilbio.2014.01.034

Zhang Y., Cong J., Lu H., Li G., Xue Y., Deng Y., Li H., Zhou J., Li D. (2015). Soil bacterial diversity patterns and drivers along an elevational gradient on Shennongjia Mountain, China. Microb Biotechnol 8 (4): 739–746. doi:10.1111/1751-7915.12288

Zhang Z., Zhao Y., Wang R., Lu Q., Wu J., Zhang D., Nie Z., Wei Z. (2018). Effect of the addition of exogenous precursors on humic substance formation during composting. Waste Manag 79: 462–471. doi:10.1016/j.wasman.2018.08.025

Zhou Z., Wang C., Luo Y. (2018). Effects of forest degradation on microbial communities and soil carbon cycling: A global meta-analysis. Glob Ecol Biogeogr 27 (1): 110–124. doi:10.1111/geb.12663

Zhu J., Li M., Whelan M. (2018a). Phosphorus activators contribute to legacy phosphorus availability in agricultural soils: A review. Sci Total Environ 612: 522–537. doi:10.1016/j.scitotenv.2017.08.095

Zhu Z., Ge T., Luo Y., Liu S., Xu X., Tong C., Shibistova O., Guggenberger G., Wu J. (2018b). Microbial stoichiometric flexibility regulates rice straw mineralization and its priming effect in paddy soil. Soil Biol Biochem 121: 67–76. doi:10.1016/j.soilbio.2018.03.003

Zimmermann M., Leifeld J., Fuhrer J. (2007). Quantifying soil organic carbon fractions by infrared-spectroscopy. Soil Biol Biochem 39 (1): 224–231. doi:10.1016/j.soilbio.2006.07.010

Curriculum vitae

Irina Tanuwidjaja was born in 1981 in Varaždin where she attended the First Grammar School Varaždin. After her second year, she won the HMC scholarship for students from Central and Eastern Europe which allowed her to enroll in St. John's School, Leatherhead, Surrey, UK where she completed her high school education. In 2010 she obtained a Bachelor's degree in Organic Agriculture and 2012 a Master's degree in Agroecology, majoring in Microbial Biotechnology in Agriculture at the University of Zagreb Faculty of Agriculture. Both theses were performed at the Department of Microbiology under the supervision of Skelin, PhD ("Isolation and genetic characterization of the indigenous enterococci isolated from the Istrian cheese", Bachelor's thesis), and assist. prof. Mrkonjić Fuka ("Genotypic and phenotypic characterization of indigenous lactococcal population isolated from the traditional Istrian cheese", Master's thesis). During her final year of graduate study, she was an intern at the Laboratory for Molecular Genetics, Ruđer Bošković Institute in the group of dr. sc. Vujaklija where she was supervised by dr. sc. Bielen. Her work there resulted in a student paper "An analysis of expression vector promotor for lipase biosynthesis *Streptomyces coelicolor*" which was rewarded with the Rector's Award in 2012. She was employed at Helmholtz Center Munich, Germany in 2012. In 2016 Irina Tanuwidjaja started to work at the Department of Microbiology, University of Zagreb Faculty of Agriculture as an assistant. As an associate, she held laboratory courses and seminars on two undergraduate, and five graduate modules of which one is taught in English. She was an immediate supervisor of four undergraduate and six graduate theses and a co-author of one faculty handbook for undergraduate students. She was an associate on seven scientific national and international projects and one teaching project. She held lectures at three international conferences and participated as an author or co-author at more than ten international and national conferences. Since 2016 she successfully trained in international institutions, including the Helmholtz Center, Munich, Germany; BOKU, Vienna, Austria; Biotechnology Research Center, LIPI, Cibinong, Indonesia; Bogor University of Agriculture, Bogor, Indonesia and Huazhong University of Agriculture, Wuhan, People's Republic of China. To date, she has published eleven A1 and three A3 papers, and is the first author of five A1 papers.

Publications in WoS:

Tanuwidjaja I., Mrkonjic Fuka M. (2022). Ozone in Droplets and Mist in Inhibition of Phytopathogenic Microbiota. Agriculture 12(11): 1875. doi:10.3390/agriculture12111875

Augustin K., **Tanuwidjaja I.**, Kovaček I., Majić I., Luković Z., Mrkonjić Fuka M. (2021). Microbiological analysis of indoor and outdoor air on a pig farm in Slavonia. J Cent Eur Agric 22(2): 260–268. doi:10.5513/JCEA01/22.2.3143

Jurić S., **Tanuwidjaja I.**, Mrkonjić Fuka M., Vlahoviček Kahlina K., Marijan M., Boras A., Udiković Kolić N., Vinceković M. (2021). Encapsulation of two fermentation agents, Lactobacillus sakei and calcium ions in microspheres. Colloids Surfaces B Biointerfaces 197: 111387. doi:10.1016/j.colsurfb.2020.111387

Mrkonjic Fuka M., Kos I., Zgomba Maksimovic A., Bacic M., **Tanuwidjaja I**. (2021). Proteolytic Lactococcus lactis and Lipolytic Enterococcus durans of Dairy Origin as Meat Functional Starter Cultures. Food Technol Biotechnol 59(1): 63–73. doi:10.17113/ftb.59.01.21.6872

Mrkonjic Fuka M., Zgomba Maksimovic A., Hulak N., Kos I., Marusic Radovcic N., Juric S., **Tanuwidjaja I.**, Karolyi D., Vincekovic M. (2021). The survival rate and efficiency of non-encapsulated and encapsulated native starter cultures to improve the quality of

artisanal game meat sausages. J Food Sci Technol 58(2): 710–719. doi:10.1007/s13197-020-04587-z

Tanuwidjaja I., Svečnjak L., Gugić D., Levanić M., Jurić S., Vinceković M., Mrkonjić Fuka M. (2021). Chemical Profiling and Antimicrobial Properties of Honey Bee (Apis mellifera L.) Venom. Molecules 26: 3049. doi:10.3390/molecules26103049

Tanuwidjaja I., Vogel C., Pronk G.J., Schöler A., Kublik S., Vestergaard G., Kögel-Knabner I., Mrkonjic Fuka M., Schloter M., Schulz S. (2021). Microbial Key Players Involved in P Turnover Differ in Artificial Soil Mixtures Depending on Clay Mineral Composition. Microb Ecol 81(4): 897–907. doi:10.1007/s00248-020-01635-1

Mrkonjic Fuka M., **Tanuwidjaja I.**, Zgomba Maksimovic A., Zunabovic-Pichler M., Kublik S., Hulak N., Domig K.J., Schloter M. (2020). Bacterial diversity of naturally fermented game meat sausages: Sources of new starter cultures. LWT - Food Sci Technol 118: 108782. doi:10.1016/j.lwt.2019.108782

Mrkonjic Fuka M., Zgomba Maksimovic A., **Tanuwidjaja I.**, Hulak N., Schloter M. (2017). Characterization of enterococcal community isolated from an Artisan Istrian raw milk cheese: Biotechnologicaland safety aspects. Food Technol Biotechnol 55(3): 368–380. doi:10.17113/ft b.55.03.17.5118

Pronk G.J., Heister K., Vogel C., Babin D., Bachmann J., Ding G.C., Ditterich F., Gerzabek M.H., Giebler J., Hemkemeyer M., Kandeler E., Kunhi Mouvenchery Y., Miltner A., Poll C., Schaumann G.E., Smalla K., Steinbach A., **Tanuwidjaja I.**, Tebbe C.C., Wick L.Y., Woche S.K., Totsche K.U., Schloter M., Kögel-Knabner I. (2017). Interaction of minerals, organic matter, and microorganisms during biogeochemical interface formation as shown by a series of artificial soil experiments. Biol Fertil Soils 53(1): 9–22. doi:10.1007/s00374-016-1161-1

Vogel C., Heister K., Buegger F., **Tanuwidjaja I.**, Haug S., Schloter M., Kögel-Knabner I. (2015). Clay mineral composition modifies decomposition and sequestration of organic carbon and nitrogen in fine soil fractions. Biol Fertil Soils 51(4): 427–442. doi:10.1007/s00374-014-0987-7